Getting to the root of the issue: characterising plant-microbial circadian interactions in the rhizosphere microbiome

Amy Laura Newman MSci

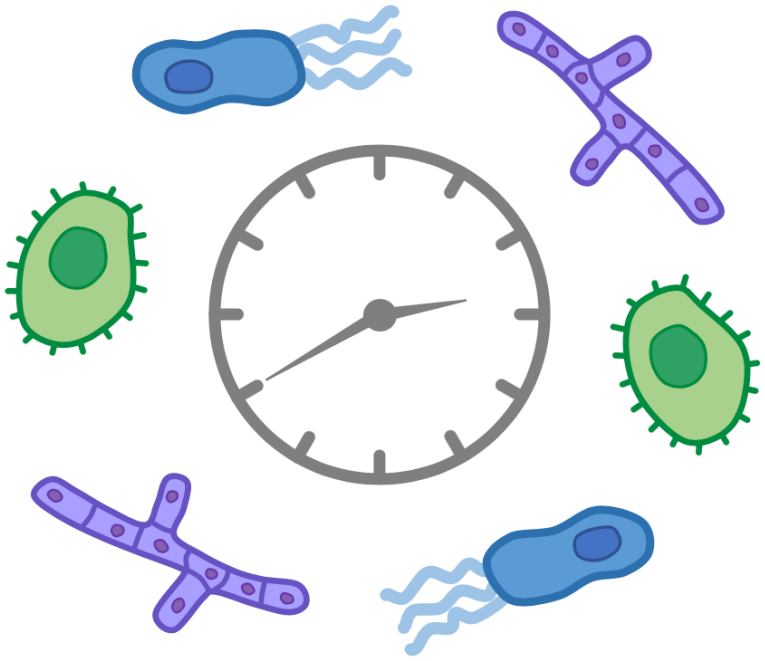

A thesis submitted for the degree of Doctor of Philosophy

School of Life Sciences, University of Warwick

November 2020

TABLE OF CONTENTS

LIST OF TABLES

LIST OF FIGURES

DEDICATION

I dedicate this thesis to my parents, Jayne and Martin Newman. I am so grateful for all the support they have given me over the years and everything they continue to do for me.

ACKNOWLEDGEMENTS

Completing this thesis was only possible with the help and contributions of many others, so several thanks are in order.

First and foremost, I wish to thank my supervisors Professor Gary Bending and Professor Isabelle Carré for helping me to grow as a scientist and being there every step of the way with guidance, encouragement and expertise. I thank Isabelle for sampling with me for Chapter 2 and for her input on the experimental design and analysis for Chapter 4 in particular. I thank Gary for sharing his microbial knowledge and always believing in me even when I didn't quite believe in myself.

Many thanks are also due to Dr Sally Hilton and Dr Emma Picot, as I benefitted greatly from their help. I thank Sally for sharing her expertise in all things MiSeq and molecular, Emma for discussions about circadian biology and her general coding magic, and both for helping with my bioinformatics and handling my endless code-related questions.

I also wish to thank the many people who have helped with the practical aspects of my project along the way. In particular, I thank everyone who gave up their time to help me take samples for Chapter 3: Gary Bending, Isabelle Carré, Sally Hilton, Jess Palmer, Ellis Monaghan, Katie Endersby, and Louisa Martin. I could not have managed the scale of the experiment without their help, and having companions made the many hours in a room with no window pass much faster. I thank Betty Sands for her help with qPCR and for being good company in the greenhouse darkrooms – when we weren't bumping into each other in the dark.

I am also grateful for the technical support I received, particularly from Paul Goode for helping with all the lab moves and making sure things were as I needed, and Michael Keenan for arranging a back-up power supply at the time my experiments needed it the most. I also thank the team from Workshop for

being there for all my repair- and DIY-based needs, particularly for Chapter 4, and the Prep Room staff for autoclaving the soil for Chapter 4.

I also thank my advisory panel members Dr John Clarkson and Professor Liz Wellington for always giving me a different perspective, and many other academics at Warwick for their feedback and discussions at various events over the years. In particular, I thank Dr Dan Franklin for his statistics advice and the demonstrating opportunities. I also wish to thank Nikki Glover for being so helpful when providing practical and administrative assistance over the years.

I wish to thank CENTA for selecting me and NERC for funding my studentship, which has led to so many opportunities for scientific and professional development. I am particularly thankful to Dr Chris Jeffs at the British Ecological Society for taking me on as a placement student and for his guidance, and CENTA for funding this experience. I also thank the International Society for Microbial Ecology for giving me the opportunity to speak at their 2018 conference.

My thanks are also due to many past and present labmates and researchers at Warwick, particularly for their company at tea breaks and contributions to the cake rota. There are too many to list individually, but to name a few, I thank Chris O'Grady, Ellis Monaghan, Emma Johnstone, Jess Palmer, and Betty Sands for their help with code, plant- and microbe-related discussions, the company on car journeys, and sharing internet memes. I also thank friends outside of the Warwick bubble for the much-needed perspective and time spent away from work.

I am very grateful to my family, particularly my parents, brother, and grandparents, for always being there for me, and could not have undertaken this without their practical and personal support. Lastly, I thank Michael Lawson, who has been the best distraction from my PhD – often in places more scenic than the Midlands – for all his encouragement and particularly for getting me through the final few months.

DECLARATION

I declare that the work presented in this thesis was conducted by myself under the direct supervision of Professor Gary Bending and Professor Isabelle Carré, with the exception of those instances where the contribution of others has been specifically acknowledged. None of the work presented in this thesis has previously been submitted for any other degree.

Amy Laura Newman

LIST OF ABBREVIATIONS

ANOSIM – Analysis of Similarity

ANOVA – Analysis of Variance

CAB – Chlorophyll a/b-binding protein

CCA1 – Circadian Clock Associated 1

cDNA – Complementary DNA

DCMU – 3-[3,4-dichlorophenyl]-1,1-dimethylurea

DNA – Deoxyribonucleic acid

EC – Evening Complex

ELF – Early Flowering

FFT-NLLS – Fast Fourier Transform Non-Linear Least Squares

FRQ – Frequency

GI – Gigantea

ITS – Internal Transcribed Spacer

LB – Lysogeny Broth

LD – Light-dark cycles

LED – Light Emitting Diode

LHY – Late Elongated Hypocotyl

LL – Constant light and temperature conditions

luc/lux – Luciferase

LUX – Lux Arrhythmo

mRNA – Messenger RNA

NCBI – National Centre for Biotechnology Information

NMDS – Non-Metric Multidimensional Scaling

OD – Optical Density

OTU – Operational Taxonomic Unit

PCR – Polymerase Chain Reaction

pH – Potential hydrogen

PRR – Pseudo-Response Regulator

QIIME – Quantitative Insights into Microbial Ecology

qPCR – Quantitative PCR

RAE – Relative Amplitude Error

RNA – Ribonucleic acid

RNAi – RNA interference

ROI – Region of Interest

rpoA – DNA-directed RNA polymerase alpha subunit

rpm – Revolutions per minute

rRNA – Ribosomal ribonucleic acid

RT-qPCR – Reverse transcriptase quantitative PCR

SEM – Standard Error of the Mean

TOC1 – Timing of CAB 1

UVR8 – Ultraviolet Resistance Locus 8

WC – White Collar

WCC – White Collar Complex

WT – Wild type

ZTL – Zeitlupe

SUMMARY

The circadian clock is an intracellular mechanism that allows organisms to synchronise their internal biological processes with predictable daily environmental changes. The circadian rhythms it generates are well studied in plants. However, very little is known about the possible influence of the plant circadian clock upon root-associated microbiota. Plants form intimate associations with microbes which are recruited from the soil into roots and the soil immediately adjacent to roots. These microbes constitute the rhizosphere microbiome and its composition can have significant implications for plant health. This thesis therefore investigated the presence of circadian changes in the rhizosphere microbiome and demonstrated the role of the plant circadian clock in shaping these interactions. To investigate the influence of the plant circadian clock on the assembly of the rhizosphere microbiome, we compared the rhizosphere bacterial and fungal communities of wild-type plants with those of plants with abnormal circadian clocks, using amplicon sequencing of the 16S rRNA and ITS regions. We found that altered clock function through overexpression or loss-of-function of the core plant clock gene *lhy* (*late elongated hypocotyl*) altered the rhizosphere microbiome after a period of plant growth, indicating that the plant circadian clock influences rhizosphere microbiome assembly. Additionally, we showed that a fraction of microbial OTUs exhibit daily changes in activity or abundance. OTUs that showed rhythmicity were found to differ between wild-type and *lhy* mutant plants, indicating that the plant clock also influences diel changes in the rhizosphere microbiome. In order to determine whether microbial rhythmicity in the rhizosphere persists in the absence of day-night cycles, we subsequently characterised microbial communities from plants transferred to constant light and temperature conditions. Here, rhythmic OTUs were observed in the wild-type rhizosphere but rhythmicity was largely abolished in the rhizosphere of arrhythmic plants overexpressing *lhy*, indicating that most free-running microbial rhythmicity was driven by the plant circadian clock. A handful of rhythmic OTUs were found in samples from arrhythmic plants, providing evidence for autonomous rhythmicity in some rhizosphere microbiota. Further, we developed a flexible imaging method for the non-destructive

visualisation of temporal interactions between plant roots and a luminescent model rhizosphere bacterium. Rhythmic bacterial luminescence was observed under light-dark cycles and persisted on the roots of wild-type plants under constant conditions. This free-running rhythmicity was disrupted on plants with loss-of-function of the circadian clock gene *gi* (*gigantea*), indicating that it was driven by the plant circadian clock. In summary, the work presented in this thesis identified circadian changes in the rhizosphere microbiome and found that the plant circadian clock drives most of these oscillations. The rhizosphere microbiome is therefore more variable over very short timescales than previously anticipated. The time of day at which samples are taken should be considered in future studies seeking to investigate rhizosphere microbiota, as this factor is not currently controlled for. Additionally, the findings of this thesis may form the basis of new strategies for more sustainable agricultural production, such as the timed application of crop management products.

CHAPTER 1: GENERAL INTRODUCTION

1.1. The plant circadian clock

1.1.1. The circadian clock

Due to the Earth's rotation around its axis, we experience changes in light levels and temperatures throughout the day. It is vital that organisms are able to anticipate and respond to this diel (i.e. 24 hour) variation in their environment in a timely fashion, as this allows them to optimise a variety of biological processes (McClung, 2006). The circadian clock has evolved to fulfil this purpose, through the generation of circadian rhythms.

The circadian clock is a widespread intracellular mechanism which may be conceptually divided into three core components (Rosbash and Hall, 1989): input pathways that couple the core oscillator to its environment; the core oscillator, which is a network of genes and their products in transcriptional-translational feedback loops; and output pathways that control downstream rhythms. Circadian rhythms generated by the circadian clock have a period (duration) of approximately 24 hours, as is demonstrated by the origins of the word 'circadian'. First coined in 1959, the term brings together the Latin words *circa* for about and *dies* for day (McClung, 2006).

The circadian clock is normally entrained (synchronised) to the day-night cycle of its environment. It can also be reset by external cues or zeitgebers (from the German 'zeit' for time and 'geber' for giver) to ensure its entrainment to the environment (McClung, 2006), of which light and temperature are particularly important for plants.

When organisms possessing circadian clocks are transferred to continuous light or darkness with no oscillations in temperature, also known as 'free-running' conditions, rhythmicity is maintained with a period of approximately 24 hours, demonstrating the endogenous nature of the circadian clock (McClung, 2006). The period of the plant circadian clock under constant conditions is also

influenced by the wavelength and intensity of the light it is receiving (Young and Kay, 2001).

The circadian clock also displays temperature compensation, whereby a relatively consistent period length is maintained even over a range of temperatures (McClung, 2006). Additionally, in plants and animals, the circadian clock is also able to perceive photoperiods, or the length of time each day where light is received, enabling them to also respond to seasonal environmental changes (Adams and Carré, 2011).

For rhythmicity to be classed as circadian, the following three criteria must therefore be met: it must be capable of entrainment to external stimuli, have a 'free-running' period of approximately 24 hours, and display temperature compensation (Bell-Pedersen et al., 2005).

Circadian clocks have been observed in organisms ranging from humans and animals, to plants, cyanobacteria, and fungi (Young and Kay, 2001). Interestingly, it is thought that circadian clocks have evolved multiple times: the oscillatory mechanisms of mammals, plants, insects, and fungi are largely composed of distinctly different sets of genes (Young and Kay, 2001).

The core oscillators of most known circadian clocks are based upon transcription-translation feedback loops, with the exception of the cyanobacterial clock, which is a post-translational oscillator (Cohen and Golden, 2015). Work to identify core circadian oscillator genes initially began with the investigation of the model insect *Drosophila melanogaster* (Tataroglu and Emery, 2015), and has since been conducted in many other model species, chiefly the fungus *Neurospora crassa* (Baker et al., 2012), mammal *Mus musculus* (Ripperger et al., 2011), plant *Arabidopsis thaliana* (McClung, 2019), and cyanobacterium *Synechococcus elongatus* (Cohen and Golden, 2015). It has been suggested that the plant circadian clock is more complex than the circadian oscillatory mechanisms in other types of organism, as many of its components belong to multi-gene families and exhibit partial redundancy in their functioning (Carré and Veflingstad, 2013).

1.1.2. The plant circadian clock and its influence

Current understanding of how the plant circadian clock operates is mostly based on work conducted on the model plant species *Arabidopsis thaliana.*

As one of the key zeitgebers for the plant circadian clock is light, plant photoreceptors are important molecules in the input pathways of the plant circadian oscillator. In *A. thaliana*, five types of photoreceptor molecules are known: red and far-red light sensing phytochromes; cryptochromes, the ZTL (ZEITLUPE) family, and phototropins, which sense blue light; and UVR8 (*Ultraviolet Resistance Locus 8*), which senses Ultraviolet-B light (Litthauer et al., 2016; Sanchez et al., 2020). Members of all five groups are known to be involved in the entrainment of the circadian clock by light, with the exception of phototropins (Litthauer et al., 2016; Sanchez et al., 2020). However, only the ZTL family is considered part of the main oscillator mechanism as its members are necessary for the entrainment of the clock and the maintenance of free-running rhythmicity (Sanchez et al., 2020). Plants use a variety of signalling cascades to integrate information from these photoreceptors and provide information to the circadian clock, allowing them to sense the intensity and spectral composition of the light they receive in addition to the photoperiod (duration of light received each day) (Sanchez et al., 2020).

The central oscillator of the plant circadian clock is composed of three main negative feedback loops, which each happen at different times of day (McClung, 2019; Figure 1.1). The mRNA levels of two closely related transcription factors *LHY* (*LATE ELONGATED HYPOCOTYL*) and *CCA1* (*CIRCADIAN CLOCK ASSOCIATED 1*) peak at dawn. In the morning, the LHY and CCA1 proteins repress expression of the *PRR* family of genes (*PSEUDO-RESPONSE REGULATORS 9*, *7*, *5*, and *1* [*PRR1* also known as *TOC1*, *TIMING OF CAB*]) and of the *EC* (*EVENING COMPLEX*, a transcriptional regulatory complex which includes *ELF3* and *ELF4 – EARLY FLOWERING 3* & *4 –* and *LUX* [*LUX ARRHYTHMO*]). As LHY and CCA1 repress their own gene expression and their protein levels decline, this repression lifts and *TOC1* and the *PRR* genes are expressed sequentially throughout the day, starting with *PRR9*. The PRRs then repress the expression of *LHY* and *CCA1* by binding to their promoters, and also

repress their own expression. In the evening, mRNA levels of the *EC* genes rise, and the EC acts to repress expression of the *PRR*s, allowing *LHY* and *CCA1* to be expressed again the following dawn and the cycle to continue.

Other components have also been implicated in the proper functioning of the circadian clock. For example, ZTL is involved with the degradation of TOC1 and PRR5, ensuring a high amplitude of their oscillation, and GI (GIGANTEA) acts to stabilise ZTL and facilitate its maturation into its active form (Cha et al., 2017).

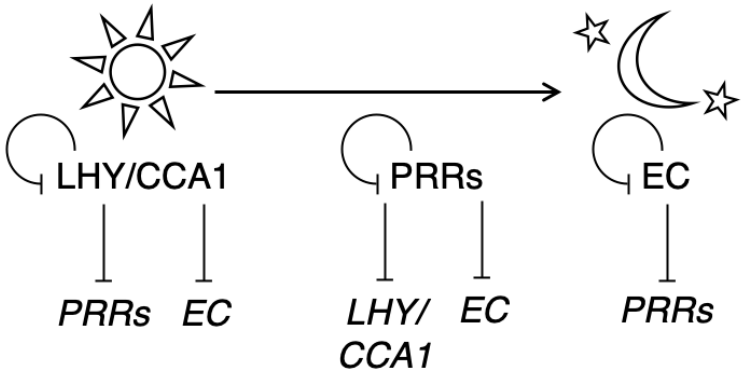

Figure 1.1. Overview of inhibitory interactions forming the core oscillator of the plant circadian clock. Lines with flat ends indicate transcriptional repression. In the morning, LHY and CCA1 repress the expression of the *PRR* family of genes and of the *EC*. LHY and CCA1 repress their own gene expression and their protein levels decline, causing their repression of the *PRRs* to lift. Throughout the afternoon, the *PRRs* are sequentially expressed. The PRRs bind to the promoters of *LHY* and *CCA1* to repress their expression, and TOC1 (also known as PRR1) represses the *EC*. Members of the PRRs also repress each other's expression, and the *EC* is then expressed in the evening. The EC represses expression of the *PRRs*, and represses its own expression, allowing *LHY* and *CCA1* to be expressed again the next day.

In addition to light, temperature is also an important zeitgeber for the plant circadian clock. Plants are capable of entrainment to thermocycles, i.e. alternations between warm and cool conditions (Eckardt, 2005). It has been demonstrated that *PRR7* and *PRR9* play a key role in this temperature entrainment in *A. thaliana*, where they have partially redundant functions (Salomé & McClung, 2005). Despite this ability to synchronise with external temperature cycles, the period of the plant circadian clock is not influenced by temperature

(McClung, 2006). This ability to maintain consistent period lengths over a range of environmental temperatures, termed temperature compensation, is thought to be due to the robustness which the plant circadian clock's multi-loop structure conveys, as opposed to the presence of specific molecular mechanisms (Gould et al., 2006; Gould et al., 2013). This robustness may be referred to as 'network balancing', whereby relatively mild effects of temperature are observed upon the individual components of the circadian oscillator, and temperature compensation is achieved due to their antagonistic interactions within the oscillator's multiple feedback loops (Gould et al., 2013). In support of this, Gould et al. (2006) demonstrated that ambient temperature influences the rhythmic accumulation of *TOC1*, *GI*, *LHY* and *CCA1* transcripts in *A. thaliana*. Further, blue light signalling via the cryptochrome photoreceptors CRY1 and CRY2 is required for temperature compensation in *A. thaliana* (Gould et al., 2013). The results of Gould et al. (2013) indicated that light and temperature share common input mechanisms to the plant circadian clock, and that this common regulatory pathway influences multiple components within the network of circadian clock genes.

Numerous aspects of plant physiology, development, metabolism and environmental responses are influenced or regulated by the circadian clock (Table 1.1). It has been demonstrated that between 6 – 31% of *A. thaliana* transcription is controlled by the circadian clock and shows rhythmicity under constant conditions (Michael et al., 2008). Additionally, as many as 89% of transcripts were demonstrated to show rhythmicity under at least one of a variety of lighting and temperature cycles (Michael et al., 2008).

Table 1.1. Key functions the plant circadian clock is known to influence.

Function	Reference
Leaf movement	Engelmann et al., 1992
Stomatal opening and photosynthesis	Somers et al., 1998
Photosynthetic gene expression	Harmer et al., 2000
Starch reserve breakdown	Graf et al., 2010
Nitrogen assimilation and utilisation	Gutiérrez et al., 2008

Hypocotyl elongation	Dowson-Day and Millar, 1999
Hormonal control of growth and development	Covington and Harmer, 2007
Season-dependent control of flowering	Yanovsky and Kay, 2002
Abiotic stress tolerance	Nakamichi et al., 2009
Rhythmic defence against herbivory	Goodspeed et al., 2012
Rhythmic defence against pathogens	Wang et al., 2011
Sensitivity to herbicides	Belbin et al., 2019

Whilst a functional circadian clock is not critical for plant viability (Green et al., 2002), the possession of a clock which is synchronised to the diel cycles of the external environment results in higher fitness (Dodd et al., 2005). Plants grown under light-dark conditions with a period matched to that of their circadian clock exhibit a higher chlorophyll content, greater carbon fixation, and higher growth and survival rates (Dodd et al., 2005). Additionally, it is now thought that a key advantage the clock confers is the ability to ration energy reserves throughout the night, breaking down starch at a steady rate so as to not run out before the anticipated dawn (Graf et al., 2010). Such anticipation of an environmental change provides an adaptive advantage by ensuring suitable allocation of metabolic efforts in preparation for the conditions ahead. However, little is known about the potential influence of the plant circadian clock below ground, and whether it may also modulate soil processes that also contribute to plant health.

1.2. The rhizosphere microbiome

1.2.1. The rhizosphere

Soils are incredibly diverse microbial habitats of great importance. A single gram of soil is estimated to contain up to approximately 9,000 different microbial species (Bardgett and van der Putten, 2014), and in the region of 10^9 prokaryotic cells alone (Torsvik et al., 2002). Bacteria, fungi, and archaea inhabit soil, in addition to protists, nematodes, and viruses. As early as the 19th century, it was known that soil microbiota are crucial in nutrient cycling and form relationships with plant roots (Hirsch and Mauchline, 2012). It is even thought that the most complex microbial communities on Earth can be found in soil ecosystems (Urich et al., 2008).

In particular, root-associated soil microbes, which comprise the rhizosphere microbiome (Figure 1.2), are highly abundant, functionally important, and show great genetic diversity (Roesch et al., 2007). The rhizosphere was first defined as “soil influenced by roots” in 1904 by the pioneering microbial ecologist Lorenz Hiltner (Hartmann et al., 2008). Hiltner was also the first to recognise that root exudation was involved in the recruitment of rhizosphere microbiota, and to link the rhizosphere microbiome with plant health (Hartmann et al., 2008). Due to the presence of plant roots, the rhizosphere contains more available carbon, and hence supports more microbial biomass, than the surrounding bulk soil (Fierer, 2017). It is estimated that up to 10^9 bacteria, 10^6 fungi, and 10^4 protists may be found in a gram of rhizosphere soil (el Zahar Haichar et al., 2014).

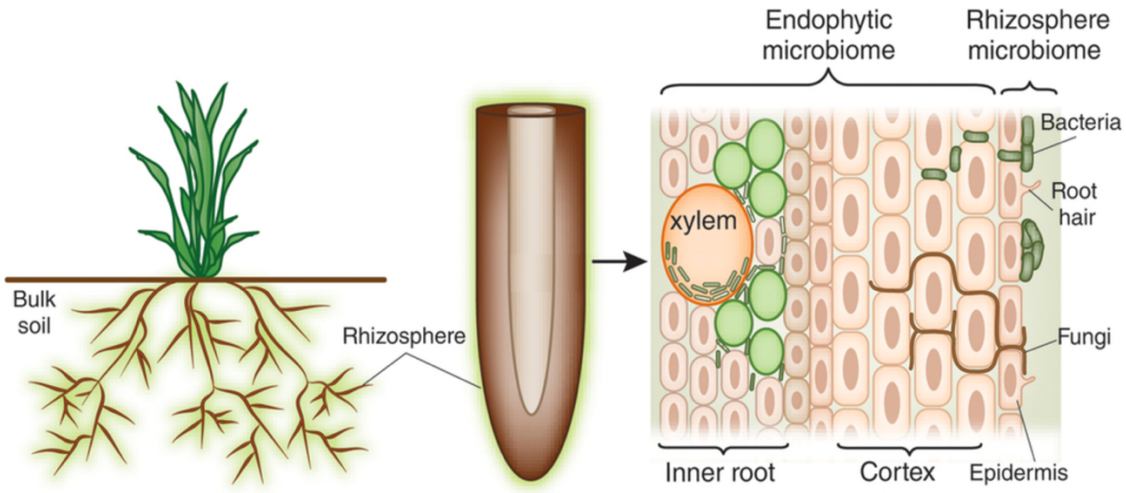

Figure 1.2. Diagram of the rhizosphere microbiome. Also shown is the proximity of the rhizosphere microbiome to the endophytic microbiome, which is comprised of only the microorganisms found living inside the root. From Hirsch and Mauchline, 2012.

Carbon enters the rhizosphere via rhizodeposition, the process by which material is released from roots into soil, subsequently acting as a nutrient source for rhizosphere microbiota (Philippot et al., 2013). Rhizodeposits are comprised of both root exudates and other material originating from plants, such as dead root cells (Philippot et al., 2013). Root exudates contain both low molecular mass compounds, such as sugars, amino acids, and secondary metabolites, and high molecular mass compounds, such as proteins or polymerised sugars in the form of mucilage (Badri and Vivanco, 2009). It has been estimated that 11% of net carbon fixed by plants ends up in rhizodeposits (Jones et al., 2009). As rhizodeposition is influenced by many plant- and soil-related biotic and abiotic factors (Jones et al., 2004), including plant species, it is almost impossible to provide one consistently applicable quantitative definition of the rhizosphere.

1.2.2. Rhizosphere microbiome interactions

The rhizosphere is a highly dynamic microbial habitat influenced by many other factors in addition to rhizodeposition (Table 1.2). Many of these, for example soil nutrient concentrations, may be influenced by plant roots themselves, and plants are also known to shape their rhizosphere microbiome to select for particular organisms (Doornbos et al., 2012). However, the community composition of the surrounding bulk soil microbiome is thought to be of greatest influence on rhizosphere microbiome composition (Bulgarelli et al., 2012; Lundberg et al.,

2012). While temporal variation in the rhizosphere microbiome has previously been characterised, work has focussed on changes over seasonal scales (Shi et al., 2015) and in relation to the development of plants (Chaparro et al., 2014). Additionally, the time of day at which samples are collected is not currently taken into account.

Table 1.2. Factors influencing the rhizosphere microbiome. Examples of factors which may influence the composition of the rhizosphere microbiome in addition to rhizodeposition, some of which may be moderated via resulting differences in rhizodeposition.

Factor	Examples	Reference
Biotic	Plant species	Kowalchuk et al., 2002
	Plant genotype	Micallef et al., 2009
	Plant developmental stage	Chaparro et al., 2014
	Plant immune system	Yu et al., 2019
	Chemical signals from other soil organisms	Lakshmanan et al., 2014
Abiotic	Soil water availability	Marasco et al., 2012
	Soil oxygen availability	Philippot et al., 2013
	Soil nutrient concentrations	
	Climate	
	Agricultural management	Schmidt et al., 2019

Just as plants play an important role in influencing the rhizosphere, the rhizosphere microbiome itself can also have important impacts on plants, many of which may be beneficial interactions (Table 1.3). The rhizosphere microbiome has been referred to as plants' "second genome" (Berendsen et al., 2012), as it is able to broaden the functional repertoire of plants (Bakker et al., 2013). Specific groups of rhizosphere microbiota also enter into symbiotic relationships with roots, which can be of particular importance to plant health. Approximately 80% of plant species host mycorrhizal fungi (Wang and Qiu, 2006), which colonise the rhizosphere and penetrate roots, receiving carbon from plants in return for providing nutrients they absorb from soil (Selosse and Roy, 2009). Rhizobial bacteria inhabit the roots of leguminous plants, converting atmospheric nitrogen into the ammonium, which can be utilised by plants (Igiehon and Babalola, 2018).

Table 1.3. Means by which the rhizosphere microbiome may influence plants.

Influence	Reference
Growth promotion	Lugtenberg and Kamilova, 2009
Plant productivity	Wagg et al., 2011
Nutrient acquisition	Philippot et al., 2013
Competitiveness and community diversity	Philippot et al., 2013
Vector for viral and nematode infection	Mendes et al., 2013
Alteration of physiology, e.g. metabolism and root growth	Vacheron et al., 2013
Tolerance of abiotic stress	Rodriguez et al., 2008
Production of regulatory compounds	Lakshmanan et al., 2014
Harbouring of pathogens	Mendes et al., 2013
Protection against soil-borne pathogens	Couillerot et al., 2009
Induction of systemic resistance	Van Loon et al., 1998

The rhizosphere microbiome has wider significance not only due to its influence on plants and therefore agricultural production, but also for its role in biogeochemical cycling. This is because, in addition to influencing nutrient acquisition by plants, rhizosphere microbiota also play an important role in the decomposition of soil organic matter and other chemical reactions, and therefore the cycling of nutrients through the environment (Philippot et al., 2013). Rhizosphere microbiota are vital in connecting above- and below-ground systems and biomass in both contexts (Philippot et al., 2013). Investigation of the composition and function of the rhizosphere microbiome, and factors which influence it, is therefore of great interest.

1.3. Circadian rhythms and the rhizosphere microbiome

1.3.1. The rhizosphere as a rhythmic environment

The circadian clock is present in plant roots, and it is thought to be a simplified version of that in shoots (James et al., 2008). Root and shoot clocks are synchronised when plants are under light-dark cycles, while under constant light and temperature conditions they become desynchronised and exhibit differences in period, phase and amplitude (James et al., 2008; Bordage et al., 2016). While the lower amplitudes and higher variability in periods generally observed in the

root circadian clock are thought to make rhythmicity in roots harder to detect, oscillations in the expression of *LHY*, *CCA1*, *PRR7*, *PRR9*, *TOC1*, and *GI* have been observed (James et al., 2008; Bordage et al., 2016).

Rhythmicity in plant roots may to some extent be directly entrained by light. Members of all five types of plant photoreceptors – phytochromes, cryptochromes, the ZTL family, phototropins, and UVR8 – are expressed in roots (Mo et al., 2015; Li et al., 2018). There is evidence that light piped from above ground is able to directly activate expression of phytochrome B in roots (Lee et al., 2016), and more recently it was proposed that the piping of light from shoots to roots entrains the root clock to light-dark cycles (Nimmo, 2018). There is also evidence that rhythms in roots are also influenced by other signals from the shoot. James et al. (2008) theorised that a photosynthesis-related signal from shoots synchronises the root circadian clock, and evidence from Takahashi et al. (2015) indicated the existence of a long-distance circadian signal between shoots and roots. Lee and Seo (2018) found that while circadian oscillations occur in an organ-specific manner, the root clock requires shoot-derived signals for the co-ordination of circadian activity across the whole plant, and Chen et al. (2020) determined that ELF4 regulates rhythms in roots by delivering a temperature-dependent signal and setting the pace of the root clock.

The plant circadian clock drives many processes which may contribute to the creation of a rhythmic environment in the rhizosphere. In particular, the fixation of carbon via photosynthesis is a rhythmic process, and the plant circadian clock is also involved in the allocation of this carbon, which may be transported, stored, or utilised in metabolism (Harmer et al., 2000). Starch turnover in roots has been demonstrated to follow diel patterns under light-dark cycles and is important for the maintenance of root growth, which also exhibits daily oscillations that peak around dawn and persist under constant conditions (Yazdanbakhsh et al., 2011). There is also evidence that the flux of carbon out of plants via root exudates oscillates over daily timescales. Iijima et al. (2003) found that the area of exudation from *Zea mays* (maize) roots was higher during dark periods and at its lowest during the middle of light periods. Diel oscillations in the presence of specific compounds within root exudates have also been reported. Badri et al.

(2010) found that while the exudation of the majority of compounds was constitutive in *A. thaliana* grown under light-dark cycles, genes involved in the synthesis of phenylpropanoid and glucosinolate secondary metabolites displayed diel expression patterns, with expression increasing during dark and decreasing during light periods. Further, when grown under light-dark cycles, quantities of the organic acid citrate within exudates of *Lupinus albus* (white lupin) and the flavonoid catechin in exudates of *Centaurea stoebe* (spotted knapweed) were observed to be higher during light periods (Watt and Evans, 1999; Tharayil and Triebwasser, 2010). A diel rhythm in the exudation of iron-bonding mugineic acids, with secretion occurring during light periods, was also reported in grasses deficient in iron (Ma and Nomoto, 1996). Additionally, while not related to diel cycles, Hughes et al. (1999) demonstrated that exposure to light increased concentrations of some flavonoids (polyphenolic secondary metabolites) in root exudates of *Alnus glutinosa* (black alder). As rhizodeposition is one of the key factors influencing the composition of rhizosphere microbial communities, such diel changes in root exudates may therefore lead to diel changes within the rhizosphere microbiome.

More recently, Staley et al. (2017) found that the abundance of many compounds within the *A. thaliana* rhizosphere differed in abundance between light and dark periods, providing further evidence that plants exhibit diel differences in rhizodeposition. Here, a higher number of compounds were observed to be more abundant in light-taken samples when compared to dark-taken samples than vice versa (Staley et al., 2017). Additionally, lipid-like compounds were observed to dominate dark-taken samples, while compounds with higher oxygen:carbon ratios, such as those likely to be flavonoids or organic acids, were more abundant in light samples (Staley et al., 2017). Evidence from a microbial perspective has also been gained, as Baraniya et al. (2018) identified diel differences in the activity of certain metabolic pathways in the *Hordeum vulgare* (barley) rhizosphere. From metatranscriptomic data, pre-dawn samples displayed significantly higher activities of pathways involved in the metabolism of amino acids, carbohydrates, cofactors and vitamins, and nucleotides than post-dawn samples (Baraniya et al., 2018). This indicates that rhizosphere microbiota may

respond to diel differences in the availability of energy sources exuded from plant roots.

Rhythmicity in plant processes which mediate plant-microbe interactions has already been demonstrated in relation to pathogens. (Zhang et al., 2013) determined that the *A. thaliana* circadian clock has a direct role in plant innate immunity, whereby plants are able to deploy nonspecific defence mechanisms against pathogens. The accumulation of jasmonates and salicylates, which are plant hormones involved in defence signalling, is known to be regulated by the circadian clock, with jasmonates peaking in the subjective day and salicylates in the subjective night (Goodspeed et al., 2012). Additionally, *A. thaliana* showed rhythmic susceptibility to the bacterium *Pseudomonas syringae* and the fungus *Botrytis cinerea*, where susceptibility was lower when infected in the morning, and this persisted under constant conditions (Bhardwaj et al., 2011; Hevia et al., 2015; Ingle et al., 2015).

Evidence of the influence of circadian clocks has been observed on both sides of rhythmic plant-pathogen interactions. *CCA1* and *LHY* are involved in *A. thaliana* defence mechanisms against *P. syringae* (Wang et al., 2011) and the oomycete pathogen *Hyaloperonospora arabidopsis* (Wang et al., 2011; Zhang et al., 2013). While the plant hormone jasmonic acid was found to be involved in bringing about rhythmic responses to *B. cinerea* infection (Ingle et al., 2015), interestingly, Hevia et al. (2015) identified a circadian clock within *B. cinerea* itself, which they determined to be primarily responsible for rhythmicity in disease severity.

Plant rhythmic defence against microbial pathogens therefore comprised the first body of evidence that the plant circadian clock is able to influence plant-microbe interactions. As the rhizosphere is an important entry site into plants for potentially pathogenic soil-borne microbes, roots are also able to detect the presence of pathogens, and induce innate immune responses (Chuberre et al., 2018). The plant circadian clock is likely also involved in defence processes within roots, providing another means by which rhythmic signals from the plant may influence rhizosphere microbiota.

Diel oscillations in several environmental parameters have also been observed in the rhizosphere. Ishikawa and Bledsoe (2000) characterised gradual increases in water potential of *Quercus douglasii* (blue oak) rhizosphere soil during the night and rapid decreases through the day.

Diel oscillations in pH were observed in *Lupinus albus* (white lupin) rhizosphere soil, where pH was highest during dark periods when under light-dark cycles, and these oscillations were found to correspond with patterns of root water uptake (Rudolph et al., 2013). Nutrient uptake by plants may also exhibit diel patterns (York et al., 2016), and it has been demonstrated that plant transpiration increases nutrient flow in soil (Matimati et al., 2014), indicating a potential mechanism for this. Additionally, as it is thought that light is able to pass through the top few millimetres of soil (Tester and Morris, 1987), environmental light-dark cycles may also be able to influence some of the rhizosphere microbiome directly. It is therefore possible that rhythmicity in the rhizosphere microbiome may also be brought about by these daily changes in the environmental conditions that microbiota in the rhizosphere face.

1.3.2. Microbial rhythmicity

A growing body of evidence exists for the presence of circadian oscillator components and circadian rhythmicity in fungi and prokaryotes, indicating that rhythmicity in the rhizosphere microbiome could be driven by autonomous oscillators possessed by rhizosphere microbiota.

The model Ascomycete fungus *Neurospora crassa* was one of the first organisms in which circadian clock components were identified, and much of what has been discovered about fungal circadian clocks since is also based on research on this model species (Baker et al., 2012). The core oscillatory components of the *N. crassa* circadian clock are FRQ (Frequency), and WC1 & 2 (White Collar 1 & 2). Briefly, WC1 and WC2 act together as the transcription factor WCC (White Collar Complex) and drive expression of *FRQ*, which peaks in the early morning (Baker et al., 2012). FRQ is then involved with the inactivation of the WCC later in the day (Baker et al., 2012).

Homologs of the FRQ and WCC proteins have now also been identified in other fungal species using *in silico* techniques, with homologs of at least one of the three being found in many other classes of fungi, including Agaricomycetes, Dothideomycetes, Eurotiomycetes and Leotiomycetes (Rodriguez-Romero et al., 2010; Salichos and Rokas, 2010), as well as in arbuscular mycorrhizal fungi (Lee et al., 2018). Interestingly, some species do not possess homologs of all three core genes but still exhibit rhythmic behaviour, suggesting the existence of a different oscillator mechanism (Rodriguez-Romero et al., 2010). For example, *Aspergillus flavus* does not possess *FRQ* but displays free-running rhythmicity in the formation of protective sclerotial structures, which is also temperature compensated at higher temperatures (Greene et al., 2003).

Few other fungi have been found to exhibit physiological rhythmicity which meets the criteria of true circadian rhythmicity. Asexual spore development of *N. crassa* is known to be controlled by its circadian clock and is easy to assay, which was in part why it was chosen as the primary model for investigation of the fungal circadian clock (Liu and Bell-Pedersen, 2006). Other examples of fungal rhythms which persist under constant conditions are the spore discharge of *Sordaria fimicola* (Austin, 1968), virulence of *B. cinerea* (Hevia et al., 2015), melanisation of hyphae in *Cercospora kikuchii* (Bluhm et al., 2010), and bioluminescence of *Neonothopanus gardneri* (Oliveira et al., 2015), the latter two of which also display temperature compensation. Additionally, while not proven to be endogenous rhythmicity, diel variability in fungal morphology has also been observed *in situ*: Hernandez and Allen (2013) observed diel growth of arbuscular mycorrhizal fungi in soil under environmental conditions, with the highest rates of growth and dieback observed late in the day.

It was previously believed that prokaryotic organisms could not possess such a complex mechanism as a circadian clock (Johnson et al., 2011). However, circadian clocks are now well-characterised in cyanobacteria, including some of the most abundant photosynthetic species in the planet's oceans (Johnson et al., 2011). In addition to gene expression, the cyanobacterial circadian clock is known to regulate the timing of chromosome compaction and cell division (Cohen and

Golden, 2015). In the model cyanobacterium *Synechococcus elongatus* PCC 7942, the circadian clock is formed of a post-translational oscillator containing the three core proteins KaiA, KaiB and KaiC (Cohen and Golden, 2015). This cyanobacterial clock does not sense light directly, instead perceiving the redox and energy state of cells, and operates via cycles of phosphorylation of KaiC (Cohen and Golden, 2015).

Homologs of cyanobacterial KaiB and KaiC proteins have been discovered in non-photosynthetic bacteria, suggesting the possible existence of Kai-based timing mechanisms outside the Cyanobacteria (Dvornyk et al., 2003; Loza-Correa et al., 2010; Schmelling et al., 2017). Homologues of *kaiB*, *kaiC* and their corresponding proteins have been identified within genomes from several bacterial phyla, namely Bacteroidetes, Chloroflexi, Planctomycetes, Chlamydiae, Acidobacteria, Verrucomicrobia, and a particularly high number of Proteobacteria (Dvornyk et al., 2003; Loza-Correa et al., 2010; Schmelling et al., 2017). This high abundance in the Proteobacteria may however be due to a higher number of genomes available for analysis rather than a greater proportion of genomes containing these homologues. It is hypothesised that bacteria possessing KaiB and KaiC but not KaiA may have some form of "hourglass"-type timing mechanism, which resets daily but is not truly a circadian oscillator (Ma et al., 2016; Schmelling et al., 2017).

There is very limited evidence for physiological rhythmicity in non-photosynthetic bacteria which exhibits any truly circadian properties. Soriano et al. (2010) demonstrated that *Pseudomonas putida*, which inhabits soil and can interact with plant roots, exhibits rhythmic rings of growth on agar. Under light-dark cycles, *P. putida* growth showed a period of ~24 hours, which was also observed for up to two cycles under constant darkness (Soriano et al., 2010). Paulose et al. (2016) provide the most robust report of bacterial circadian rhythmicity, in *Enterobacter aerogenes*, which inhabits the human intestine. In the presence of the hormone melatonin, *E. aerogenes* displayed rhythmicity in its swarming behaviour, which was temperature compensated (i.e. displayed a consistent period length over a range of temperatures) and persisted under constant conditions for four cycles (Paulose et al., 2016). Additionally, while not proven to be endogenous

rhythmicity, Hörnlein et al. (2018) characterised rhythmicity in some gene transcripts from Proteobacteria and Firmicutes as well as Cyanobacteria within a marine microbial mat growing under environmental conditions.

Very little is therefore known about potential circadian rhythmicity of both fungi and non-photosynthetic bacteria within microbial habitats in the environment. It has been speculated that the importance and functionality of circadian clocks or clock-like timekeeping mechanisms in microbes may only be revealed via *in situ* studies of the complex environments they reside in, as opposed to culture-based approaches alone (Sartor et al., 2019). Sartor et al. (2019) also suggest that even non-photosynthetic microbes may experience evolutionary pressure to develop timekeeping mechanisms due to zeitgeber cycles within their environment. The ideas of Sartor et al. (2019) are reinforced by the 'Choir-Choirmaster' theory proposed by Hörnlein et al. (2018) concerning rhythmicity in marine microbial mats. Hörnlein et al. (2018) proposed that rhythmicity in community members known to have a truly autonomous circadian clock may serve as a zeitgeber for other members whose timekeeping mechanisms may only be entrained by a combination of cues, including photosynthate and metabolites from those photosynthetic members.

Soriano et al. (2010) suggested that a circadian clock could be advantageous for bacteria colonising plant surfaces, as it could allow them to anticipate alterations in resource availability, which could be caused by the plant's own rhythms, or oscillations in light and temperature conditions. Similarly, Lee et al. (2019) argued, in the context of arbuscular mycorrhizal fungal specifically, that considering the circadian clocks of plants and their associated microbes in the context of their symbioses may lead to a greater understanding of temporal organisation in both. These studies therefore highlight the importance of adopting a holistic approach and studying complex environments *in situ* in order to characterise rhythmic microbial behaviour.

1.3.3. Circadian influences on the rhizosphere microbiome

A small number of existing published works have examined the interaction between the plant circadian clock and the rhizosphere microbiome, and characterised diel changes in the rhizosphere microbiome (Hubbard et al., 2017; Staley et al., 2017; Baraniya et al., 2018). All these previous studies were based upon the molecular characterisation of rhizosphere microbial communities (Hubbard et al., 2017; Staley et al., 2017; Baraniya et al., 2018).

It has been demonstrated that the plant circadian clock influences the assembly of the rhizosphere microbiome after a period of plant growth. Evidence for this was gained by Hubbard et al. (2017) and Staley et al. (2017), who characterised DNA extracted from the *A. thaliana* rhizosphere to profile the bacterial communities present. Loss-of-function of the plant circadian clock genes *toc1* and *ztl* were found to influence overall community composition of the bacterial component of the rhizosphere microbiome (Hubbard et al., 2017). Loss of *toc1* function was also found to influence bacterial alpha diversity, which takes into account the number of unique species present in addition to the equality in their abundances. Hubbard et al. (2017) also demonstrated the potential influence of the plant circadian clock upon the recruitment of a rhizosphere microbiome which contributes to plant health. Wild-type plants grown in soil which previously harboured plants with *toc1* or *ztl* loss-of-function grew smaller and took longer to germinate (Hubbard et al., 2017).

Diel changes in both the composition and transcriptomic activity of the rhizosphere microbiome have also been characterised in the model organisms *A. thaliana* and *Brachypodium distachyon* and the crop plant *H. vulgare* (Hubbard et al., 2017; Staley et al., 2017). Significant differences in overall bacterial community composition were observed between light- and dark-collected samples of wild-type *A. thaliana* (Hubbard et al., 2017; Staley et al., 2017). Staley et al. (2017) found that OTUs which significantly differed in their relative abundance between light- and dark-collected samples accounted for ~13 – 18% and ~8 – 10% of bacterial communities by relative abundance from bulk soil and *A. thaliana* rhizosphere samples respectively. Additionally, OTUs which significantly differed in their relative abundance between light- and dark- collected

samples accounted for ~11% of bacterial communities by relative abundance in the *B. distachyon* rhizosphere (Staley et al., 2017). Hubbard et al. (2017) also observed that the proportional changes found in the relative abundance of individual OTUs between light- and dark-taken *A. thaliana* rhizosphere samples were relatively consistent on both of the two days over which sampling took place. Diel variation in the rhizosphere microbiome was also observed at other taxonomic levels. Bacterial families which exhibited 'cycling dynamics' in their relative abundance were also identified within 6-hourly rhizosphere samples of *A. thaliana* grown under light-dark cycles (Staley et al., 2017). These cycling families accounted for differing proportions of microbial communities from different samples: ~13% of the community from the wild-type *A. thaliana* rhizosphere, ~1% of that from bulk soil, and ~4% of that from the rhizosphere of plants overexpressing *CCA1*. Additionally, Baraniya et al. (2018) demonstrated that the transcriptional activity of some microbial orders in the *H. vulgare* rhizosphere, namely the protist order Plasmodiophorida and the bacterial orders Burkholderiales, Caulobacterales, Rhizobiales, Sphingomonadales, and Xanthomonadales, significantly differed between pre- and post-dawn sampling points.

However, it is not known whether the plant circadian clock influences these diel changes observed in the rhizosphere microbiome, or whether they display spatial heterogeneity. For example, the majority of exudation from roots occurs at the growing tip (Canarini et al., 2019) and higher microbial populations are found in its vicinity (Massalha et al., 2017) so rhythmicity could be localised to, or more pronounced in, rhizosphere soil adjacent to this region. The rhythmicity of microbiota could also vary with their proximity to roots, with rhizosphere soil closer to roots potentially receiving more exudation and containing a higher amount of rhythmic microbes. Additionally, the mechanisms causing rhizosphere microbial diel changes are unknown, and the relative importance of potential drivers, such as light-dark cycles, the plant circadian clock, or autonomous microbial clocks, have not been investigated. There is also much scope to further explore the implications of circadian interactions in the rhizosphere microbiome for plant health, and the recruitment of particular groups of rhizosphere-inhabiting microbial taxa.

1.3.4. Thesis aims

In Chapter 2, we conducted the molecular characterisation of rhizosphere microbial communities from *Arabidopsis thaliana* mutants with abnormal circadian clocks in order to:

1. Determine whether the plant circadian clock influences the recruitment of microbiota into the rhizosphere.
2. Determine whether diel changes in the composition of the rhizosphere microbiome are influenced by the plant circadian clock.

In Chapter 3, we transferred *A. thaliana* wild-type and mutant plants to constant conditions and conducted sampling at a higher time resolution. The molecular characterisation of rhizosphere microbial communities was conducted in order to:

1. Determine whether microbial rhythmicity in the rhizosphere microbiome persists under constant conditions.
2. Test whether this rhythmicity is dependent on the plant circadian clock or upon autonomous microbial oscillators.
3. Investigate the relationship between microbial rhythmicity in the rhizosphere microbiome and the possession of homologues of known circadian clock components.

In Chapter 4, we developed a model system and non-invasive imaging method to monitor bacterial populations in the *Brassica rapa* rhizosphere with high time resolution. This allowed us to:

1. Determine whether *P. fluorescens* SBW25::*luxCDABE* displays rhythmic luminescence in the rhizosphere.
2. Determine whether the plant circadian clock influences rhythmic luminescence of *P. fluorescens* SBW25::*luxCDABE* in the rhizosphere.
3. Determine whether rhythmic bioluminescence of *P. fluorescens* SBW25::*luxCDABE* is due to oscillations in cell abundance or *lux* gene expression.

CHAPTER 2: THE PLANT CIRCADIAN CLOCK INFLUENCES RHIZOSPHERE MICROBIOME ASSEMBLY AND DIEL CHANGES

2.1. Introduction

2.1.1. Introduction

It has been demonstrated that the plant circadian clock influences the assembly of the rhizosphere microbiome (Hubbard et al., 2017; Staley et al., 2017). Diel changes in the composition and transcriptomic activity of the rhizosphere microbiome have also been observed (Hubbard et al., 2017; Staley et al., 2017; Baraniya et al., 2018). All previous investigations concerning circadian influences upon the rhizosphere microbiome have utilised molecular approaches.

Hubbard et al. (2017) demonstrated that the plant circadian clock components *toc1* and *ztl* influence the overall composition of bacterial communities within the *Arabidopsis thaliana* rhizosphere microbiome. Evidence was also found that *toc1* influences bacterial alpha diversity (Hubbard et al., 2017), which takes into account the number of species present and the equality in their abundances. Additionally, Staley et al. (2017) found that OTUs which significantly differed in their relative abundance between wild-type *A. thaliana*, bulk soil, and plants overexpressing the clock gene *CCA1* formed approximately 70% of bacterial communities. This indicated that the plant circadian clock influences the relative abundance of many microbial community members which are recruited into the rhizosphere microbiome.

Diel changes in rhizosphere microbial communities have been demonstrated in wild-type *A. thaliana*, *Hordeum vulgare* (barley), and the model grass *Brachypodium distachyon* (Hubbard et al., 2017; Staley et al., 2017). Both Hubbard et al. (2017) and Staley et al. (2017) observed significant differences in overall bacterial community composition between light- and dark-collected wild-type *A. thaliana* samples. Staley et al. (2017) also found that OTUs which significantly differed in their relative abundance between light- and dark-collected

samples accounted for ~13 – 18% and ~8 – 10% of bacterial communities by relative abundance from bulk soil and *A. thaliana* rhizosphere samples respectively. Additionally, OTUs which significantly differed in their relative abundance between light- and dark- collected samples accounted for ~11% of bacterial communities by relative abundance in the *B. distachyon* rhizosphere (Staley et al., 2017). Further work by Staley et al. (2017) characterised bacterial families which were deemed to display 'cycling dynamics' under light-dark cycles when sampled every 6 hours. These cycling families formed ~13% of the community from the wild-type *A. thaliana* rhizosphere, ~1% of the bulk soil community, and ~4% of the community from the rhizosphere of plants overexpressing *cca1*. Additionally, Baraniya et al. (2018) found that the transcriptional activity of some microbial metabolic pathways and bacterial and protist orders in the *H. vulgare* rhizosphere significantly differed between pre- and post-dawn sampling points. While Hubbard et al. (2017), Staley et al. (2017) and Baraniya et al. (2018) characterised diel variation in the rhizosphere microbiome, the possibility that plant circadian clock dysfunction may also alter these diel changes was not investigated.

2.1.2. Aims

The aims of this work were to:

1. Determine whether dysfunction of the plant circadian clock influences the recruitment of microbiota into the rhizosphere
2. Determine whether diel changes in the composition of the rhizosphere microbiome are influenced by the plant circadian clock

2.1.3. Experimental design

In order to address the aims of this work, we investigated the rhizosphere microbiome of two *A. thaliana* lines with mutations in the core circadian clock gene *LHY*: *lhy-11* and *lhy-ox*. As each displays different circadian phenotypes, investigating these mutants would allow us to determine whether each form of dysfunction brought about different effects on the rhizosphere microbiome. This is because it was already demonstrated by Hubbard et al. (2017) that mutant plants with different circadian phenotypes, namely the short period *toc1-21*

mutant and the long period *ztl-30* mutant, which display loss-of-function of the circadian clock genes *toc1* and *ztl* respectively, contained significantly different rhizosphere communities. Under constant conditions, plants with *lhy* loss-of-function (*lhy-11*) display a short circadian period (approximately 2 – 3 hours shorter) relative to wild-type plants, while under light-dark cycles, a phase advance was demonstrated in plants with *lhy* loss-of-function (Green and Tobin, 1999; Mizoguchi et al., 2002). Contrastingly, *lhy-ox* plants constitutively express the *LHY* gene throughout the day at levels close to the maximum of *LHY* expression in wild-type plants (Green et al., 2002). Under constant conditions, the circadian clock of *lhy-ox* plants is arrhythmic (Schaffer et al., 1998). However, under light-dark cycles, driven rhythms initiated by switches from dark to light conditions are observed in *lhy-ox* mutants, but these plants are incapable of anticipatory behaviour (Kim et al., 2003). While both display a period of 24 hours under light-dark cycles, the abnormal timing of rhythmic processes in these *lhy* mutants could lead to the altered timing of rhythmicity in the rhizosphere microbiome. Additionally, because *LHY* influences output pathways such as metabolism and immune responses (Graf et al., 2010; Zhang et al., 2013), processes such as root exudation may be altered in these *lhy* mutants. This could also lead to altered patterns of rhythmicity in the rhizosphere microbiome or, over the course of plant growth, different microbiota being recruited into the rhizosphere.

We decided to investigate circadian influences upon the rhizosphere microbiome by profiling both DNA and RNA from the microbial communities present, in order to determine whether the examination of RNA could prove a more sensitive approach to detect microbial rhythmicity. These approaches have not previously been compared, as Hubbard et al. (2017) and Staley et al. (2017) both characterised DNA extracted from the rhizosphere microbiome only, while Baraniya et al. (2018) used a metatranscriptomic approach to characterise total rhizosphere mRNA. The profiling of DNA present in samples allows the characterisation of all taxa which accumulate in the rhizosphere over the lifetime of plants, including dead, dormant and live members (Emerson et al., 2017). Contrastingly, RNA is less stable and its profiling has been used to identify microbiota transcribing their rRNA genes in order to detect the so-called ‘active’

members of microbial communities (Duineveld et al., 2001; Gaidos et al., 2011; Blazewicz et al., 2013; Kang et al., 2013; Emerson et al., 2017; De Vrieze et al., 2018), and thus it may present a more sensitive approach to detect changes in microbial growth and activity compared to community profiling using DNA. As per previous studies which used both approaches (De Vrieze et al., 2018; Li et al., 2019; Nawaz et al., 2019), communities identified from the characterisation of microbial DNA will henceforth be referred to as 'total communities' while those identified based upon the characterisation of RNA, which signifies gene transcription, will be referred to as 'active communities'.

Additionally, our current understanding of diel variability in the rhizosphere microbiome is based almost entirely upon bacterial communities (Hubbard et al., 2017; Staley et al., 2017; Baraniya et al., 2018). However, many other groups of microorganisms inhabit the rhizosphere and fungi in particular are a key component of the rhizosphere microbiome. Rhizosphere fungi play important roles as endophytic symbionts, pathogens, antagonists of pathogens and by contributing to biogeochemical cycles (Raaijmakers et al., 2009; Bardgett and van der Putten, 2014). Fungi are also of interest because many fungal species are known to possess circadian clocks (Salichos and Rokas, 2010) and therefore fungal rhythms could potentially be synchronised with plant rhythms in the rhizosphere. In this study we therefore sought to profile the responses of both bacterial and fungal communities within the rhizosphere microbiome.

2.2. Methods

2.2.1. Plant growth and sampling

Wild-type L*er* (Landsberg *erecta* ecotype) and *lhy-11* and *lhy-ox* mutant *A. thaliana* plants were used in this study.

All plants were grown in Wick series sandy loam soil (16.3% clay, 16.6% silt and 67.1% sand; Whitfield, 1974) which was sampled from a depth of 0-20 cm at Cottage Field West, University of Warwick Wellesbourne Campus, UK. The soil has a carbon content of 0.9 % and a pH of 6.8 (Whitfield, 1974), and was determined to have a mean moisture content of 12.3%. Soil was collected at the

margins of an oilseed rape crop in October 2016. Following sampling, all soil was homogenised by passage through a 3 mm sieve.

lhy-11, *lhy-ox* and wild-type seeds were planted in modular pots then grown for 8 weeks in a Sanyo Versatile Environment Test Chamber MLR-350 growth cabinet (Sanyo, Moriguchi, Japan). Each genotype was grown in a separate tray, with up to four plants occupying each modular pot. To minimise the effects of cabinet position on plants, trays were rotated and their position changed daily. Plants were watered as required to maintain the original moisture content of the soil, experienced 12L:12D lighting cycles at 22°C, and received 54 – 100 μmol/m^2/sec of light (dependent on position within the cabinet) as measured by a light meter which quantified photosynthetically active radiation (Skye Instruments, Llandrindod, UK). As they grew, we noted that while the speed of growth and overall visual appearance of the *lhy-11* mutant seedlings were indistinguishable from the wild-type plants, *lhy-ox* seedlings were markedly slower to grow and displayed a severely altered growth phenotype whereby plants' overall biomass was notably lower, including both smaller leaves and root systems.

Sampling was conducted at two time points on one day, at dawn and dusk (12 hours after dawn). Plants from at least two modular pots were combined to form a single sample containing 3 or 4 plants, and seven such replicate samples were taken at each sampling point. Plants were carefully removed from their pots and non-adhering soil was gently brushed off root systems using tweezers, and then roots were cut from the shoot just below the stem. This resulted in a composite rhizosphere sample which included microbes inside roots, on their surface, and in the closely root-adhering soil. These samples will henceforth be referred to as "rhizosphere samples". Samples of bulk soil were also taken at each time point from pots kept under the same conditions but containing only soil. This was performed by sampling 0.5 g of soil from approximately 1 cm below the surface, discarding the uppermost layer. All samples were put into Lysing Matrix E tubes (MP Biomedicals, Irvine, USA) and immediately frozen in liquid nitrogen then transferred to -80 °C.

2.2.2. Microbial community profiling

2.2.2.1. Nucleic acid extraction and cDNA generation

Both DNA and RNA were extracted from rhizosphere and bulk soil samples. Nucleic acids were co-extracted using a modified version of a protocol by Griffiths et al. (2000). 450 *µ*l each of phenol-chloroform-isoamyl alcohol (25:24:1) and extraction buffer were added to each sample tube. The extraction buffer was comprised of equal volumes of 12% CTAB (hexadecyltrimethylammonium bromide) in 0.7 M NaCl and 240 mM potassium phosphate buffer. Samples were lysed using a FastPrep-24™ homogeniser (MP Biomedicals, Irvine, USA) for 30 seconds at a speed of 5.5 m s^{-1}, and then the aqueous phase containing nucleic acids was separated by centrifugation at 16,000 *g* for 5 minutes at 4 °C. An equal volume of chloroform-isoamyl alcohol (24:1) was added to the aqueous phase, and another short centrifugation step conducted in order to remove phenol from the sample. To precipitate total nucleic acids, two volumes of 30% PEG (polyethylene glycol) in 1.6 M NaCl were added, along with 5 *µ*l of glycogen to aid the formation of a visible nucleic acid pellet, and samples were incubated at room temperature for 2 hours. A centrifugation step at 17,200 *g* for 20 minutes at 4 °C was then conducted to form nucleic acid pellets, which were then washed using 1000 *µ*l ice-cold 70% ethanol, followed by another centrifugation step at 17,200 *g* for 10 minutes at 4 °C. All ethanol was then removed and the pellets air-dried at room temperature. The resultant nucleic acid pellets were resuspended in 50 *µ*l of sterile nuclease-free water.

Concentrations of DNA and RNA in the samples were checked with an Invitrogen Qubit fluorometer 2.0 (Thermo Fisher Scientific, Waltham, USA) using the broad range DNA and high sensitivity RNA assays. 5 *µ*l of the eluted nucleic acids were diluted to a concentration of 5 ng/*µ*l using sterile nuclease-free water and set aside for DNA amplicon sequencing, and 44 *µ*l were used to generate cDNA from the extracted RNA. Two additional extractions were also performed at this stage, using empty Lysing Matrix E tubes. These samples were used as negative controls throughout the library preparation process and during MiSeq sequencing.

Samples to be used for RNA were treated with DNAse I using the DNAse Max Kit (MO Bio, Carlsbad, USA) according to the manufacturer's instructions, where each reaction contained 10 units of the DNAse I enzyme and 11 μl of the original RNA sample. To confirm that all DNA was removed from the samples, PCRs were conducted using non-modified primers for the 16S rRNA V4 region (detailed in Section 2.2.2.2). In these confirmatory PCRs, the following volumes of reagents were used: 12.5 μl Q5 High Fidelity 2X Readymix (New England Biolabs, Hitchin, UK), 1 μl forward primer (10 μM), 1 μl reverse primer (10 μM), 9 μl sterile nuclease-free water, and 1 μl DNAse-treated RNA. The reaction was conducted under the following conditions: denaturation at 94 °C for 5 minutes; 25 cycles of denaturation at 94 °C for 30 seconds, annealing at 50 °C for 30 seconds, elongation at 72 °C for 30 seconds; elongation at 72 °C for 5 minutes. PCR products were added to a 1% agarose gel and run at a voltage of 100 V for 20 minutes before visualisation under ultraviolet light using a transilluminator.

After confirming that all DNA was removed, cDNA was then generated from the DNAse-treated RNA using the SuperScript III Reverse Transcriptase kit (Invitrogen brand, Thermo Fisher Scientific, Waltham, USA) and RNAse OUT ribonuclease inhibitor (Invitrogen brand, Thermo Fisher Scientific, Waltham, USA) according to the manufacturer's instructions. Random hexamers and oligo(dT) were used at the first incubation step. To confirm that cDNA was present, PCRs and gel electrophoresis were conducted again.

2.2.2.2. Library preparation

PCR amplification of the target bacterial 16S rRNA and fungal Internal Transcribed Spacer (ITS) regions of both DNA and cDNA samples was conducted. The V4 region of the 16S rRNA gene was amplified using the 515f/806r primers (515f: 5' GTG CCA GCM GCC GCG GTA A 3', 806r 5' GGA CTA CHV GGG TWT CTA AT 3'; Caporaso et al., 2011) and the ITS2 region of the ITS gene was amplified using the 3f/4r primers (3f: 5' GCA TCG ATG AAG AAC GCA GC 3', 4r: 5' TCC TCC GCT TAT TGA TAT GC 3'; White et al., 1990). These primers were modified at the 5' end with the following Illumina adaptors:

forward adaptor TCG TCG GCA GCG TCA GAT GTG TAT AAG AGA CAG; reverse adaptor GTC TCG TGG GCT CGG AGA TGT GTA TAA GAG ACA G.

In these PCRs the final volumes of reagents were 12.5 μl Q5 High Fidelity 2X Readymix, 1.25 μl forward primer (10 μM), 1.25 μl reverse primer (10 μM), 5 μl sterile molecular grade water, and 5μl template DNA or cDNA. For amplification of the 16S rRNA V4 region, the following cycling conditions were used: denaturation at 98 °C for 30 seconds; 25 cycles of denaturation at 98 °C for 10 seconds, annealing at 50 °C for 15 seconds, elongation at 72 °C for 20 seconds; elongation at 72 °C for 5 minutes. For amplification of the ITS2 region, the following cycling conditions were used: denaturation at 98 °C for 30 seconds; 35 cycles of denaturation at 98 °C for 10 seconds, annealing at 57 °C for 15 seconds, elongation at 72 °C for 20 seconds; elongation at 72 °C for 5 minutes.

The products from these PCRs were purified using Agencourt AMPure XP beads (Beckman Coulter, High Wycombe, UK) according to the manufacturer's instructions. A second round of PCRs then took place for library preparation using short Illumina Nextera index primers, in order to multiplex the samples ready for pooling and sequencing. Indexing PCRs included 13 μl Q5 High Fidelity 2X Readymix, 4 μl sterile nuclease-free water, 2.5 μl Index primer 1 (10 μM), 2.5 μl Index primer 2 (10 μM), and 4 μl amplified PCR product (from initial amplicon PCR). The following reaction conditions were used: denaturation at 95 °C for 3 minutes; 8 cycles of denaturation at 98 °C for 20 seconds, annealing at 55 °C for 15 seconds, elongation at 72 °C for 15 seconds; elongation at 72 °C for 5 minutes.

Following the addition of indexing primers, all samples were processed using the SequalPrep Normalisation Kit (Invitrogen brand, Thermo Fisher Scientific, Waltham, USA) according to the manufacturer's instructions. This ensured that the final PCR product was purified and that the DNA and cDNA from each sample were equalised to 25 ng. All samples were then combined, and the resultant pooled samples diluted to 4 nM. Sequencing of 300 bp paired-end reads was then performed on an Illumina MiSeq machine (Illumina, San Diego, USA) at the University of Warwick Genomics Facility, Coventry, UK.

2.2.3. Processing of amplicon sequencing data

Raw sequences were automatically de-multiplexed by the Illumina MiSeq machine. Low-quality bases were removed from the ends of sequences using Trimmomatic v0.36 (Bolger et al., 2014). USEARCH 9 (Edgar, 2010) was used to join paired-end reads, conduct quality filtering, trim off primer sequences, and dereplicate the data to determine the number of unique sequences. USEARCH 9 was also used to cluster the reads into Operational Taxonomic Units (OTUs) – groups with ≥97% sequence similarity – and conduct chimera filtering. QIIME (Quantitative Insights Into Microbial Ecology) 1.9.1 (Caporaso et al., 2010) was used to assign taxonomy to the OTUs, using version 13.8 of the GreenGenes database (DeSantis et al., 2006) for the 16S rRNA gene data and version 7.0 of the UNITE database (Kõljalg et al., 2005) for the ITS data. Filtering was undertaken using QIIME 1.9.1 to remove reads that were annotated as mitochondria or chloroplasts in the 16S rRNA gene dataset. Additionally, the ITS dataset was manually investigated for *A. thaliana* sequences known to be mis-annotated as fungal taxa, and these were removed.

All subsequent analyses were conducted in R Studio (running R Version 3.6.0). Data were first normalised using the DESeq2 package (Love et al., 2014), which also removed samples with under 1000 reads and OTUs with 0 reads. OTUs present in under 10% of samples were manually removed.

Raw sequence files were uploaded to the NCBI (National Centre for Biotechnology Information) Sequence Read Archive (https://www.ncbi.nlm.nih.gov/sra) under the BioProject accession number PRJNA675000. Nucleotide sequences of the highly abundant plant pathogenic fungal OTUs identified were uploaded to the NCBI GenBank (https://www.ncbi.nlm.nih.gov/genbank/) under submission number SUB8478023.

2.2.4. Statistical analyses

To investigate whether altered function of the plant circadian clock influences the assembly of the rhizosphere microbiome, data from the dawn and dusk sampling

points were combined and microbial communities compared between wild-type, *lhy-11* and *lhy-ox* plants. Bray-Curtis dissimilarity matrices (Bray and Curtis, 1957), which account for both presence-absence and relative abundance of OTUs, were generated and used to conduct ANOSIM (Analysis of Similarity) (Clarke, 1993) and create NMDS (Non-Metric Multidimensional Scaling) (Minchin, 1987) plots to investigate beta diversity, which compares the assemblages of species present in different sample groups. Alpha diversity, which indicates the diversity of species present in a given sample, was calculated using Shannon's Index (Shannon, 1948), using the vegan package in R (Oksanen et al., 2007). Alpha diversity takes into account both the number of OTUs present in each sample (also known as species richness) and the equitability in their abundances (species evenness). Species evenness was calculated using Shannon's Equitability Index (Sheldon, 1969) and species evenness was determined by calculating the mean numbers of OTUs found within samples. The FUNGuild annotation tool (Nguyen et al., 2016) was used to parse fungal OTUs into relevant ecological 'guilds' or functional groups. The FUNGuild output was manually curated to ensure only contextually relevant guilds (arbuscular mycorrhizal fungi, endophytes, fungal parasites, plant pathogens and saprotrophs) were considered. The relative abundances of rhizosphere taxa (bacterial phyla and fungal classes) and fungal guilds were compared using Kruskal-Wallis tests, followed by pairwise Wilcoxon rank sum tests for multiple comparisons. For all analyses, fungi were investigated at the class level due to low numbers of fungal phyla present and the domination of samples by Ascomycota.

To investigate diel changes in the composition of the rhizosphere microbiome and whether these are influenced by the plant circadian clock, the two time points were compared for each sample type. ANOSIM was used to determine whether the overall composition of microbial communities significantly differed between dawn and dusk samples. Kruskal-Wallis pairwise testing was used to compare microbial alpha diversity and the relative abundances of fungal ecological guilds, bacterial phyla, fungal classes, and individual microbial OTUs, between dawn and dusk samples. The rhythmic OTUs we identified, which displayed significant

differences in their relative abundance between dawn and dusk samples, were then compared across sample types.

2.3. Results

We sought to investigate whether 1). dysfunction of the plant circadian clock influences the recruitment of microbiota into the rhizosphere and 2). whether diel changes in the composition of the rhizosphere microbiome are influenced by the plant circadian clock. To do this, we collected rhizosphere samples from wild-type, *lhy-11* and *lhy-ox A. thaliana* plants at dawn and dusk on a single day and conducted amplicon sequencing to characterise the bacterial and fungal communities present.

A total of 24,094,802 raw reads were obtained from the MiSeq run. After all pre-processing was complete, 1,859,738 reads were obtained for the bacterial (16S rRNA gene V4 region) amplicon, and 1,722,782 reads were obtained for the fungal (ITS2 region) amplicon. A range of 11 – 58,904 raw reads with an average of 16,032 per sample were obtained for the 16S rRNA gene, and a range of 11 – 44,528 with an average of 5,836 per sample were obtained for the ITS region. After DESeq2 normalisation, where samples with under 1,000 reads and OTUs with 0 reads were removed, 4,392 OTUs and 53 of the original 56 samples remained in the data from total bacterial communities, 4,096 OTUs and 44 samples remained in the data from active bacterial communities, 488 OTUs and 47 samples remained in the data from total fungal communities, and 183 OTUs and 44 samples remained in the data from active fungal communities.

2.3.1. Dysfunction of the plant circadian clock influences the recruitment of microbiota into the rhizosphere

We investigated whether dysfunction of the plant circadian clock influences the assembly of the rhizosphere microbiome by comparing rhizosphere samples from wild-type *A. thaliana* with those from plants with *lhy* loss-of-function and overexpression. While sampling was conducted at two time points on a single day, we found that in both total and active bacterial and fungal communities, overall community composition and alpha diversity did not significantly differ

between the dawn and dusk samples (Table A2.1; Table A2.2). We therefore combined the data from the two time points for all analyses investigating the influence of the plant circadian clock upon the assembly of the rhizosphere microbiome.

2.3.1.1. Community composition and diversity

We compared the overall community composition of wild-type, *lhy-11* and *lhy-ox* rhizosphere samples using NMDS plots and ANOSIM analyses based on Bray-Curtis dissimilarities, which are used to represent the dissimilarity between populations of species from different sample groups. We also used Shannon's Index to assess for differences in microbial alpha diversity between samples. Alpha diversity indicates the diversity of microbial species present within a given habitat and takes into account both the number of OTUs present in each sample (also known as species richness) and the equitability in their abundances (species evenness). Species richness and evenness were also quantified separately, using mean numbers of OTUs and Shannon's Equitability Index respectively.

The overall composition of the total and active bacterial, and total fungal, communities of *lhy-11*, *lhy-ox* and wild-type plant rhizosphere samples all were significantly dissimilar from bulk soil (Figure 2.1; Table 2.1), confirming that a distinct rhizosphere compartment was present as anticipated. While no significant differences in community composition were found between wild-type and *lhy-11* or *lhy-ox* samples within total and active bacterial, or active fungal, communities, *lhy-ox* and wild-type plant rhizospheres displayed significant dissimilarity between their total fungal community composition (Figures 2.1.e and 2.1.f; Table 2.1). Additionally, *lhy-11* and *lhy-ox* rhizosphere samples also contained significantly dissimilar active bacterial and total fungal communities to each other (Figures 2.1.c to 2.1.f; Table 2.1). The altered community composition observed in *lhy-ox* plants relative to wild-type and *lhy-11* therefore indicates that the overexpression of *lhy* influenced the composition of total fungal communities within the rhizosphere microbiome while the lack of *lhy* expression did not have an effect. As more significant differences were observed in total microbial

communities than active, this indicates that the overall composition of active communities was less affected by *lhy* dysfunction, and that the profiling of total microbial communities was better suited to identifying the effects of *lhy* dysfunction upon overall community composition in the rhizosphere.

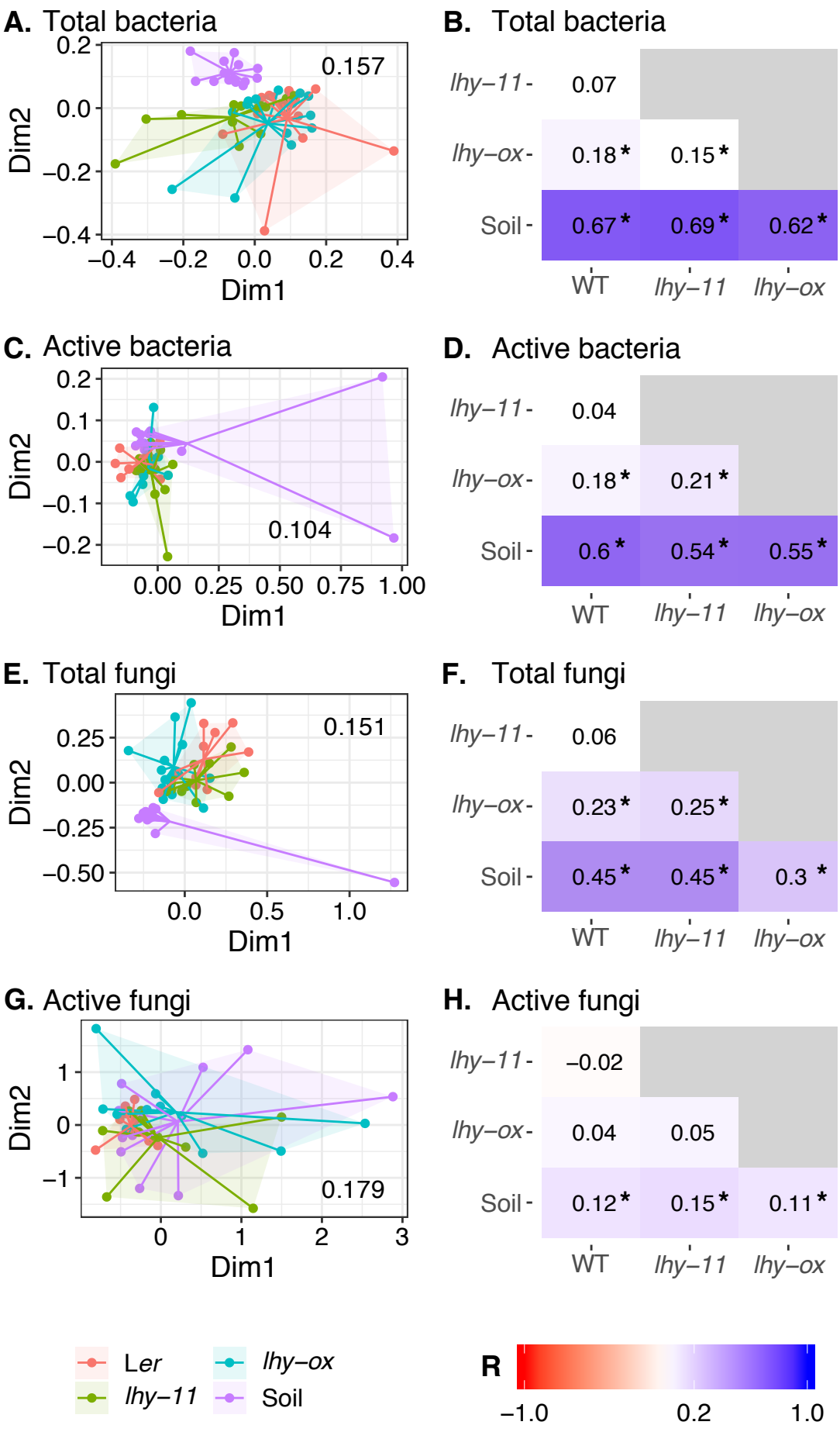
A. Total bacteria
0.157
Dim2
Dim1
B. Total bacteria
lhy−11
lhy−ox
Soil
0.07
0.18*
0.15*
0.67*
0.69*
0.62*
WT
lhy−11
lhy−ox
C. Active bacteria
0.104
D. Active bacteria
0.04
0.18*
0.21*
0.6*
0.54*
0.55*
E. Total fungi
0.151
F. Total fungi
0.06
0.23*
0.25*
0.45*
0.45*
0.3*
G. Active fungi
0.179
H. Active fungi
−0.02
0.04
0.05
0.12*
0.15*
0.11*
Ler
lhy−11
lhy−ox
Soil
R
−1.0
0.2
1.0

Figure 2.1. *lhy* overexpression, but not loss-of-function, alters overall rhizosphere microbiome composition. Total and active bacterial and fungal communities were compared between samples using NMDS plots and ANOSIM based on Bray-Curtis dissimilarity matrices. For NMDS plots (a), (c), (e), and (g), stress values (indications of how well data are represented in reduced dimensionality) are displayed on each. For ANOSIM plots (b), (d), (f) and (h), samples compared are considered significantly different if R (dissimilarity score displayed on each tile) ≥ 0.2 and $p \leq 0.05$ (* indicates that $p \leq 0.05$: see Table 2.1 for p values).

Table 2.1. p values accompanying ANOSIM analysis in Figure 2.1. $p \leq 0.05$ (denoted by *) indicates a suitably robust comparison where the R value (displayed in Figure 2.2) generated can be regarded as reliable.

	Bacteria		**Fungi**	
	Total	**Active**	**Total**	**Active**
WT vs soil	<0.001*	<0.001*	<0.001*	0.010*
***lhy-11* vs soil**	<0.001*	<0.001*	<0.001*	0.019*
***lhy-ox* vs soil**	<0.001*	<0.001*	<0.001*	0.017*
WT vs *lhy-11*	0.063	0.214	0.109	0.563
WT vs *lhy-ox*	0.005*	0.007*	0.003*	0.162
lhy-11* vs *lhy-ox	0.008*	0.011*	<0.001*	0.112

As expected, alpha diversity was generally reduced in almost all rhizosphere samples relative to bulk soil in both total and active bacterial communities and total fungal communities (Figure 2.2). No significant differences in alpha diversity were observed between any of the rhizosphere samples in active bacterial or fungal communities (Figures 2.2.b and 2.2.d). Additionally, in total communities, the alpha diversity of *lhy-11* samples did not significantly differ from that of wild-type plants (Figures 2.2.a and 2.2.c). However, alpha diversity of the *lhy-ox* rhizosphere was significantly reduced relative to wild-type plants in both total bacterial ($p = <0.001$) and fungal ($p = 0.027$) communities, and relative to *lhy-11* ($p = 0.05$) in total fungal communities (Figures 2.2.a and 2.2.c). While species richness did not significantly differ between rhizosphere samples (Table A2.3), species evenness of *lhy-ox* was significantly reduced relative to wild-type and *lhy-11* plants in both total bacterial and fungal communities (Table A2.4). The altered

alpha diversity and species evenness observed in *lhy-ox* therefore indicate that only overexpression of *lhy* influences the microbial diversity of total rhizosphere communities, specifically by influencing the distribution of relative abundances of species present as opposed to the number of species detected. Similarly to the results observed for overall community composition, as significant differences were only observed in total microbial communities, this indicates that the alpha diversity of active communities was not affected by *lhy* dysfunction, and therefore only the profiling of total microbial communities was suitable for identifying the effects of *lhy* dysfunction upon rhizosphere microbial diversity.

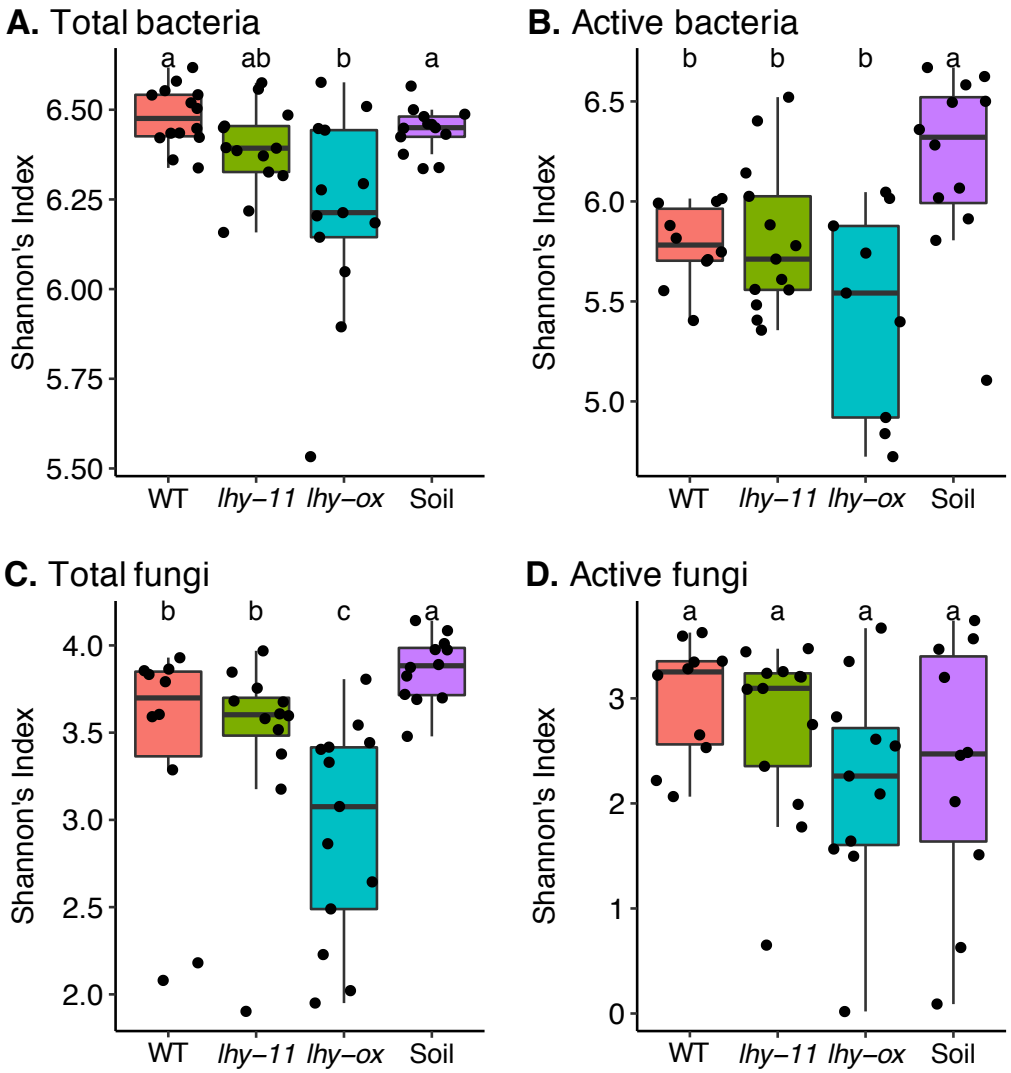

Figure 2.2. *lhy* overexpression, but not loss-of-function, alters alpha diversity of the rhizosphere microbiome. Alpha diversity was quantified using Shannon's Index (Shannon, 1948). Samples displaying different letters possess significantly different diversity scores ($p \leq 0.05$; Kruskal-Wallis followed by pairwise Wilcoxon rank sum tests).

2.3.1.2. Relative abundances of taxa

Across all sample types, the relative abundances of bacterial phyla and fungal classes differed between total and active rhizosphere microbial communities.

Both total and active bacterial communities were dominated by Actinobacteria and Proteobacteria (Figures 2.3.a and 2.3.b). However, Proteobacteria formed higher relative abundances in active than total communities (Figures 2.3.a and 2.3.b; Table A2.5) while the reverse occurred for Actinobacteria, which typically displayed over 1.5-fold higher relative abundances in total communities (Figures 2.3.a and 2.3.b; Table A2.5). Additionally, Cyanobacteria were found in high relative abundances only in the active communities of rhizosphere samples, with relative abundances in wild-type and *lhy-11* samples over five-fold higher than in total communities (Figures 2.3.a and 2.3.b; Table A2.5).

Both total and active fungal communities were dominated by Dothideomycetes and Sordariomycetes (Figure 2.3.c and 2.3.d). While Dothideomycetes formed higher relative abundances in active than total communities, these differences were only significant in *lhy-11* rhizosphere samples (Figures 2.3.c and 2.3.d; Table A2.5). Contrastingly, Sordariomycetes were found in higher relative abundances in total than active communities, with significant differences in all samples except *lhy-ox* (Figures 2.3.c and 2.3.d; Table A2.5).

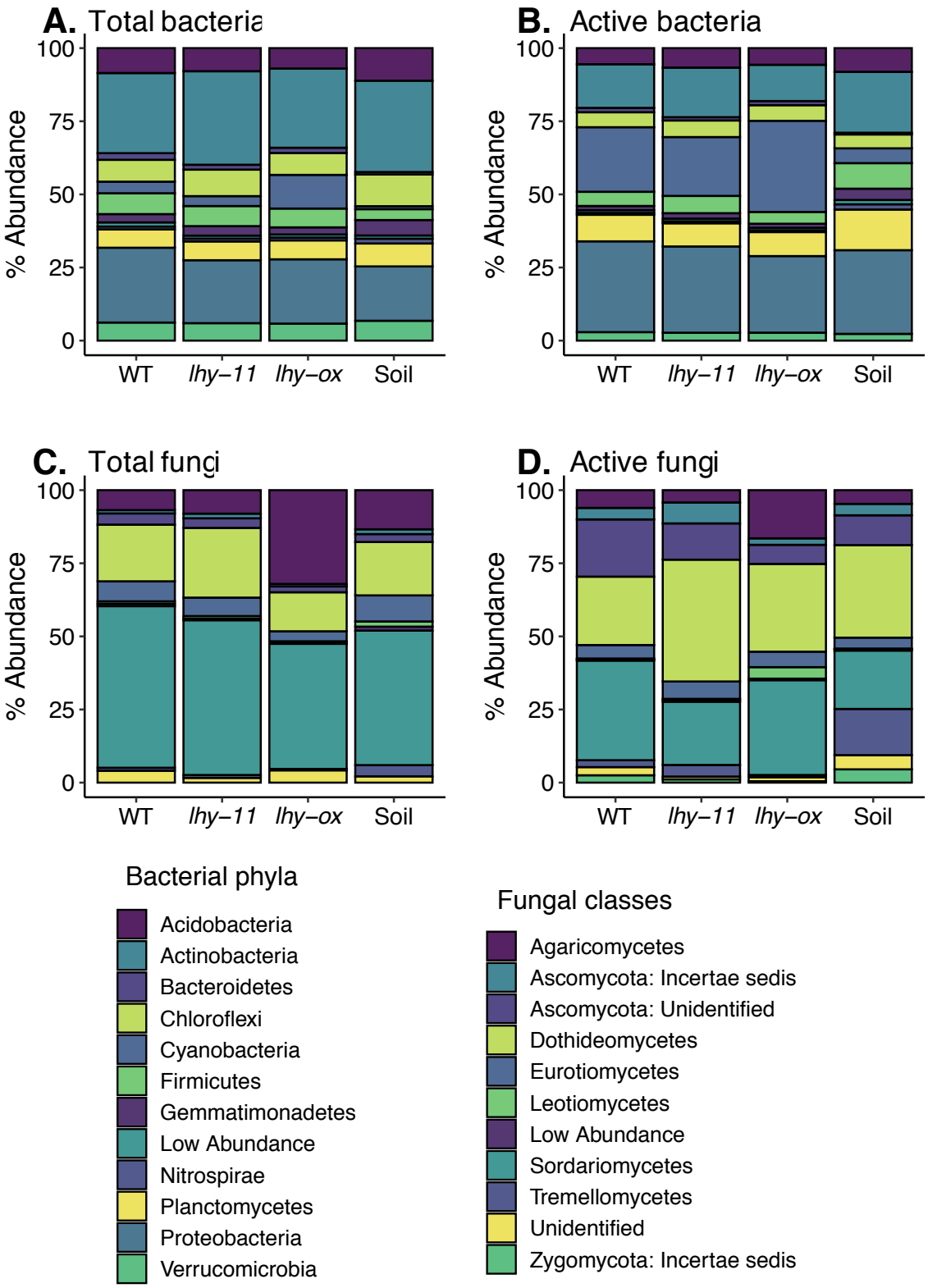

Figure 2.3. Relative abundances of bacterial phyla and fungal classes in wild-type, *lhy-11*, *lhy-ox*, and bulk soil samples. Taxa present were identified in (a) total and (b) active bacterial communities, and (c) total and (d) active fungal communities. Mean relative abundances shown. Taxa with individual mean relative abundances of less than 1% across all samples were merged to create the “Low Abundance” category.

In order to determine whether dysfunction of the plant circadian clock influences the relative abundances of microbial taxa, we compared the relative abundances of bacterial phyla and fungal classes between wild-type, *lhy-11* and *lhy-ox* samples. Significant differences between wild-type, *lhy-11,* and *lhy-ox* samples were observed within total and active rhizosphere communities.

In total bacterial communities, both *lhy-11* and *lhy-ox* samples showed significant differences in their relative abundances of phyla when compared to wild-type plants (Figure 2.4.a; Table A2.6). *lhy-11* contained significantly higher relative abundances of Actinobacteria and Chloroflexi, and significantly lower relative abundances of Bacteroidetes and Proteobacteria, while *lhy-ox* contained significantly lower relative abundances of Acidobacteria and Proteobacteria (Figure 2.4.a; Table A2.6). Additionally, when compared to *lhy-11*, *lhy-ox* contained significantly lower relative abundances of Actinobacteria, Chloroflexi, and Gemmatimonadetes, and significantly higher relative abundances of Cyanobacteria, the latter being over three-fold greater in *lhy-ox* relative to *lhy-11* (Figure 2.4.a; Table A2.6).

Contrastingly, in active bacterial communities, only one significant difference was observed in the relative abundances of phyla between rhizosphere samples. As was also observed in total bacterial communities, and with a similar fold-change, *lhy-ox* contained a significantly lower relative abundance of Proteobacteria than wild-type plants (Figure 2.4.b; Table A2.6).

In total fungal communities, only *lhy-ox* samples showed significant differences in their relative abundances of classes when compared to wild-type plants (Figure 2.4.c; Table A2.7). *lhy-ox* contained significantly lower relative abundances of Dothideomycetes and Eurotiomycetes, and a significantly higher relative abundance of Agaricomycetes, than wild-type and *lhy-11* plants (Figure 2.4.c; Table A2.7). Additionally, when compared to *lhy-11*, *lhy-ox* contained a significantly lower relative abundance of Sordariomycetes (Figure 2.4.c; Table A2.7).

In active fungal communities, fewer differences were observed in the relative abundances of classes between rhizosphere samples. Similarly to total fungal communities, only *lhy-ox* displayed alterations relative to wild-type plants (Figure 2.4.d; Table A2.7). *lhy-ox* contained lower relative abundances of Tremellomycetes than wild-type and *lhy-11* plants, which were not observed in total fungal communities, with the latter being a particularly large decrease at approximately six-fold (Figure 2.4.d; Table A2.7). As was also observed in total fungal communities, when compared to *lhy-11*, *lhy-ox* contained a significantly higher relative abundance of Agaricomycetes (Figure 2.4.d; Table A2.7).

The relative abundances of a wide range of microbial taxa, across both total and active bacterial and fungal communities, were therefore altered in *lhy-11* and *lhy-ox* plants. However, these differences occurred across a wider range of taxa in *lhy-ox* than in *lhy-11* samples. Additionally, in general, greater fold-changes in relative abundance were observed in fungal classes than bacterial phyla, suggesting that the influence of plant circadian clock dysfunction may be greater for fungi. These results therefore indicate that both overexpression and loss-of-function of *lhy* influenced the relative abundances of bacterial and fungal taxa in the rhizosphere microbiome but did not bring about the same effects.

In both bacterial and fungal communities, more differences were observed in the relative abundances of taxa between rhizosphere samples from total than active microbial communities. This indicates that the relative abundances of microbial taxa in active communities were less affected by *lhy* dysfunction, and that the profiling of total microbial communities was better suited to identifying the effects of *lhy* dysfunction upon the relative abundances of microbial taxa in the rhizosphere.

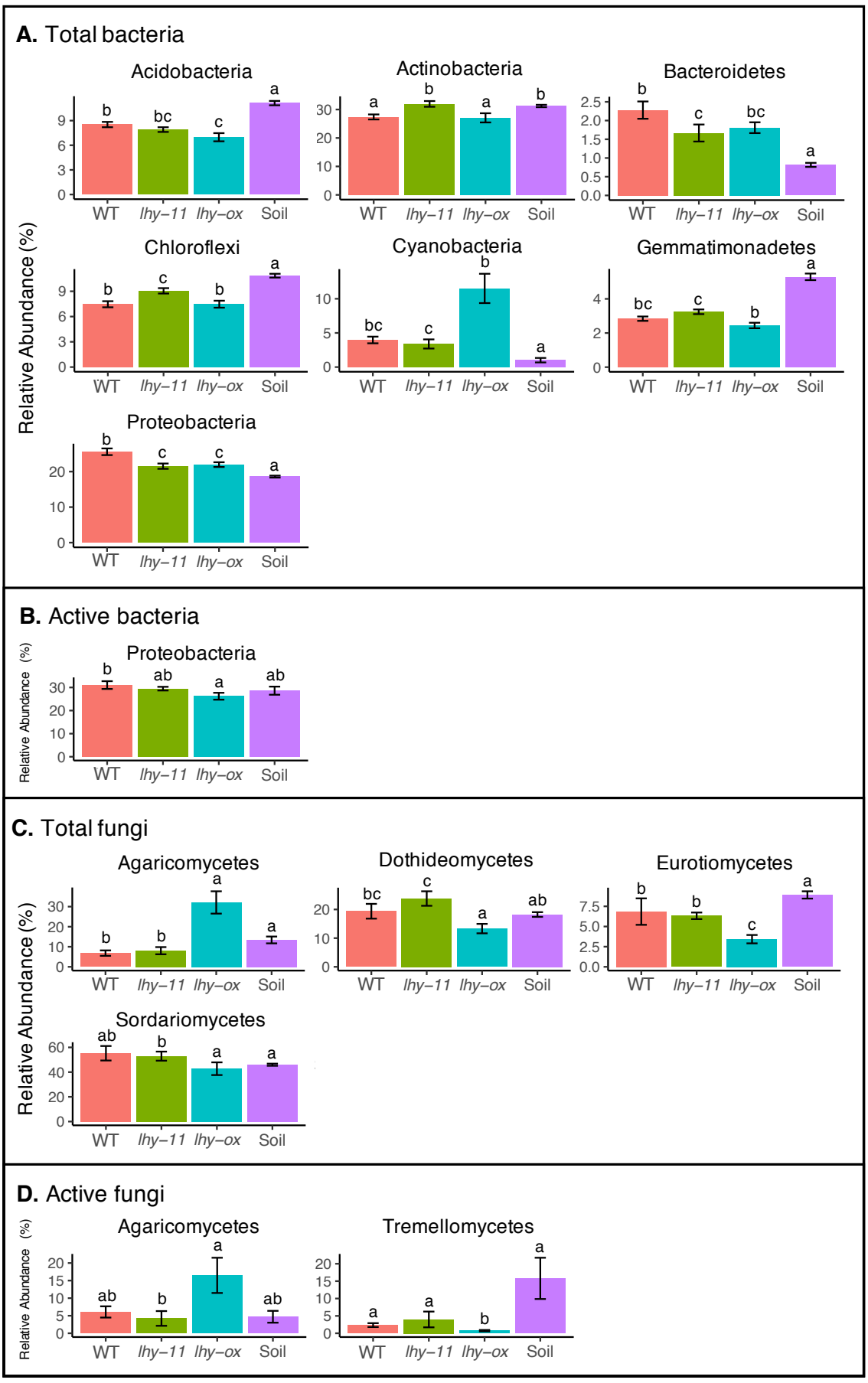
A. Total bacteria
Acidobacteria
Actinobacteria
Bacteroidetes
Chloroflexi
Cyanobacteria
Gemmatimonadetes
Proteobacteria
Relative Abundance (%)
WT
lhy−11
lhy−ox
Soil
B. Active bacteria
Proteobacteria
Relative Abundance (%)
C. Total fungi
Agaricomycetes
Dothideomycetes
Eurotiomycetes
Sordariomycetes
Relative Abundance (%)
D. Active fungi
Agaricomycetes
Tremellomycetes
Relative Abundance (%)

Figure 2.4. *lhy* loss-of-function and overexpression alter the relative abundances of bacterial phyla and fungal classes in the rhizosphere microbiome. Relative abundances of taxa were compared between samples using Kruskal-Wallis testing. Taxa shown displayed significant differences ($p \leq 0.05$) in their relative abundances within at least one comparison between wild-type, *lhy-11*, and *lhy-ox* rhizosphere samples, and constitute greater than 1% relative abundance in at least one sample. Samples displaying different letters possess significantly different relative abundances. Mean relative abundances ± SEM (Standard Error of the Mean) shown.

2.3.1.3. Relative abundances of fungal guilds

217 fungal OTUs from total communities (44% of all OTUs) and 55 OTUs from active communities (30% of all OTUs) were assigned to one of the five following ecological guilds using the FUNGuild tool: arbuscular mycorrhizal fungi, endophytes, fungal parasites, plant pathogens, and saprotrophs. Significant differences in the relative abundance of these guilds were observed between plant rhizosphere samples but only in total communities (Figure 2.5). The *lhy-ox* rhizosphere contained a higher relative abundance of arbuscular mycorrhizal fungi than both wild-type ($p = 0.0017$) and *lhy-11* ($p = 0.0065$), with a particularly high increase of almost eight-fold observed between wild-type and *lhy-ox* plants (Figure 2.5). Additionally, *lhy-ox* samples contained lower relative abundances of saprotrophs than both wild-type ($p = 0.034$) and *lhy-11* ($p = 0.047$), and a lower relative abundance of endophytes than wild-type samples ($p = 0.029$) (Figure 2.5).

As the relative abundances of fungal guilds were only significantly altered in the rhizosphere of *lhy-ox* plants relative to wild-type, this indicates that overexpression of *lhy* influences the acquisition of potentially ecologically significant fungi within the rhizosphere, but loss of *lhy* function does not. Additionally, as differences were only observed between rhizosphere samples in total fungal communities, only the profiling of total microbial communities was suitable for detecting of the effects of *lhy* dysfunction on the relative abundances of rhizosphere fungal guilds.

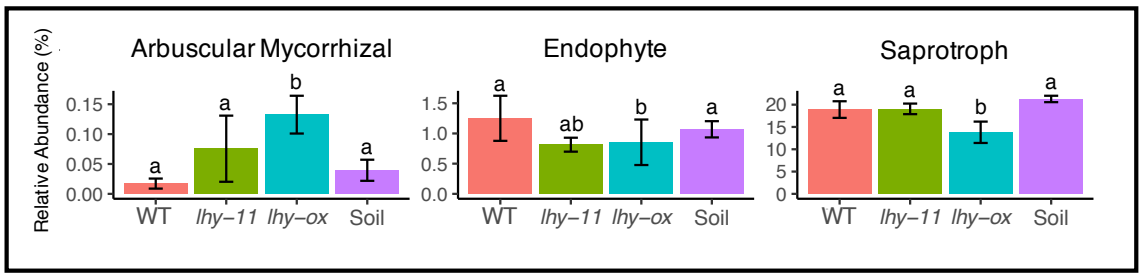

Figure 2.5. *lhy* overexpression, but not loss-of-function, alters the relative abundance of ecological guilds within total fungal rhizosphere communities. Relative abundances of guilds were compared between samples using Kruskal-Wallis testing. Guilds shown displayed significant differences ($p \leq 0.05$) in their relative abundances in at least one comparison between wild-type, *lhy-11*, and *lhy-ox* rhizosphere samples. Samples displaying different letters possess significantly different relative abundances. Mean relative abundances ± SEM shown.

FUNGuild annotation also revealed that plant pathogenic OTUs were highly abundant across all samples, with total fungal communities containing higher total relative abundances than active communities (Figure 2.6; Table A2.8). While a high pathogen load was also present in bulk soil samples, the total relative abundances of plant pathogenic OTUs in soil were significantly reduced compared to *lhy-11* in total, and wild-type samples in active, communities (Figure 2.6).

Several highly abundant plant pathogenic OTUs, with a mean relative abundance of greater than 1% in more than one rhizosphere sample, were found in total and active fungal communities. 6 of these 9 OTUs found in total communities significantly differed in their relative abundance between rhizosphere samples (Table 2.2), while 4 of the 9 found in active communities differed (Table 2.3). In the majority of cases, these OTUs were found in lower relative abundances in *lhy-ox* and *lhy-11* compared to wild-type samples, and in *lhy-ox* compared to *lhy-11*, with only two displaying the reverse.

In total communities, when compared to wild-type plants, *lhy-11* contained a higher relative abundance of OTU4 (*Fusarium* sp.), and *lhy-ox* contained lower relative abundances of OTU5 (*Plectosphaerella* sp.), OTU16 (*Dendryphionnanum*), and OTU60 (*Fusarium neocosmosporiellum*), the latter

two displaying particularly high changes of approximately six-fold (Table 2.2). *lhy-ox* also contained a higher relative abundance of OTU4 and lower relative abundances of OTU3 (*Cladosporium exasperatum*), OTU7 (*Alternaria* sp.), OTU5, and OTU16 than *lhy-11* (Table 2.2).

In active communities, the significant changes in relative abundance of pathogenic OTUs between rhizosphere samples differed to those observed in total communities. Here, when compared to wild-type plants, *lhy-11* contained a lower relative abundance of OTU28 (*Devriesia* sp.), and *lhy-ox* contained lower relative abundances of OTU5, OTU7, and OTU60, the latter two displaying particularly high changes of over twenty- and ten-fold respectively (Table 2.3).

The altered relative abundances of specific highly abundant pathogenic OTUs observed in the *lhy-11* and *lhy-ox* rhizospheres relative to wild-type samples indicates that both *lhy* overexpression and loss-of-function influenced the pathogenic fungi present in the rhizosphere, but that each form of dysfunction had different effects. Additionally, significant differences between wild-type, *lhy-11* and *lhy-ox* samples were observed in both total and active communities but differed between the two, indicating that while the profiling of both total and active communities was able to detect the influence of circadian clock dysfunction upon pathogenic rhizosphere fungi, these communities responded differently.

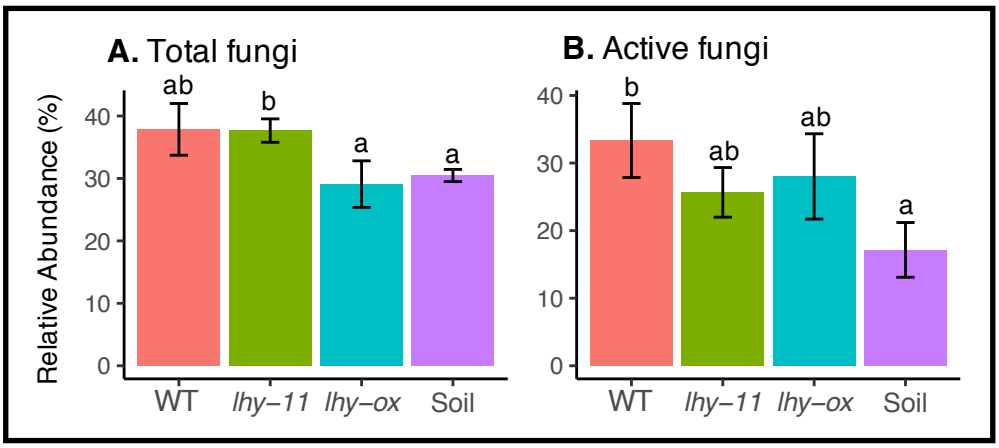

Figure 2.6. Relative abundances of pathogenic OTUs in wild-type, *lhy-11*, *lhy-ox* and bulk soil samples. Total relative abundances of pathogenic OTUs from (a) total and (b) active fungal communities were identified using the FUNGuild annotation tool.

Samples displaying different letters possess significantly different relative abundances. Mean relative abundances ± SEM shown.

Table 2.2. Highly abundant plant pathogenic OTUs from total fungal communities significantly differ in relative abundance between rhizosphere samples from wild-type, *lhy-11* and *lhy-ox* plants. OTUs with a mean relative abundance greater than 1% in at least one sample were investigated using Kruskal-Wallis testing. Fold changes displayed indicate the difference in relative abundance within the second sample listed when compared to the first.

Comparison	OTU ID	Relative Abundance	Fold change	p
WT vs *lhy-11*	4; *Fusarium* sp.	7.4% vs 11.4%	1.5 ↑	0.003
WT vs *lhy-ox*	5; *Plectosphaerella* sp.	8.5% vs 1.3%	6.5 ↓	0.002
	16; *Dendryphionnanum*	2.2% vs 0.9%	2.4 ↓	0.031
	60; *Fusarium neocosmosporiellum*	1.8% vs 0.3%	6.0 ↓	<0.001
lhy-11* vs *lhy-ox	3; *Cladosporium exasperatum*	7.9% vs 3.7%	2.1 ↓	0.002
	4; *Fusarium* sp.	11.4% vs 13.8%	1.2 ↑	0.009
	5; *Plectosphaerella* sp.	6.6% vs 1.3%	5.1 ↓	<0.001
	7; *Alternaria* sp.	3.0% vs 1.4%	2.1 ↓	0.002
	16; *Dendryphionnanum*	1.6% vs 0.9%	1.8 ↓	0.015

Table 2.3. Highly abundant plant pathogenic OTUs from active fungal communities significantly differ in relative abundance between rhizosphere samples from wild-type, *lhy-11* and *lhy-ox* plants. OTUs with a mean relative abundance greater than 1% in at least one sample were investigated using Kruskal-Wallis testing. Fold changes displayed indicate the difference in relative abundance within the second sample listed when compared to the first.

Comparison	OTU ID	Relative Abundance	Fold change	p
WT vs *lhy-11*	28; *Devriesia* sp.	2.0% vs 0.7%	2.5 ↓	0.020
WT vs *lhy-ox*	5; *Plectosphaerella* sp.	6.4% vs 2.6%	3.3 ↓	0.032
	7; *Alternaria* sp.	5.3% v 1.6%	3.2 ↓	0.029
	60; *Fusarium neocosmosporiellum*	1.2% vs 0.05%	2.9 ↓	0.029
lhy-11* vs *lhy-ox	7; *Alternaria* sp.	5.1% vs 1.6%	24 ↓	0.034
	60; *Fusarium neocosmosporiellum*	0.7% vs 0.05%	14 ↓	0.011

2.3.2. Diel changes in the composition of the rhizosphere microbiome are influenced by the plant circadian clock

Having established that mutations in the *lhy* gene affect the assembly of the rhizosphere microbiome, we wanted to determine whether diel changes in the composition of the rhizosphere microbiome are also influenced by dysfunction of the plant circadian clock. To do this, we used the rhizosphere samples which were taken at dawn and dusk from wild-type *A. thaliana* and those with *lhy* loss-of-function and overexpression, and compared their microbial communities between the two time points. In order to characterise diel changes, dawn and dusk time points were compared within each sample type with respect to the following: overall community composition; alpha diversity; the relative abundances of fungal ecological guilds, bacterial phyla, and fungal classes; and the relative abundances of individual OTUs.

No significant diel differences were observed in overall rhizosphere microbial community composition (Table A2.1) or alpha diversity (Table A2.2). Additionally, no fungal ecological guilds (Table A2.9) and few bacterial phyla (Table A2.10) and fungal classes (A2.11) differed in their relative abundance between dawn and dusk samples. In total bacterial communities, Acidobacteria and

Cyanobacteria were significantly rhythmic in the wild-type rhizosphere, while Gemmatimonadetes and Proteobacteria were in *lhy-11* and *lhy-ox* samples respectively (Table A2.10). For active bacterial communities, Acidobacteria were significantly rhythmic in *lhy-11* and Verrucomicrobia were in *lhy-ox* samples (Table A2.10). In total fungal communities, Leotiomycetes were significantly rhythmic in the wild-type rhizosphere, and Tremellomycetes were in *lhy-ox* samples (Table A2.11). For active fungal communities, Eurotiomycetes were significantly rhythmic in wild-type and Eurotiomycetes and Tremellomycetes were in *lhy-ox* samples (Table A2.11).

2.3.2.1. Rhythmic OTUs

Significant differences between dawn and dusk samples were also found in the relative abundance of individual OTUs. These OTUs, subsequently termed rhythmic OTUs, were found across all sample types. Because they were more numerous and ubiquitous than the rhythmic bacterial phyla and fungal classes, we focussed on these rhythmic OTUs for our subsequent investigation into whether diel changes in the rhizosphere microbiome are influenced by the plant circadian clock. To determine whether *lhy* loss-of-function and overexpression influence diel changes in the rhizosphere microbiome, we compared the rhythmic OTUs, their taxonomy, and total relative abundances across sample types.

Rhythmic OTUs displaying significant differences in their relative abundance between dawn and dusk samples were found in total and active communities across wild-type, *lhy-11*, *lhy-ox* and bulk soil samples, with the exception of the active fungal community of soil (Table 2.4). Similar proportions of these rhythmic OTUs were found across samples, with rhythmic OTUs forming 4.0 – 4.6% of total bacterial, 1.6 – 5.3% of active bacterial, 2.6 – 7.7% of total fungal, and 3.5 – 5.8% of active fungal communities as a proportion of the total number of OTUs present (Table 2.4).

Table 2.4. Rhizosphere and bulk soil samples contain rhythmic OTUs. Relative abundances of individual OTUs were compared between dawn and dusk sampling points

using Kruskal-Wallis testing. Rhythmic OTUs displayed significantly different ($p \leq 0.05$) relative abundances between dawn and dusk samples and are reported as a proportion of the total number of OTUs found in each sample.

	Bacteria		Fungi	
	Total	**Active**	**Total**	**Active**
WT	4.7% (202/4328)	2.9% (111/3854)	4.0% (15/373)	3.5% (6/172)
lhy-11	4.5% (192/4226)	5.3% (210/3943)	2.6% (11/416)	5.3% (9/170)
lhy-ox	4.6% (194/4260)	2.3% (87/3742)	7.7% (33/427)	5.8% (9/154)
Soil	4.0% (161/4067)	1.6% (64/3883)	3.3% (16/487)	0.0% (0/169)

2.3.2.2. Rhythmic OTUs are influenced by the plant circadian clock and differ between total and active communities

While over 87% of rhythmic OTUs were present in all samples (Figure A2.1), no OTUs were found to be rhythmic in every sample (Figure 2.7), across total and active bacterial and fungal communities. Small numbers of OTUs were found to be rhythmic in more than one sample, and total bacterial communities contained the highest numbers of OTUs observed as rhythmic in multiple samples (Figure 2.7). For example, 15 OTUs were determined to be rhythmic in total bacterial communities of both wild-type and *lhy-11* rhizosphere samples while 165 were rhythmic in wild-type and 156 in *lhy-11* samples alone (Figure 2.7). Just one OTU was determined to be rhythmic in all three rhizosphere samples and was found in active fungal communities (Figure 2.7.d). Additionally, very few rhythmic OTUs were found in common between bulk soil and any of the rhizosphere samples (Figure 2.7). For example, the highest number was in total bacterial communities, where five OTUs were rhythmic in both wild-type rhizosphere samples and also bulk soil, while 165 were rhythmic in wild-type and 139 in bulk soil samples alone (Figure 2.7.a).

Similarly, while approximately 90% of bacterial and over 65% of fungal rhythmic OTUs were present in both total and active communities (Figure A2.2), very few OTUs were found to be rhythmic in both total and active communities (Figure

2.8). For bacteria, all four of wild-type, *lhy-11*, *lhy-ox* and bulk soil samples contained OTUs which were rhythmic in both total and active communities (Figures 2.8.a, 2.8.c, 2.8.e, and 2.8.g). For example, eight OTUs were found to be rhythmic in both total and active bacterial communities of wild-type rhizosphere samples, while 194 were rhythmic in total communities only and 103 in active only. (Figure 2.8.a). Contrastingly, only one fungal OTU was found to be rhythmic in both total and active communities (Figure 2.8). This OTU was found in wild-type rhizosphere samples, where 14 were rhythmic in total communities only and five in active only (Figure 2.8.b).

When compared to wild-type plants, both loss-of-function and overexpression of *lhy* therefore altered which members of the rhizosphere microbiome were rhythmic. Distinct subsets of organisms were rhythmic in the rhizosphere of each mutant, indicating that *lhy* loss-of-function and overexpression each affected diel changes in the rhizosphere microbiome differently. Additionally, the minimal overlap between the rhythmic OTUs from bulk soil and rhizosphere samples suggests that the presence of plant roots also alters the subset of soil microbial communities which may show rhythmicity.

While the profiling of both total and active microbial communities was able to identify diel changes in the composition of the rhizosphere microbiome, the rhythmic OTUs found differed between total and active communities.

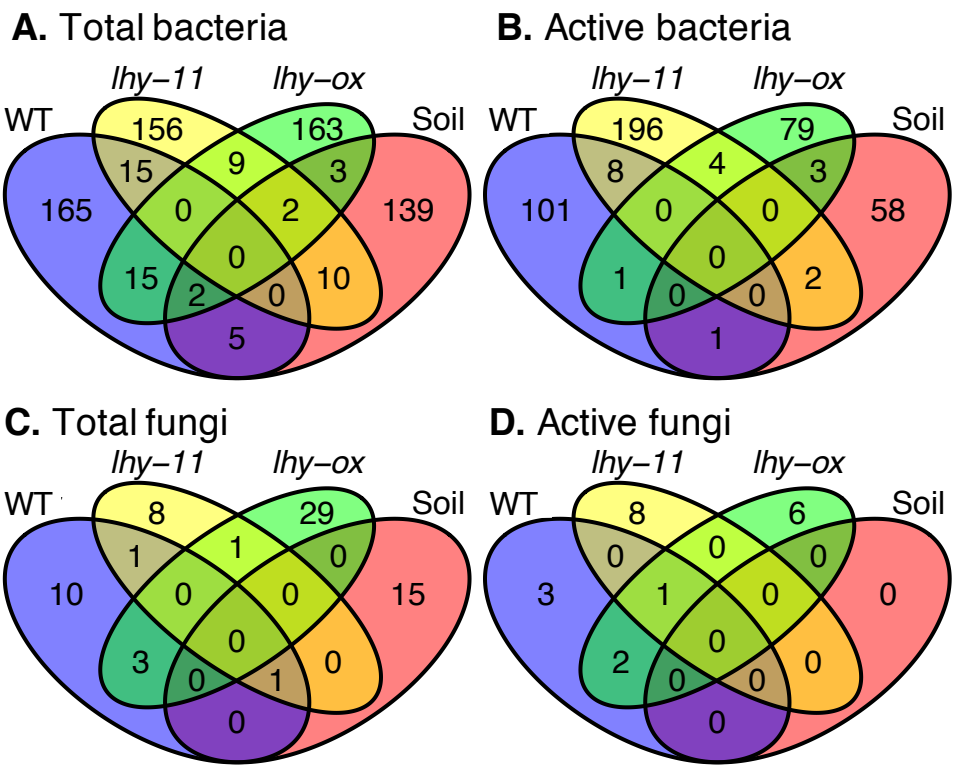

Figure 2.7. Rhythmic OTUs differ across rhizosphere and bulk soil samples. Numbers of OTUs from (a) total and (b) active bacterial communities and (c) total and (d) active fungal communities. Numbers in overlapping sections indicate OTUs detected as rhythmic in common between that particular combination of samples.

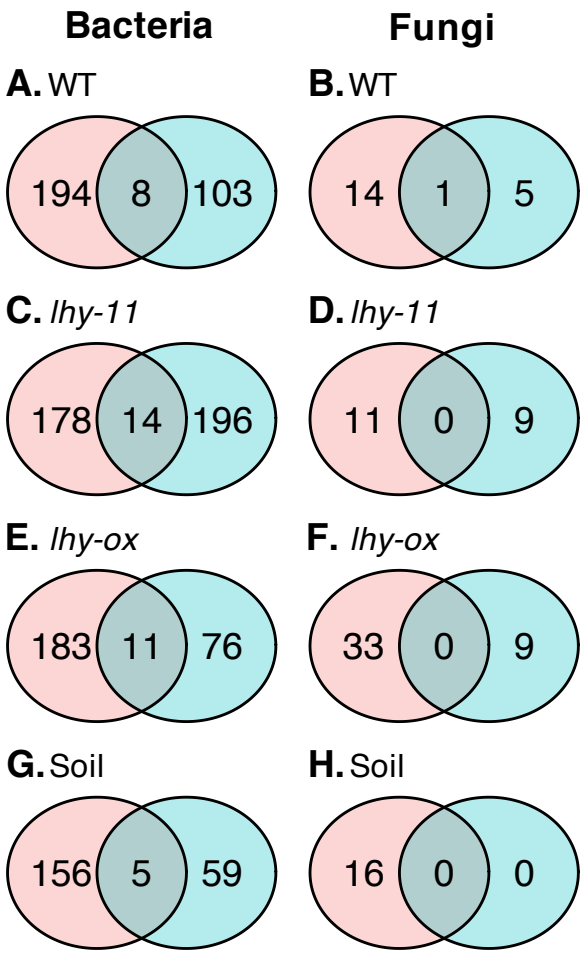

Figure 2.8. Rhythmic OTUs differ between total and active microbial communities. Rhythmic OTUs from (a), (c), (e), and (g): bacterial and (b), (d), (f), and (h): fungal communities. Left (pink) circles represent OTUs detected as rhythmic in total communities and right (blue) represent those from active communities.

2.3.2.3. Taxonomy and overall relative abundances of rhythmic OTUs

Both the taxonomy and total relative abundances of rhythmic OTUs were found to differ across rhizosphere and bulk soil samples (Figure 2.9; Tables A2.12 and A2.13).

Within total bacterial communities, Actinobacteria contained the greatest relative abundance of rhythmic OTUs across all samples, including bulk soil (Figures 2.9.a to 2.9.d; Table A2.12). Contrastingly, Proteobacteria contained the greatest relative abundance of rhythmic OTUs in active bacterial communities (Figures 2.9.e to 2.9.h; Table A2.12). For both total and active bacterial communities, no other phylum was consistently highly abundant within the rhythmic OTUs across

wild-type, *lhy-11* and *lhy-ox* rhizosphere samples (Figures 2.9.a to 2.9.h; Table A2.12). For example, in total bacterial communities, Chloroflexi were the second most highly abundant phylum within rhythmic OTUs from the wild-type rhizosphere whereas Proteobacteria were the second most abundant phylum within rhythmic OTUs in *lhy-ox* samples (Figures 2.9.a and 2.9.c; Table A2.12.

Within total fungal communities, Sordariomycetes contained the greatest relative abundance of rhythmic OTUs across all samples including bulk soil, but only at dusk (Figures 2.9.i to 2.9.l; Table A2.13). Contrastingly, Dothideomycetes contained the greatest relative abundance of rhythmic OTUs in dusk samples from active communities (Figures 2.9.m to 2.9.o; Table A2.13). As with the bacterial results, in total and active fungal communities, no other class was consistently highly abundant within the rhythmic OTUs across rhizosphere samples (Figures 2.9.i to 2.9.o; Table A2.13). For example, in dawn samples from active fungal communities, Eurotiomycetes were the second most highly abundant class within rhythmic OTUs from the wild-type rhizosphere, whereas rhythmic Sordariomycete OTUs were also highly abundant in *lhy-11* samples (Figures 2.9.m and 2.9.n; Table A2.13).

Across all samples, these rhythmic OTUs formed varying proportions of microbial communities, accounting for between 1.3 – 14.6% of bacterial and 0.3 – 30.1% of fungal communities by relative abundance (Figure 2.9). These overall relative abundances of rhythmic OTUs were generally higher in total than active bacterial communities, whereas the opposite was true for fungi, where active communities contained higher overall relative abundances of rhythmic OTUs. For example, in wild-type rhizosphere samples, rhythmic OTUs accounted for ~10 – 12% of total bacterial communities compared to ~6% of active bacterial communities, whereas ~1 – 4% of total fungal communities were comprised of rhythmic OTUs compared to ~4 – 12% of active fungal communities (Figures 2.9.a, 2.9.e, 2.9.i, and 2.9.m).

Additionally, the fungal rhythmic OTUs generally displayed greater differences in their overall relative abundance between dawn and dusk samples than the bacterial rhythmic OTUs. (Figure 2.9). In particular, large differences in overall

relative abundances of rhythmic OTUs were observed between dawn and dusk samples in active fungal communities of wild-type and *lhy-ox* rhizosphere samples (Figures 2.9.m and 2.9.o).

In addition to altering which OTUs within microbial communities were rhythmic, dysfunction of the plant circadian clock also caused a change in the type of OTUs which were rhythmic, in terms of the representation of different taxonomic groups. While the same taxa usually formed the highest relative abundance within rhythmic OTUs across all samples, the degree to which other taxa were represented, in terms of both their presence and relative abundances, differed between all samples. Similarly to the results which demonstrated that the plant clock influences which community members display rhythmicity, the taxonomy and overall relative abundances of rhythmic OTUs within *lhy-ox* and *lhy-11* samples differed from the wild-type rhizosphere and from each other. This also indicates that *lhy* loss-of-function and overexpression both influenced diel changes in the rhizosphere microbiome in different ways. Additionally, the taxonomy and overall relative abundances of rhythmic OTUs differed between total and active microbial communities. As with the results concerning differences in rhythmic community members, this indicates that while the profiling of both total and active microbial communities was able to detect diel changes in community composition, different rhythmic subsets of the rhizosphere microbiome were detected with each method.

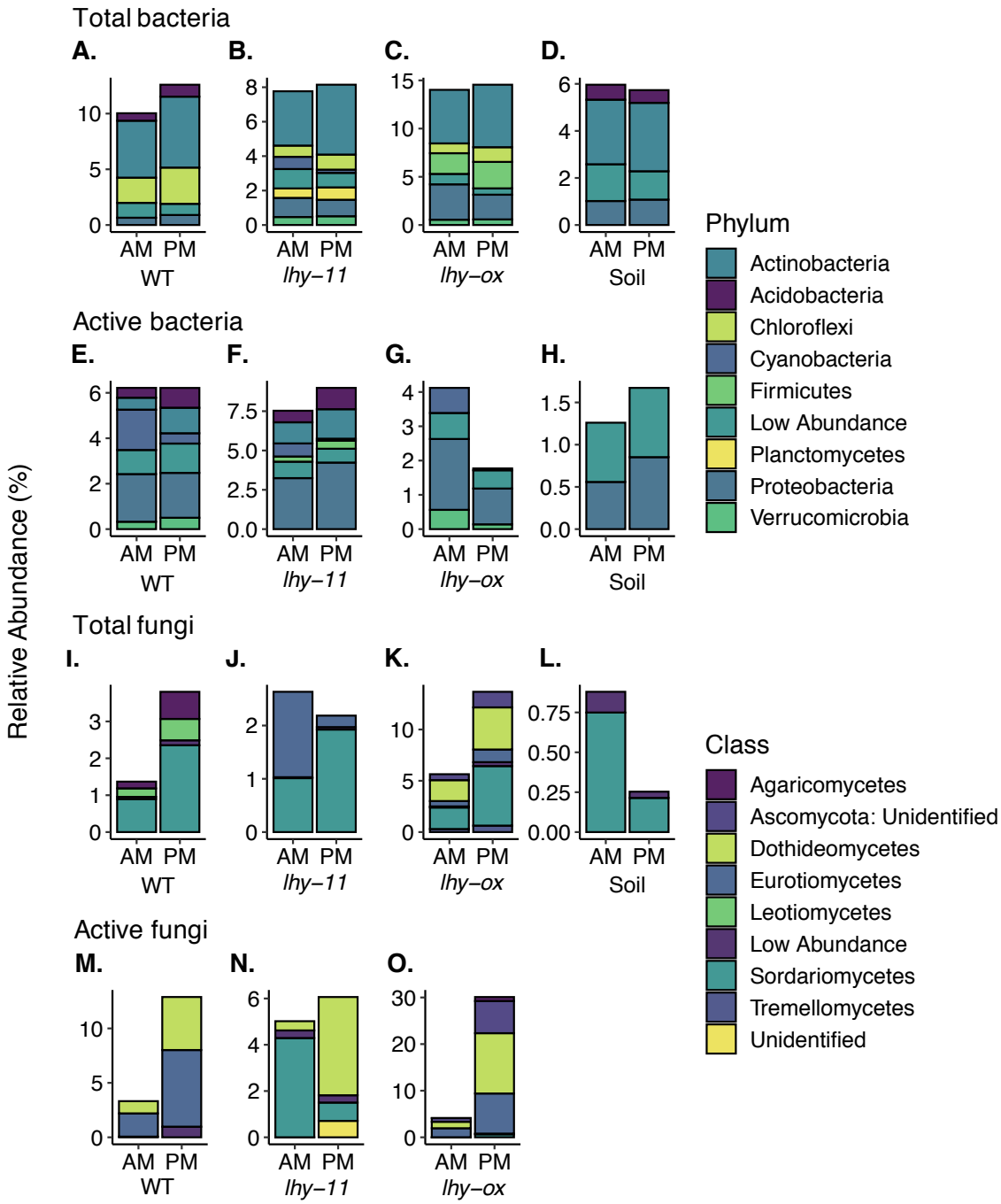

Figure 2.9. The taxonomy of rhythmic OTUs differs across wild-type, *lhy-11*, *lhy-ox*, and bulk soil samples, and between total and active microbial communities. Rhythmic OTUs displayed a significant difference in their relative abundance between dawn (AM) and dusk (PM) samples. Phyla within rhythmic OTUs in (a) to (d): total and (e) to (h): active bacterial communities, and classes of rhythmic OTUs in (i) to l: total and (m) to (o): active fungal communities. Active fungal communities of soil samples did not contain any rhythmic OTUs. Taxa with individual relative abundances of less than 0.5% across all samples were merged to create the “Low Abundance” category. Mean relative abundances shown.

2.4. Discussion

2.4.1. Dysfunction of the plant circadian clock influences the recruitment of microbiota into the rhizosphere

Previous works investigating the influence of the plant circadian clock upon the assembly of the rhizosphere microbiome investigated the total bacterial communities of plants possessing mutations in the circadian clock genes *cca1* (Staley et al., 2017), *toc1*, and *ztl* (Hubbard et al., 2017). In this study we found that the influence of the plant clock upon the assembly of the rhizosphere microbiome is not restricted to bacterial taxa, as fungal communities were also altered by *lhy* loss-of-function and overexpression.

We found that many aspects of the assembly of the *A. thaliana* rhizosphere microbiome were influenced by loss-of-function and overexpression of the core circadian clock gene *LHY*. Specifically, overall community composition, alpha diversity, and the relative abundances of microbial taxa and fungal ecological guilds significantly differed when compared to rhizosphere samples from wild-type plants.

2.4.1.1. The influence of plant circadian clock dysfunction upon the assembly of the rhizosphere microbiome

Across the analyses concerning community assembly, we observed differing microbial responses in the rhizosphere of plants with *lhy* loss-of-function when compared to those overexpressing *lhy*, and fewer significant differences between wild-type plants and those with *lhy* loss-of-function than between the wild type and those overexpressing *lhy*. When compared to wild-type samples, significant alterations in the overall composition, microbial diversity, and relative abundances of fungal guilds in the rhizosphere microbiome were only caused by the overexpression of *lhy*. Further, while the relative abundances of bacterial phyla, fungal classes, and highly abundant pathogenic OTUs were altered by both *lhy* loss-of-function and overexpression, different microbial taxa were influenced differently in the rhizosphere of each mutant. Plants with *lhy* loss-of-function display a phase advance when grown under light-dark cycles (Mizoguchi et al., 2002), while those overexpressing *lhy* are only capable of driven rhythms

triggered by dark-to-light environmental switches (Kim et al., 2003). These results therefore demonstrate that each *lhy* mutation influenced the assembly of the rhizosphere microbiome differently, and that the circadian phenotype of plants overexpressing *lhy* had a greater influence upon the microbiota recruited into the rhizosphere microbiome. This could be because in the *A. thaliana* circadian clock *LHY* exhibits a partially redundant function with *CCA1* (Mizoguchi et al., 2002). Loss of *lhy* function may therefore result in a more subtle phenotype than *lhy* overexpression because *CCA1* is still able to partially substitute for *LHY* function (Mizoguchi et al., 2002).

Hubbard et al. (2017) investigated the effects of the *toc1-21* and *ztl-30* mutations upon the assembly of total bacterial communities within the rhizosphere microbiome. *toc1-21* plants, which possess a shortened endogenous circadian period of ~20 hours that mismatches with exogenous 24-hour cycles (Somers et al., 1998), displayed differing overall community composition and reduced alpha diversity when compared to wild-type plants (Hubbard et al., 2017). Contrastingly, while *ztl-30* plants possess an elongated endogenous circadian period of ~28 hours that also mismatches with exogenous 24-hour cycles (Kevei et al., 2006), this mutation did not significantly alter community composition and diversity (Hubbard et al., 2017). In our study, we found that contrasting mutations in the plant circadian clock gene *lhy*, which brought about different circadian phenotypes, resulted in differing alterations to the community composition and alpha diversity of rhizosphere microbiota. Plants overexpressing *lhy* displayed significant differences in the overall composition of total fungal communities and in the alpha diversity of total bacterial and fungal communities, but those with loss of *lhy* function did not. Further, while Hubbard et al. (2017) demonstrated reduced microbial alpha diversity in the *toc1-21* rhizosphere, in this study we provided additional insight into the reduced alpha diversity we observed in *lhy-ox* plants as we determined that this was caused by a reduction in species evenness specifically. This indicates that the overexpression of *lhy* caused a more unequal distribution of microbial species, and that fewer OTUs may dominate the rhizosphere microbiome of *lhy-ox* plants.

Previous works by Hubbard et al. (2017) and Staley et al. (2017) also determined that dysfunction of the plant circadian clock influenced the relative abundance of individual microbial OTUs. Hubbard et al. (2017) identified 'indicator OTUs' which contributed to the differences observed in community composition between wild-type, *toc1-21*, and *ztl-30* rhizosphere samples. Staley et al. (2017) identified OTUs which significantly differed in their relative abundance between bulk soil, the rhizosphere of wild-type plants, and the rhizosphere of *cca1-ox* plants, which exhibit only driven rhythms under light-dark cycles. Contrastingly, when considering the assembly of the rhizosphere microbiome in this study, we mainly characterised the influence of plant circadian clock dysfunction upon higher level taxonomic groups (bacterial phyla and fungal classes). However, we observed some commonalities between the taxa identified in our study and those of Hubbard et al. (2017) and Staley et al. (2017). Of the 23 indicator OTUs identified by Hubbard et al. (2017), 17 belonged to phyla which we identified as being influenced by *lhy* loss-of-function and overexpression. In particular, a large proportion – seven of the 23 – of these indicator OTUs belonged to the Proteobacteria (Hubbard et al., 2017). In our study, the relative abundance of Proteobacteria was influenced by both *lhy* loss-of-function and overexpression in both total and active communities. Additionally, the OTUs identified by Staley et al. (2017) as being significantly different between wild-type, *cca1-ox*, and bulk soil samples most commonly belonged to Proteobacteria. The phylum Proteobacteria contains high physiological and metabolic diversity, with members of importance in global carbon, nitrogen and sulphur cycling (Spain et al., 2009). It is therefore particularly interesting that members of the Proteobacteria and the phylum as a whole have emerged from multiple works identifying impacts of the plant circadian clock on the assembly of the rhizosphere microbiome.

Other highly abundant taxa which we determined to be influenced by plant circadian clock dysfunction were Actinobacteria, Sordariomycetes, and Dothideomycetes. Similar to Proteobacteria, Actinobacteria contains a high diversity of members, which are also of importance in the decomposition of organic matter and therefore carbon cycling (Lewin et al., 2016). Both Sordariomycetes and Dothideomycetes also contain a wide variety of members, including endophytic, plant pathogenic, and saprotrophic fungi (Zhang et al.,

2006; Goodwin, 2014) and are therefore also important for nutrient cycling and plant health. The significance of these taxa indicate that the plant circadian clock is involved in the recruitment of rhizosphere microbiota which are able to perform a range of key ecological roles.

2.4.1.2. Ecological significance of the influence of plant circadian clock dysfunction upon rhizosphere fungi

Characterising the effects of the plant circadian clock on rhizosphere fungi in addition to bacteria allowed us to utilise the FUNGuild database, which assigns ecological functions to fungal taxa present (Nguyen et al., 2016). We were therefore also able to provide evidence that the plant circadian clock influences the relative abundances of specific ecologically important functional groups of rhizosphere microbiota. The relative abundances of arbuscular mycorrhizal, endophytic, and saprotrophic fungi within total communities were found to be influenced by *lhy* overexpression and given their significance for plant health, indicate that the normal functioning of the plant circadian clock plays an important role in the recruitment of a rhizosphere microbiome which facilitates plant health.

A. thaliana is a non-mycorrhizal plant, and its growth is reduced when its roots are in the presence of an arbuscular mycorrhizal mycelium (Veiga et al., 2013). The significantly higher relative abundance of arbuscular mycorrhizal fungi observed in the *lhy-ox* rhizosphere may therefore reduce plant fitness and biomass. Concurrent with this possibility are our observations of a growth phenotype in *lhy-ox* plants, where we observed lower overall biomass, including both smaller leaves and root systems. Similarly, the lower relative abundances of endophytic and saprotrophic fungi observed in *lhy-ox* plants may also have implications for plant health. Living symbiotically within plant tissues for at least part of their life cycle, endophytic fungi can act to increase plants' water and nutrient intake and confer biotic and abiotic stress tolerance (Rodriguez et al., 2009). Saprotrophic fungi, which feed on dead and decaying matter, have been demonstrated to stimulate some antifungal bacteria, and it has been suggested that they may be able to enhance natural biocontrol against soil-borne plant pathogenic fungi (de Boer et al., 2015). Additionally, as the main means of litter

decomposition, saprotrophic fungi play an important role in the cycling of nutrients through ecosystems (Crowther et al., 2012), indicating that the normal function of the plant circadian clock may be of importance in the maintenance of microbial communities capable of contributing to biogeochemical cycles.

The total relative abundances of pathogenic OTUs were similarly high across all samples, indicating that a high pathogen load was present in the soil used. However, plants with *lhy* loss-of-function and overexpression harboured differing communities of pathogens to each other and to wild-type plants, as several of the most highly abundant pathogenic OTUs significantly differed in relative abundance between rhizosphere samples. Identifying that *lhy* dysfunction influences the recruitment of particular OTUs within this important functional group is significant as the complex microbial communities present in the rhizosphere interact to determine the outcome of pathogen infection (Raaijmakers et al., 2009), and it is of importance to determine the factors which affect this.

2.4.1.3. Differing responses to plant circadian clock dysfunction between total and active rhizosphere communities

The responses of rhizosphere bacteria and fungi to *lhy* loss-of-function and overexpression differed between total and active microbial communities. These *lhy* mutations influenced the overall community composition, microbial diversity, and relative abundances of fungal guilds within total microbial communities only. Additionally, while the *lhy* mutations influenced the relative abundance of bacterial phyla, fungal classes and highly abundant pathogenic OTUs in both total and active communities, the responses of each differed, providing further evidence that the assembly of total and active rhizosphere communities responded differently to circadian clock dysfunction. However, these results also suggest that *lhy* loss-of-function and overexpression exerted a greater influence upon all of the taxa which accumulate in the rhizosphere microbiome over the course of plant growth, including those members which may become dead or dormant by the time of sampling. As such, the characterisation of total microbial

communities was found to be more capable of detecting the influence of plant circadian clock dysfunction upon rhizosphere microbiome assembly.

2.4.2. Diel changes in the composition of the rhizosphere microbiome are influenced by the plant circadian clock

We observed diel changes in the composition of the rhizosphere microbiome in the form of rhythmic OTUs, which significantly differed in relative abundance between dawn and dusk time points. These diel changes were widely observed as they were characterised within the total and active bacterial and fungal communities we examined from rhizosphere samples, and were also present in the microbiome of bulk soil. We found that *lhy* loss-of-function and overexpression influenced which OTUs were rhythmic in rhizosphere samples. Due to the timing of the sampling we conducted, the proportions of rhythmic OTUs observed here could be an underestimate, as other OTUs which peaked in relative abundance at other points during the day may have been missed.

In addition to the rhizosphere microbiome of wild-type plants (Hubbard et al., 2017; Staley et al., 2017; Baraniya et al., 2018), diel changes have previously been observed in the rhizosphere microbiome of plants with a dysfunctional circadian clock (Staley et al., 2017) and also in the bulk soil microbiome (Staley et al., 2017). However, previous studies only investigated bacterial communities from the rhizosphere (Hubbard et al., 2017; Staley et al., 2017; Baraniya et al., 2018). We therefore extended our observations to both bacteria and fungi, and we identified rhythmic OTUs within bacterial and fungal communities of wild-type, *lhy-11*, and *lhy-ox* rhizosphere microbiomes, and in the bulk soil microbiome.

2.4.2.1. Diel changes in the rhizosphere microbiome of wild-type plants

Previous investigations identified significant differences in the overall composition of total bacterial communities between light- and dark-taken rhizosphere samples of wild-type plants (Hubbard et al., 2017; Staley et al., 2017). However, in this study we did not observe diel differences in the overall composition of total or active bacterial or fungal rhizosphere communities. This may be due to the timing

of the sampling conducted here or the high relative abundances of pathogens observed in our samples, which could have overwhelmed any such differences.

Additional work on rhizosphere samples from wild-type *A. thaliana* plants was conducted by Staley et al. (2017). Staley et al. (2017) identified rhythmic bacterial taxa in two ways: rhythmic OTUs which significantly differed in their relative abundance between light- and dark-taken samples, and secondly, families which exhibited 'cycling dynamics' in their relative abundance within samples taken every 6 hours. There, rhythmic OTUs comprised ~8 – 10% of the relative abundance of total bacterial communities, while cycling families formed ~13% of the relative abundance (Staley et al., 2017). Similar proportions of rhythmic OTUs were found in our study, as we found that rhythmic bacterial OTUs from total communities comprised 10.0 – 12.6% of the wild-type rhizosphere.

We also observed parallels between our data and the findings of Baraniya et al. (2018). The transcriptional activity of several microbial orders from the rhizosphere of wild-type *H. vulgare* plants significantly differed between pre- and post-dawn sampling points (Baraniya et al., 2018). All five bacterial orders showing diel changes in transcription belonged to Proteobacteria (Baraniya et al., 2018). Similarly, in the active rhizosphere community of wild-type *A. thaliana*, we also identified Proteobacteria as containing the highest relative abundance of rhythmic bacterial OTUs. Additionally, the rhythmic OTUs from total bacterial communities identified by Staley et al. (2017) most commonly belonged to Proteobacteria. Proteobacteria is therefore of particular interest in relation to circadian influences upon the rhizosphere microbiome. This is because, in multiple studies, this phylum and its members have been prominent within both rhythmic taxa and those which are influenced by the effect of plant circadian clock dysfunction on rhizosphere composition (Hubbard et al., 2017; Staley et al., 2017; Baraniya et al., 2018; as also mentioned in Section 2.4.3 of this thesis).

2.4.2.2. Diel changes in the microbiome of bulk soil

Staley et al. (2017) observed diel changes in microbiota from bulk soil samples. ~13 – 18% of the relative abundance of bulk soil communities were comprised of

rhythmic OTUs, while cycling families comprised ~1% (Staley et al., 2017). Contrastingly, in our study, rhythmic OTUs formed ~5 – 6% of the relative abundance of total bacterial communities from bulk soil. We found that there was little overlap between the rhythmic OTUs observed in rhizosphere and bulk soil samples. This suggests that while diel changes in microbial community composition could be found in soil alone, the presence of plant roots changed the subsets of OTUs which displayed rhythmicity. As bulk soil is not influenced by plant roots and therefore not subject to rhythmic plant-derived signals such as root exudation, environmental light-dark cycles must therefore drive diel changes in the bulk soil microbiome.

2.4.2.3. The influence of plant circadian clock dysfunction upon diel changes in the rhizosphere microbiome

Diel changes in the rhizosphere microbiome of plants with circadian clock dysfunction were also characterised by Staley et al. (2017). Staley et al. (2017) found that cycling families comprised ~4% of the relative abundance of total bacterial communities within the *cca1-ox34* rhizosphere. *cca1-ox34* plants overexpress the circadian clock gene *CCA1* and under light-dark cycles exhibit driven rhythms only (Green et al., 2002). By comparison, the work presented here found that rhythmic OTUs from the rhizosphere of *lhy-11* and *lhy-ox* plants formed higher proportions of total bacterial communities (~8% and ~13 – 15% respectively by total relative abundance). *CCA1* and *LHY* are thought to have overlapping functions as part of the plant circadian clock (Mizoguchi et al., 2002) and both *cca1-ox34* and *lhy-ox* plants both possess a circadian phenotype of driven rhythms under light-dark cycles (Green et al., 2002; Kim et al., 2003), so we anticipated potentially similar effects of these mutations upon rhythmicity in the rhizosphere. Contrastingly, *lhy-11* plants display a phase advance under light-dark cycles (Mizoguchi et al., 2002). The differing proportions of rhythmicity observed between the *cca1-ox34* rhizosphere and our *lhy-11* and *lhy-ox* samples could be explained by the different statistical tests which were used, as the method we employed could be less stringent than that Staley et al. (2017) used to identify cycling families. Additionally, the differing sampling times or soil types used may also contribute, as we sampled at dawn and dusk while Staley et al.

(2017) collected samples at 6-hourly intervals during both light and dark periods for their analysis of cycling families. Further, the differing circadian phenotype of *lhy-11* when compared to *cca1-ox34* plants could also contribute to the differing degrees of rhythmicity observed between these two mutants specifically.

As it had not previously been investigated whether dysfunction of the plant circadian clock influences diel changes in rhizosphere microbiome composition, we compared our rhythmic OTUs from wild-type plants with those identified in the rhizosphere of plants with *lhy* loss-of-function and overexpression. Loss-of-function and overexpression of *lhy* influenced the specific community members which displayed rhythmicity, as well as the taxonomic groupings and total relative abundances of these rhythmic OTUs. In addition to differing between *lhy* mutant and wild-type plants, we also found that these aspects of the rhythmic OTUs also differed between the two mutants.

The circadian phenotype of host plants therefore influenced diel changes in the rhizosphere microbiome, and different subsets of rhizosphere communities displayed rhythmicity in different host plants. These results suggest that the rhythmic potential of some OTUs may only be visible in the rhizosphere of plants with particular circadian phenotypes. This could explain the observed differences in rhythmic OTUs between rhizosphere samples, as the rhythmicity of only some rhizosphere microbiota may be compatible with that of the circadian clock of wild-type plants. This may be because particular OTUs may respond differently to the potential impacts of circadian clock dysfunction upon the expression of other genes. For example, *LHY* also controls the expression of many genes involved in biotic and abiotic stress responses (Adams et al., 2018). Relatedly, in the fungal communities we characterised, particularly high differences in the total relative abundances of rhythmic OTUs were observed between dawn and dusk samples. This is of interest as many fungi possess their own circadian clocks (Baker et al., 2012), which could potentially be acting in resonance with the plant circadian clock and therefore amplifying the diel changes observed.

2.4.2.4. Differing diel changes in the rhizosphere microbiome between total and active rhizosphere communities

We observed diel changes in both the total and active communities within the rhizosphere microbiome, and similar proportions of rhythmic OTUs were found within total (DNA-based) and active (RNA-based) communities. This was surprising as we anticipated that while DNA-based approaches have previously characterised diel changes in the rhizosphere microbiome (Hubbard et al., 2017; Staley et al., 2017), the profiling of active communities using RNA, which is less stable and degraded faster than DNA (Wang and Kool, 1995), would be a more sensitive approach capable of identifying more diel changes in rhizosphere composition. Both DNA- and RNA-based approaches were therefore sufficient for detecting diel changes in the rhizosphere microbiome.

However, the limitations and concerns regarding the use of RNA as an indicator of 'active' microbiota within environmental samples must be discussed. The previously generally accepted paradigm that rRNA sequencing can identify currently 'active' community members has faced criticism, as the assumptions it is based upon may be false in many circumstances (Blazewicz et al., 2013). While cells considered to be active may be metabolising but not necessarily dividing, it is assumed that growth accounts for the majority of cells' activity (Blazewicz et al., 2013). However, rRNA concentrations are not a robust proxy for microbial growth, as rRNA levels do not always correlate with microbial growth rates and this correlation also differs between taxa and environmental conditions (Blazewicz et al., 2013; Emerson et al., 2017). Most studies concerning the relationship between rRNA concentration and growth rates were conducted in pure culture under laboratory conditions, and the relationship between rRNA and other non-growth-related indicators of activity, such as osmoregulation or conjugation, has not yet been investigated (Blazewicz et al., 2013). Additionally, increased concentrations of rRNA have been observed in bacterial cells transitioning to dormancy in preparation for their emergence from this state (Sukenik et al., 2012), indicating that increases in rRNA abundance may not always indicate increases in activity. Taking into account these possible limitations of using rRNA to identify currently active community members, we therefore acknowledge that, as suggested by Blazewicz et al. (2013), the

microbiota identified in this study using rRNA sequencing could be better described as those displaying protein synthesis potential.

While similar proportions of rhythmic OTUs were observed in each, the specific rhythmic members, their taxonomy, and total relative abundances differed between DNA- and RNA-based approaches within each sample type. This indicates that the profiling of microbial DNA and RNA each detected rhythmicity within different subsets of the rhizosphere microbiome, and therefore the diel dynamics in this region appear to be more complex than expected.

Active microbes, which may include those with protein synthesis potential that we identified using the sequencing of rRNA, must be metabolising in order to be termed active but may also be dividing (Blazewicz et al., 2013). Contrastingly, the microbiota we identified via DNA sequencing could be termed 'growing', whereby they may not be currently metabolising but are still dividing (Blazewicz et al., 2013). Such 'growing' and 'active' community members could respond differently to factors which may contribute to rhythmicity in the rhizosphere microbiome, which could explain why the communities based upon the characterisation of DNA and RNA each contained different rhythmic members. Additionally, the differing rhythmicity in these two subsets of the rhizosphere microbiome could be due to different mechanisms. The rhythmicity we identified in OTUs from RNA-based communities could be due to diel changes in cell abundance or rRNA production, while the rhythmicity in OTUs from DNA-based communities could be due to changes in cell abundance only. Additionally, it is also possible that due to the use of relative abundance metrics in this work, the observed changes in OTUs' relative abundance may not be reflective of absolute differences in cell abundance *in situ*, as these may also be affected by alterations to the absolute or relative abundance of other OTUs.

Rhythmicity in the rhizosphere could be driven by the plant circadian clock, such as changes in the volume or composition of root exudates, or by interactions with other rhizosphere microbiota, such as possible oscillations in predation pressure from protists. Diel changes in microbial movement could also occur as some microbes may capable of relatively quick movement through water-filled soil

pores (Watt et al., 2006). Additionally, the rapid turnover of microbial communities may occur, as diel changes in the rates of growth and dieback have been observed in soil fungi (Hernandez and Allen, 2013). These mechanisms could potentially lead to the rhythmicity we observed by characterising both DNA and RNA. Additionally, Lepp and Schmidt (1998) demonstrated that the rRNA content of cyanobacterial cells increased in dark periods when grown under light-dark cycles. Such accumulation of rRNA during periods of lower metabolic activity may confer an advantage in more favourable conditions (Blazewicz et al., 2013). In the rhizosphere, favourable conditions for any given microbial species could occur at any time of the day, for example due to the presence of a particular substrate which may be rhythmically exuded from plant roots. Such patterns of rRNA accumulation could provide an additional explanation for the rhythmicity observed in our characterisation of microbial RNA in the rhizosphere.

CHAPTER 3: RHYTHMICITY IN THE RHIZOSPHERE MICROBIOME PERSISTS UNDER CONSTANT CONDITIONS

3.1. Introduction

3.1.1. Introduction

Persistence of circadian oscillations under constant conditions, commonly described as free-running rhythmicity, with a period of approximately 24 hours is a key indicator of rhythmicity caused by an endogenous circadian oscillator. While it has been demonstrated that there are rhythmic changes in the rhizosphere microbiome under diel light-dark cycles (Chapter 2; Hubbard et al., 2017; Staley et al., 2017; Baraniya et al., 2018), it is not known whether such oscillations persist under constant environmental conditions. Three different factors may drive rhythmicity in the rhizosphere microbiome: (i) a direct effect of environmental light-dark cycles; (ii) rhythmic changes caused by the plant circadian clock, particularly due to rhythmic changes in root exudation; and (iii) autonomous circadian clocks within rhizosphere microbiota. Rhythmicity in the rhizosphere microbiome which is driven by the latter two factors will persist under constant conditions.

Rhizosphere microbiota may be directly influenced by light-dark cycles as light is able to penetrate soil to some degree. It is thought that light is able to pass through the top few millimetres of soil directly (Tester and Morris, 1987). Alternatively, rhythmicity in the rhizosphere microbiome under constant conditions may be driven by the plant circadian clock. Many processes which likely contribute to the creation of a rhythmic environment within the rhizosphere are under the influence of the plant circadian clock, and therefore persist under constant conditions. While it is not known whether the diel changes previously observed in root exudation (Ma and Nomoto, 1996; Watt and Evans, 1999; Iijima et al., 2003; Tharayil and Triebwasser, 2010) also persist under constant conditions, the plant circadian clock is known to control other processes relating to energy use, namely photosynthesis, the allocation of fixed carbon, and nutrient

utilisation (Somers et al., 1998; Gutiérrez et al., 2008; Graf et al., 2010). The plant circadian clock also regulates the production of defence molecules and controls rates of root growth (Yazdanbakhsh et al., 2011; Goodspeed et al., 2012). Members of the rhizosphere microbiome may therefore respond to free-running rhythmic changes in their environment caused by the presence of plant roots.

Another possibility is that some members of the rhizosphere microbiome may themselves possess a circadian clock that could cause potential free-running rhythmicity in this region. Microbial circadian clocks have been well characterised in some model fungi and cyanobacteria (Baker et al., 2012; Cohen and Golden, 2015), and homologues of their components have also been identified in other species (Dvornyk et al., 2003; Loza-Correa et al., 2010; Rodriguez-Romero et al., 2010; Salichos and Rokas, 2010; Schmelling et al., 2017; Lee et al., 2018). Work in the model Ascomycete *Neurospora crassa* elucidated the mechanism of the fungal circadian clock, which involves a negative feedback loop of transcription between Frequency (FRQ) and the White Collar Complex (composed of WC1 and WC2) (Baker et al., 2012). There is evidence that members of some other fungal classes possess homologues of the FRQ and WCC proteins. For example, Agaricomycetes and Eurotiomycetes contain WC1 and WC2 homologues, and Dothideomycetes and Leotiomycetes contain homologues of WC1, WC2 and FRQ (Salichos and Rokas, 2010) suggesting that members of these classes may also possess some form of circadian oscillator. A circadian clock was identified in cyanobacteria chiefly through the study of *Synecococcus elongatus*. The cyanobacterial circadian clock is a post-translational oscillator involving rhythmic phosphorylation cycles and the components KaiA, KaiB, and KaiC (Cohen and Golden, 2015). Homologues of cyanobacterial *kaiB* and *kaiC* genes (and also their corresponding proteins) have also been found in some non-photosynthetic bacterial phyla, namely members of Proteobacteria, Chloroflexi, Bacteroidetes, Chlamydiae, Planctomycetes and Acidobacteria (Dvornyk et al., 2003; Loza-Correa et al., 2010; Schmelling et al., 2017), suggesting that these may also contain a timekeeping mechanism.

While many bacterial and fungal taxa may possess possible circadian clock components, little is known about the potential rhythmic behaviour of non-

photosynthetic microbiota. *N. crassa* displays well-characterised rhythms in its alternation between mycelial and conidial production (Baker et al., 2012), and a handful of other fungal species have been demonstrated to display rhythmicity in various physiological processes under constant conditions. These included spore discharge, virulence, bioluminescence, hyphal melanisation and sclerotial formation, with the latter three also displaying temperature compensated rhythms whereby their period remained relatively constant over a range of temperatures (Austin, 1968; Greene et al., 2003; Bluhm et al., 2010; Hevia et al., 2015; Oliveira et al., 2015).

Less still is known about free-running circadian behaviour in bacteria outside of the cyanobacteria and to date just two bacterial species have been demonstrated to display such rhythmicity. The rhythmic growth of *Pseudomonas putida* persisted under constant darkness for one daily cycle (Soriano et al., 2010), and the swarming behaviour of *Enterobacter aerogenes* displayed temperature compensated rhythmicity for four cycles under constant conditions in the presence of melatonin (Paulose et al., 2016).

All previous studies characterising both bacterial and fungal free-running rhythmicity have been conducted using culture-based methods, where single species were investigated alone. However, it has been suggested that in order to best capture the circadian capabilities of non-photosynthetic organisms, studies should instead focus on the complex environments they are found within, such as soil. Sartor et al. (2019) proposed that such an approach should prove more fruitful for the detection of microbial circadian rhythmicity than culture-based experiments on single species, because these natural environments contain complex signals from the growth substrate and other microbial community members present. The rhizosphere is an ecologically important complex environment, containing a diverse array of microbiota under the influence of a host plant with well-characterised circadian processes. It is therefore likely that the rhizosphere microbiome may contain some microbes which display rhythmicity under constant conditions, whether this is due to their responses to the circadian clock of their host plant or an autonomous oscillator of their own.

3.1.2. Aims

The aims of this work were to:

1. Determine whether microbial rhythmicity in the rhizosphere microbiome persists under constant conditions.
2. Test whether this rhythmicity is dependent on the plant circadian clock or upon autonomous microbial oscillators.
3. Investigate the relationship between microbial rhythmicity in the rhizosphere microbiome and the possession of homologues of known circadian clock components.

3.2. Methods

3.2.1. Plant growth and sampling

Wild-type L*er* (Landsberg *erecta* ecotype) and *lhy-ox A. thaliana* plants were used in this study and are described in Chapter 2.

All plants were grown in the Wick series sandy loam soil described in Chapter 2, which was collected in April 2019 and then homogenised by passage through a 3 mm sieve. Following stratification of seeds at 4 °C for 7 days, wild-type and *lhy-ox* plants were grown in modular pots for 6 weeks in a Sanyo Versatile Environment Test Chamber MLR-350 (Sanyo, Moriguchi, Japan). Wild-type and *lhy-ox* plants were grown in separate trays, with up to four plants occupying each modular pot. To minimise the effects of cabinet position on plants, trays were rotated and their position changed daily. Plants experienced 12L:12D lighting cycles at 22 °C, received 55 – 100 μmol/m^2/sec of light (dependent on position within the cabinet), and were watered as required to maintain the original moisture content of the soil.

Trays of plants were split equally into two growth cabinets which were both set to the same conditions but were each under oppositely phased lighting cycles. This allowed sampling at three-hour intervals to take place during working hours. Sampling was undertaken at dawn, then three, six and nine hours after dawn, from both cabinets simultaneously. As a result of the growth of plants in these two oppositely phased cabinets, samples were also obtained for time points

representing 12, 15, 18 and 21 hours after dawn. Sampling under dark conditions was conducted under green lighting so as to not influence the plants' circadian clocks. Sampling was conducted over three days – the first under light-dark cycles, then the following two days after switching to constant conditions and a gap of 24 hours to adjust (Figure 3.1).

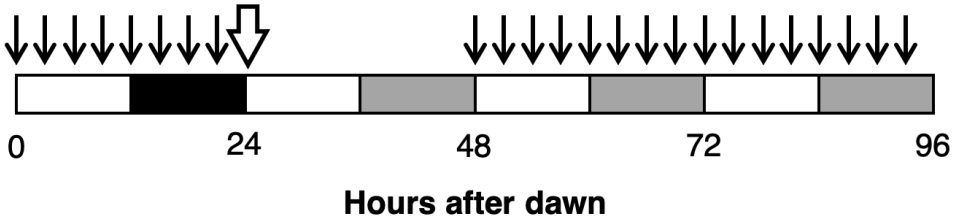

Figure 3.1. Sampling strategy employed to investigate rhythmicity in the rhizosphere microbiome under constant conditions. The black bar represents night; grey bars represent subjective night. The large arrow indicates the switch to constant conditions; all other arrows indicate sampling points.

A minimum of eight plants were pooled to form one sample, and four such replicate samples were taken at each sampling point. Root systems were carefully removed from pots and non-adhering soil was gently brushed off using tweezers, and then roots were cut from the shoot just below the stem. Root and rhizosphere compartments were then separated using a miniature version of the root washing protocol as described by Hilton et al (in press). For each sample, all excised roots were firstly combined into a single pre-prepared 2ml Cryovial tube containing 750 μl sterile water. This was shaken 20x, then the roots removed using fine tweezers cleaned with ethanol. Roots were placed in a microcentrifuge tube containing 750 μl sterile water and shaken a further 20x. After the roots were again removed from this tube, its contents were poured into the first Cryovial. These two washes combined formed the rhizosphere compartment for each sample. The roots were transferred to another microcentrifuge tube containing 1000 μl sterile water and shaken 20x again before being transferred to a Cryovial. This was the root compartment – the water from this final washing step was discarded.

At each time point, one additional sample was collected for RNA analyses. A minimum of 8 plants were pooled to form each additional sample. Root systems were carefully removed from pots and non-adhering soil was gently brushed off using tweezers. Roots were cut from the shoot just below the stem and placed into Lysing Matrix E tubes (MP Biomedicals, Irvine, USA). This resulted in a composite root and rhizosphere sample.

All samples were immediately frozen in liquid nitrogen and then transferred to -80 °C. In this study, only the rhizosphere compartment samples were analysed.

3.2.2. Microbial community profiling

3.2.2.1. Nucleic acid extraction

DNA was extracted from rhizosphere samples using the FastDNA® SPIN Kit for Soil (MP Biomedicals, Irvine, USA) according to the manufacturer's instructions. Extracted nucleic acids were resuspended in 50 μl of Elution Buffer at the final step, or 100 μl when larger amounts of residue were present in the SPIN™ Filter.

Concentrations of DNA in the samples were checked with a Qubit fluorometer 2.0 (Life Technologies) using the high sensitivity DNA assay. 5 μl of each sample was diluted ten-fold using sterile nuclease-free water, and this diluted DNA was used for downstream analysis. Two additional extractions were also performed at this stage, using empty Lysing Matrix E tubes. These samples were used as negative controls throughout the library preparation process and during MiSeq sequencing.

3.2.2.2. Library preparation

PCR amplification of DNA from the target bacterial 16S rRNA and fungal Internal Transcribed Spacer (ITS) regions was conducted. The V4 region of the 16S rRNA gene was amplified using the 515f/806r primers (515f: 5' GTG YCA GCM GCC GCG GTA A 3'; 806r 5' GGA CTA CNV GGG TWT CTA AT 3'; Apprill et al., 2015; Parada et al., 2016) and the ITS2 region of the ITS gene was amplified using the 3f/4r primers (3f: 5' GCA TCG ATG AAG AAC GCA GC 3'; 4r: 5' TCC TCC GCT TAT TGA TAT GC 3'; White et al., 1990). These primers were modified at the 5'

end with Illumina adaptors, and PCRs were conducted as described in Chapter 2.

The products from these PCRs were purified using SPRI beads, a homemade alternative (Rohland and Reich, 2012) to Agencourt AMPure XP beads (Beckman Coulter, High Wycombe, UK), according to the manufacturer's instructions. In order to multiplex the samples ready for pooling and sequencing, a second round of PCRs took place for library preparation using short Illumina Nextera index primers as described in Chapter 2.

Following the addition of indexing primers, all samples were processed using the SequalPrep Normalisation Kit (Invitrogen brand, Thermo Fisher Scientific, Waltham, USA) according to the manufacturer's instructions. This ensured that the final PCR product was purified, and that the DNA and cDNA from each sample were equalised to 25 ng. All samples were then combined, and the resultant pooled samples diluted to 4 nM. Sequencing of 300 bp paired-end reads was then performed on an Illumina MiSeq machine (Illumina, San Diego, USA) at the Earlham Institute, Norwich, UK.

3.2.3. RNA analyses

3.2.3.1. RNA extraction and cDNA generation

RNA was extracted from the composite root and rhizosphere samples using the method described in Chapter 2.

DNA was removed and cDNA subsequently generated from the extracted RNA as described in Chapter 2.

3.2.3.2. RT-qPCR assays

The relative expression of the genes of interest at each time point was quantified using the $2^{\Delta\Delta Ct}$ method (Livak and Schmittgen, 2001). The *LUX* circadian clock gene (At3g46640) was amplified using the forward primer (5' – 3') TGG CGG TAG CAG CGG TAA and reverse primer (5' – 3') TCA TCT GTT GCG TTC CAT ACG) and the *ACTIN2* housekeeping gene (At3g18780) was amplified using the

forward primer (5' – 3') TCA GAT GCC CAG AAG TCT TGT TCC and reverse primer (5' – 3') CCG TAC AGA TCC TTC CTG ATA TCC.

All qPCR reactions were performed on an Agilent MX3005P machine (Agilent, Santa Clara, US) using the SYBR Green™ reagent (Sigma-Aldrich, Missouri, USA). Reactions were run in triplicate and final volumes in each were as follows: 10 μl SYBR Green 2x Readymix, 4 μl sterile molecular-grade water, 2 μl forward primer (3 μM), 2μl reverse primer (3 μM), 2 μl template cDNA. Reactions were conducted under the following conditions: denaturation at 95 °C for 10 minutes; 40 cycles of denaturation at 94 °C for 30 seconds, annealing at 58 °C for 1 minute, and elongation at 72 °C for 1 minute. To check that amplicons of only one size were generated, a dissociation curve was produced by running the following additional cycle at the end: 95 ºC for 1 minute, 58 ºC for 30 seconds, 95 ºC for 30 seconds. The annealing temperature of all primers used was 58 ºC.

3.2.4. Processing of amplicon sequencing data

Raw sequences were automatically de-multiplexed by the Illumina MiSeq machine. Low-quality bases were removed from the ends of sequences using Trimmomatic v0.39 (Bolger et al., 2014). USEARCH 9 (Edgar, 2010) was used to join paired-end reads, conduct quality filtering, trim off primer sequences, and dereplicate the data to determine the number of unique sequences. USEARCH 9 was also used to cluster the reads into Operational Taxonomic Units (OTUs) – groups with ≥97% sequence similarity – and conduct chimera filtering. QIIME (Quantitative Insights Into Microbial Ecology) 1.9.1 (Caporaso et al., 2010) was used to assign taxonomy to the OTUs, using release 132 of the SILVA database (Quast et al., 2012) for the 16S rRNA data and version 7.2 of the UNITE database (Kõljalg et al., 2005) for the ITS data. Filtering was undertaken using QIIME 1.9.1 to remove reads that were annotated as mitochondria or chloroplasts in the 16S rRNA dataset. Additionally, the ITS dataset was manually investigated for *A. thaliana* sequences known to be mis-annotated as fungal taxa, and these were removed.

All subsequent analyses were conducted in R Studio (running R Version 3.6.0). Data were first normalised using the DESeq2 package (Love et al., 2014), which also removed samples with under 1,000 reads and OTUs with 0 reads.

Raw sequence files were uploaded to the NCBI (National Centre for Biotechnology Information) Sequence Read Archive (https://www.ncbi.nlm.nih.gov/sra) under the BioProject accession number PRJNA678539. Nucleotide sequences of rhythmic OTUs identified under constant conditions were uploaded to the NCBI GenBank (https://www.ncbi.nlm.nih.gov/genbank/) under submission number SUB8586379 for bacteria and SUB8586077 for fungi.

3.2.5. Rhythmicity analyses

For all rhythmicity analyses, OTUs were only considered if they were present in more than 50% of sampling points from both the light-dark and constant conditions portions of the experiment. Kruskal-Wallis pairwise testing was used to identify rhythmic OTUs under light-dark cycles, which displayed significant differences in their mean relative abundance in samples taken between 9 to 15 hours apart. The R package MetaCycle (Wu et al., 2016) was used to identify rhythmic OTUs under constant conditions. MetaCycle detected periodicity in the mean relative abundances of individual OTUs using the JTK_Cycle (Hughes et al., 2010) and Lomb-Scargle (Glynn et al., 2006) algorithms, and Fisher's method (Fisher, 1925) was used to integrate the p values from both algorithms. OTUs with a corrected p value of ≤ 0.05 were considered significantly rhythmic. MetaCycle analysis was repeated on randomised versions of the OTU tables, resulting in 0 rhythmic OTUs found, thereby confirming the rhythmicity observed was reliable. The FUNGuild annotation tool (Nguyen et al., 2016) was used to identify the ecological functional guild of fungal rhythmic OTUs of interest.

3.2.6. Identification of circadian clock protein homologues

Homologues of microbial circadian clock proteins were identified by using TBLASTN searches of the NCBI non-redundant nucleotide database, where the amino acid sequences of known core components of bacterial and fungal circadian clocks were used as queries (Sayers et al., 2020). Protein sequences

of KaiA, KaiB, and KaiC from the cyanobacterium *Synechococcus elongatus* PCC 7942 were used for bacteria, and FRQ (Frequency), WC1 (White Collar 1), and WC2 (White Collar 2) from the fungus *Neurospora crassa* were used for fungi. Search results were determined to show evidence of homology when their E value was lower than 0.01, percentage identity was greater than 20%, and query cover was greater than 80% for bacteria and ~40% for fungi.

3.3. Results

To investigate rhythmicity in the rhizosphere microbiome under constant conditions, sampling of wild-type and *lhy-ox A. thaliana* plants was conducted every three hours over a period of three days (Figure 3.1). The first day of sampling was conducted while plants were still under light-dark cycles, to allow rhythmicity in the rhizosphere microbiome to be compared between light-dark cycles and constant conditions. Plants were then switched to constant conditions, and 24 hours later, two further days of sampling under these conditions began. As it was already demonstrated in Chapter 2 that the profiling of DNA from microbial communities was sufficient to detect rhythmic changes in rhizosphere microbiota, amplicon sequencing of DNA only was conducted in this chapter.

A total of 22,647,198 raw reads were obtained from the MiSeq run. After all pre-processing was complete, 2,714,477 reads were obtained for the bacterial (16S rRNA gene) amplicon, and 4,152,598 reads were obtained for the fungal (ITS region) amplicon. A range of 29 – 49,827 raw reads with an average of 14,136 per sample were obtained for the 16S rRNA gene, and a range of 12 – 65,977 with an average of 21,628 per sample were obtained for the ITS region. After DESeq2 normalisation, where samples with under 1,000 reads and OTUs with 0 reads were removed, 7,965 OTUs and 178 of the original 189 samples remained in the bacterial data, and 2,032 OTUs and 166 of the 189 samples remained in the fungal data.

3.3.1. Microbial rhythmicity in the rhizosphere microbiome persists under constant conditions in the rhizosphere of wild-type plants

To identify whether rhythmicity in the rhizosphere microbiome persisted under constant conditions in the rhizosphere of wild-type plants, rhythmic OTUs were identified from the constant light and temperature (LL) portion of the experiment using MetaCycle (Wu et al., 2016). The normal functioning of the plant circadian clock under LL was confirmed by quantifying the relative expression of the evening-phased circadian clock gene *LUX ARRHYTHMO* (Figure 3.2).

1,381 bacterial and 201 fungal OTUs were rhythmic under LD, as determined by Kruskal-Wallis pairwise testing of samples taken between 9 – 15 hours apart. This represented 46.5% and 54.7% respectively of all bacterial and fungal OTUs analysed (Figures 3.3.a and 3.3.c) and 67.2% and 76.8% of overall microbial communities.

Fewer OTUs were found to be rhythmic under LL, which may be because MetaCycle is much more stringent than the method used to test for rhythmicity under LD. Under LL, 49 bacterial and 44 fungal rhythmic OTUs were found (Table A3.1), comprising 1.6% and 12% of all OTUs analysed and forming 6.2% and 42.3% of overall microbial communities by relative abundance respectively (Figures 3.3.a, 3.3.c, and 3.3.e). The majority of these rhythmic OTUs had also been identified as rhythmic under LD (Figures 3.3.a and 3.3.c). No correlation was observed between the rhythmicity and relative abundance of all the OTUs analysed (Figure 3.3.f). These results therefore demonstrate rhythmicity in the relative abundance of many OTUs from the rhizosphere microbiome in the absence of external cues.

The relative abundances of the rhythmic OTUs under LL from the wild-type rhizosphere are visualised over the duration of the experiment in Figures 3.4.a and 3.4.c. Two distinct waves of microbial rhythmicity were observed in both bacterial and fungal communities, with most phases of rhythmic OTUs occurring in either the middle of the night or the middle of the day (Figures 3.4.a, 3.4.c, 3.4.e and 3.4.f). These patterns were observed under LD and persisted with similar timing under LL (Figures 3.4.a and 3.4.c).

To investigate the potential ecological significance of the fungal rhythmic OTUs identified under LL, the FUNGuild annotation tool (Nguyen et al., 2016) was used and 33 of the 44 OTUs were assigned a relevant ecological guild. Most common were saprotrophs, with 19 rhythmic OTUs assigned this guild, followed by seven plant pathogenic OTUs, six endophytic, and one fungal parasitic OTU. Interestingly, the most highly abundant OTU within fungal communities was also found to be rhythmic under LL. It was identified as *Gibellulopsis nigrescens*, which was assigned as a probable plant pathogen by FUNGuild and had a mean relative abundance of 15.5% over the duration of the experiment. Many fungal rhythmic OTUs therefore belonged to guilds which form intimate associations with plants.

3.3.2. Rhythmicity in the rhizosphere microbiome under constant conditions is disrupted by circadian clock dysfunction

To investigate whether the plant circadian clock influences rhythmicity in the rhizosphere microbiome under constant conditions, we compared samples from wild-type and *lhy-ox* mutant *A. thaliana* plants. *lhy-ox* plants constitutively express the *lhy* gene throughout the day at levels close to the maximum of *LHY* expression in wild-type plants (Green et al., 2002), and under constant conditions the circadian clock of *lhy-ox* plants is arrhythmic (Schaffer et al., 1998). The abnormal functioning of the *lhy-ox* circadian clock under constant conditions was confirmed by quantifying the relative expression of the evening-phased circadian clock gene *LUX* (Figure 3.2). While the expected pattern of *LUX* expression was observed in wild-type samples, this rhythmicity was abolished in *lhy-ox* plants (Figure 3.2).

The rhythmic OTUs found in wild-type samples were also investigated in the *lhy-ox* rhizosphere (Figures 3.4.b and 3.4.d). Clearly rhythmic patterns in their mean relative abundance were no longer observed under either LD or LL, demonstrating the loss of rhythmicity in the rhizosphere of plants overexpressing *lhy* (Figures 3.4.b and 3.4.d).

Under LD, rhythmicity was observed in the *lhy-ox* rhizosphere in similar proportions to that found in wild-type samples (Figures 3.3.a to 3.3.d). 890 bacterial and 87 fungal OTUs were rhythmic under LD, comprising 33.1% and 31.0% of all OTUs analysed (Figures 3.3.b and 3.3.d) and forming 43.7% and 50.8% of overall microbial communities by relative abundance respectively. These proportions were higher than those observed in Chapter 2, where rhythmic OTUs from plants under LD formed up to ~15% of both bacterial and fungal communities by relative abundance in both wild-type and *lhy-ox* plants. This could possibly be because the rhizosphere was separated from roots in this chapter, or due to the increased time resolution of this experiment. Contrastingly, very few rhythmic OTUs were identified in *lhy-ox* samples under LL. Only 4 bacterial and 3 fungal OTUs were found to be rhythmic, representing 0.1% and 1.1% of all OTUs analysed (Figures 3.3.b, 3.3.d, and 3.3.e) and forming total relative abundances of 0.3% and 4.7% of overall bacterial and fungal communities respectively. As in wild-type *A. thaliana* samples, no correlation was observed between the rhythmicity and relative abundance of OTUs from *lhy-ox* plants under LL (Figure 3.3.g). Rhythmicity was therefore not restricted to either rare or abundant taxa.

These results therefore indicate that microbial rhythmicity in the rhizosphere microbiome is largely disrupted under constant conditions in arrhythmic plants overexpressing *lhy*. This suggests that the plant circadian clock drives most of the rhythmic changes in the rhizosphere microbiome which persist under constant conditions.

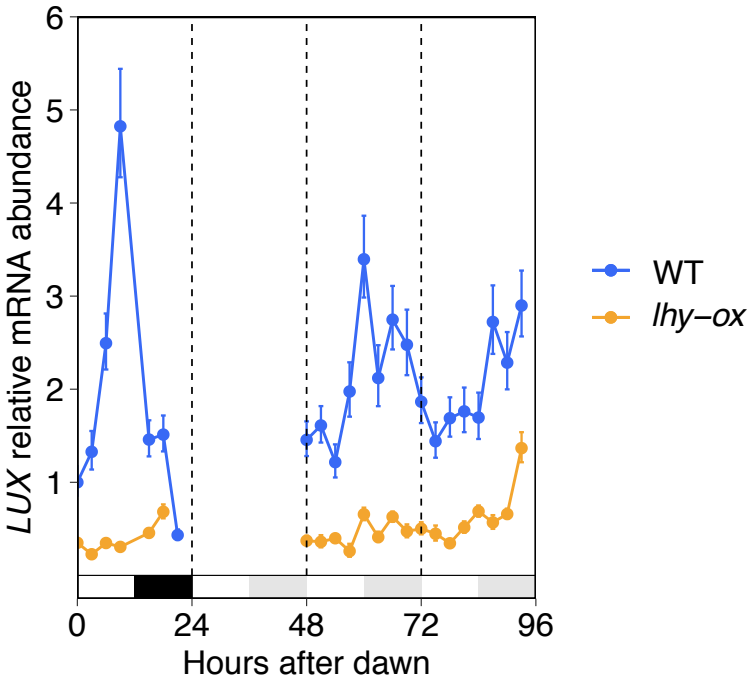

Figure 3.2. Plants with *lhy* overexpression possess a dysfunctional circadian clock under constant conditions. Expression of the evening-phased clock gene *LUX* relative to *ACTIN* in roots of wild-type and *lhy-ox* plants. All expression data were normalised to the first time point from wild-type samples. Mean from 3 technical replicates ± SEM shown.

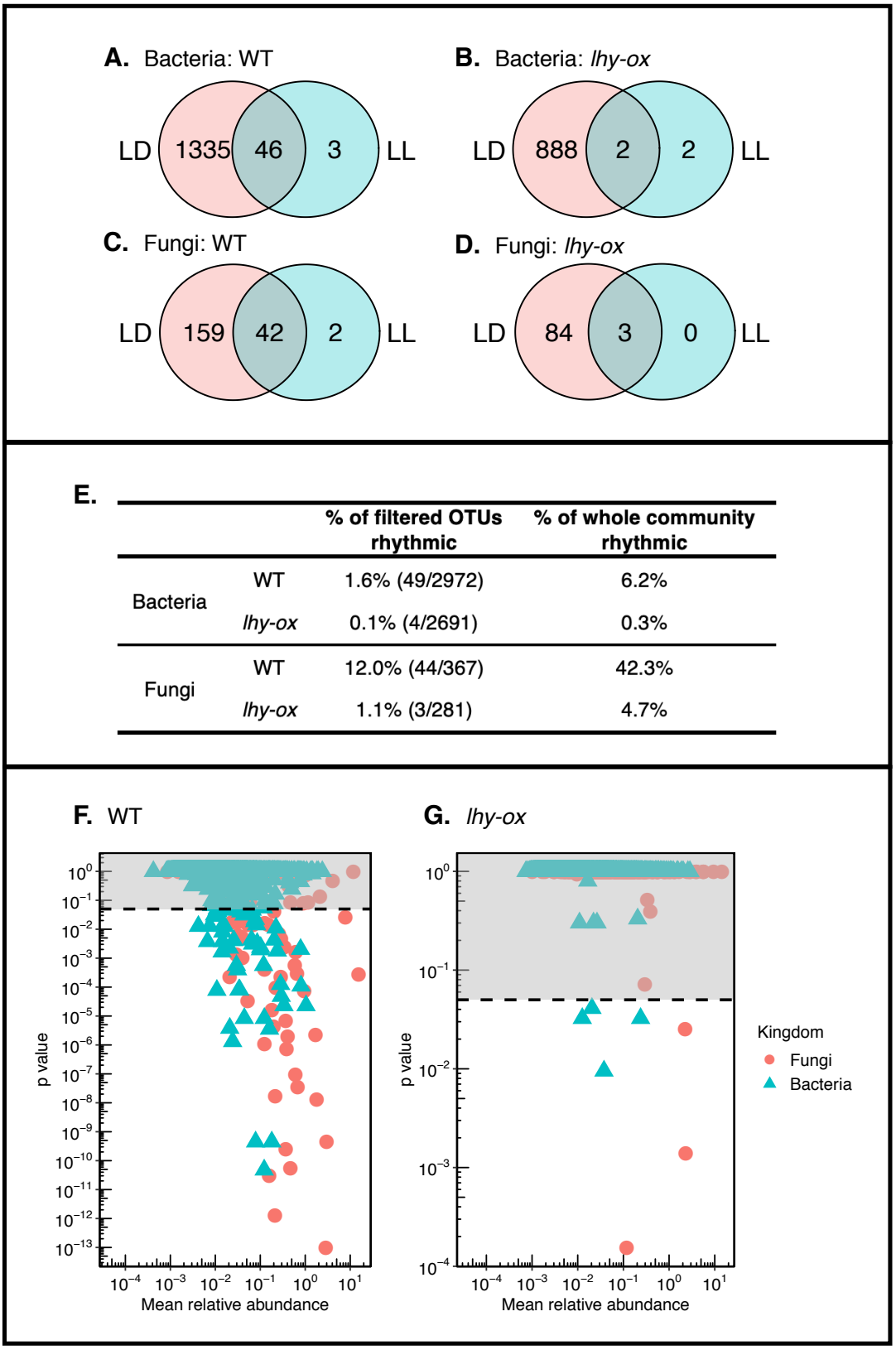

E.

		% of filtered OTUs rhythmic	% of whole community rhythmic
Bacteria	WT	1.6% (49/2972)	6.2%
	lhy-ox	0.1% (4/2691)	0.3%
Fungi	WT	12.0% (44/367)	42.3%
	lhy-ox	1.1% (3/281)	4.7%

Figure 3.3. Rhythmicity of some microbial OTUs persists in the wild-type rhizosphere under constant conditions, but not in plants overexpressing *lhy*. Rhythmic OTUs under light-dark cycles were identified as displaying a significant difference in relative abundance between any samples taken 9 to 15 hours apart. Rhythmic OTUs under constant conditions were identified using MetaCycle analysis (Wu

et al., 2016), where a meta2d.BHQ value (corrected using Fishers' method) of $p \leq 0.05$ was considered significantly rhythmic. (a) to (d) Numbers of rhythmic OTUs observed in (a) and (b) bacterial and (c) and (d) fungal communities. Left (pink) circles represent OTUs rhythmic under light-dark cycles, right (blue) circles represent OTUs rhythmic under constant conditions, and the overlap between these represents OTUs rhythmic under both light-dark cycles and constant conditions. (e) Proportions of communities rhythmic under constant conditions. (f) and (g) Mean relative abundances of all OTUs over the duration of the constant conditions portion of the experiment, compared to their p values from the MetaCycle analysis to detect rhythmicity. Dashed black lines and grey shading represent the significance cut-off for rhythmicity of $p \leq 0.05$.

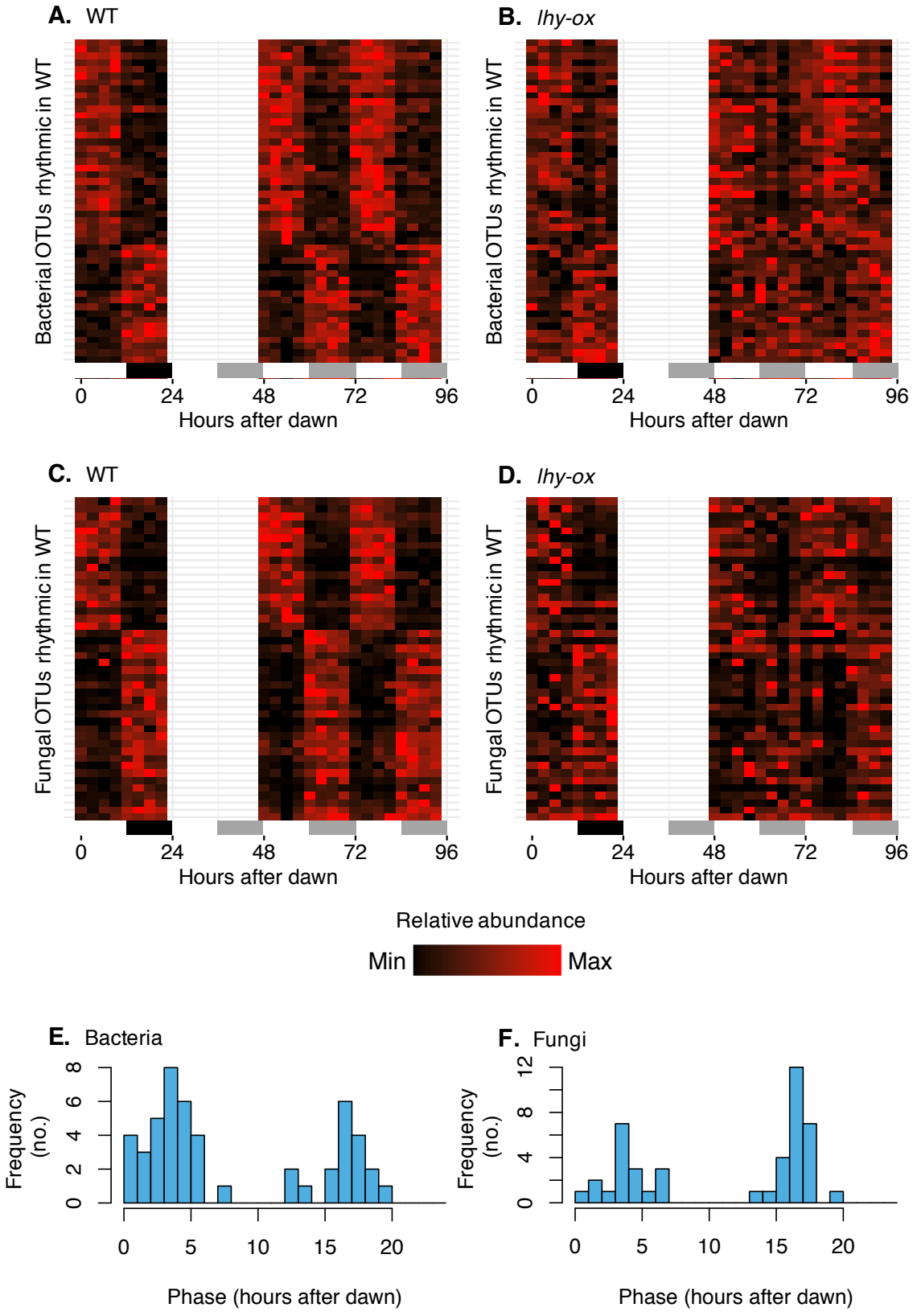

Figure 3.4. Microbial rhythmicity under constant conditions is disrupted in plants overexpressing *lhy*. Rhythmic OTUs under constant conditions were identified using MetaCycle analysis (Wu et al., 2016) where a meta2d.BHQ value (corrected using Fishers' method) of $p \leq 0.05$ was considered significantly rhythmic. Normalised relative abundances of rhythmic OTUs from wild-type *A. thaliana* plotted in (a) and (c) wild-type

and (b) and (d) *lhy-ox* rhizosphere samples. OTUs are ordered vertically by the phase of their relative abundance in the constant conditions portion of the experiment. (e) and (f) Histograms of the phase under constant conditions of (e) bacterial and (f) fungal rhythmic OTUs.

3.3.3. Autonomous rhythmicity in the rhizosphere microbiome of arrhythmic plants

A small number of rhythmic OTUs were found in the rhizosphere of arrhythmic *lhy-ox* plants under constant conditions and therefore displayed autonomous rhythmicity (Figure 3.5). Four were bacterial OTUs, including a member of *Solirubrobacterales,* and species of *Geobacter, Lutispora* and *Desulfosporosinus*, and three were fungal OTUs, identified as the probable plant pathogen *Musicillium theobromae,* the probable saprotroph *Pseudeurotium bakeri*, and the possible saprotroph *Penicillium astrolabium*. Five OTUs were rhythmic in both wild-type and *lhy-ox* samples, but the bacteria identified as *Lutispora* sp. and *Desulfosporosinus* sp. were only rhythmic in *lhy-ox* samples, suggesting that their autonomous rhythmicity was incompatible with that of the wild-type plant circadian clock. All seven OTUs peaked in relative abundance during the subjective day (Figure 3.5). Of those OTUs which were rhythmic in both the wild-type and *lhy-ox* rhizosphere, oscillations in their relative abundance were similar between wild-type and *lhy-ox* samples with the exception of *Penicillium astrolabium*, which displayed higher amplitude rhythms and higher relative abundances in wild-type samples (Figure 3.5.g).

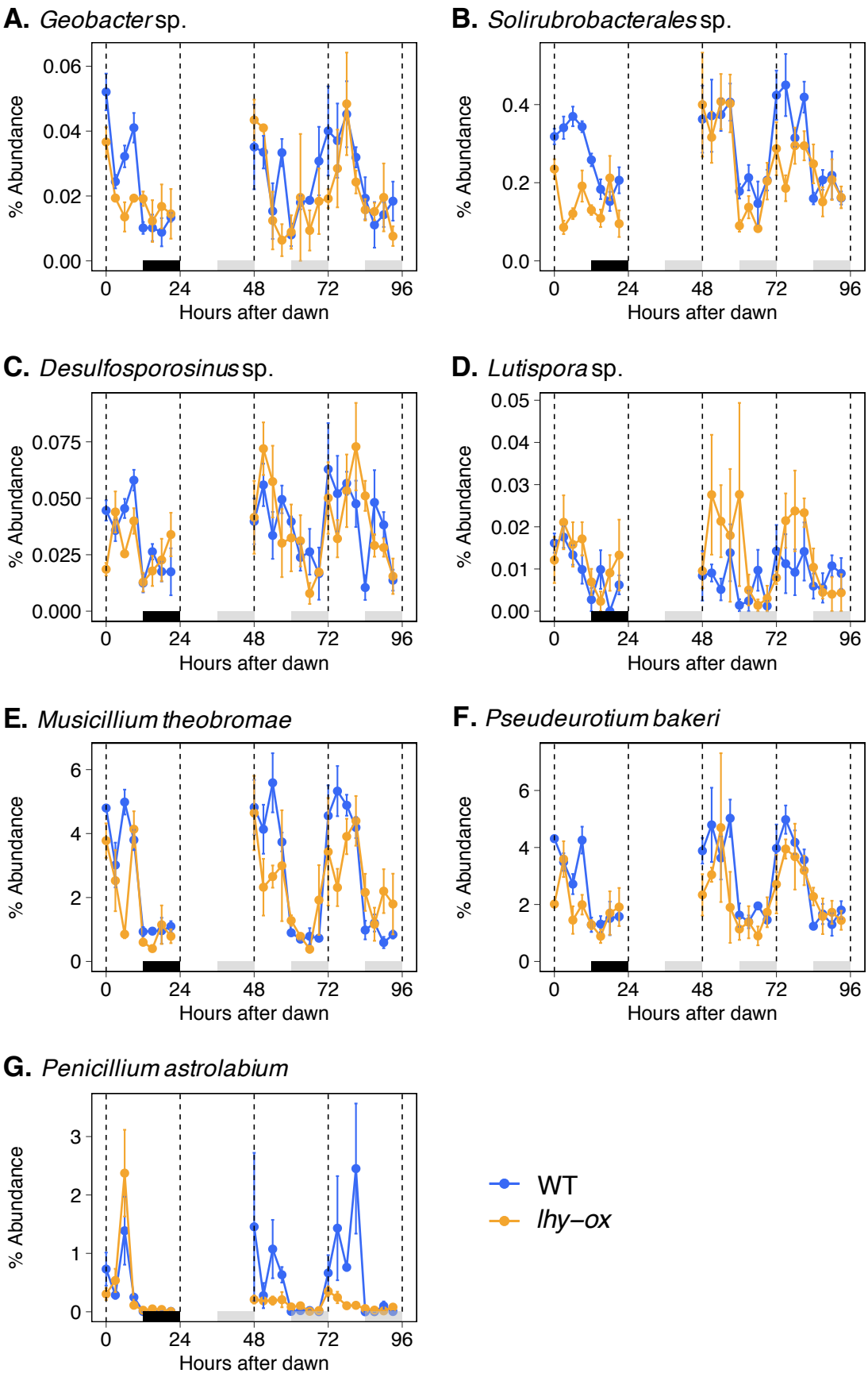

Figure 3.5. Rhythmicity of a few OTUs persists under constant conditions in the rhizosphere of plants overexpressing *lhy*. OTUs detected as rhythmic in *lhy-ox* rhizosphere samples using MetaCycle analysis (Wu et al., 2016). Mean relative

abundances in the rhizosphere of wild-type (blue lines) and *lhy-ox* (orange lines) plants ± SEM. Relative abundance of the bacterial OTUs identified as (a) *Geobacter* sp., (b) from the Solirubrobacterales family, (c) *Desulfosporosinus* sp. and (d) *Lutispora* sp., and fungal OTUs identified as (e) *Musicillium theobromae*, (f) *Pseudeurotium bakeri*, and (g) *Penicillium astrolabium*.

3.3.4. Relationship between circadian clock component homologue possession and microbial rhythmicity

To investigate the relationship between microbial rhythmicity and the possession of putative circadian clock components, we grouped the rhythmic OTUs by the phyla (for bacteria) and classes (for fungi) they belonged to. We then searched for the presence of homologues to known clock components within members of these taxa. The sequences of bacterial and fungal core oscillator proteins were used as search queries within the NCBI non-redundant nucleotide sequence database (Sayers et al., 2020) and homologues of *S. elongatus* KaiA, KaiB and KaiC and *N. crassa* FRQ, WC1 and WC2 were found (Tables 3.1 and 3.2).

3.3.4.1. Light driven rhythmicity

Greater numbers of taxa contained rhythmic OTUs under LD than under LL, which may be explained by the less stringent method used to test for rhythmicity in samples taken under LD (Tables 3.1 and 3.2). The taxa which contained rhythmic OTUs from the rhizosphere of either wild-type or *lhy-ox* plants under LD displayed rhythmicity which was driven by environmental light-dark cycles but may still be modulated through the plant. Many OTUs that were only rhythmic under LD belonged to taxa that did not possess homologues of circadian clock components (Tables 3.1 and 3.2).

Under LD, a total of 23 different bacterial phyla contained rhythmic OTUs from either wild-type or *lhy-ox* samples (Table 3.1). Of these phyla displaying evidence of light-driven rhythmicity, 11 possessed homologues of cyanobacterial circadian clock Kai proteins (Table 3.1). No evidence for Kai homologues was found in 12 phyla, suggesting that these bacterial taxa either do not possess a circadian clock or that they possess a clock based upon a different mechanism. Of the phyla which contained rhythmic OTUs under LD and also possessed Kai homologues,

most possessed KaiB and KaiC, with just two phyla (Firmicutes and Cyanobacteria) possessing homologues for all three of KaiA, KaiB, and KaiC (Table 3.1).

For fungi, 18 different classes contained rhythmic OTUs from either wild-type or *lhy-ox* samples (Table 3.2). Of these classes displaying evidence of light-driven rhythmicity, 11 possessed homologues of *N. crassa* circadian clock proteins (Table 3.2). No evidence for such homologues was found in 7 classes, suggesting that these fungal taxa either do not possess a circadian clock or that they possess a clock based upon a different mechanism. Of the classes which contained rhythmic OTUs under LD and also possessed clock component homologues, most possessed WC1 and WC2, with four classes (Dothideomycetes, Eurotiomycetes, Leotiomycetes and Sordariomycetes) possessing homologues for all three of FRQ, WC1, and WC2 (Table 3.2).

Rhythmicity which was driven by environmental light-dark cycles and did not persist under constant conditions was therefore observed in many microbial taxa, and the possession of homologues of known circadian clock components was not required for this rhythmicity.

3.3.4.2. Plant driven rhythmicity

We found evidence for circadian clock component homologues within all the taxa containing rhythmic OTUs from the wild-type rhizosphere under LL, with the exception of the Mortierellomycetes (Tables 3.1 and 3.2). The majority of these taxa contained OTUs which were rhythmic in the wild-type rhizosphere but not in that of arrhythmic *lhy-ox* plants, suggesting that their rhythmicity was driven by the plant circadian clock.

Firmicutes possessed homologues of cyanobacterial KaiA, KaiB and KaiC and contained rhythmic members in the wild-type rhizosphere under LL. Acidobacteria, Actinobacteria, Chloroflexi, Cyanobacteria, Firmicutes, Gemmatimonadetes, Proteobacteria, and Verrucomicrobia only possessed homologues of KaiB and KaiC but also contained rhythmic members.

Actinobacteria contained the highest number of rhythmic OTUs (26 in total, representing 5% of all Actinobacterial OTUs detected), followed by Proteobacteria (nine in total, representing 1% of all Proteobacterial OTUs).

Dothideomycetes, Eurotiomycetes, Leotiomycetes and Sordariomycetes possessed homologues of *N. crassa* circadian clock components FRQ, WC1 and WC2 and contained rhythmic members in the wild-type rhizosphere under LL. Pezizomycetes, Agaricomycetes, and Microbotryomycetes only possessed homologues of WC1 and WC2 but also contained rhythmic members. Evidence for homologues of *N. crassa* clock genes was not found in Mortierellomycetes, but this class still contained rhythmic members. Most of these fungal classes belong to the phylum Ascomycota, and a small number to the Basidiomycota and Mortierellomycota. Sordariomycetes, Dothideomycetes and Eurotiomycetes were also the most highly abundant fungal classes in wild-type samples. Sordariomycetes contained the highest number of rhythmic OTUs at 26 (representing 18% of all OTUs in this class), followed by Leotiomycetes and Eurotiomycetes with five (23% of the class) and four (14% of the class) respectively.

Rhythmicity under constant conditions that was driven by the plant circadian clock was therefore observed in several microbial taxa, and the possession of homologues of known circadian clock components was not necessarily required for this rhythmicity.

3.3.4.3. Autonomous rhythmicity

We found evidence for homologues of circadian clock components within all the taxa which contained rhythmic OTUs from the *lhy-ox* rhizosphere under LL. As they contained the few OTUs which were rhythmic in the rhizosphere of arrhythmic *lhy-ox* plants, within these taxa we found evidence for rhythmicity driven by an autonomous circadian clock.

Bacterial OTUs that were rhythmic in the *lhy-ox* rhizosphere under LL belonged to Actinobacteria, Firmicutes and Proteobacteria (Table 3.1). Half of these

rhythmic OTUs were found in Firmicutes, which was also the only phylum outside of Cyanobacteria found to possess a KaiA homologue (Table 3.1). Additionally, all three phyla possessed KaiB and KaiC homologues (Table 3.1).

The three fungal OTUs that were rhythmic in the *lhy-ox* rhizosphere under LL belonged to Eurotiomycetes, Leotiomycetes, and Sordariomycetes, which all possessed homologues of FRQ, WC1 and WC2 (Table 3.2).

Autonomous rhythmicity was therefore observed in a handful of microbial taxa, and as all these taxa contained evidence for homologues of known circadian clock components, such homologues may be required for this rhythmicity.

3.3.4.4. Co-occurrence of circadian clock component homologues and microbial rhythmicity

Circadian clock component homologues were therefore found within almost all taxa containing OTUs displaying plant-dependent or autonomous rhythmicity, and many taxa containing OTUs displaying light-driven rhythmicity. However, some taxa possessing circadian clock homologues were not found to contain rhythmic OTUs. Spirochaetes possessed a KaiC homologue, and Mucoromycetes possessed WC1 and WC2 homologues, but neither taxon contained rhythmic OTUs under LD or LL in either wild-type or *lhy-ox* plants (Tables 3.1 and 3.2). This therefore indicates that while the possession of circadian clock component homologues did not always co-occur with microbial rhythmicity in our experiment, the majority of the microbial rhythmicity observed was within taxa that did possess such homologues.

Table 3.1. Relationship between putative circadian clock gene possession and bacterial rhythmicity in the rhizosphere microbiome. TBLASTN searching was conducted to identify homologues of the *Synechococcus elongatus* PCC 7942 KaiA, KaiB and KaiC proteins within each taxon using the BLAST non-redundant nucleotide database (Sayers et al., 2020). Search results were determined to show evidence of homology when their E value was lower than 0.01, percentage identity was greater than 20%, and query cover was greater than 80%. ✗ indicates no evidence for a homologue, ✓ indicates evidence for a homologue in at least one record, and ? indicates that this taxon was not found in the database. Numbers of rhythmic OTUs under light-dark cycles and constant conditions were summarised for wild-type and *lhy-ox* plants. Rhythmic OTUs under light-dark cycles were identified as displaying a significant difference in relative abundance between any samples taken 9 to 15 hours apart. Rhythmic OTUs under constant conditions were identified using MetaCycle analysis (Wu et al., 2016), where a meta2d.BHQ value (corrected using Fishers' method) of $p \leq 0.05$ was considered significantly rhythmic. ☀ indicates rhythmicity driven by light-dark cycles (i.e. present in wild-type or *lhy-ox* samples under light-dark cycles), 🍃 indicates rhythmicity driven by the plant circadian clock (i.e. present in wild-type samples under constant conditions), and 🕒 indicates rhythmicity driven by an autonomous circadian oscillator (i.e. present in *lhy-ox* samples under constant conditions).

Phylum	KaiA	KaiB	KaiC	Rhythmic in LD: WT	Rhythmic in LL: WT	Rhythmic in LD: *lhy-ox*	Rhythmic in LL: *lhy-ox*	
Acidobacteria	✗	✓	✓	112/226	1/226	83/226	0/226	🍃
Actinobacteria	✗	✓	✓	273/522	26/522	172/478	1/478	🕒
Armatimonadetes	✗	✓	✓	6/23	0/23	9/20	0/20	☀
Bacteroidetes	✗	✓	✓	62/144	0/144	40/141	0/141	☀
BRC1	✗	✗	✗	2/4	0/4	1/2	0/2	☀
Chlamydiae	✗	✗	✗	2/17	0/17	2/14	0/14	☀
Chloroflexi	✗	✓	✓	125/233	3/233	87/209	0/209	🍃
Cyanobacteria	✓	✓	✓	6/15	1/15	3/18	0/18	🍃
Dependentiae	✗	✗	✗	2/9	0/9	3/6	0/6	☀

Elusimicrobia	✗	✗	✗	2/12	0/12	2/8	0/8	☀
Entotheonellaeota	?	?	?	1/10	0/10	2/8	0/8	☀
FCPU426	?	?	?	1/4	0/4	n/a	n/a	☀
Fibrobacteres	✗	✗	✗	2/4	0/4	0/5	0/5	☀
Firmicutes	✓	✓	✓	76/165	4/165	55/136	2/136	🕓
Gemmatimonadetes	✗	✓	✓	30/64	2/64	22/59	0/59	🍃
Latescibacteria	✗	✗	✗	9/23	0/23	7/22	0/22	☀
Nitrospirae	✗	✗	✗	8/12	0/12	1/10	0/10	☀
Omnitrophicaeota	✗	✗	✗	0/1	0/1	0/1	0/1	-
Patescibacteria	✗	✗	✗	4/8	0/8	0/2	0/2	☀
Planctomycetes	✗	✓	✓	201/512	0/512	121/445	0/445	☀
Proteobacteria	✗	✓	✓	370/803	9/803	225/736	1/736	🕓
Rokubacteria	✗	✗	✗	11/15	0/15	7/14	0/14	☀
Spirochaetes	✗	✗	✓	0/1	0/1	0/1	0/1	-
Verrucomicrobia	✗	✓	✓	75/142	3/142	48/129	0/129	🍃
WS2	✗	✗	✗	0/2	0/2	0/1	0/1	-
WS4	?	?	?	1/1	0/1	n/a	n/a	☀

Table 3.2. Relationship between putative circadian clock gene possession and fungal rhythmicity in the rhizosphere microbiome. TBLASTN searching was conducted to identify homologues of the *Neurospora crassa* FRQ, WC1, and WC2 proteins within each taxon using the BLAST non-redundant nucleotide database (Sayers et al., 2020). Search results were determined to show evidence of homology when their E value was lower than 0.01, percentage identity was greater than 20%, and query cover was greater than ~40%. ✗ indicates no evidence for a homologue, ✓ indicates evidence for a homologue in at least one record, and ? indicates that this taxon was not found in the database. Numbers of rhythmic OTUs under light-dark cycles and constant conditions were summarised for wild-type and *lhy-ox* plants. Rhythmic OTUs under light-dark cycles were identified as displaying a significant difference in relative abundance between any samples taken 9 to 15 hours apart. Rhythmic OTUs under constant conditions were identified using MetaCycle analysis (Wu et al., 2016), where a meta2d.BHQ value (corrected using Fishers' method) of $p \leq 0.05$ was considered significantly rhythmic. ☀ indicates rhythmicity driven by light-dark cycles (i.e. present in wild-type or *lhy-ox* samples under light-dark cycles), 🍃 indicates rhythmicity driven by the plant circadian clock (i.e. present in wild-type samples under constant conditions), and 🕒 indicates rhythmicity driven by an autonomous circadian oscillator (i.e. present in *lhy-ox* samples under constant conditions).

Phylum	Class	FRQ	WC1	WC2	Rhythmic in LD: WT	Rhythmic in LL: WT	Rhythmic in LD: *lhy-ox*	Rhythmic in LL: *lhy-ox*	
Ascomycota	Dothideomycetes	✓	✓	✓	21/39	1/39	7/32	0/32	🍃
	Eurotiomycetes	✓	✓	✓	13/28	4/28	8/16	1/16	🕒
	Laboulbeniomycetes	✗	✗	✗	1/1	0/1	0/1	0/1	☀
	Lecanoromycetes	✗	✓	✓	1/2	0/2	0/2	0/2	☀
	Leotiomycetes	✓	✓	✓	9/22	5/22	4/18	1/18	🕒
	Pezizomycetes	✗	✓	✓	2/6	1/6	0/3	0/3	🍃
	Saccharomycetes	✗	✓	✓	1/5	0/5	2/3	0/3	☀
	Sordariomycetes	✓	✓	✓	90/145	26/145	40/113	1/113	🕒

Basidiomycota	Agaricomycetes	✗	✓	✓	9/22	1/22	2/11	0/11	
	Agaricostilbomycetes	✗	✗	✗	1/1	0/1	0/1	0/1	
	Cystobasidiomycetes	✗	✗	✗	0/1	0/1	0/1	0/1	-
	Microbotryomycetes	✗	✓	✓	6/10	1/10	4/8	0/8	
	Tremellomycetes	✗	✓	✓	10/18	0/18	3/14	0/14	
	Ustilaginomycetes	✗	✓	✓	1/1	0/1	1/1	0/1	
Chytridiomycota	Rhizophlyctidomycetes	?	?	?	0/2	0/2	1/1	0/1	
	Rhizophydiomycetes	?	?	?	6/12	0/12	1/8	0/8	
Mortierellomycota	Mortierellomycetes	✗	✗	✗	8/14	2/14	3/15	0/15	
Mucoromycota	Mucoromycetes	✗	✓	✓	0/1	0/1	0/1	0/1	-
Olpidiomycota	Olpidiomycetes	✗	✗	✗	1/1	0/1	1/1	0/1	
Rozellomycota	Rozellomycotina (Class Incertae Sedis)	✗	✗	✗	4/9	0/9	2/7	0/7	
Unidentified	Unidentified	N/A	N/A	N/A	17/25	3/25	8/22	0/22	
Zoopagomycota	Zoopagomycetes	✗	✗	✗	0/2	0/2	0/2	0/2	-

3.4. Discussion

In this chapter we characterised microbial rhythmicity in the rhizosphere under constant conditions, as this has not been investigated in previous studies concerning circadian changes in the rhizosphere microbiome. Most of the rhythmicity we observed in the rhizosphere under light-dark cycles did not persist after plants were transferred to constant conditions, indicating that it was driven by light-dark cycles. However, rhythmicity was observed in a subset of the rhizosphere microbiome from wild-type plants under constant conditions. This rhythmicity was largely disrupted in rhizosphere samples of arrhythmic *lhy-ox* plants, indicating that it was driven by the plant circadian clock. Additionally, a handful of microbes displayed rhythmicity in the rhizosphere of *lhy-ox* plants, providing evidence for autonomous oscillators within these organisms.

3.4.1. Rhythmicity in the rhizosphere microbiome driven by environmental light-dark cycles

While higher proportions of bacterial and fungal rhythmic OTUs were present under light-dark cycles than under constant conditions, a direct comparison is not possible due to the different methods used to analyse rhythmicity. However, these results suggest that the rhythmicity of OTUs in the rhizosphere microbiome was mostly driven by diel changes in environmental conditions as opposed to by plant or microbial circadian oscillators.

Within the light-dark portion of the experiment, wild-type and *lhy-ox* rhizosphere samples contained similar proportions of rhythmic OTUs, which was consistent with the findings of Chapter 2 and indicates that a dysfunctional circadian clock did not prevent OTUs displaying rhythmicity under diel conditions. Additionally, greater numbers and total relative abundances of rhythmic OTUs were observed under light-dark cycles in this chapter than in Chapter 2. This is likely due to the increased frequency of sampling points employed in this experiment, and possibly also because we separated the rhizosphere from roots.

About half of all bacterial and fungal taxa which contained rhythmic OTUs under light-dark cycles also possessed homologs of circadian clock components,

indicating that the possession of such homologs was not required for microbial rhythmicity under light-dark cycles. As it appears that a known timekeeping mechanism was not a prerequisite, rhythms under light-dark cycles may be direct responses to light or indirect responses driven by light responses of the plant, such as the higher amplitudes of rhythms which may be observed under light-dark cycles when compared to constant conditions (as in Figure 3.2).

3.4.2. Plant-dependent rhythmicity in the rhizosphere

As previous studies investigating circadian changes in the rhizosphere microbiome only carried out experiments under diel light-dark cycles (Hubbard et al., 2017; Staley et al., 2017; Baraniya et al., 2018), it was unclear whether rhythmicity in the rhizosphere microbiome persists under constant conditions and is therefore driven by a circadian oscillator. Such rhythmicity could be driven by an oscillator within either the host plant or the rhizosphere microbiota themselves.

Rhythmicity in some members of the rhizosphere microbiome of wild-type plants was observed under constant conditions, indicating that a subset of both bacterial and fungal communities is capable of rhythmicity driven by a circadian oscillator. *lhy-ox* plants possess an arrhythmic circadian clock under constant conditions, and the rhythmicity observed in the wild-type rhizosphere was largely disrupted in *lhy-ox* samples, for both bacterial and fungal rhythmic OTUs. 92% of bacterial and 93% of fungal rhythmic OTUs we identified under constant conditions were present in wild-type rhizosphere samples only. These results therefore indicate that the plant circadian clock was the main driver of microbial rhythmicity under constant conditions.

All the taxa containing rhythmic OTUs from the wild-type rhizosphere under constant conditions possessed homologs of circadian clock components, with the exception of the fungal Mortierellomycetes, which did not possess homologs of FRQ, WC1 or WC2. All the other fungal classes containing rhythmic OTUs possessed homologs of either the WCC or both FRQ and the WCC, while all the bacterial phyla containing rhythmic OTUs possessed KaiB and KaiC but not KaiA.

This indicates that such homologs were not necessarily required for microbial rhythmicity driven by the plant circadian clock.

Much of the rhythmicity in rhizosphere microbiota under constant conditions could therefore simply be driven by plant processes which are controlled by the plant circadian clock, such as exudation and defence signalling, without any requirement for a microbial clock. Alternatively, it has been suggested that bacteria and fungi which possess homologues of only some of the known core circadian clock components could contain a clock which functions as an 'hourglass' as opposed to an autonomous oscillator (Correa et al., 2003; de Paula et al., 2006; Holtzendorff et al., 2008; Mullineaux and Stanewsky, 2009; Ma et al., 2016). Such a timer would be capable of responding to rhythmic signals from its external environment but unable to maintain oscillations under constant conditions. Another possibility as suggested by Brody (2019) is that circadian clock components may have become so divergent in some species that they are no longer able to be detected as homologous.

3.4.3. Autonomous rhythmicity in the rhizosphere microbiome

Little is known about whether non-photosynthetic microbiota may display autonomous circadian rhythmicity, of which a key indicator is rhythmicity that persists under constant conditions. Evidence for rhythmic processes that persist under constant conditions already exists within just a handful of fungi and two non-photosynthetic bacteria (Austin, 1968; Greene et al., 2003; Bluhm et al., 2010; Soriano et al., 2010; Hevia et al., 2015; Oliveira et al., 2015; Paulose et al., 2016).

In this experiment, a few OTUs were determined to be rhythmic under constant conditions in the rhizosphere of arrhythmic *lhy-ox* plants. Their rhythmicity in the absence of potential zeitgebers from host plants indicates that these few microbes may possess some form of autonomous circadian oscillator of their own. Two of these OTUs were determined to be rhythmic in *lhy-ox* samples but not in the wild-type rhizosphere, suggesting that their rhythmicity may be incompatible with or interrupted by that of the plant host. Of the OTUs which were

rhythmic in both the wild-type and *lhy-ox* rhizosphere, their rhythmicity was not altered by plant circadian clock dysfunction as very similar patterns of relative abundance were generally observed between wild-type and *lhy-ox* samples. That the three fungal OTUs rhythmic in both wild-type and *lhy-ox* samples under constant conditions were identified as a plant pathogen and saprotrophs indicates that these microbes with putative autonomous rhythmicity may have potential significance for plant health and nutrient cycling.

All the bacterial and fungal taxa which contained rhythmic OTUs from the *lhy-ox* rhizosphere possessed homologs of circadian clock components. This indicates that the possession of such homologs may be required for free-running rhythmicity which is autonomous within members of the rhizosphere microbiome.

All three rhythmic fungal OTUs from *lhy-ox* samples belonged to classes which possessed FRQ, WC1 and WC2 together, suggesting that all three components may be required for autonomous free-running fungal rhythmicity. Contrastingly, only half of the rhythmic bacterial OTUs belonged to phyla which possessed KaiA, KaiB and KaiC. A KaiA homologue was identified here in the Firmicutes, which was unexpected as it is thought that only Cyanobacteria possess KaiA (Kawamoto et al., 2020). Two rhythmic bacterial OTUs from *lhy-ox* samples were Firmicutes, suggesting that these may possess an autonomous circadian oscillator of their own involving a functional KaiA. However, the other two free-running rhythmic OTUs belonged to the Actinobacteria and Proteobacteria, which were found to possess homologues of just KaiB and KaiC. KaiA was therefore not required for all autonomous bacterial rhythmicity, and it is possible that an autonomous KaiBC-based circadian oscillator could have driven rhythmicity in the *lhy-ox* rhizosphere. This is reinforced by recent findings by Kawamoto et al. (2020) which demonstrated that KaiB and KaiC were sufficient to maintain free-running oscillations in a *Synechococcus* strain with inactivated KaiA, although damping (reducing amplitudes over time) of rhythmic activity of the KaiBC promoter was observed.

3.4.4. Fungal guilds and highly abundant taxa within rhythmic OTUs from the rhizosphere microbiome under constant conditions

Most of the rhythmic fungal OTUs from constant conditions were assigned an ecological guild, with the most common guild being saprotrophs, followed by pathogens and endophytes. Rhythmicity under constant conditions was therefore observed within fungi which form intimate associations with plants and may perform a variety of ecological functions within the rhizosphere microbiome, demonstrating that such OTUs may directly interact with the plant circadian clock. Interestingly, the most highly abundant OTU from the rhizosphere community of wild-type plants was also rhythmic under constant conditions. This fungal OTU, identified as *G. nigrescens*, was found to be a probable plant pathogen. However, it has previously been considered both saprotrophic and weakly pathogenic (Zare et al., 2007; Vagelas and Leontopoulos, 2015) and has also been demonstrated to protect plants from infection by *Verticillium* pathogens (Melouk and Horner, 1975; Vagelas and Leontopoulos, 2015). While the function of *G. nigrescens* appears to vary, that this OTU was highly abundant and also rhythmic may have implications for plant health. Whether it displays pathogenic or protective effects in any given context, rhythmicity in the relative abundance of *G. nigrescens* could lead to circadian variation in the severity of infection caused by this OTU or by other pathogenic fungi.

For both bacterial and fungal communities, the microbial taxa which contained the highest numbers of rhythmic OTUs were also the most abundant. Actinobacteria and Proteobacteria were the most highly abundant phyla within bacterial communities and contained 50% and 20% of all rhythmic OTUs under constant conditions from the wild-type rhizosphere respectively. Sordariomycetes was the most highly abundant class within fungal communities by a large margin and contained 60% of all rhythmic OTUs. Actinobacteria, Proteobacteria and Sordariomycetes are commonly found in the *A. thaliana* rhizosphere microbiome as well as in bulk soil (Bulgarelli et al., 2012; Urbina et al., 2018) and some prior evidence exists for rhythmicity within these taxa. Actinobacteria, Proteobacteria and Sordariomycetes were already highlighted in Chapter 2 of this thesis, where they were highly abundant within the rhythmic OTUs from the rhizosphere of wild-type plants grown under light-dark cycles. The two previous demonstrations of

free-running rhythmicity in non-photosynthetic bacterial species were both in members of Proteobacteria, *Enterobacter aerogenes* and *Pseudomonas putida* (Soriano et al., 2010; Paulose et al., 2016). Similarly, in this experiment two of the bacterial OTUs found to display rhythmicity in the wild-type rhizosphere under constant conditions were identified as members of the genus Pseudomonas. Additionally, Sordariomycetes contain the model species used to investigate the fungal circadian clock, *N. crassa*, and another member of this class, *Sordaria fimicola*, has been demonstrated to display free-running circadian rhythmicity in its spore discharge (Austin, 1968). These results therefore present evidence that microbial rhythmicity in the rhizosphere microbiome may be particularly prevalent in specific taxa.

3.4.5. Limitations and conclusions

When investigating the relationship between microbial rhythmicity and the possession of circadian clock component homologs, we sought out evidence for such homologues within the different taxonomic groups which were represented in the samples, as opposed to within the specific OTUs we detected in this experiment. It is possible that the presence of circadian clock components could be a feature of a taxonomic group, and as such all members could contain them. However, circadian clock components could occur in only some members of any given taxon, as their presence could be a result of horizontal gene transfer or other members could have selectively lost the genes. We therefore cannot be certain that the specific rhythmic OTUs we identified in this experiment contained circadian clock component homologues, but were able to determine that they belonged to taxa which did contain evidence of homologues. Despite this limitation, we identified clear associations between the presence or absence of circadian clock components and rhythmic microbial behaviour within particular taxa under different conditions, suggesting that our analysis revealed real trends.

In this chapter, we extended observations of microbial rhythmicity in the rhizosphere by examining samples taken under constant conditions. This allowed us to determine that a subset of the rhizosphere microbiome displays rhythmicity indicative of control by a circadian oscillator, which has not previously been

investigated. Most of this rhythmicity under constant conditions was driven by the plant circadian clock, indicating that a subset of rhizosphere microbiota display an intimate association with their host's oscillator. In a few community members we also identified autonomous rhythmicity, which has rarely been demonstrated in non-photosynthetic microbiota.

CHAPTER 4: CIRCADIAN RHYTHMICITY OF A MODEL RHIZOSPHERE BACTERIUM

4.1. Introduction

4.1.1. Introduction

All of the existing evidence for circadian changes in the rhizosphere microbiome has been gained by the molecular characterisation of rhizosphere communities. Hubbard et al. (2017), Staley et al. (2017) and Baraniya et al. (2018) used such molecular methods to identify diel changes in the composition and transcriptomic activity of the rhizosphere microbiome. In the first two experimental chapters of this thesis, molecular characterisation was also used and rhythmic OTUs were identified within the rhizosphere microbiome. The studies by Hubbard et al. (2017), Staley et al. (2017) and Baraniya et al. (2018) were based either upon discrete sampling points or on time-course experiments with low time resolution and short durations, with the most frequent sampling intervals being 6 hours apart and the longest experiment lasting two days. Similarly, the work conducted for Chapter 2 of this thesis was conducted at low time resolution, with samples being taken 12 hours apart on the same day. More frequent sampling intervals were employed for Chapter 3, where samples were collected at 3-hour intervals over three days.

The protocols involved in rhizosphere microbiome sampling are time-consuming and often technically demanding, particularly when working with *Arabidopsis thaliana*. Common techniques used for the molecular characterisation of microbial communities, such as amplicon sequencing and metatranscriptomic analysis, can also be costly and require significant laboratory work for sample processing. The frequency of sampling and duration of experiments may therefore be limited within studies concerning circadian rhythmicity in rhizosphere microbiota, reducing their capacity to examine interactions at fine temporal resolution and accurately capture rhythmicity.

Additionally, the possibility of spatial variation in circadian plant-microbe interactions in the rhizosphere has not been investigated, as previous works

concerning circadian changes in the rhizosphere microbiome have either used rhizosphere compartment samples only (Chapter 3 of this thesis; Hubbard et al., 2017; Staley et al., 2017) or composite root and rhizosphere samples which are homogenised and all spatial structure lost (Chapter 2 of this thesis; Baraniya et al., 2018).

We therefore sought to develop a new method for the detection of circadian rhythms in the rhizosphere microbiome which was cheaper, more flexible, and enabled faster collection of results than the methods used thus far. Such a method would also allow us to further examine the influence of the plant circadian clock upon, and to begin to establish spatial variation in, circadian plant-microbe interactions in the rhizosphere.

4.1.2. Bioluminescence imaging

Bioluminescence-based imaging techniques have been frequently employed in circadian biology studies since their advent in the 1990s (Millar et al., 1992; Kondo et al., 1993). Bioluminescence is the generation of light as a by-product of a biological reaction. For bioluminescence reactions to be completed and luminescence emitted, the presence of both luciferase enzyme genes and those encoding their substrates is required, or the substrate must be applied exogenously. Luciferase genes originating from both prokaryotic and eukaryotic organisms have been widely utilised in circadian biology. Most commonly, these may be fused to promoter regions as reporters of the expression of particular genes of interest, but they may also be expressed constitutively within organisms.

The relatively short-lived enzymatic activity of luciferase enzymes ensure that they are suitable for the reporting of circadian rhythms (McClung, 2006). The firefly *luc* gene is the most commonly used luciferase for studies of eukaryotic organisms (McClung, 2006). The luciferase substrate which is not already present in cells, luciferin, must be applied exogenously for the generation of luminescence (Millar et al., 1992) and has no reported toxic effects. In prokaryotes, the *luxCDABE* cassette contains all the genes necessary for luminescence. *luxA* and *luxB* produce the luciferase enzyme, and *luxC*, *luxD* and

luxE produce its substrate required for luminescence, a long-chain aldehyde, which isn't already present within cells (Dennis et al., 2006; Craney et al., 2007). Some experimental approaches utilise just the *luxAB* genes, and require exogenous application of the aldehyde substrate, which may be toxic to cells under prolonged exposure (Nunes-Halldorson and Duran, 2003).

The use of luciferase reporter genes was a major advance in circadian biology, as it allowed for non-invasive real-time monitoring and could be used to image gene expression within specific tissues. Its potential was first demonstrated by Millar et al. (1992), who used the firefly *luc* gene fused with the promoter of *CHLOROPHYLL A/B-BINDING 2* to identify circadian regulation of its expression in *Nicotiana tabacum* seedlings. *lux* reporter genes have also been used extensively to monitor circadian rhythms in the gene expression of cyanobacteria (Berla et al., 2013) and, using *Synechococcus* sp., provided the first evidence of circadian rhythmicity in cyanobacterial gene expression (Kondo et al., 1993).

Previous bioluminescence-based investigations of circadian rhythmicity in roots have focussed on plant gene expression. For example, fusions of the firefly *luc* gene with circadian clock gene promoter regions have been utilised to demonstrate the co-ordination of circadian oscillations in newly produced root cells (Fukuda et al., 2012), and that the circadian clock runs at different speeds in different organs (Greenwood et al., 2019).

Bioluminescence-based rhizosphere imaging approaches utilising *lux* reporter genes to image prokaryotes were pioneered as early as the 1980s. Across these works, bacterial luminescence was only assessed at single time points, typically after 7 days of growth. *lux* reporter genes have been used to investigate the colonisation of wheat (*Triticum* sp.) roots by *Enterobacter cloacae* (Rattray et al., 1995) and *Pseudomonas fluorescens* (de Weger et al., 1997), and the colonisation of *Brassica rapa* roots by *P. fluorescens* (Dennis et al., 2006). A *lux* tagged *P. fluorescens* strain was also used by Darwent et al. (2003), who used it as a biosensor to determine spatial variation in, and the effects of nitrate concentration upon, root exudates of barley (*Hordeum vulgare*). Additionally, some previous works have assayed the expression of specific target genes using

bioluminescent rhizosphere bacteria in which the promoter control of the *lux* reporter was known. Pini et al. (2017) used *lux* promoter fusions of *Rhizobium leguminosarum* transporter genes to detect the presence of specific compounds within exudates of pea (*Pisum sativum*) and vetch (*Vicia hirsuta*) plants. Additionally, O'Kane et al. (1988) used lux reporter genes to investigate the gene expression of *Bradyrhizobium japonicum* in infected root nodules of soybean (*Glycine max*).

4.1.3. Development of a model system

Imaging is a powerful approach for the investigation of fine resolution temporal and spatial variation in plant-microbe interactions, making it possible to conduct experiments that would be difficult to do using molecular characterisation of the rhizosphere microbiome. As it does not require destructive sampling, time-lapse imaging of a bioluminescent reporter strain could enable the visualisation of plant-microbe interactions in the rhizosphere over longer experiments with a finer temporal resolution. Imaging could also enable the investigation of spatial variation in circadian interactions in the rhizosphere. An imaging-based approach would be flexible and less resource-intensive, allowing the investigation of multiple plant genotypes simultaneously as well as differing light conditions. This would enable the investigation of a variety of hypotheses relating to rhizosphere microbial rhythmicity and the plant circadian clock. In this chapter we therefore developed a novel bioluminescence-based imaging method using the luminescent strain *Pseudomonas fluorescens* SBW25::*luxCDABE*, in order to investigate rhythmicity in the rhizosphere microbiome.

4.1.4. Aims

The aims of this work were to:

1. Determine whether *P. fluorescens* SBW25::*luxCDABE* displays rhythmic luminescence in the rhizosphere
2. Determine whether the plant circadian clock influences rhythmic luminescence of *P. fluorescens* SBW25::*luxCDABE* in the rhizosphere

3. Determine whether rhythmic bioluminescence of *P. fluorescens* SBW25::*luxCDABE* is due to oscillations in cell abundance or *lux* gene expression

4.1.5. Experimental design

In order to achieve the experimental aims and test whether luminescence could be used to detect bacterial rhythmicity in the rhizosphere, a model system was developed using the luminescent model bacterium *Pseudomonas fluorescens* SBW25::*luxCDABE* and *Brassica rapa* plants.

P. fluorescens is commonly found within the rhizosphere and is recognised as a plant growth-promoting rhizobacterium (PGPR) (Rainey, 1999). This species is able to positively influence plant health via a combination of its competition with pathogens, production of antimicrobial compounds, induction of systemic resistance, and production of plant growth hormones (Haas and Defago, 2005; Jackson et al., 2005; Mavrodi et al., 2007; Silby et al., 2009). *P. fluorescens* SBW25 is often used in microbial ecology studies, particularly those investigating the rhizosphere (Haas and Défago, 2005; Silby et al., 2009), and its genome has been sequenced (Silby et al., 2009). *P. fluorescens* SBW25 can also act as a mycorrhizal helper bacterium, facilitating interactions between plant roots and beneficial mycorrhizal fungi (Shinde et al., 2019). Considered a model plant-associated bacterium (Berg et al., 2014), *P. fluorescens*, and the SBW25 strain in particular, is therefore of importance when considering factors influencing the microbial ecology of the rhizosphere and impacts this may have on the health of host plants.

The initial *P. fluorescens* SBW25 strain was isolated from the phyllosphere (leaf surface) of *Beta vulgaris* (sugar beet) plants at Rothamstead Research (De Leij et al., 1995; Thompson et al., 1995). *P. fluorescens* SBW25::*luxCDABE* contains a stable chromosomal insertion of the *Photorhabdus luminescens luxCDABE* cassette (Winson et al., 1998), which was generated by introducing a mini-Tn*5* transposon into a spontaneous rifampicin-resistant mutant of the wild-type SBW25 strain (Lilley et al., 2003). The production of light using the *luxCDABE*

cassette is thought to be energetically expensive, due to the synthesis and activity of the lux proteins (Dunlap and Urbanczyk, 2013), making this strain potentially less competitive. This was accounted for in the development of the experimental method, whereby soil used for growth of inoculated plants in the rhizotrons was autoclaved before use in order to reduce initial competition from native bacteria. *Pseudomonas fluorescens* SBW25::*luxCDABE* will henceforth be referred to as *P. fluorescens*::*lux.*

The *B. rapa* genotype used in this work, R-o-18, is an inbred line of *B. rapa* subsp. *trilocularis* (yellow sarson) and is developmentally similar to oilseed rape (*B. napus*) (Stephenson et al., 2010). The roots of *B. rapa* seedlings are larger and more robust than those of *A. thaliana*, enabling their easy inoculation and imaging. Additionally, the investigation of this oilseed rape-like genotype allowed the potential presence of rhizosphere circadian rhythmicity to be assessed in a context which may be more applicable to agriculturally and economically relevant crops than *A. thaliana*. It is thought that the overall network of core *B. rapa* circadian clock gene interactions is the same as that in *A. thaliana* (Lou et al., 2012).

4.2. Methods

4.2.1. Imaging of bioluminescent *Pseudomonas* in the rhizosphere

4.2.1.1. Plant growth for rhizosphere imaging

Transparent plastic rhizotrons based on those developed by Rellan-Alvarez et al. (2015) were created for the growth of plants. Rhizotrons were constructed using custom-cut transparent Perspex (Figure 4.1). Each rhizotron was slotted into an open-ended opaque black plastic sleeve to prevent root systems being exposed to light whilst not being imaged.

Soil used in all rhizotrons was as described in Chapter 2 and was collected in January and April 2019. Following sampling, all soil was homogenised by passage through a 3 mm sieve. Soil was autoclaved for 28 minutes at 121 °C in order to encourage the survival and establishment of *P. fluorescens*::*lux* by reducing competition from other existing microbes. Rhizotrons were filled by

gradually adding soil and spraying with deionised water. Six four-to-seven-day-old *B. rapa* seedlings were able to comfortably fit in to each rhizotron at once.

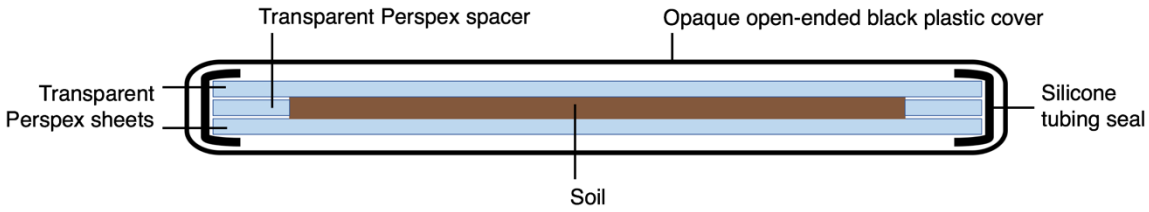

Figure 4.1. Rhizotron design for rhizosphere imaging. Labelled top-down schematic of the transparent rhizotrons constructed for the growth and imaging of *B. rapa* roots inoculated with *P. fluorescens*::*lux*. The opaque plastic cover was removed when the rhizotron was transferred to be imaged. The transparent Perspex used was 3 mm thick, and the total internal dimensions of each rhizotron measured 10 cm x 10 cm x 0.3 cm. A gap of approximately 1.2 cm was left along the bottom edge when applying soil to each rhizotron, to allow for it to be placed in a tray containing water of the same depth without the soil slumping and falling out.

4.2.1.2. Inoculation of *B. rapa* roots with *P. fluorescens*::*lux*

The bioluminescent strain *P. fluorescens*::*lux* was constructed as described in Lilley et al. (2003) and supplied by Professor Hirsch at Rothamsted Research, UK. *B. rapa* R-o-18 wild type and *gi-1* seeds were supplied by Professor McClung at Dartmouth College, US. R-o-18 was first described by Stephenson et al. (2010) and *gi-1* was first described by Xie et al. (2015). The *gi-1* mutation was identified in the R-o-18 background (Xie et al., 2015). *gi-1* plants were used in this study due to their lack of function of the circadian oscillator component GI, and previously observed temperature-dependent impaired circadian clock function under constant conditions (Xie et al., 2015).

Roots of *B. rapa* seedlings were inoculated with a nutrient-starved culture of *P. fluorescens*::*lux* before being planted in the rhizotrons. To prepare this strain for the comparatively less nutrient-rich environment of soil (relative to LB broth growth media), cultures of the bacterium were starved using a modified version of a protocol by Dennis et al. (2006).

P. fluorescens::*lux* was grown on LB agar plates for three to seven days at 20 – 30 ºC, then plates were flooded with 3 ml of LB broth. The bacterial colonies were disturbed using a pipette and thoroughly mixed into the liquid. The cell suspension was then diluted using LB broth to an optical density at 600 nm of 0.050 (± 10%). 200 *µ*l of diluted cell suspension was added to 100 ml of LB broth and then incubated at 25 ºC and 175 rpm for 20 hours to a mean OD of 2.18. This method was used to ensure that the concentration of the initial bacterial inoculum remained constant across all required replicate experiments.

In order to starve this culture of *P. fluorescens*::*lux*, it was centrifuged at 4,000 rpm (3220 *g*) for 20 minutes in order to collect the cells then the supernatant was discarded. Sterile water of the same volume as the original supernatant was added and the cells resuspended by shaking. These two centrifuging and resuspending steps were repeated twice more, and then the washed cells were returned to incubate at 25 °C and 175 rpm for a further 48 hours. After this time, it was estimated using a dilution series plated onto LB agar that this starved cell culture contained 1.3 – 4.8 x 10^8 CFU/ml, and a mean OD of 1.57 was calculated.

B. rapa wild type (genotype R-o-18) seedlings were germinated for three days and *gi-1* for seven days on moist filter paper, as the initial germination and growth of *gi-1* plants was found to be slower. Seedlings were then inoculated by submerging their roots in sterile plastic vials containing the starved *P. fluorescens*::*lux* culture and incubating at room temperature for 24 hours. Inoculated seedlings were planted in rhizotrons, which were placed in a plant growth cabinet for seven days before time-lapse imaging began. Plants in this growth cabinet experienced 22°C, 12L:12D light cycles, and 54 – 100 *µ*mol/m^2/sec of light (dependent on position within the cabinet).

4.2.1.3. Time-lapse imaging of luminescence

Luminescence was imaged in a light-tight box within a purpose-built darkroom imaging facility (Figure 4.2). The box was lit by white LED lighting (Philips, Amsterdam, Netherlands) and a photon counting Retiga R6 camera (QImaging, Surrey, Canada) was used to capture images. The imaging process was co-

ordinated using Micro-Manager v1.4 software (Vale lab, University of California San Francisco, USA). To ensure images were captured in darkness to allow the detection of bacterial bioluminescence, the lights were switched on and off as appropriate via an Arduino microprocessor (Somerville, Massachusetts, USA).

Two rhizotrons containing a total of twelve plants were imaged at once. In each experiment, three seedlings of each *B. rapa* genotype were planted in each of the two rhizotrons imaged, their positions within these randomly assigned. Their roots were shielded from the light by an opaque tunnel covering the rhizotrons and water tray. The plants grown in this system received 12 – 15 μmol/m^2/sec of light (dependent on position within the box) and experienced an average temperature of 21 °C (+/- 1 °C) over the course of each experiment, as determined by measurements taken every 10 minutes using a temperature probe (Rotronic, Crawley, UK).

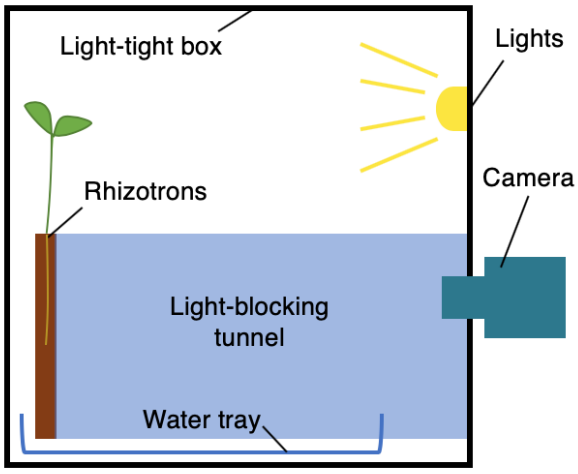

Figure 4.2. Imaging box layout for rhizosphere imaging. Labelled side-view schematic of the light-tight imaging box used for the time-lapse imaging of *P. fluorescens*::*lux* luminescence on *B. rapa* roots.

Every two hours, an image with a 20 minute exposure time was taken. Each image was preceded by a 5 minute delay, in order to allow any interfering fluorescence from the plants' own tissues to decay. A series of images depicting the luminescence of *P. fluorescens*::*lux* on *B. rapa* roots was therefore amassed over the duration of the time-course.

4.2.1.4. Luminescence data analysis

The series of images generated by time-lapse experiments were analysed using ImageJ (Schneider et al., 2012). The magic wand tool was used to automatically generate a Region of Interest (ROI) outlining each root based on a projection of the average intensity of its luminescence across the full image series. The bacterial luminescence within each ROI was quantified at each time point by determining its mean grey value within each image. In order to remove background signal, the mean grey values of five regions containing no roots were quantified in every image and subtracted from the mean grey value of every ROI. Luminescence values at each time point from each replicate root were then normalised to the mean luminescence of that root across the whole experiment, giving relative luminescence data for each time point.

Applying the FFT-NLLS (Fast Fourier Transform Non-Linear Least Squares) method using the BioDare2 online platform (biodare2.ed.ac.uk; Moore et al., 2014), relative luminescence data were baseline detrended then assessed for rhythmicity. This analysis determined which roots exhibited circadian rhythmicity in their bacterial luminescence, by attempting to fit cosine waves with periods of 18 – 34 hours to the data. Goodness of fit was assessed manually, and those deemed to be a poor fit were discarded from subsequent analyses.

Pairwise Wilcoxon rank sum tests were used to test for differences in period, phase, and RAE between wild-type and *gi-1* mutant plants.

4.2.2. Leaf movement analyses

As leaf movement is an easily assayable output of the plant circadian clock, we conducted leaf movement analyses in order to confirm the circadian phenotype of the *B. rapa gi-1* plants under our experimental conditions.

Plants were initially grown in general potting compost (Wilko, Worksop, UK) in modular pots, as opposed to the rhizotrons used for the luminescence imaging experiment described in Section 4.2.1. Pots were placed in a growth cabinet under 12L:12D conditions and 48 – 69 μmol/m^2/sec of light (dependent on position within the cabinet), with the same average temperature as was recorded

during the luminescence imaging work (21 ºC) ± 0.5 ºC. Time-lapse imaging began after the first two true leaves were longer than approximately 2 cm; for wild-type *B. rapa* this was 15 days post-sowing and for *gi-1* 26 days. For this, plants of both genotypes were transferred into a randomly generated configuration under constant light conditions and 36 - 102 μmol/m^2/sec of light (dependent on position within the cabinet), also with the same average temperature. A Brinno TLC200 time-lapse camera (Brinno, Taipei City, Taiwan) captured one image every 10 minutes, and plants were imaged in these conditions for 7 days.

The series of images generated by this time-lapse imaging were analysed using ImageJ. ROIs were created to delineate areas that individual leaves occupied over the course of the experiment. Images were converted to greyscale and then binary, so that the position of leaves within this ROI would be quantified at each time point using the 'centre of mass' function. Position values at each time point for each leaf were then normalised to the mean position of that leaf across the whole experiment, giving relative position data.

Circadian rhythmicity in this leaf position data was assessed using the FFT-NLLS (Fast Fourier Transform Non-Linear Least Squares) method using the BioDare2 online tool (biodare2.ed.ac.uk; Moore et al., 2014) as described above for luminescence imaging.

4.2.3. Bacterial RNA analyses

As the rhythmic luminescence of *P. fluorescens*::*lux* observed in the imaging experiment (demonstrated in Sections 4.3.1 and 4.3.2) could be due to rhythmic changes in either bacterial cell abundance or *lux* gene expression, or both, the possible mechanisms causing this rhythmicity were investigated using RT-qPCR.

4.2.3.1. Plant growth and sampling

Seedlings were planted in modular pots, as opposed to the rhizotrons used in the imaging experiment. Soil was prepared and wild-type *B. rapa* seedlings inoculated with *P. fluorescens::lux* in the same way as for the luminescence

imaging experiment described in Section 4.2.1. Inoculated plants were grown in a growth cabinet under 12L:12D conditions and 17 – 28 μmol/m^2/sec of light at 22 °C (dependent on position within the cabinet).

Prior to sampling, inoculated plants were grown for 10 days, three days longer than for the imaging experiments. This enabled roots to become larger and therefore easier to sample, and also increased the amount of material from which to extract RNA. Trays of plants were split equally into two growth cabinets which were both set to the same conditions but were each under oppositely phased lighting cycles. This allowed sampling at six-hour intervals to take place during working hours. Sampling began 10 days after inoculation and was conducted for a period of five days. Samples were taken at dawn and six hours after dawn, from both cabinets simultaneously. As a result of the growth of plants in these two oppositely phased cabinets, samples were also obtained for timepoints representing 12 and 18 hours after dawn. At each time point, one sample comprised of material from the root systems of 10 – 12 individual plants was taken.

Sampling involved a compartment separation step in order to determine any spatial variation in the rhythmicity of *P. fluorescens*::*lux* in the root and rhizosphere. Root and rhizosphere compartments were separated using a miniature version of a root washing protocol developed by Hilton et al (in press). Root washing may not dislodge all rhizoplane microbes (Richter-Heitmann et al., 2016), so it was assumed that this procedure would result in root compartment samples containing both endophytic and some rhizoplane bacteria.

Plants were carefully removed from pots and non-adhering soil was gently brushed off roots using tweezers. Root systems were then cut from the plant just below the base of the shoot. For each sample, all excised roots with adhering rhizosphere soil were firstly combined into a single pre-prepared 15 ml tube containing 6 ml sterile water. This was shaken 20x, then the roots removed using fine tweezers which had been cleaned with 70% ethanol. Roots were placed in another 15 ml tube containing 6 ml sterile water and shaken a further 20x. After the roots were again removed from this tube, its contents were poured into the

first 15 ml tube. These two washes combined formed the rhizosphere compartment for each sample. The roots were transferred to another 15 ml tube containing 9 ml sterile water, and shaken 20x again, before being transferred to an empty 15 ml tube. This formed the root compartment sample, and the water from the final washing step was discarded.

Upon completion of compartment separation, all samples were immediately frozen in liquid nitrogen and then transferred to -80 °C. Tweezers and all other sampling equipment were cleaned with 70% ethanol between samples.

Samples were placed in a freeze drier (Christ, Osterode, Germany) and incubated at a low temperature and pressure (-55 ºC, 0.05 mbar) until all water was removed and only rhizosphere soil remained.

4.2.3.2. RNA extraction and cDNA generation

RNA was extracted from root and rhizosphere soil samples, and cDNA subsequently generated for use in RT-qPCR. All samples were transferred to Lysing Matrix E tubes (MP Biomedicals, Irvine, USA), then a modified version of a protocol by Griffiths et al. (2000) was used to extract RNA as described in Section 2.2.2.1. All contaminating DNA was removed by treatment with DNAse I using the DNAse Max Kit (MO Bio, Carlsbad, USA) according to the manufacturer's instructions. Each reaction contained 10 units of the DNAse I enzyme and 11 μl of the original RNA sample. To confirm that all DNA had been removed from the samples, PCRs were conducted using the Eub338/518 general bacterial primer set, which targets the 16S rRNA gene of bacteria (Table 4.1). In these confirmatory PCRs, the following volumes of reagents were used: 12.5 μl RedTaq 2x Readymix (Sigma-Aldrich, Missouri, USA), 9 μl sterile molecular-grade water, 1.25 μl forward primer (3 μM), 1.25 μM reverse primer (3 μM), and 1 μl DNAse-treated RNA. The reaction was conducted under the following conditions: denaturation at 95 °C for 10 minutes; 40 cycles of denaturation at 94 °C for 30 seconds, annealing at 60 °C for 1 minute, elongation at 72 °C for 1 minute. PCR products were added to a 1% agarose gel and 100 V of electricity were applied for 20 minutes, before visualisation under ultraviolet light using a

transilluminator. After confirming that all DNA was removed, cDNA was then generated from the DNAse-treated RNA as described in Section 2.2.2.1. To confirm that cDNA was present, PCRs and gel electrophoresis were conducted again.

4.2.3.3. RT-qPCR assays

To investigate the potential mechanisms causing the rhythmic luminescence of *P. fluorescens::lux* that we observed in the imaging experiment (demonstrated in Sections 4.3.1 and 4.3.2), we investigated the relative expression of its *luxC* gene and the relative quantity of its cells (by investigating the relative expression of its 16S rRNA gene). We also confirmed the rhythmicity of the plant circadian clock by quantifying the relative expression of *CCA1* and *GI*.

The relative expression of the genes of interest (Table 4.1) at each time point was quantified using the $2^{\Delta\Delta Ct}$ method (Livak and Schmittgen, 2001). Some primers used were designed specifically for this study using the Primer3 online tool (http://www.bioinformatics.nl/cgi-bin/primer3plus/primer3plus.cgi).

All qPCR reactions were performed as described in Section 3.2.3 and the annealing temperature of all primers used was 60 ºC.

Table 4.1. Primer pairs used for RT-qPCR investigation of *P. fluorescens*::*lux* gene expression in the *B. rapa* root and rhizosphere.

NCBI GenBank Gene ID numbers are included for plant genes of interest.

Gene of interest	Primer pair	Reference	Nucleotide sequence (forward and reverse respectively)	Product size (base pairs)
P. fluorescens luxC	luxC	This study	5'-CCT GCC AAT ATT GAA TGA CTC TC-3' 5'-AAT GTA TGT CCT GCG TCT TGA GT-3'	148
P. fluorescens rpoA – reference gene for *luxC* expression	rpoA	This study	5'-TAT CGC ATA CGT GGT GGA AA-3' 5'-TCT CGT CTT CCT GCT CGA TT-3'	200
P. fluorescens::lux 16S rRNA	PF16S	This study	5'-TGC ATT CAA AAC TGA CTG-3' 5'-GTC CAG GTG GTC GCC TTC-3'	113
General bacterial 16S rRNA gene – reference gene for *P. fluorescens::lux* 16S rRNA expression	Eub338/ Eub518	Fierer et al., 2005	5'-ACT CCT ACG GGA GGC AGC AG-3' 5'-ATT ACC GCG GCT GCT GG-3'	~200
B. rapa GI (103249166)	GI	Kim et al., 2019	5'-ACG TCC ACG TCA CGT AAT GA-3' 5'-AGC GAA ACA ACG GAG AAA GA-3'	245
B. rapa CCA1 (103866427)	CCA1	Kim et al., 2019	5'-TCT CTG TCA CAT GCT CCT CCT T-3' 5'-CGG CTA AGT TCC CTT GTG G-3'	184
B. rapa ACTIN (103865925) – reference gene for *GI* and *CCA1* expression	ACTIN	Xiao et al., 2012	5'-GGA GCT GAG AGA TTC CGT TG-3' 5'-GAA CCA CCA CTG AGG ACG AT-3'	158

4.3. Results

4.3.1. Rhythmicity of bioluminescent *Pseudomonas* on roots

In order to test whether luminescence could be used to detect bacterial rhythmicity in the rhizosphere, we imaged *P. fluorescens*::*lux* within the rhizosphere of *Brassica rapa* plants. Roots of *B. rapa* were inoculated with *P. fluorescens*::*lux* and subjected to time-lapse imaging within a light-tight box, where bacterial luminescence was captured every two hours by a photon-counting camera.

When overlaid with reference images taken of the rhizotrons under white light, detectable bacterial luminescence was observed to be concentrated over the outline of roots (Figure 4.3.e). This luminescence was not detected on all regions of the root systems, rather remaining on the parts which were originally inoculated, and generally towards the top of the root, closest to the stem. Example images of *P. fluorescens*::*lux* luminescence from the series obtained from one replicate root under light-dark cycles are shown in Figure 4.3.d.

Imaging experiments were conducted to characterise rhythmic bacterial luminescence on the roots of *B. rapa* plants grown under both light-dark cycles and constant light and temperature conditions.

Under light-dark cycles, *P. fluorescens*::*lux* exhibited rhythmic changes in its luminescence on the roots of wild-type *B. rapa* plants (Figure 4.3). 16% of roots examined displayed rhythmic luminescence under light-dark cycles with a mean period of about 25 hours (Figures 4.3.a and 4.3.c). Peaks in relative luminescence occurred during the first half of the light period each day (Figures 4.3.a and 4.3.c).

When plants were transferred to constant conditions, an almost identical proportion of roots showed rhythmic luminescence as under light-dark cycles (Figure 4.3). Here, bacterial luminescence was rhythmic on 17% of roots, and a mean period of 25.99 hours was observed (Figures 4.3.b and 4.3.c). That rhythmicity of *P. fluorescens*::*lux* luminescence was maintained in the absence

of external time cues indicates that this bacterial rhythm exhibited a key property of circadian rhythmicity.

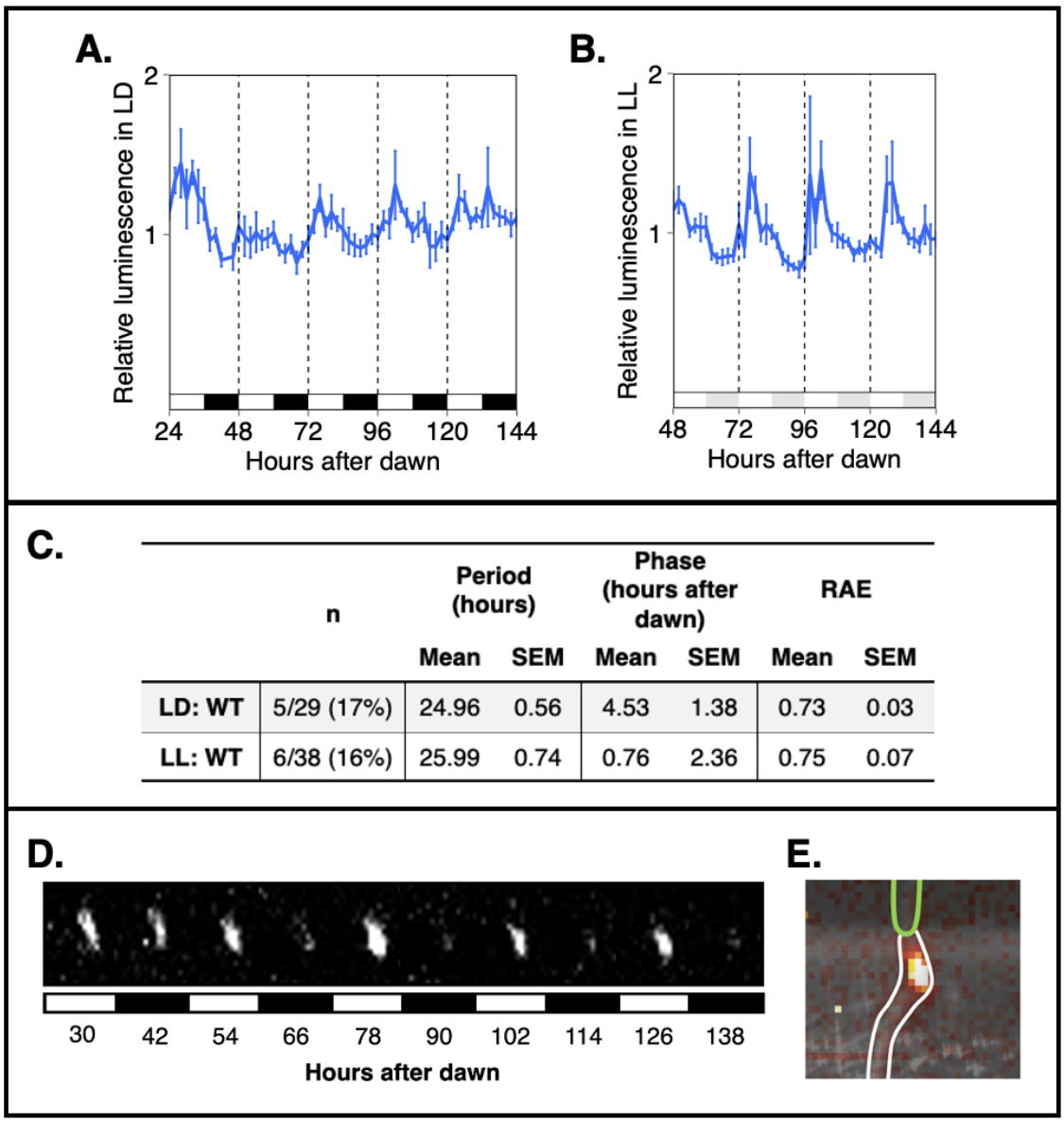

C.

	n	Period (hours)		Phase (hours after dawn)		RAE	
		Mean	SEM	Mean	SEM	Mean	SEM
LD: WT	5/29 (17%)	24.96	0.56	4.53	1.38	0.73	0.03
LL: WT	6/38 (16%)	25.99	0.74	0.76	2.36	0.75	0.07

Figure 4.3. *P. fluorescens*::*lux* displays rhythmic luminescence on wild-type *B. rapa* roots under both light-dark cycles and constant conditions. Mean bacterial luminescence ± SEM of rhythmic roots under (a) light-dark cycles and (b) constant conditions. (c) Summary statistics. Units are hours for period, hours after dawn for phase, and arbitrary for RAE. RAE refers to the Relative Amplitude Error, a measure of the quality of the period and phase estimate. RAE = 0 indicates a perfect fit to the data; RAE = 1 indicates a very poor fit. (d) Example images of rhythmic luminescence on one root from an experiment conducted under light-dark cycles. (e) Example image of luminescence at 30 hours after dawn overlaid with bright-field image of seedling (root outline emphasised in white; stem position outlined in green). Colour indicates intensity

of luminescence signal, with white representing the highest and red the lowest. Roots in (d) and (c) are approximately 1.5mm in diameter. Rhythmicity was determined using the FFT-NLLS method within the BioDare2 platform.

4.3.2. The plant circadian clock influences rhythmicity of bioluminescent *Pseudomonas* on roots

To investigate the influence of the plant circadian clock on *P. fluorescens::lux* rhythms, we tested whether loss of function of *gigantea* (*gi*), which encodes of one of the oscillator components, altered the rhythmic patterns of luminescence of *P. fluorescens*::*lux* on *B. rapa* roots. *GI* is involved in the maintenance of circadian rhythms (Fowler et al., 1999; Park et al., 1999; Swarup et al., 1999).

We used leaf movement assays to determine the circadian phenotype of *gi-1* mutants under constant conditions, as the movement of leaves is a well-characterised output of the circadian clock (Engelmann et al., 1992). The phenotype of the *B. rapa gi-1* mutant was described previously (Xie et al., 2015). Xie et al. (2015) found that *gi-1* plants displayed temperature-dependent impaired circadian clock function under constant conditions: the circadian period was unaffected at 18 °C but at 22 °C, 69% of seedlings were arrhythmic and those which displayed rhythmic leaf movement showed increased RAE (a measure of the strength of a circadian rhythm) and lengthened period. It was also necessary to test the *gi-1* phenotype under the experimental conditions we used in this work. Similarly, in our experiments, a smaller proportion of *gi-1* leaves displayed rhythmic movement than in wild-type plants (24% as compared to 64%) (Figure 4.4). A significantly higher mean RAE ($p = 0.005$) was observed, indicating poorer fits to the data, and a consensus could not be reached upon the period values, which were spread over the full 18 – 34 hour range (Figure 4.4). This showed that, while driven rhythms would still be observed under light-dark cycles, the circadian clock of *gi-1* plants was dysfunctional under our experimental constant conditions.

We also conducted imaging experiments to characterise rhythmic bacterial luminescence on the roots of *B. rapa gi-1* plants. Under light-dark cycles, 19% of *gi-1* roots displayed rhythmic luminescence of *P. fluorescens*::*lux*, a similar

proportion to that found for wild-type *B. rapa*, and their period values were tightly clustered around 24-25 hours (Figure 4.5). In these conditions, no significant differences in the period, phase or RAE of bacterial luminescence were observed between *gi-1* and wild-type plants (period: p = 1.00; phase: p = 1.00; RAE: p = 0.46; Figure 4.5.e). Additionally, period values from individual replicates were plotted against their RAE values, and it was observed that the period lengths and quality of period estimates (as indicated by the RAE) of bacterial rhythmicity were very similar between *gi-1* and wild-type plants in these conditions (Figure 4.5.c).

Contrastingly, under constant conditions, the results obtained for bacterial luminescence on *gi-1* roots differed to those from wild-type plants (Figures 4.5.b, 4.5.d, and 4.5.e). Luminescence rhythms damped (displayed reduced amplitudes over time) within 96 hours of transfer to constant conditions. Based on data from 48 to 144 hours under constant conditions, Biodare2 only fitted a cosine wave to data from one root out of 30 tested (Figures 4.5.b, 4.5.d, and 4.5.e). The rhythmicity in bacterial luminescence on this one root was only clearly observed for the first half of the experiment, and the signal damped thereafter (Figure 4.5.b).

The lack of rhythmicity in luminescence detected on most *gi-1* roots under constant conditions, and the damping of the oscillations observed in the single rhythmic root, suggest that the rhythmicity of *P. fluorescens*::*lux* luminescence was disrupted when *gi* function was disrupted and plant host rhythms were abolished. This suggests that the plant circadian clock influenced the rhythmicity of *P. fluorescens*::*lux* in the rhizosphere. Whether GI plays a direct role in this remains to be demonstrated.

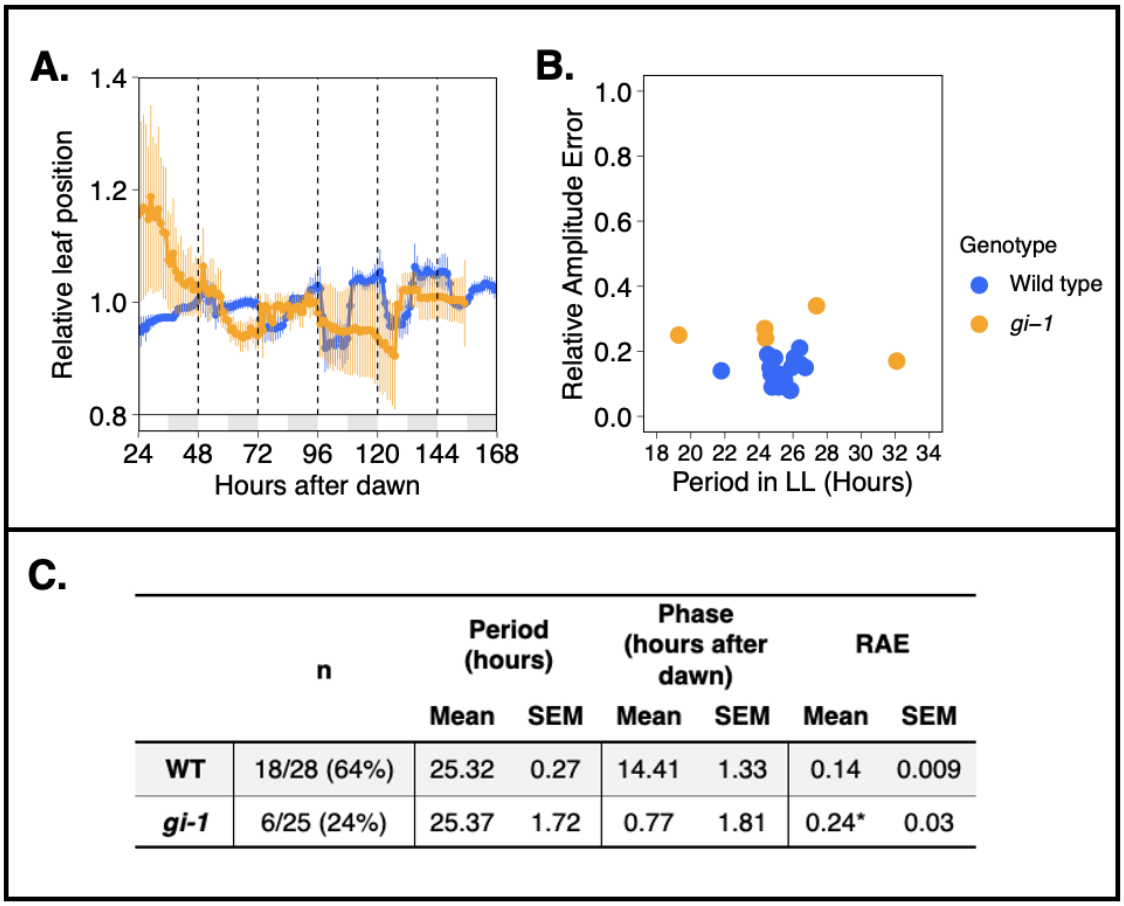

	n	Period (hours)		Phase (hours after dawn)		RAE	
		Mean	SEM	Mean	SEM	Mean	SEM
WT	18/28 (64%)	25.32	0.27	14.41	1.33	0.14	0.009
gi-1	6/25 (24%)	25.37	1.72	0.77	1.81	0.24*	0.03

Figure 4.4. Circadian rhythms of leaf movement are disrupted in *gi-1* plants relative to wild-type *B. rapa*. (a) Relative leaf position of leaves determined to display rhythmicity under constant conditions after growth under light-dark cycles. (b) Period and RAE values of rhythmic leaves. RAE refers to the Relative Amplitude Error, a measure of the quality of the period and phase estimate. RAE = 0 indicates a perfect fit to the data; RAE = 1 indicates a very poor fit. (c) Summary statistics. Units are hours for period, hours after dawn for phase, and arbitrary for RAE. * indicates a significant difference between *gi-1* and wild-type plants. Rhythmicity was determined using the FFT-NLLS method within the BioDare2 platform.

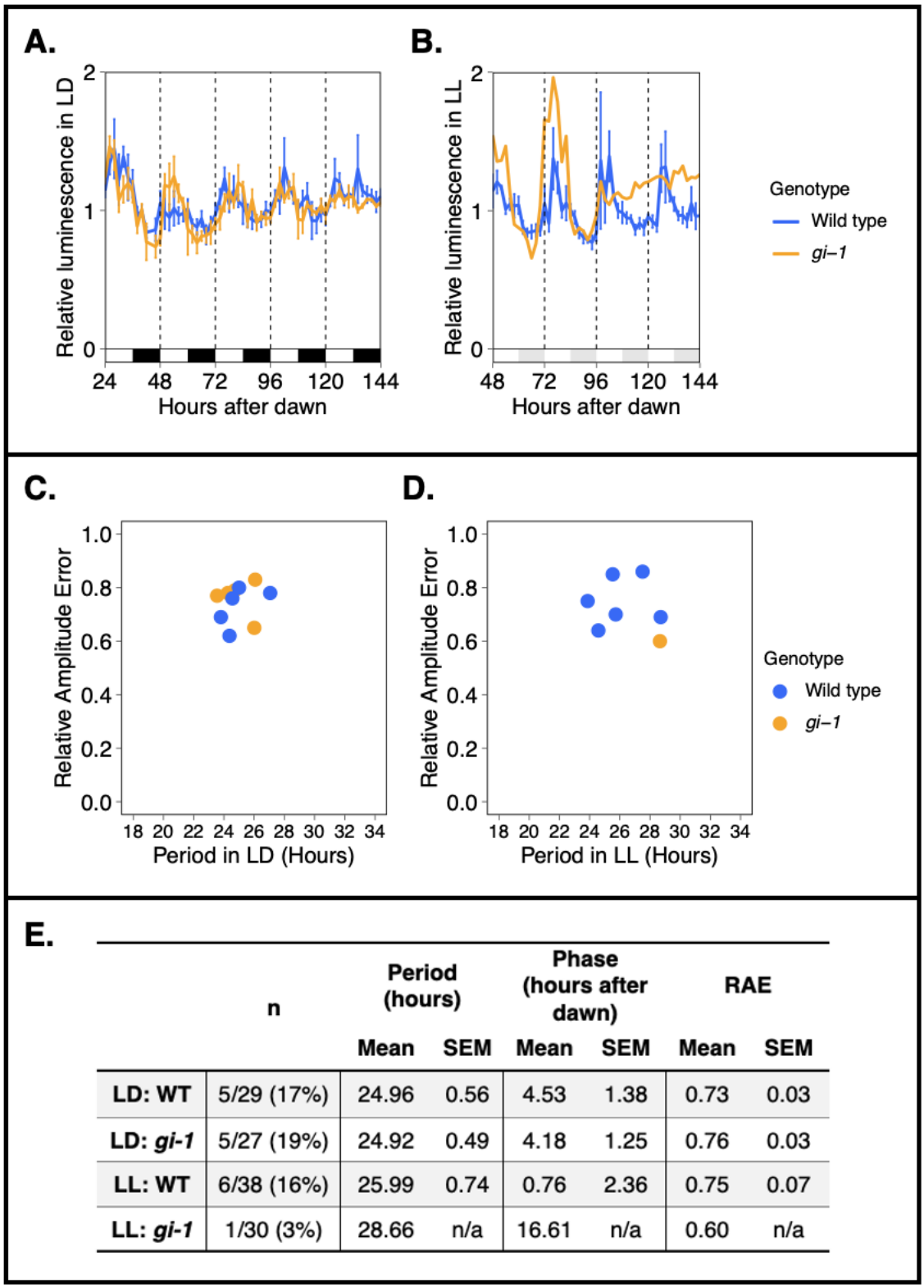

E.

	n	Period (hours)		Phase (hours after dawn)		RAE	
		Mean	SEM	Mean	SEM	Mean	SEM
LD: WT	5/29 (17%)	24.96	0.56	4.53	1.38	0.73	0.03
LD: *gi-1*	5/27 (19%)	24.92	0.49	4.18	1.25	0.76	0.03
LL: WT	6/38 (16%)	25.99	0.74	0.76	2.36	0.75	0.07
LL: *gi-1*	1/30 (3%)	28.66	n/a	16.61	n/a	0.60	n/a

Figure 4.5. Rhythmic luminescence of *P. fluorescens*::*lux* under constant conditions is disrupted on *gi-1* roots compared to wild-type *B. rapa*. Mean bacterial luminescence ± SEM of all roots under (a) light-dark cycles (n = 29 for wild type and 27 for *gi-1*) and (b) constant conditions (n = 38 for wild type and 30 for *gi-1*). Period and RAE values of rhythmic luminescence under (c) light-dark cycles and (d) constant conditions. RAE refers to the Relative Amplitude Error, a measure of the quality of the

period and phase estimate. RAE = 0 indicates a perfect fit to the data; RAE = 1 indicates a very poor fit. (c) Summary statistics. Units are hours for period, hours after dawn for phase, and arbitrary for RAE. Rhythmicity was determined using the FFT-NLLS method within the BioDare2 platform.

4.3.3. Mechanism of luminescence rhythms of *Pseudomonas* in the root and rhizosphere

The rhythmic luminescence of *P. fluorescens*::*lux* could be due to rhythmic changes in either bacterial cell abundance or *lux* gene expression, or both. These possible mechanisms were investigated using RT-qPCR. Root and rhizosphere compartment samples were examined separately, allowing the investigation of potential spatial variation in rhythmic changes. The timing of these rhythms was compared to those of plant clock genes *LHY* and *CCA1* in root tissues.

Rhythmic changes in the relative quantity of bacterial cells were investigated by quantifying levels of *P. fluorescens* 16S rRNA gene expression, relative to total expression of the 16S rRNA gene from all bacterial cells present.

The relative abundance of *P. fluorescens*::*lux* 16S rRNA in the root compartment displayed rhythmic changes, peaking 0-6 hours after dawn (Figure 4.6.b). While no peaks were observed on day 4, peaks on days 1, 2, 3, and 5 occurred with similar regularity to the peaks of *GI* and *CCA1* expression in the plant host (Figures 4.6.b and 4.6.c), suggesting possible synchronisation with the plant circadian clock.

Rhythmic changes in the relative abundance of *P. fluorescens*::*lux* 16S rRNA were also observed in the rhizosphere compartment (Figure 4.6.b). While these oscillations had a similar amplitude to those observed in the root compartment, they were not synchronised with those observed in the root compartment and peaked about 6 hours earlier (Figure 4.6.b).

In order to determine whether expression of the *lux* operon displayed circadian changes, mRNA levels of the *luxC* gene were quantified relative to those of *rpoA*

(DNA-directed RNA polymerase), a commonly used and constitutively expressed reference gene.

Relative expression of bacterial *luxC* in the root compartment displayed rhythmic changes, with a period of approximately 24 hours and peaks occurring in the morning (Figure 4.6.a). Days 1, 3 and 5 showed distinct single peaks in expression, while on days 2 and 4 broader peaks were observed, where relative expression was elevated in multiple samples taken during the light period (Figure 4.6.a). These peaks occurred with similar timing to those observed in *B. rapa GI* and *CCA1* expression (Figures 4.6.a and 4.6.c), suggesting possible synchronisation with the plant circadian clock.

While oscillations in relative *luxC* expression were observed in the rhizosphere compartment, these were not synchronised with those observed in the root compartment and peaks did not occur at regular intervals in the rhizosphere (Figure 4.6.a).

The data gained from RT-qPCR analyses cannot be directly overlaid with that obtained from the luminescence imaging experiments, as inoculated plants were two days older when sampling for RT-qPCR commenced. However, the timing of peaks may be compared across these experiments. Under light-dark cycles, the mean phase of *P. fluorescens*::*lux* luminescence was determined to be 4.5 hours after dawn (Figure 4.3.c). This occurred with similar timing to the peaks observed in both relative *luxC* expression and bacterial abundance in the root compartment, which all occurred in samples taken at, or 6 hours after, dawn. These results therefore indicate that diel oscillations in both the relative abundance and *luxC* expression of *P. fluorescens*::*lux* contribute to its rhythmic luminescence observed on *B. rapa* roots.

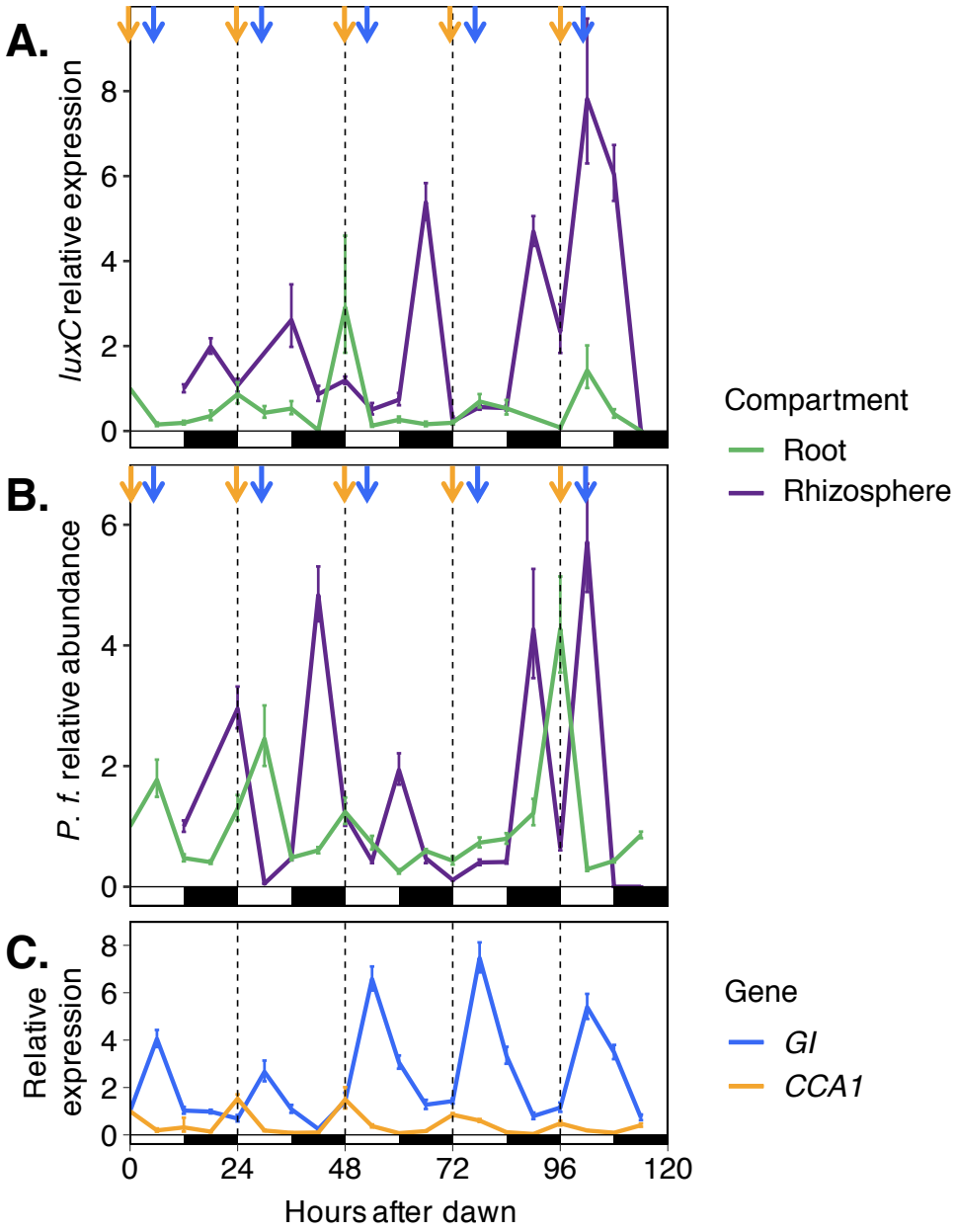

Figure 4.6. *P. fluorescens*::*lux* displays diel oscillations in *luxC* expression and relative cell abundance in root and rhizosphere compartments of inoculated wild-type *B. rapa*. (a) Expression of *P. fluorescens*::*lux luxC* relative to the housekeeping gene *rpoA*. (b) Relative abundance of *P. fluorescens*::*lux* cells as determined by expression of its 16S rRNA gene relative to total bacterial 16S rRNA expression. (c) Relative expression of *B. rapa GI* and *CCA1* relative to *ACTIN* to confirm rhythmicity of the plant circadian clock in roots. Blue and orange arrows on (a) and (b) represent peaks of plant *GI* and *CCA1* expression for reference. All expression data were normalised to the first time point in each series. Mean from 3 technical replicates ± SEM shown.

4.4. Discussion

4.4.1. A method for imaging bioluminescent *Pseudomonas* on roots

In this chapter, we developed a system for the growth and observation of plant roots inoculated with a luminescent model rhizosphere bacterium, inspired by methods by Dennis et al (2006) and Rellán-Álvarez et al (2015). Our method allowed the non-destructive analysis of root-inhabiting and rhizosphere populations of *P. fluorescens*::*lux* over time-course experiments lasting several days. It brings several advantages over the use of molecular characterisation of microbial communities, as it is cheaper and does not require labour intensive sampling. It also allowed us to investigate with high time resolution and to obtain spatial information on these interactions.

It is however worth noting that, unlike in the works of Pini et al. (2017) and O'Kane et al. (1988) where *lux* promoter fusions were created in order to investigate bacterial gene expression, the location of the *lux* cassette within the genome of the *P. fluorescens* strain used here is not known, and therefore the promoter control of *lux* expression is unknown.

4.4.2. Rhythmicity of bioluminescent *Pseudomonas* in the rhizosphere and the influence of the plant circadian clock

Circadian rhythmicity in *P. fluorescens*::*lux* luminescence was observed on roots of inoculated wild-type *B. rapa*, and found to persist under constant conditions (Figure 4.3). Persistence in the absence of external cues is a key characteristic of circadian rhythmicity (McClung, 2006), and an important differentiator between this and simply reactionary responses to diel environmental changes. These results therefore indicate that the rhythmicity of this model bacterium on wild-type *B. rapa* roots truly exhibited a circadian rhythm controlled by a biological oscillator. This led us to question whether this rhythm was endogenous to the bacterium or driven by the circadian clock of the plant host.

B. rapa gi-1 plants, which possess a loss-of-function mutation in the circadian clock gene *gigantea*, were used to investigate the influence of the plant circadian clock upon rhythmic bioluminescence of *P. fluorescens*::*lux*.

Under light-dark cycles, circadian rhythmicity in bacterial luminescence on the roots of *gi-1* plants followed the same pattern as that on the roots of wild-type plants (Figure 4.5). Contrastingly, under constant conditions, rhythmic bacterial luminescence on *gi-1* roots was effectively abolished (Figure 4.5). This is therefore evidence to suggest that the rhythmicity in luminescence of this reporter bacterium was disrupted on *B. rapa gi-1* roots under constant conditions. This alteration when compared to its behaviour on wild-type roots indicates that the *B. rapa* circadian clock does influence circadian rhythms in plant-microbe interactions in the rhizosphere. However, it remains to be seen whether this is because GI influences microbial rhythmicity directly or via its effect on the plant circadian clock.

On wild-type and *gi-1* plants under both light-dark cycles and constant conditions, bacterial luminescence exhibited relatively weak rhythmicity and high variability between roots (Figures 4.3 and 4.5). Additionally, low proportions of roots were found to display rhythmic bacterial luminescence. This may be because rhythmicity in the rhizosphere microbiome could be a response to an output of the plant clock, such as exudation, and therefore subject to greater variation, and may also be disrupted by local factors within the rhizosphere. Weak rhythmicity may also be due to relatively weak coupling between the plant and bacteria, as coupling between cells is important for maintaining the synchrony of circadian rhythms (Takahashi et al., 2015). Additionally, the luminescence signal used in this method is weak and therefore the signal to noise ratio is high, making it difficult to detect a rhythmic signal. Imaging at a closer range would mitigate this issue but would reduce the throughput of the experiments.

4.4.3. Mechanism of luminescence rhythms of *Pseudomonas* in the root and rhizosphere

Gene expression of *P. fluorescens*::*lux* in root and rhizosphere compartment samples was investigated in order to characterise spatial variation in its interaction with *B. rapa* roots, and to determine the mechanisms causing its rhythmic behaviour. Diel rhythms were observed in both the relative quantity of

P. fluorescens::*lux* cells and relative expression of the *luxC* gene, in root and rhizosphere compartment samples (Figure 4.6), indicating that both mechanisms may cause the rhythmicity observed in its bioluminescence.

While we demonstrated rhythmic changes in the relative abundance of *P. fluorescens::lux* 16S rRNA when investigating the relative quantity of its cells, it is worth nothing that as we did not experimentally validate the specificity of the primers used when amplifying this gene, the contribution of other *P. fluorescens* strains or *Pseudomonas* species cannot be excluded. However, we anticipate that autoclaving the soil which inoculated seedlings were planted in should have reduced the risk of this.

That genes from this model bacterium were detected and amplified from root samples, from which adhering rhizosphere soil was removed during the sampling protocol, implies that *P. fluorescens*::*lux* was living endophytically, or that it closely adhered to the rhizoplane (root surface) and could not be removed via standard mechanical means. Results from Thompson et al. (1995) suggested that *P. fluorescens* strain SBW25 was able to colonise the cortex of *B. vulgaris* roots, so it is possible that in this study the reporter strain was also inside the root itself. It was expected, as stated by Richter-Heitmann et al. (2016), that many microbes living on the rhizoplane may not become detached simply by root washing procedures such as that used in this study. Therefore, in order to more definitively determine whether this bacterium is able to live endophytically within *B. rapa* roots, sonication or treatment with hypochlorite could be used on samples in future. In this study, root compartment samples are therefore assumed to contain both endophytic microbes and a proportion of those living on the root surface.

In root compartment samples, daily oscillations in both *P. fluorescens*::*lux* cell abundance and gene expression were observed (Figure 4.6). Bacterial cell abundance and *luxC* expression were highest during the light periods each day. Contrastingly, the oscillations observed in bacterial cell abundance observed in rhizosphere samples were out of phase with those in the root compartment, with peaks occurring during dark periods each day. Moreover, *luxC* expression in the

rhizosphere was not synchronised with that in the root compartment and did not follow a rhythmic pattern. These results therefore suggest that the *B. rapa* circadian clock exerts a spatially variable influence on both microbial abundance and gene expression, where those microbes in closest proximity to roots are affected differently to those further away.

One explanation for the oscillations observed in the relative abundance of *P. fluorescens*::*lux* cells is that this bacterium may be able to physically move through its environment over daily time scales. It is thought that as some bacteria, including *P. fluorescens*, are able to move rapidly through aqueous media, they may also be able to move similarly quickly through water-filled pore spaces both in soil and root surfaces (Watt et al., 2006). Such movement is therefore possible and could be due to, for example, attraction towards exudates from plant roots or interactions with plant defence signalling molecules. The accumulation of jasmonates and salicylates, which are plant hormones involved in defence signalling, are regulated by the circadian clock, with jasmonates peaking in the subjective day and salicylates in the subjective night (Goodspeed et al., 2012). *Pseudomonas* species are already known to be influenced by salicylic acid, which was found to downregulate the fitness of *Pseudomonas aeruginosa* in the *A. thaliana* rhizosphere and led to a decrease in its virulence factor production (Prithiviraj et al., 2005). Salicylic acid is also thought to inhibit the motility and growth of *P. aeruginosa* by decreasing expression of *fliC*, which produces flagellin, an important component of the flagellum it requires for motility (Dong et al., 2012). The circadian rhythms in *P. fluorescens*::*lux* luminescence observed in this chapter were out of phase with those previously characterised in salicylic acid, and could therefore be explained by the known inhibitory effects of this molecule on *Pseudomonas* motility and fitness.

Due to the similar amplitudes but contrasting peaks observed in cell abundance between root and rhizosphere samples, it is possible that *P. fluorescens*::*lux* may be moving towards the root surface or into its interior during light periods, then dispersing in dark periods into the rhizosphere and potentially also further afield into bulk soil. This possibility would also explain the patterns of rhythmic luminescence observed in the imaging experiments. Higher relative

luminescence during light periods could be due to the congregation of bacterial cells in the root compartment, while lower relative luminescence during dark periods could be due to these cells becoming more diffuse over a wider area and thus their luminescence becoming undetectable.

In support of this hypothesis, the peaks observed in both *luxC* expression and the relative quantity of *P. fluorescens*::*lux* cells within root compartment samples coincided with the mean phase of luminescence observed in the imaging experiments, which occurred during the light periods. These results therefore suggest that compartment-specific daily oscillations in both gene expression and cell movement may be contributing to the rhythmic luminescence of *P. fluorescens*::*lux* on *B. rapa* roots under light-dark cycles.

CHAPTER 5: GENERAL DISCUSSION

5.1. Research findings

In the work presented in this thesis, the plant circadian clock was found to influence daily changes in relative abundance of rhizosphere microbes as well as the recruitment of microbiota into the rhizosphere microbiome.

Molecular profiling was used to identify rhythmic taxa within the rhizosphere microbiome and to investigate the assembly of the rhizosphere microbiome. In addition, a novel imaging method was developed for the non-destructive visualisation of circadian interactions between plant roots and a model rhizosphere bacterium. Work using this imaging method allowed for investigation at a fine temporal scale with a degree of spatial resolution, and the model system we developed for this also enabled us to determine whether microbial rhythmicity was associated with changes in bacterial relative abundance or transcriptional activity.

To determine the influence of the plant circadian clock, microbial rhythms in the rhizosphere of plants with mutations in the genes *lhy* and *gi* were compared to those of wild-type plants. *Arabidopsis thaliana* plants with overexpression and loss-of-function of the core circadian clock gene *lhy* were utilised for work involving molecular characterisation of the rhizosphere. For the luminescence-based experiments, *Brassica rapa* plants with *gi* loss-of-function were investigated.

In this thesis we also began to establish whether circadian rhythmicity in the rhizosphere microbiome exhibits spatial variation. Evidence for this was provided in Chapter 4, where spatial variation was observed in the patterns of bacterial relative transcriptional activity and cell abundance between root and rhizosphere compartment samples. While the imaging method developed in this chapter showed where the model rhizosphere bacterium was localised after its application to roots, further work could investigate more specifically whether there are locations with higher amplitudes of its rhythmic luminescence. It has been

suggested that rhythmic rhizosphere microbiota could act as pioneer species and colonise freshly emerging root tissues (Staley et al., 2017), as root growth is controlled by the circadian clock and shows rhythmicity (Yazdanbakhsh et al., 2011). The imaging method developed here could therefore be used to investigate this hypothesis, by determining whether microbial rhythmicity occurs throughout the rhizosphere or displays hotspots in areas which may be experiencing greater root growth. Additionally, while Chapter 2 used composite root and rhizosphere samples, Chapter 3 investigated samples taken from the rhizosphere compartment alone. It would therefore be interesting to analyse the corresponding root compartment samples which were taken in Chapter 3 but set aside. This would allow us to determine whether a higher amount of free-running microbial rhythmicity may be observed in those microbes living in closer proximity to plants.

Any potential functional consequences of circadian rhythmicity in the rhizosphere microbiome remain to be uncovered. In order to explore these, future work could determine whether specific biochemical pathways utilised by rhizosphere microbiota exhibit circadian rhythms and assess for circadian oscillations in expression of a wider range of genes than those studied here. This would enable us to determine whether rhizosphere processes which involve intimate associations with plants or have wider significance, such as nitrogen fixation or nutrient transformations, are rhythmic. These possibilities could be investigated through meta-omics techniques, which involve characterising the totality of genomic, transcriptomic, proteomic or metabolomic material from samples containing complex microbial communities (White et al., 2017). Of particular use could be metatranscriptomics and metabolomics, which investigate the totality of transcriptional and metabolic activity within a microbiome (White et al., 2017).

In addition to the model plant *A. thaliana*, a genotype of *B. rapa* (field mustard) which is developmentally similar to oilseed rape was investigated in this thesis. Circadian clock component homologs have also been identified in several commercial crop species, including soybean (Marcolino-Gomes et al., 2014), rice (Murakami et al., 2007), wheat (Alvarez et al., 2016), and the bioenergy crop

sorghum (Kebrom et al., 2020). A wider range of species, such as these commercial crops, should also be investigated in future work concerning circadian influences on the rhizosphere microbiome. This would enable us to determine whether this is a widespread phenomenon which could have potential commercial impacts. Circadian interactions in the rhizosphere could then also be compared across host plants, as it is possible that some species could display a higher degree of rhythmicity than others. This is because root exudation, which may be one of the main drivers of microbial rhythmicity in the rhizosphere, can show considerable qualitative and quantitative differences between species (Preece and Peñuelas, 2020). Circadian influences on the rhizosphere microbiome should also be investigated in field-grown plants, to determine whether they are also present under natural environmental conditions where transitions between day and night are more gradual than those experienced in growth chambers.

5.2. Mechanisms of microbial rhythmicity in the rhizosphere microbiome

While previous works on the topic have speculated that oscillating availabilities of carbon, water or nutrients may drive circadian rhythmicity in the rhizosphere microbiome (Hubbard et al., 2017; Staley et al., 2017; Baraniya et al., 2018), the causes have not yet been determined and many possible mechanisms may contribute.

The plant circadian clock regulates the timing of photosynthesis and the allocation of fixed carbon to three main fates: metabolic use, transport, and storage (Harmer et al., 2000). In addition to utilising carbon during the day, plants store it by accumulating starch, which is then used to support growth and metabolism through the night (Sulpice et al., 2014). The circadian clock ensures that starch reserves are degraded at a constant rate throughout the night to ensure that they do not run out before dawn (Graf et al., 2010). The exudation of some specific compounds is known to differ throughout the day (Ma and Nomoto, 1996; Watt and Evans, 1999; Tharayil and Triebwasser, 2010) and diel changes in the overall volume of root exudates have also been reported (Iijima et al.,

2003). As root exudates attract microbiota to the rhizosphere and stimulate microbial activity around roots (Doornbos et al., 2012), circadian changes in their quantity or composition could induce circadian changes in the rhizosphere microbiome. It is thought that some bacterial species are capable of relatively rapid movement through water-filled spaces in soil (Watt et al., 2006), so some members of the rhizosphere microbiome may be able to move into the rhizosphere at particular times of day in response to changes in plant exudation. Additionally, daily changes in available carbon sources could cause circadian changes in microbial transcriptional activity.

The plant immune system could provide another form of signal which may cause rhythmicity in the rhizosphere microbiome. The plant circadian clock is involved in the co-ordination of immune responses to pathogens and pests (Lu et al., 2017) and plants show circadian variation in their susceptibility to damage by pests and pathogens (Sharma and Bhatt, 2015). The production of many classes of molecules relating to defence signalling, namely jasmonates, salicylates and Reactive Oxygen Species, display daily oscillations (Goodspeed et al., 2012; Lai et al., 2012). For example, the accumulation of jasmonates peaks in the subjective day while salicylates peak in the subjective night (Goodspeed et al., 2012). Roots are able to detect the presence of pathogens and induce innate immune responses (Chuberre et al., 2018), and there is already evidence that defence signalling in roots influences rhizosphere community composition. It was found that activation of the jasmonic acid defence signalling pathway altered the composition of rhizosphere bacterial communities (Carvalhais et al., 2013) and that salicylic acid influenced the colonisation of the endophytic microbiome by specific bacterial taxa (Lebeis et al., 2015). Additionally, the fitness of pathogenic *Pseudomonas aeruginosa* in the rhizosphere was found to be downregulated by elevated levels of salicylic acid (Prithiviraj et al., 2005). While plant defences are primarily targeted towards microbial pathogens, it is therefore possible that the relative abundances of other members of the rhizosphere microbiome could be influenced by plant rhythmic defences, and that rhythmic changes in rhizosphere microbial transcriptional activity could also be induced in response.

Circadian influences on root exudation and defence processes could also explain why plants with a dysfunctional circadian clock accumulated differing rhizosphere microbial communities relative to wild-type plants over the course of plant growth. Plants possessing circadian clock mutations may display altered physiological phenotypes that can alter their fitness (Dodd et al., 2004; Dodd et al., 2005), which could result in the assembly of distinct groups of rhizosphere microbiota over the plant's lifespan.

In most plants, stomata open to enable photosynthesis during the day and close at night (Webb, 2003). While stomata are open, water loss occurs via transpiration, and the transpiration stream draws water up through the plant all the way from the roots to stomata. Transpiration rates are reduced at night and are typically between 5 and 15% of the rates during the day as stomatal closure may often be incomplete (Caird et al., 2007). It is therefore possible that some microbes could be passively drawn towards the rhizosphere when transpiration rates are at their highest each day. Plant transpiration has also been linked with the flow of nutrients though soil (Cardon and Gage, 2006; Matimati et al., 2014). Possible daily oscillations in rhizosphere nutrient availability, caused by changes in the distribution of water, may therefore also contribute to microbial rhythmicity in this region. Such oscillations in nutrient availability could potentially lead to rhythmic responses in both the relative abundance and transcriptional activity of rhizosphere microbiota.

While the work in this thesis focussed on the characterisation of bacterial and fungal communities, many other types of unicellular and multicellular organisms are found within the rhizosphere microbiome, such as protists, nematodes, collembola, and mites, as well as viruses (Moore et al., 2003; Gao et al., 2018; Pratama et al., 2020). Interactions between these organisms may exhibit as-yet uncharacterised daily variation. For example, protists can consume bacteria and fungi, and can shape the composition of the rhizosphere microbiome (Gantner et al., 2006; Gao et al., 2018) and some marine protists are known to display diel cycles in their growth and feeding rates (Jakobsen and Strom, 2004; Arias et al., 2020; Deng et al., 2020). While relatively little is known about the role of bacteriophage (viruses which infect and may kill bacteria) in the rhizosphere, it is

thought that they may also influence the ecological dynamics of the microbiota here (Pratama et al., 2020). There is evidence that marine cyanophage exhibit diel rhythms during infection and oscillations in their abundance (Ni and Zeng, 2016; Liu et al., 2019). It is therefore possible that such rhythmic interactions could also be occurring in the rhizosphere. Circadian rhythms in predation may exert direct effects on microbial relative abundances and could also impose a selection pressure leading to rhythmicity in the transcriptional activity of microbiota.

Another explanation for rhythmicity in the rhizosphere could be potential daily rhythms in microbial growth and dieback. Hernandez and Allen (2013) previously found that rates of growth and dieback of arbuscular mycorrhizal fungi were highest in the interval between midday and 6pm, when plant photosynthetic activity is also at its highest. Such variability could explain the peaks and troughs observed in the relative abundance of fungi in particular. This is because fungal hyphae are generally larger than bacteria (Watt et al., 2006) and unable to physically move over short timescales. However, while rhythmic dieback would account for the rhythmicity observed in members of active rhizosphere communities when characterising microbial RNA, dieback alone does not necessarily explain why rhythmicity was also observed when microbial DNA was characterised. This is because the amplicon sequencing of DNA is able to detect dead and dormant taxa in addition to live community members (Emerson et al., 2017). DNA from dead bacterial cells has been found to remain detectable in soil for as long as 70 days (Selenska and Klingmüller, 1991), and other studies observed persistence in the region of days to weeks (Nielsen et al., 2007). This indicates that for rhythmicity to be observed in the relative abundance of microbial DNA, other rhythmic processes such as predation must also be occurring to ensure that the DNA of dead cells does not persist in the rhizosphere environment.

It therefore follows that in reality, circadian changes in the rhizosphere microbiome are likely caused by a combination of multiple of the possible mechanisms discussed here, which could affect both microbial relative abundance and transcriptional activity. For example, during light periods, some

bacteria could be drawn into the rhizosphere by the plant's transpiration stream, and then if they remain in the vicinity during dark periods they may be consumed by other organisms such as protists. Peaks in microbial relative abundance may occur at times when their growth rate is greater than the rate at which they are being consumed. At other times of day where their relative abundance is low, this may be because carbon flow into the rhizosphere for use in microbial growth is at a minimum, or dieback rates are at their highest, while predation is also occurring.

A major direction for further study should therefore be to elucidate the mechanisms causing circadian rhythmicity in the rhizosphere microbiome by examining the possible mechanisms discussed here. In particular, the potential influence of plant exudates and immune responses should be examined, by comparing rhythmicity in wild-type plants to that observed in the rhizosphere of plants possessing mutations relating to these pathways. For example, the protein JAZ6 has been demonstrated to be a key link between jasmonic acid signalling pathways and the plant circadian clock (Ingle et al., 2015), so mutant plants with *jaz6* loss-of-function would be a promising avenue for determining whether plant defence signalling influences rhythmicity in the rhizosphere microbiome. Badri et al. (2010) found that the expression of some genes involved in the biosynthesis of secondary metabolites, such as flavonol synthases, followed diel patterns within roots. Plants with mutations in these genes would be a suitable starting point for the investigation of whether root exudates also influence rhizosphere microbial rhythmicity.

Future work could also examine the possibility of rhythmic predation pressure in the rhizosphere, such as using amplicon sequencing of the 18S rRNA gene to profile protist communities. While this would determine whether any protists also show oscillations in their relative abundance and could be used as part of co-occurrence analyses, it would not necessarily show definitive causation of other microbial rhythms. Alternately, interactions between protists and bacteria or fungi could be examined using competition assays, which could be based upon the introduction of a protist grazer into the model system setup developed in Chapter 4 of this thesis. The imaging method from Chapter 4 could also be used to

establish whether plant photosynthesis influences circadian rhythmicity in the rhizosphere microbiome. This could be investigated by determining whether rhythmicity of the model rhizosphere bacterium persists after application of DCMU (3-[3,4-dichlorophenyl]-1,1-dimethylurea), a chemical inhibitor of photosystem II of photosynthesis (Haydon et al., 2013), or when plants are subjected to constant darkness. While relatively low throughput in its current form, the flexibility of this imaging method means it is well suited for manipulating plant growth conditions, which would be particularly useful for testing the influence of photosynthesis or different lighting regimes. It could also be utilised to compare the effects of plant genotypes with different exudation profiles on root-associated microbial rhythmicity, for example.

5.3. Implications of research findings

The global population is predicted to reach between 9.6 and 12.3 billion people by the year 2100 (Gerland et al., 2014). The challenge of increasing food production accordingly is exacerbated by the threats which global crop production faces. Such threats, many of which are caused or worsened by climate change, include increasing temperatures, more frequent and severe extreme weather events such as drought, and the spread of pests and diseases (Sundström et al., 2014). Indeed, evidence now indicates that our changing climate has already negatively affected global food production (Ray et al., 2019). It is therefore vital that more sustainable methods are developed for maintaining and increasing crop yields in the face of these challenges. As the rhizosphere microbiome has important effects on plant health, productivity and stress tolerance, it is of importance to understand the mechanisms by which plants attract and maintain relationships with soil microbiota. Such knowledge may enable the development of new strategies for the manipulation of rhizosphere plant-microbial interactions, with a view towards enhancing crop production.

The knowledge of circadian influences on the rhizosphere microbiome gained from this work could inform the development of novel chronobiology-based strategies for crop management. Belbin et al. (2019) proposed the concept of agricultural chronotherapy, which is similar to the principle in medicine, where treatment is delivered in synchrony with the circadian rhythms of the human body

to maximise efficacy (Kaur et al., 2013). Belbin et al. (2019) determined that plants exhibit clock-mediated circadian rhythmicity in their susceptibility to a herbicide, with application at dawn causing the greatest reduction in hypocotyl length. In a similar vein, the existence of circadian variation in the rhizosphere microbiome indicates that the success of soil-based agricultural interventions, such as the establishment of microbial inoculants, could differ depending on the time of application. Additionally, some mutations in circadian clock genes, for example those of *cca1-ox* and *toc1-RNAi* plants, have been demonstrated to increase plants' ability to tolerate environmental stresses (Grundy et al., 2015). This thesis demonstrates that mutations in plant circadian clock genes also alter the assembly of, and circadian changes within, the rhizosphere microbiome, and that different mutations cause differing effects. Therefore, when considering such clock-based strategies to modulate plant stress responses, other unintended effects on the rhizosphere microbiome are possible and should be considered.

The work presented in this thesis also has implications for future studies seeking to investigate rhizosphere microbiota. The findings of this research contribute to the growing body of evidence indicating that the rhizosphere microbiome is a highly dynamic environment, which is more variable over short-term timescales than previously anticipated (Hubbard et al., 2017; Staley et al., 2017; Baraniya et al., 2018). The influence of other factors, such as plant genotype and the abiotic environment of soil, upon the composition of the rhizosphere microbiome is well characterised (Micallef et al., 2009; Marasco et al., 2012; Philippot et al, 2013). Contrastingly, comparatively little is known about the influence of time, except for in the context of changes across seasons (Shi et al., 2015). The circadian variation in the rhizosphere microbiome as characterised in this thesis indicates that future studies seeking to investigate rhizosphere microbiota should control for the timing of sampling, which is not currently considered.

APPENDIX

Table A2.1. Microbial community composition does not significantly differ between dawn and dusk samples. Dawn and dusk time points were compared within sample types using ANOSIM. * indicates the only comparison where community composition significantly differed between dawn and dusk (i.e. $R > 0.2$ and $p \leq 0.05$).

Sample		R	p
Total bacteria	WT	0.152	0.027
	lhy-11	0.022	0.328
	lhy-ox	0.146	0.083
	Soil	-0.028	0.569
Active bacteria	WT	0.079	0.262
	lhy-11	0.217	0.050*
	lhy-ox	-0.025	0.493
	Soil	-0.067	0.700
Total fungi	WT	0.080	0.202
	lhy-11	0.0175	0.359
	lhy-ox	0.357	0.348
	Soil	0.070	0.206
Active fungi	WT	0.112	0.157
	lhy-11	0.026	0.298
	lhy-ox	0.147	0.111
	Soil	-0.108	0.910

Table A2.2. Microbial alpha diversity does not significantly differ between dawn and dusk samples. Alpha diversity was compared between dawn and dusk time points within sample types using Kruskal-Wallis testing. * indicates the only significant comparison where $p \leq 0.05$.

	Bacteria		Fungi	
	Total	**Active**	**Total**	**Active**
WT	0.064	0.286	0.347	0.465
lhy-11	0.668	0.886	0.291	0.668
lhy-ox	0.568	1.00	0.153	0.029*
Soil	0.199	0.808	0.200	0.917

Table A2.3. *lhy* loss-of-function and overexpression do not influence species richness of the rhizosphere microbiome. Mean number of OTUs per sample ± SEM. Values displaying different superscript letters significantly differ ($p \leq 0.05$; Kruskal-Wallis followed by pairwise Wilcoxon rank sum tests).

	Total bacteria	Active bacteria	Total fungi	Active fungi
WT	2234 ± 103 [a]	1821 ± 98 [a]	160 ± 12 [a]	70 ± 7 [a]
lhy-11	2056 ± 90 [a]	1816 ± 73 [a]	177 ± 11 [a]	57 ± 10 [a]
lhy-ox	2136 ± 95 [a]	1797 ± 85 [a]	191 ± 11 [a]	46 ± 10 [a]
Soil	2025 ± 51 [a]	1915 ± 173 [a]	312 ± 24 [b]	52 ± 14 [a]

Table A2.4. *lhy* overexpression, but not loss-of-function, alters species evenness of the rhizosphere microbiome. Species evenness was quantified using Shannon's Equitability Index. Values displaying different superscript letters significantly differ ($p \leq 0.05$; Kruskal-Wallis followed by pairwise Wilcoxon rank sum tests).

	Total bacteria	Active bacteria	Total fungi	Active fungi
WT	0.84 ± 0.004 [a]	0.77 ± 0.006 [a]	0.67 ± 0.039 [a]	0.71 ± 0.039 [a]
lhy-11	0.84 ± 0.003 [a]	0.77 ± 0.011 [a]	0.67 ± 0.029 [a]	0.71 ± 0.045 [a]
lhy-ox	0.81 ± 0.009 [b]	0.73 ± 0.019 [a]	0.56 ± 0.027 [b]	0.59 ± 0.068 [a]
Soil	0.85 ± 0.002 [a]	0.83 ± 0.008 [b]	0.68 ± 0.012 [a]	0.61 ± 0.083 [a]

Table A2.5. Dominant microbial taxa differ in relative abundance between total and active communities of many samples. Relative abundances of taxa were compared between total and active bacterial and fungal communities using Kruskal-Wallis testing. * indicates a significant difference in relative abundance between total and active communities ($p \leq 0.05$).

	WT	***lhy-11***	***lhy-ox***	**Soil**
Actinobacteria	Total > active p < 0.001*	Total > active p < 0.001*	Total > active p < 0.001*	Total > active p < 0.001*
Proteobacteria	Total < active p < 0.001*	Total < active p < 0.001*	Total < active p = 0.030*	Total < active p < 0.001*
Cyanobacteria	Total < active p < 0.001*	Total < active p < 0.001*	Total < active p = 0.0012*	Total < active p < 0.001*
Dothideomycetes	Total < active p = 0.450	Total < active p = 0.017*	Total < active p = 0.235	Total < active p = 0.742
Sordariomycetes	Total > active p = 0.041*	Total > active p < 0.001*	Total > active p = 0.173	Total > active p < 0.001*

Table A2.6. *lhy* loss-of-function and overexpression alter the relative abundances of bacterial phyla in the rhizosphere microbiome. Relative abundances of taxa were compared between samples using Kruskal-Wallis testing. Taxa shown displayed significant differences ($p \leq 0.05$) in their relative abundances in at least one comparison between *lhy-11*, *lhy-ox* and wild-type rhizosphere samples, and constitute greater than 1% relative abundance in at least one sample. Mean relative abundances shown.

	Comparison	Phylum	Relative Abundance	Fold change	p
Total communities	WT vs *lhy-11*	Actinobacteria	27.4% vs 32.0%	1.2 ↑	0.003*
		Bacteroidetes	2.3% vs 1.7%	1.4 ↓	0.046*
		Chloroflexi	7.5% vs 9.0%	1.2 ↑	0.022*
		Proteobacteria	25.6% vs 21.5%	1.2 ↓	0.008*
	WT vs *lhy-ox*	Acidobacteria	8.5% vs 7.0%	1.2 ↓	0.046*
		Proteobacteria	25.6% vs 22.0%	1.2 ↓	0.027*
	lhy-11 vs *lhy-ox*	Actinobacteria	32.0% vs 27.0%	1.2 ↓	0.006*
		Cyanobacteria	3.4% vs 11.5%	3.4 ↑	0.025*
		Chloroflexi	9.0% vs 7.5%	1.2 ↓	0.026*
		Gemmatimonadetes	3.2% vs 2.4%	1.3 ↓	0.013*
Active communities	WT vs *lhy-ox*	Proteobacteria	29.5% vs 26.2%	1.1 ↓	0.045*

Table A2.7. *lhy* overexpression, but not loss-of-function, alters the relative abundances of fungal classes in the rhizosphere microbiome. Relative abundances of taxa were compared between samples using Kruskal-Wallis testing. Taxa shown displayed significant differences ($p \leq 0.05$) in their relative abundances in at least one comparison between *lhy-11*, *lhy-ox* and wild-type rhizosphere samples, and constitute greater than 1% relative abundance in at least one sample. Mean relative abundances shown.

	Comparison	Class	Relative Abundance	Fold Change	p
Total communities	**WT vs *lhy-ox***	Agaricomycetes	6.8% vs 32.1%	4.7 ↑	<0.001*
		Dothideomycetes	19.4% vs 13.3%	1.5 ↓	0.020*
		Eurotiomycetes	6.8% vs 3.4%	2.0 ↓	0.022*
	lhy-11* vs *lhy-ox	Agaricomycetes	8.0% vs 32.1%	4.0 ↑	<0.001*
		Dothideomycetes	23.8% vs 13.3%	1.8 ↓	<0.001*
		Eurotiomycetes	6.3% vs 3.4%	1.9 ↓	0.012*
		Sordariomycetes	52.9% vs 42.8%	1.2 ↓	0.013*
Active communities	**WT vs *lhy-ox***	Tremellomycetes	2.4% vs 0.7%	3.4 ↓	0.027*
	lhy-11* vs *lhy-ox	Agaricomycetes	4.2% vs 16.5%	3.9 ↑	0.027*
		Tremellomycetes	4.0% vs 0.7%	5.7 ↓	0.041*

Table A2.8. Plant pathogenic OTUs form higher relative abundances in total fungal communities than active. Total relative abundances of pathogenic OTUs were compared between total and active fungal communities within sample types using Kruskal-Wallis testing. Mean relative abundances shown. * indicates a significant difference in relative abundance between total and active communities ($p \leq 0.05$).

	Total	Active	p
WT	37.9%	33.3%	0.364
lhy-11	37.7%	25.7%	0.002*
lhy-ox	29.1%	28.0%	0.794
Soil	30.5%	17.1%	0.007*

Table A2.9. Fungal ecological guilds do not significantly differ in relative abundance between dawn and dusk samples. Relative abundances of guilds were compared between dawn and dusk time points within samples using Kruskal-Wallis testing. No significant comparisons ($p \leq 0.05$) were observed.

	Total				Active			
	WT	***lhy-11***	***lhy-ox***	**Soil**	**WT**	***lhy-11***	***lhy-ox***	**Soil**
Arbuscular mycorrhizal	0.814	0.862	0.886	0.688	0.368	0.820	0.176	0.136
Endophyte	0.076	0.372	0.568	0.200	0.465	0.774	0.852	0.116
Fungal parasite	0.076	0.088	0.317	0.337	0.054	0.562	n/a	0.882
Plant pathogen	0.754	0.465	0.253	1.00	0.602	0.886	1.00	0.602
Saprotroph	0.917	0.372	0.886	0.749	0.602	0.317	0.465	0.917

Table A2.10. Bacterial phyla predominantly do not significantly differ in relative abundance between dawn and dusk samples. Relative abundances of phyla were compared between dawn and dusk time points within samples using Kruskal-Wallis testing. * indicates significant comparisons where $p \leq 0.05$.

	Total				Active			
	WT	***lhy-11***	***lhy-ox***	**Soil**	**WT**	***lhy-11***	***lhy-ox***	**Soil**
Acidobacteria	0.035*	0.116	0.886	0.668	0.286	0.046*	0.624	0.808
Actinobacteria	0.085	0.253	0.253	0.199	0.670	0.317	1.0	0.465
Bacteroidetes	0.064	0.317	0.087	0.568	0.088	0.153	0.327	0.372
Chloroflexi	0.085	0.475	0.063	0.317	0.286	0.668	0.807	0.291
Cyanobacteria	0.048*	0.668	0.668	0.568	0.522	0.568	0.462	0.570
Firmicutes	0.749	0.391	0.063	1.0	0.394	0.116	0.142	0.935
Gemmatimonadetes	0.338	0.046*	0.253	0.153	0.286	0.668	1.0	0.935
Nitrospirae	0.848	0.317	0.153	0.475	1.0	0.199	1.0	0.570
Planctomycetes	0.749	0.087	0.886	0.116	1.0	0.391	0.462	0.685
Proteobacteria	0.142	0.116	0.022*	0.668	0.522	0.886	0.221	0.935
Verrucomicrobia	0.655	0.087	0.668	0.568	1.0	0.775	0.050*	0.291

Table A2.11. Fungal classes predominantly do not significantly differ in relative abundance between dawn and dusk samples. Relative abundances of classes were compared between dawn and dusk time points within samples using Kruskal-Wallis testing. * indicates significant comparisons where $p \leq 0.05$.

	Total				Active			
	WT	***lhy-11***	***lhy-ox***	**Soil**	**WT**	***lhy-11***	***lhy-ox***	**Soil**
Agaricomycetes	0.117	0.685	1.00	0.522	0.347	0.252	0.067	0.347
Ascomycota: Incertae sedis	0.917	0.570	0.199	0.337	0.465	0.668	0.400	0.245
Ascomycota: Unidentified	0.754	0.685	0.087	0.631	0.465	0.668	0.018*	0.341
Dothideomycetes	0.117	0.685	0.116	0.522	0.117	0.116	0.361	0.754
Eurotiomycetes	0.602	0.685	0.116	0.423	0.009*	0.617	0.011*	0.602
Leotiomycetes	0.009*	0.808	0.391	0.337	0.009	1.00	0.848	0.578
Sordariomycetes	0.602	0.685	0.775	1.00	0.251	0.116	0.465	0.465
Tremellomycetes	0.465	0.223	0.022*	0.873	0.465	0.391	0.027*	0.754
Zygomycota: Incertae sedis	0.917	0.465	0.032*	0.631	0.465	0.474	0.200	0.747

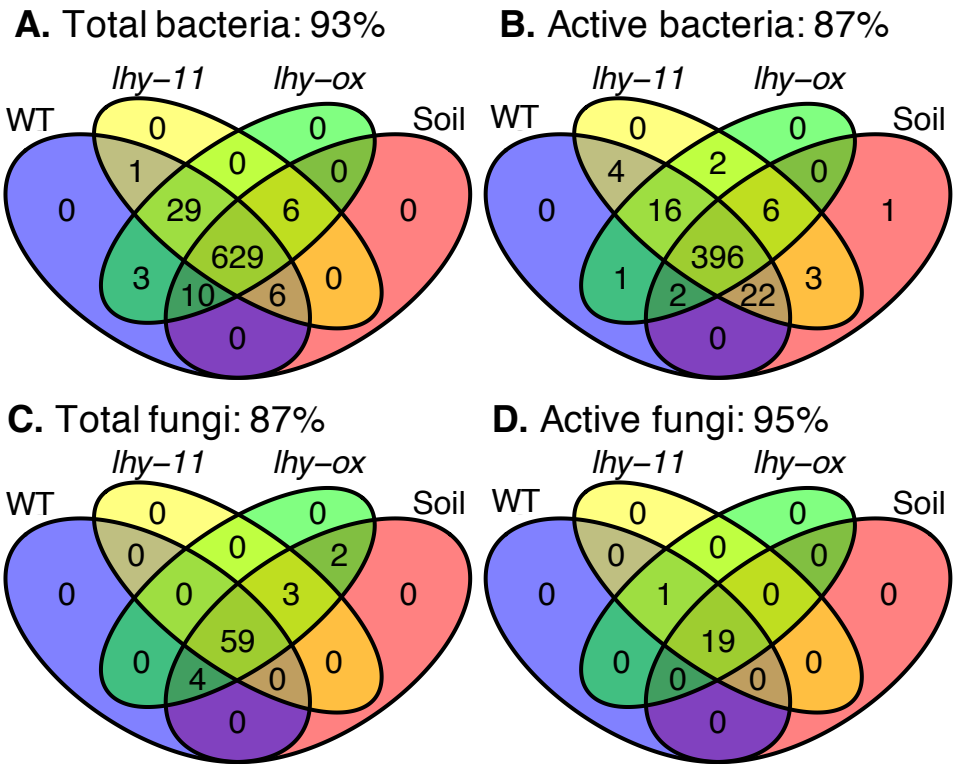

Figure A2.1. The majority of rhythmic OTUs are present across all samples. The presence of OTUs which were identified as rhythmic in one or more samples was investigated across all samples. Numbers in overlapping sections indicate rhythmic OTUs which were present in multiple samples, whether or not they were rhythmic in all. Percentages indicate the number of rhythmic OTUs which were found to be present in all samples, whether or not they were also rhythmic in these.

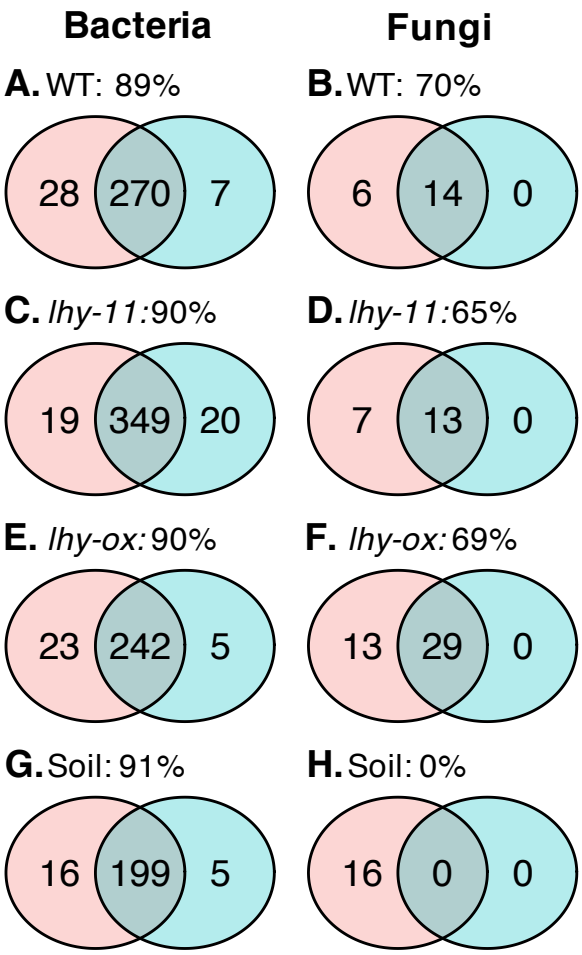

Figure A2.2. OTUs identified as rhythmic in either total or active microbial communities are generally not present in both. The presence of OTUs which were rhythmic in either total or active communities was investigated across both. Percentages indicate the amount of rhythmic OTUs which were present in both communities, whether or not they were rhythmic in these.

Table A2.12. Relative abundances of bacterial phyla present in rhythmic OTUs differ across samples. Rhythmic OTUs were identified as displaying a significant difference in their relative abundance between dawn and dusk samples. The taxonomy of these rhythmic OTUs was investigated. Mean relative abundances are as a proportion of just the rhythmic OTUs shown. “AM” and “PM” represent dawn and dusk sampling points respectively. Taxa with individual relative abundances of less than 0.5% across all samples were merged to create the “Low Abundance” category.

	Total								Active							
%	**WT**		***lhy-11***		***lhy-ox***		**Soil**		**WT**		***lhy-11***		***lhy-ox***		**Soil**	
	AM	**PM**	**AM**	**PM**	**AM**	**PM**	**AM**	**PM**	**AM**	**PM**	**AM**	**PM**	**AM**	**PM**	**AM**	**PM**
Acidobacteria	6.7	8.5	-	-	-	-	10.7	9.4	7.0	14.0	9.8	15.1	-	-	-	-
Actinobacteria	50.9	50.6	40.6	49.8	39.6	44.5	46.0	50.7	8.5	18.1	17.9	20.9	-	-	-	-
Chloroflexi	22.5	25.8	8.4	10.7	7.3	10.5	-	-	-	-	-	-	-	-	-	-
Cyanobacteria	-	-	9.2	2.3	-	-	-	-	28.5	7.3	11.0	1.4	17.8	3.1	-	-
Firmicutes	-	-	-	-	15.3	18.9	-	-	-	-	4.4	5.7	-	-	-	-
Low Abundance	13.3	8.0	14.5	10.3	7.7	4.5	26.2	21.0	17.1	20.8	13.9	9.8	18.4	30.1	55.7	49.1
Planctomycetes	-	-	7.1	8.8	-	-	-	-	-	-	-	-	-	-	-	-
Proteobacteria	6.5	7.1	14.3	11.8	26.2	17.6	17.1	18.8	33.7	31.8	43.1	47.1	50.2	59.0	44.3	50.9
Verrucomicrobia	-	-	6.0	6.2	3.9	4.0	-	-	5.2	8.0	-	-	13.6	7.9	-	-

Table A2.13. Relative abundances of fungal classes present in rhythmic OTUs differ across samples. Rhythmic OTUs were identified as displaying a significant difference in their relative abundance between dawn and dusk samples. The taxonomy of these rhythmic OTUs was investigated. Mean relative abundances are as a proportion of just the rhythmic OTUs shown. “AM” and “PM” represent dawn and dusk sampling points respectively. Taxa with individual relative abundances of less than 0.5% across all samples were merged to create the “Low Abundance” category.

%	Total								Active							
	WT		*lhy-11*		*lhy-ox*		Soil		WT		*lhy-11*		*lhy-ox*		Soil	
	AM	PM	AM	PM	AM	PM	AM	PM	AM	PM	AM	PM	AM	PM	AM	PM
Agaricomycetes	13.4	19.3	-	-	-	-	-	-	-	-	-	-	-	2.9	-	-
Ascomycota: Unidentified	-	-	-	-	10.3	11.1	-	-	-	-	-	-	19.2	22.9	-	-
Dothideomycetes	-	-	-	-	36.1	30.0	-	-	33.9	37.8	8.0	70.0	33.6	43.0	-	-
Eurotiomycetes	-	-	60.9	9.9	9.3	9.0	-	-	64.3	54.7	-	-	47.2	28.6	-	-
Leotiomycetes	16.8	15.3	-	-	-	-	-	-	-	-	-	-	-	-	-	-
Low Abundance	4.3	3.5	0.7	2.1	1.9	2.8	14.8	15.5	1.8	7.5	6.6	5.2	-	0.5	-	-
Sordariomycetes	65.5	61.9	38.4	88.1	37.2	42.5	85.2	84.5	-	-	85.5	13.0	-	2.1	-	-
Tremellomycetes	-	-	-	-	5.3	4.6	-	-	-	-	-	-	-	-	-	-
Unidentified	-	-	-	-	-	-	-	-	-	-	-	11.7	-	-	-	-

Table A3.1. Output of MetaCycle analysis used to identify rhythmic OTUs in the rhizosphere microbiome under constant conditions. Rhythmic OTUs under constant conditions were identified using MetaCycle analysis (Wu et al., 2016), where a meta2d.BHQ value (corrected using Fishers' method) of $p \leq 0.05$ was considered significantly rhythmic. Information on the ecological guild of fungal OTUs was obtained using the FUNGuild annotation tool (Nguyen et al., 2016).

Rhythmic in	OTU ID	Full taxonomy	p value	Period	Phase	Amplitude	Ecological guild (fungi only)
Bacteria - WT	OTU2508	Bacteria; Proteobacteria; Deltaproteobacteria; Myxococcales; Archangiaceae; Anaeromyxobacter; NA	0.004	23.5	3.8	0.01	n/a
Bacteria - WT	OTU29	Bacteria; Actinobacteria; Thermoleophilia; Solirubrobacterales; 67-14; NA; NA	0.000	23.7	17.6	0.20	n/a
Bacteria - WT	OTU27	Bacteria; Actinobacteria; Acidimicrobiia; IMCC26256; uncultured bacterium; uncultured bacterium; uncultured bacterium	0.002	26.5	1.2	0.14	n/a
Bacteria - WT	OTU23	Bacteria; Actinobacteria; Actinobacteria; Micrococcales; Intrasporangiaceae; NA; NA	0.000	27.5	1.4	0.16	n/a
Bacteria - WT	OTU349	Bacteria; Chloroflexi; Anaerolineae; Anaerolineales; Anaerolineaceae; Anaerolinea; uncultured bacterium	0.001	29.6	1.1	0.02	n/a
Bacteria - WT	OTU345	Bacteria; Cyanobacteria; Melainabacteria; Vampirovibrionales; NA; NA; NA	0.013	24.4	16.6	0.02	n/a
Bacteria - WT	OTU663	Bacteria; Actinobacteria; Thermoleophilia; Gaiellales; uncultured; uncultured bacterium; uncultured bacterium	0.000	26.0	3.8	0.02	n/a
Bacteria - WT	OTU471	Bacteria; Gemmatimonadetes; Gemmatimonadetes; Gemmatimonadales; Gemmatimonadaceae; uncultured; uncultured bacterium	0.000	24.4	17.7	0.02	n/a
Bacteria - WT	OTU291	Bacteria; Firmicutes; Clostridia; Clostridiales; Clostridiaceae 1; Clostridium sensu stricto 13; uncultured bacterium	0.000	25.6	5.1	0.02	n/a
Bacteria - WT	OTU49	Bacteria; Actinobacteria; Rubrobacteria; Rubrobacterales; Rubrobacteriaceae; Rubrobacter; NA	0.004	23.6	19.2	0.05	n/a

Bacteria - WT	OTU763	Bacteria; Gemmatimonadetes; Gemmatimonadetes; Gemmatimonadales; Gemmatimonadaceae; Gemmatimonas; uncultured bacterium	0.000	26.5	17.9	0.01	n/a
Bacteria - WT	OTU7238	Bacteria; Acidobacteria; Subgroup 6; uncultured bacterium; uncultured bacterium; uncultured bacterium; uncultured bacterium	0.032	23.7	18.0	0.02	n/a
Bacteria - WT	OTU511	Bacteria; Actinobacteria; Thermoleophilia; Solirubrobacterales; 67-14; uncultured bacterium; uncultured bacterium	0.000	25.9	5.6	0.02	n/a
Bacteria - WT	OTU236	Bacteria; Actinobacteria; MB-A2-108; uncultured bacterium; uncultured bacterium; uncultured bacterium; uncultured bacterium	0.000	25.8	4.2	0.02	n/a
Bacteria - WT	OTU113	Bacteria; Actinobacteria; Actinobacteria; Propionibacteriales; Nocardioidaceae; Nocardioides; Nocardioides sp.	0.002	26.3	14.1	0.03	n/a
Bacteria - WT	OTU111	Bacteria; Proteobacteria; Gammaproteobacteria; Betaproteobacteriales; Rhodocyclaceae; Dechloromonas; uncultured bacterium	0.018	27.9	2.7	0.05	n/a
Bacteria - WT	OTU1116	Bacteria; Actinobacteria; Acidimicrobiia; Microtrichales; uncultured; uncultured bacterium; uncultured bacterium	0.000	27.6	3.0	0.10	n/a
Bacteria - WT	OTU5966	Bacteria; Actinobacteria; Actinobacteria; Pseudonocardiales; Pseudonocardiaceae; Crossiella; uncultured bacterium	0.028	23.5	16.5	0.01	n/a
Bacteria - WT	OTU276	Bacteria; Actinobacteria; Actinobacteria; Frankiales; NA; NA; NA	0.046	30.0	28.8	0.02	n/a
Bacteria - WT	OTU342	Bacteria; Chloroflexi; Gitt-GS-136; uncultured bacterium; uncultured bacterium; uncultured bacterium; uncultured bacterium	0.003	23.8	17.9	0.03	n/a
Bacteria - WT	OTU135	Bacteria; Proteobacteria; Deltaproteobacteria; Desulfuromonadales; uncultured; uncultured bacterium; uncultured bacterium	0.000	26.7	3.3	0.06	n/a
Bacteria - WT	OTU154	Bacteria; Actinobacteria; Actinobacteria; Streptosporangiales; Nocardiopsaceae; Nocardiopsis; NA	0.000	24.8	5.1	0.09	n/a

Bacteria - WT	OTU1386	Bacteria; Firmicutes; Clostridia; Clostridiales; Clostridiaceae 1; Clostridium sensu stricto 9; uncultured bacterium	0.041	24.9	3.9	0.01	n/a
Bacteria - WT	OTU94	Bacteria; Actinobacteria; Thermoleophilia; Solirubrobacterales; 67-14; uncultured bacterium; uncultured bacterium	0.000	24.6	4.1	0.06	n/a
Bacteria - WT	OTU95	Bacteria; Actinobacteria; Thermoleophilia; Gaiellales; uncultured; uncultured bacterium; uncultured bacterium	0.011	29.8	0.9	0.05	n/a
Bacteria - WT	OTU97	Bacteria; Firmicutes; Clostridia; Clostridiales; Clostridiaceae 1; Clostridium sensu stricto 13; uncultured bacterium	0.000	26.0	4.7	0.05	n/a
Bacteria - WT	OTU315	Bacteria; Actinobacteria; Thermoleophilia; Solirubrobacterales; Solirubrobacteraceae; Conexibacter; uncultured bacterium	0.003	25.9	2.4	0.03	n/a
Bacteria - WT	OTU2144	Bacteria; Firmicutes; Clostridia; Clostridiales; Ruminococcaceae; Ruminiclostridium 1; NA	0.032	23.9	5.2	0.01	n/a
Bacteria - WT	OTU3814	Bacteria; Proteobacteria; Alphaproteobacteria; Rhizobiales; Xanthobacteraceae; uncultured; uncultured bacterium	0.002	28.1	1.3	0.02	n/a
Bacteria - WT	OTU783	Bacteria; Proteobacteria; Deltaproteobacteria; Myxococcales; Sandaracinaceae; uncultured; uncultured bacterium	0.013	24.0	4.4	0.01	n/a
Bacteria - WT	OTU371	Bacteria; Proteobacteria; Deltaproteobacteria; Desulfuromonadales; Geobacteraceae; Geobacter; uncultured bacterium	0.004	27.6	27.2	0.01	n/a
Bacteria - WT	OTU1032	Bacteria; Actinobacteria; Rubrobacteria; Rubrobacterales; Rubrobacteriaceae; Rubrobacter; uncultured bacterium	0.004	24.0	16.8	0.01	n/a
Bacteria - WT	OTU8477	Bacteria; Verrucomicrobia; Verrucomicrobiae; Verrucomicrobiales; Rubritaleaceae; Luteolibacter; uncultured bacterium	0.046	30.0	16.2	0.02	n/a
Bacteria - WT	OTU5531	Bacteria; Actinobacteria; Rubrobacteria; Rubrobacterales; Rubrobacteriaceae; Rubrobacter; uncultured bacterium	0.002	24.0	15.6	0.02	n/a
Bacteria - WT	OTU77	Bacteria; Actinobacteria; Thermoleophilia; Solirubrobacterales; 67-14; uncultured bacterium; uncultured bacterium	0.000	26.3	3.4	0.08	n/a
Bacteria - WT	OTU631	Bacteria; Chloroflexi; Chloroflexia; Thermomicrobiales; JG30-KF-CM45; uncultured bacterium; uncultured bacterium	0.046	23.5	17.0	0.01	n/a

Bacteria - WT	OTU496	Bacteria; Proteobacteria; Gammaproteobacteria; Pseudomonadales; Pseudomonadaceae; Pseudomonas; uncultured bacterium	0.013	26.6	17.2	0.01	n/a
Bacteria - WT	OTU564	Bacteria; Actinobacteria; Thermoleophilia; Solirubrobacterales; 67-14; uncultured bacterium; uncultured bacterium	0.002	26.2	15.1	0.01	n/a
Bacteria - WT	OTU217	Bacteria; Verrucomicrobia; Verrucomicrobiae; Verrucomicrobiales; Rubritaleaceae; Luteolibacter; uncultured bacterium	0.040	24.0	5.8	0.03	n/a
Bacteria - WT	OTU3670	Bacteria; Actinobacteria; Thermoleophilia; Solirubrobacterales; 67-14; metagenome; metagenome	0.002	25.7	3.8	0.08	n/a
Bacteria - WT	OTU509	Bacteria; Actinobacteria; Thermoleophilia; Solirubrobacterales; 67-14; uncultured bacterium; uncultured bacterium	0.000	25.6	3.6	0.02	n/a
Bacteria - WT	OTU860	Bacteria; Verrucomicrobia; Verrucomicrobiae; Chthoniobacterales; Chthoniobacteraceae; Chthoniobacter; uncultured Verrucomicrobia bacterium	0.008	26.8	18.8	0.01	n/a
Bacteria - WT	OTU261	Bacteria; Proteobacteria; Gammaproteobacteria; Pseudomonadales; Pseudomonadaceae; Pseudomonas; NA	0.004	21.4	7.1	0.03	n/a
Bacteria - WT	OTU3249	Bacteria; Actinobacteria; MB-A2-108; uncultured bacterium; uncultured bacterium; uncultured bacterium; uncultured bacterium	0.000	24.3	3.6	0.07	n/a
Bacteria WT	OTU103	Bacteria; Actinobacteria; Thermoleophilia; Solirubrobacterales; 67-14; metagenome; metagenome	0.001	23.7	16.9	0.05	n/a
Bacteria WT	OTU80	Bacteria; Actinobacteria; Thermoleophilia; Solirubrobacterales; 67-14; uncultured bacterium; uncultured bacterium	0.000	24.3	4.5	0.13	n/a
Bacteria WT	OTU5896	Bacteria; Actinobacteria; Thermoleophilia; Solirubrobacterales; 67-14; uncultured bacterium; uncultured bacterium	0.013	24.5	5.6	0.01	n/a
Bacteria WT	OTU161	Bacteria; Actinobacteria; Thermoleophilia; Solirubrobacterales; 67-14; uncultured bacterium; uncultured bacterium	0.014	28.7	3.3	0.02	n/a
Bacteria WT	OTU165	Bacteria; Proteobacteria; Alphaproteobacteria; Rhizobiales; Beijerinckiaceae; uncultured; uncultured bacterium	0.022	25.9	18.0	0.03	n/a

Bacteria *lhy-ox*	OTU438	Bacteria; Firmicutes; Clostridia; Clostridiales; Peptococcaceae; Desulfosporosinus; uncultured bacterium	0.010	29.0	4.4	0.02	n/a
Bacteria *lhy-ox*	OTU371	Bacteria; Proteobacteria; Deltaproteobacteria; Desulfuromonadales; Geobacteraceae; Geobacter; uncultured bacterium	0.041	30.0	29.7	0.01	n/a
Bacteria *lhy-ox*	OTU1036	Bacteria; Firmicutes; Clostridia; Clostridiales; Gracilibacteraceae; Lutispora; uncultured bacterium	0.032	25.1	6.7	0.01	n/a
Bacteria *lhy-ox*	OTU80	Bacteria; Actinobacteria; Thermoleophilia; Solirubrobacterales; 67-14; uncultured bacterium; uncultured bacterium	0.032	28.2	3.2	0.10	n/a
Fungi WT	OTU197	Fungi; Ascomycota; Pezizomycetes; Pezizales; Pyronemataceae; unidentified; unidentified	0.005	24.2	17.6	0.04	Possible Saprotroph
Fungi WT	OTU219	Fungi; Ascomycota; Sordariomycetes; Sordariales; Chaetomiaceae; Humicola; olivacea	0.006	25.1	16.1	0.04	Probable Saprotroph
Fungi WT	OTU189	Fungi; Basidiomycota; Agaricomycetes; Agaricales; Psathyrellaceae; Psathyrella; fusca	0.000	24.8	4.1	0.07	Probable Saprotroph
Fungi WT	OTU186	Fungi; Ascomycota; Sordariomycetes; Sordariales; Lasiosphaeriaceae; Podospora; unidentified	0.015	22.8	3.9	0.05	Possible Saprotroph
Fungi WT	OTU223	Fungi; Ascomycota; Sordariomycetes; Hypocreales; Clavicipitaceae; Paecilomyces; unidentified	0.018	24.1	17.1	0.02	Possible Saprotroph
Fungi WT	OTU21	Fungi; Ascomycota; Sordariomycetes; Hypocreales; Cordycipitaceae; Cordyceps; polyarthra	0.000	25.3	17.2	0.98	Possible Animal Pathogen
Fungi WT	OTU235	Fungi; Ascomycota; Eurotiomycetes; Eurotiales; Aspergillaceae; Penicillium; jensenii	0.001	25.7	17.8	0.03	Possible Saprotroph
Fungi WT	OTU230	Fungi; Ascomycota; Leotiomycetes; Helotiales; unidentified; unidentified; unidentified	0.001	23.7	16.2	0.04	Unknown
Fungi WT	OTU34	Fungi; Ascomycota; Sordariomycetes; Chaetosphaeriales; Chaetosphaeriaceae; unidentified; unidentified	0.000	23.8	17.0	0.66	Probable Saprotroph
Fungi WT	OTU35	Fungi; Ascomycota; Sordariomycetes; unidentified; unidentified; unidentified; unidentified	0.000	26.0	16.4	0.30	Unknown

Fungi WT	OTU32	Fungi; Ascomycota; unidentified; unidentified; unidentified; unidentified; unidentified	0.000	25.7	3.2	0.53	Possible Plant Pathogen
Fungi WT	OTU249	Fungi; unidentified; unidentified; unidentified; unidentified; unidentified; unidentified	0.018	23.6	6.2	0.08	Unknown
Fungi WT	OTU15	Fungi; Ascomycota; Sordariomycetes; Chaetosphaeriales; Chaetosphaeriaceae; unidentified; unidentified	0.000	23.4	16.4	0.42	Probable Saprotroph
Fungi WT	OTU10	Fungi; Ascomycota; Sordariomycetes; Hypocreales; Clavicipitaceae; Metarhizium; carneum	0.000	23.8	17.8	0.42	Probable Animal Pathogen
Fungi WT	OTU12	Fungi; Ascomycota; Leotiomycetes; Thelebolales; Pseudeurotiaceae; Pseudeurotium; bakeri	0.000	24.0	4.8	0.58	Probable Saprotroph
Fungi WT	OTU2237	Fungi; Ascomycota; Sordariomycetes; Hypocreales; unidentified; unidentified; unidentified	0.002	26.0	5.1	0.30	Possible Saprotroph
Fungi WT	OTU114	Fungi; Ascomycota; unidentified; unidentified; unidentified; unidentified; unidentified	0.007	26.3	3.8	0.16	Unknown
Fungi WT	OTU115	Fungi; Ascomycota; Sordariomycetes; Hypocreales; Hypocreaceae; Trichoderma; hamatum	0.000	24.6	16.9	0.13	Possible Saprotroph
Fungi WT	OTU111	Fungi; Ascomycota; Sordariomycetes; Hypocreales; unidentified; unidentified; unidentified	0.000	24.1	17.0	0.08	Probable Fungal Parasite
Fungi WT	OTU62	Fungi; Ascomycota; Sordariomycetes; Coniochaetales; Coniochaetaceae; Lecythophora; unidentified	0.000	23.7	16.1	0.23	Highly Probable Endophyte
Fungi WT	OTU67	Fungi; Mortierellomycota; Mortierellomycetes; Mortierellales; Mortierellaceae; Mortierella; alpina	0.000	24.1	18.0	0.18	Possible Endophyte
Fungi WT	OTU290	Fungi; Mortierellomycota; Mortierellomycetes; Mortierellales; Mortierellaceae; Mortierella; amoeboidea	0.000	24.1	16.7	0.02	Possible Endophyte
Fungi WT	OTU292	Fungi; Ascomycota; Sordariomycetes; Coniochaetales; Coniochaetaceae; Coniochaeta; unidentified	0.013	24.0	16.6	0.03	Possible Plant Pathogen

Fungi WT	OTU77	Fungi; Ascomycota; Sordariomycetes; unidentified; unidentified; unidentified; unidentified	0.000	23.8	16.7	0.13	Unknown
Fungi WT	OTU74	Fungi; Ascomycota; Sordariomycetes; Hypocreales; Hypocreaceae; Trichoderma; reesei	0.000	24.4	16.6	0.29	Possible Saprotroph
Fungi WT	OTU75	Fungi; Ascomycota; Sordariomycetes; Hypocreales; fam_Incertae_sedis; Acremonium; persicinum	0.001	23.8	17.5	0.36	Possible Plant Pathogen
Fungi WT	OTU78	Fungi; Basidiomycota; Microbotryomycetes; Sporidiobolales; unidentified; unidentified; unidentified	0.000	26.0	16.9	0.18	Unknown
Fungi WT	OTU42	Fungi; Ascomycota; Eurotiomycetes; Eurotiales; Aspergillaceae; Penicillium; astrolabium	0.002	26.3	4.0	0.76	Possible Saprotroph
Fungi WT	OTU41	Fungi; Ascomycota; Leotiomycetes; Helotiales; Vibrisseaceae; Phialocephala; humicola	0.000	23.8	17.0	0.34	Highly Probable Endophyte
Fungi WT	OTU127	Fungi; Ascomycota; Sordariomycetes; Microascales; unidentified; unidentified; unidentified	0.017	28.7	15.6	0.08	Unknown
Fungi WT	OTU6	Fungi; Ascomycota; Sordariomycetes; Glomerellales; Plectosphaerellaceae; Musicillium; theobromae	0.000	26.0	3.7	0.87	Probable Plant Pathogen
Fungi WT	OTU4	Fungi; Ascomycota; Eurotiomycetes; Chaetothyriales; Herpotrichiellaceae; Exophiala; equina	0.025	21.3	17.1	0.18	Probable Animal Pathogen
Fungi WT	OTU1	Fungi; Ascomycota; Sordariomycetes; Hypocreales; unidentified; unidentified; unidentified	0.000	24.3	5.6	0.15	Probable Unknown
Fungi WT	OTU59	Fungi; Ascomycota; Sordariomycetes; Hypocreales; Hypocreaceae; Trichoderma; piluliferum	0.000	25.6	4.2	0.24	Possible Saprotroph
Fungi WT	OTU51	Fungi; Ascomycota; Sordariomycetes; Magnaporthales; Magnaporthaceae; Macgarvieomyces; juncicola	0.000	23.8	6.0	0.40	Probable Plant Pathogen
Fungi WT	OTU52	Fungi; Ascomycota; Sordariomycetes; Hypocreales; Nectriaceae; Ilyonectria; mors-panacis	0.000	26.1	1.6	0.37	Possible Saprotroph

Fungi WT	OTU55	Fungi; Ascomycota; Sordariomycetes; Hypocreales; Nectriaceae; unidentified; unidentified	0.005	26.5	3.3	0.15	Possible Saprotroph
Fungi WT	OTU80	Fungi; Ascomycota; Dothideomycetes; Valsariales; Valsariaceae; Valsaria; neotropica	0.000	23.5	6.1	0.12	Highly Probable Saprotroph
Fungi WT	OTU86	Fungi; Ascomycota; Eurotiomycetes; Onygenales; fam_Incertae_sedis; Chrysosporium; lobatum	0.000	26.4	3.5	0.19	Highly Probable Saprotroph
Fungi WT	OTU89	Fungi; Ascomycota; Leotiomycetes; Helotiales; fam_Incertae_sedis; Chalara; piceae-abietis	0.000	28.9	0.2	0.10	Probable Plant Pathogen
Fungi WT	OTU326	Fungi; Ascomycota; Leotiomycetes; Helotiales; fam_Incertae_sedis; Cadophora; unidentified	0.018	30.0	17.5	0.03	Highly Probable Endophyte
Fungi WT	OTU143	Fungi; Ascomycota; Sordariomycetes; Hypocreales; Nectriaceae; unidentified; unidentified	0.015	27.0	17.2	0.04	Probable Plant Pathogen
Fungi WT	OTU1094	Fungi; Ascomycota; Sordariomycetes; Coniochaetales; Coniochaetaceae; Lecythophora; unidentified	0.015	23.6	16.6	0.10	Highly Probable Endophyte
Fungi WT	OTU98	Fungi; Ascomycota; Sordariomycetes; Hypocreales; Hypocreaceae; Trichoderma; paraviridescens	0.041	25.4	1.7	0.08	Possible Saprotroph
Fungi *lhy-ox*	OTU12	Fungi; Ascomycota; Leotiomycetes; Thelebolales; Pseudeurotiaceae; Pseudeurotium; bakeri	0.025	25.8	4.9	0.55	Probable Saprotroph
Fungi *lhy-ox*	OTU42	Fungi; Ascomycota; Eurotiomycetes; Eurotiales; Aspergillaceae; Penicillium; astrolabium	0.000	23.9	4.5	0.09	Possible Saprotroph
Fungi *lhy-ox*	OTU6	Fungi; Ascomycota; Sordariomycetes; Glomerellales; Plectosphaerellaceae; Musicillium; theobromae	0.001	29.6	1.8	0.55	Probable Plant Pathogen

Table A3.2. Evidence for homologues of cyanobacterial KaiABC circadian clock proteins within phyla found in rhizosphere samples. Homologues were identified using TBLASTN searches of the non-redundant nucleotide database (Sayers et al., 2020), using the amino acid sequences of KaiA, KaiB and KaiC from the cyanobacterium *Synechococcus elongatus* PCC 7942 as queries. Hits were determined to show evidence of homology when their E value was lower than 0.01, % identity was greater than 20%, and query cover was greater than 80%. For E values reported, 'E-x' signifies multiplication by 10^{-x}.

Phylum	Homologous to	Best hit	Query Cover	E value	% Identity	Accession number
Acidobacteria	KaiA	No evidence				
	KaiB	Acidisarcina polymorpha strain SBC82 chromosome, complete genome	86%	6.00E-20	43.18	CP030840.1
	KaiC	Luteitalea pratensis strain DSM 100886, partial sequence	97%	2.00E-25	22.76	CP015136.1
Actinobacteria	KaiA	No evidence				
	KaiB	Nocardioides sp. HDW12B chromosome, complete genome	87%	3.00E-16	46.07	CP049867.1
	KaiC	Nocardioides sp. HDW12B chromosome, complete genome	94%	4.00E-129	43.2	CP049867.1
Armatimonadetes	KaiA	No evidence				
	KaiB	Fimbriimonas ginsengisoli Gsoil 348, complete genome	83%	6.00E-24	50.59	CP007139.1
	KaiC	Fimbriimonas ginsengisoli Gsoil 348, complete genome	94%	9.00E-80	34.69	CP007139.1
Bacteriodetes	KaiA	No evidence				
	KaiB	Sphingobacteriaceae bacterium GW460-11-11-14-LB5, complete genome	96%	4.00E-25	58.62	CP021237.1
	KaiC	Hymenobacter sp. BRD72 chromosome, complete genome	96%	1.00E-137	46.63	CP044285.1
BRC1	KaiA	No evidence				
	KaiB	No evidence				
	KaiC	No evidence				
Chlamydiae	KaiA	No evidence				

	KaiB	No evidence				
	KaiC	No evidence				
Chloroflexi	KaiA	No evidence				
	KaiB	Chloroflexus aggregans DSM 9485, complete genome	84%	2.00E-19	49.41	CP001337.1
	KaiC	Roseiflexus castenholzii DSM 13941, complete genome	96%	5.00E-158	50.2	CP000804.1
Dependentiae	KaiA	No evidence				
	KaiB	No evidence				
	KaiC	No evidence				
Elusimicrobia	KaiA	No evidence				
	KaiB	No evidence				
	KaiC	No evidence				
Entotheonellaeota	KaiA	No records of taxon found for search				
	KaiB	No records of taxon found for search				
	KaiC	No records of taxon found for search				
FCPU426	KaiA	No records of taxon found for search				
	KaiB	No records of taxon found for search				
	KaiC	No records of taxon found for search				
Fibrobacteres	KaiA	No evidence				
	KaiB	No evidence				
	KaiC	No evidence				
Firmicutes	KaiA	Bacillus subtilis BEST7613 DNA, complete genome	98%	6.00E-59	40.75	AP012495.1
	KaiB	Bacillus subtilis BEST7613 DNA, complete genome	98%	9.00E-48	86.14	AP012495.1
	KaiC	Bacillus subtilis BEST7613 DNA, complete genome	97%	0	74.55	AP012495.1
Gemmatimonadetes	KaiA	No evidence				
	KaiB	Gemmatirosa kalamazoonesis strain KBS708, complete genome	90%	6.00E-17	46.74	CP007128.1

	KaiC	Gemmatirosa kalamazoonesis strain KBS708, complete genome	94%	3.00E-141	46.12	CP007128.1
Latescibacteria	KaiA	No evidence				
	KaiB	No evidence				
	KaiC	No evidence				
Nitrospirae	KaiA	No evidence				
	KaiB	No evidence				
	KaiC	No evidence				
Omnitrophicaeota	KaiA	No evidence				
	KaiB	No evidence				
	KaiC	No evidence				
Patescibacteria	KaiA	No evidence				
	KaiB	No evidence				
	KaiC	No evidence				
Planctomycetes	KaiA	No evidence				
	KaiB	Planctomycetes bacterium Pla85_3_4 chromosome, complete genome	88%	2.00E-23	53.33	CP036433.1
	KaiC	Candidatus Kuenenia stuttgartiensis strain CSTR1 chromosome, complete genome	97%	5.00E-81	32.15	CP049055.1
Proteobacteria	KaiA	No evidence				
	KaiB	Bradyrhizobium sp. ORS278,complete sequence	93%	3.00E-24	56.47	CU234118.1
	KaiC	Candidatus Thiodictyon syntrophicum strain Cad16T chromosome, complete genome	99%	2.00E-149	48.93	CP020370.1
Rokubacteria	KaiA	No evidence				
	KaiB	No evidence				
	KaiC	No evidence				
Spirochaetes	KaiA	No evidence				
	KaiB	No evidence				

	KaiC	Spirochaeta thermophila DSM 6578, complete genome	93%	1.00E-21	22.69	CP002903.1
Verrucomicrobia	KaiA	No evidence				
	KaiB	Luteolibacter sp. G-1-1-1 chromosome, complete genome	93%	8.00E-23	52.33	CP051774.1
	KaiC	Roseimicrobium sp. ORNL1 chromosome, complete genome	96%	2.00E-81	32.29	CP049143.1
WS2	KaiA	No evidence				
	KaiB	No evidence				
	KaiC	No evidence				
WS4	KaiA	No records of taxon found for search				
	KaiB	No records of taxon found for search				
	KaiC	No records of taxon found for search				

Table A3.3. Evidence for homologues of fungal FRQ, WC1, and WC2 circadian clock proteins within classes found in rhizosphere samples. Homologues were identified using TBLASTN searches of the non-redundant nucleotide database (Sayers et al., 2020), using the amino acid sequences of FRQ, WC1 and WC2 from the fungus *Neurospora crassa* as queries. Hits were determined to show evidence of homology when their E value was lower than 0.01, % identity was greater than 20%, and query cover was greater than ~40%. For E values reported, 'E-x' signifies multiplication by 10^{-x}.

Class	Homologous to	Best hit	Query Cover	E value	% Identity	Accession number
Dothideomycetes	FRQ	Coniosporium apollinis CBS 100218 hypothetical protein partial mRNA	64%	7.00E-137	61.14	XM_007784311.1
	WC1	Pseudocercospora fijiensis CIRAD86 blue-light-activated transcription factor (WCO1), partial mRNA	57%	0	51.24	XM_007933703.1
	WC2	Leptosphaeria australiensis frequency clock protein (frq) gene, complete cds	97%	0	40.99	U25851.1
Eurotiomycetes	FRQ	Cladophialophora carrionii CBS 160.54 hypothetical protein partial mRNA	77%	6.00E-46	27.34	XM_008728758.1
	WC1	Exophiala mesophila hypothetical protein mRNA	58%	0	53.13	XM_016364407.1
	WC2	Exophiala dermatitidis NIH/UT8656 hypothetical protein mRNA	72%	9.00E-115	49.5	XM_009158635.1
Laboulbenio-mycetes	FRQ	No evidence				
	WC1	No evidence				
	WC2	No evidence				
Lecanoro-mycetes	FRQ	No evidence				
	WC1	Cladonia metacorallifera strain KoLRI002260 white collar-1 (wc-1) gene, complete cds	53%	0	58.35	MN325842.1
	WC2	Cladonia metacorallifera strain KoLRI002260 white collar-2 (wc-2) gene, partial cds	64%	1.00E-137	58.21	MN325843.1
Leotiomycetes	FRQ	Sclerotinia sclerotiorum 1980 UF-70 hypothetical protein partial mRNA	79%	3.00E-80	30.27	XM_001586765.1
	WC1	Glarea lozoyensis ATCC 20868 PYP-like sensor (PAS) mRNA	76%	0	47.53	XM_008078525.1
	WC2	Hyaloscypha bicolor E white-collar 2 (K444DRAFT_525844), partial mRNA	64%	3.00E-149	62.75	XM_024874488.1

Pezizomycetes	FRQ	Tuber melanosporum Mel28 hypothetical protein (GSTUM_00006869001) mRNA, complete cds	6%	0.23	36.07	XM_002839011.1
	WC1	Tuber borchii mRNA for tuber borchii white collar-1 (Tbwc-1 gene)	53%	0	53.58	AJ575418.1
	WC2	Tuber melanosporum Mel28 hypothetical protein (GSTUM_00001635001) mRNA, complete cds	64%	4.00E-116	52.86	XM_002835809.1
Saccharomycetes	FRQ	No evidence				
	WC1	Candida hispaniensis genome assembly, chromosome: B	41%	6.00E-50	27.57	LS992271.1
	WC2	Yarrowia lipolytica CLIB122 YALI0F05346p partial mRNA	61%	2.00E-24	25.3	XM_505029.1
Agaricomycetes	FRQ	Fibroporia radiculosa predicted protein partial mRNA	14%	4.2	25.81	XM_012328319.1
	WC1	Trametes hirsuta strain 072 chromosome 8, complete sequence	49%	6.00E-61	29.01	CP019381.1
	WC2	Serpula lacrymans var. lacrymans S7.9 white collar 2 type of transcription factor (SERLADRAFT_475940), mRNA	64%	5.00E-38	29.75	XM_007322049.1
Agaricostilbo-mycetes	FRQ	No evidence				
	WC1	No evidence				
	WC2	No evidence				
Cystobasidio-mycetes	FRQ	No evidence				
	WC1	No evidence				
	WC2	No evidence				
Microbotryo-mycetes	FRQ	Rhodotorula toruloides NP11 Frequency clock protein partial mRNA	19%	8.00E-10	41.43	XM_016421037.1
	WC1	Rhodotorula graminis WP1 uncharacterized protein (RHOBADRAFT_14207), partial mRNA	54%	2.00E-136	38.98	XM_018412189.1
	WC2	Rhodotorula graminis WP1 uncharacterized protein (RHOBADRAFT_52765), partial mRNA	39%	4.00E-33	42.86	XM_018416495.1
Tremello-mycetes	FRQ	No evidence				
	WC1	Kwoniella shandongensis uncharacterized protein (CI109_001289), partial mRNA	47%	3.00E-119	38.91	XM_032002476.1

	WC2	Kwoniella mangroviensis CBS 8507 hypothetical protein partial mRNA	48%	4.00E-08	23.97	XM_019149521.1
Ustilagino-mycetes	FRQ	No evidence				
	WC1	Moesziomyces antarcticus conserved hypothetical protein partial mRNA	48%	1.00E-94	31.8	XM_014801700.1
	WC2	Sporisorium scitamineum strain SSC39 chromosome 6, complete sequence	64%	5.00E-21	33.33	CP010918.1
Rhizophlyctido-mycetes	FRQ	No records of taxon found for search				
	WC1	No records of taxon found for search				
	WC2	No records of taxon found for search				
Rhizophydio-mycetes	FRQ	No records of taxon found for search				
	WC1	No records of taxon found for search				
	WC2	No records of taxon found for search				
Mortierello-mycetes	FRQ	Lobosporangium transversale Ion transport protein-domain-containing protein (BCR41DRAFT_420766), mRNA	6%	0.81	28.77	XM_022029939.1
	WC1	Lobosporangium transversale hypothetical protein (BCR41DRAFT_294365), partial mRNA	4%	1.00E-07	46.81	XM_022020397.1
	WC2	Lobosporangium transversale hypothetical protein (BCR41DRAFT_418793), mRNA	32%	1.00E-07	23.79	XM_022029671.1
Mucoro-mycetes	FRQ	No evidence				
	WC1	Rhizopus microsporus ATCC 52813 putative white-collar-1a protein (RHIMIDRAFT_287091), partial mRNA	52%	1.00E-150	38.68	XM_023613442.1
	WC2	Phycomyces blakesleeanus NRRL 1555(-) GATA-type zinc finger transcription factor (WctC), partial mRNA	64%	5.00E-48	33.04	XM_018441430.1
Olpidio-mycetes	FRQ	No evidence				
	WC1	No evidence				
	WC2	No evidence				
Rozello-	FRQ	Uncultured Cryptomycota partial 26S rRNA gene, clone Ao0mple7	1%	8.3	50	HE806171.1
	WC1	No evidence				

Mycotina (class Incertae Sedis)	WC2	No evidence
Unidentified	FRQ	N/A
	WC1	N/A
	WC2	N/A
Zoopago-mycetes	FRQ	No evidence
	WC1	No evidence
	WC2	No evidence

BIBLIOGRAPHY

ADAMS, S. & CARRÉ, I. A. 2011. Downstream of the plant circadian clock: output pathways for the control of physiology and development. *Essays in Biochemistry,* 49**,** 53-69.

ADAMS, S., GRUNDY, J., VEFLINGSTAD, S. R., DYER, N. P., HANNAH, M. A., OTT, S. & CARRÉ, I. A. 2018. Circadian control of abscisic acid biosynthesis and signalling pathways revealed by genome-wide analysis of LHY binding targets. *New Phytologist*, 220, 893-907.

ALVAREZ, M., TRANQUILLI, G., LEWIS, S., KIPPES, N. & DUBCOVSKY, J. 2016. Genetic and physical mapping of the earliness *per se* locus *Eps-A (m)1* in *Triticum monococcum* identifies *EARLY FLOWERING 3* (*ELF3*) as a candidate gene. *Functional & Integrative Genomics,* 16**,** 365-382.

APPRILL, A., MCNALLY, S., PARSONS, R. & WEBER, L. 2015. Minor revision to V4 region SSU rRNA 806R gene primer greatly increases detection of SAR11 bacterioplankton. *Aquatic Microbial Ecology,* 75**,** 129-137.

ARIAS, A., SAIZ, E. & CALBET, A. 2020. Towards an understanding of diel feeding rhythms in marine protists: consequences of light manipulation. *Microbial Ecology,* 79**,** 64-72.

AUSTIN, B. 1968. An endogenous rhythm of spore discharge in *Sordaria fimicola*. *Annals of Botany,* 32**,** 262-278.

BADRI, D. V. & VIVANCO, J. M. 2009. Regulation and function of root exudates. *Plant, Cell & Environment,* 32**,** 666-681.

BADRI, D. V., LOYOLA-VARGAS, V. M., BROECKLING, D. D., & VIVANCO, J. M. 2010. Root secretion of phytochemicals in *Arabidopsis* is predominantly not influenced by diurnal rhythms. *Molecular Plant*, 3, 491-498.

BAKER, C. L., LOROS, J. J. & DUNLAP, J. C. 2012. The circadian clock of *Neurospora crassa*. *Federation of European Microbiological Societies Microbiology Reviews,* 36**,** 95-110.

BAKKER, P. A., BERENDSEN, R. L., DOORNBOS, R. F., WINTERMANS, P. C. & PIETERSE, C. M. 2013. The rhizosphere revisited: root microbiomics. *Frontiers in Plant Science,* 4**,** 165.

BARANIYA, D., NANNIPIERI, P., KUBLIK, S., VESTERGAARD, G., SCHLOTER, M. & SCHOLER, A. 2018. The impact of the diurnal cycle on the microbial transcriptome in the rhizosphere of barley. *Microbial Ecology,* 75**,** 830-833.

BARDGETT, R. D. & VAN DER PUTTEN, W. H. 2014. Belowground biodiversity and ecosystem functioning. *Nature,* 515**,** 505-511.

BELBIN, F. E., HALL, G. J., JACKSON, A. B., SCHANSCHIEFF, F. E., ARCHIBALD, G., FORMSTONE, C. & DODD, A. N. 2019. Plant circadian rhythms regulate the effectiveness of a glyphosate-based herbicide. *Nature Communications,* 10**,** 1-11.

BELL-PEDERSEN, D., CASSONE, V. M., EARNEST, D. J., GOLDEN, S. S., HARDIN, P. E., THOMAS, T. L. & ZORAN, M. J. 2005. Circadian rhythms from multiple oscillators: lessons from diverse organisms. *Nature Reviews Genetics,* 6**,** 544-556.

BERENDSEN, R. L., PIETERSE, C. M. & BAKKER, P. A. 2012. The rhizosphere microbiome and plant health. *Trends in Plant Science,* 17**,** 478-486.

BERG, G., GRUBE, M., SCHLOTER, M. & SMALLA, K. 2014. Unraveling the plant microbiome: looking back and future perspectives. *Frontiers in Microbiology,* 5**,** 148.

BERLA, B. M., SAHA, R., IMMETHUN, C. M., MARANAS, C. D., MOON, T. S. & PAKRASI, H. 2013. Synthetic biology of cyanobacteria: unique challenges and opportunities. *Frontiers in Microbiology,* 4**,** 246.

BHARDWAJ, V., MEIER, S., PETERSEN, L. N., INGLE, R. A. & RODEN, L. C. 2011. Defence responses of *Arabidopsis thaliana* to infection by Pseudomonas syringae are regulated by the circadian clock. *PloS One,* 6**,** e26968.

BLAZEWICZ, S. J., BARNARD, R. L., DALY, R. A. & FIRESTONE, M. K. 2013. Evaluating rRNA as an indicator of microbial activity in environmental communities: limitations and uses. *The ISME Journal,* 7**,** 2061-2068.

BLUHM, B. H., BURNHAM, A. M. & DUNKLE, L. D. 2010. A circadian rhythm regulating hyphal melanization in *Cercospora kikuchii*. *Mycologia,* 102**,** 1221-1228.

BOLGER, A. M., LOHSE, M. & USADEL, B. 2014. Trimmomatic: a flexible trimmer for Illumina sequence data. *Bioinformatics,* 30**,** 2114-20.

BORDAGE, S., SULLIVAN, S., LAIRD, J., MILLAR, A. J. & NIMMO, H. G. 2016. Organ specificity in the plant circadian system is explained by different light inputs to the shoot and root clocks. *New Phytologist,* 212**,** 136-149.

BRAY, J. R. & CURTIS, J. T. 1957. An ordination of the upland forest communities of southern Wisconsin. *Ecological Monographs,* 27**,** 325-349.

BRODY, S. 2019. Circadian rhythms in fungi: Structure/function/evolution of some clock components. *Journal of Biological Rhythms,* 34**,** 364-379.

BULGARELLI, D., ROTT, M., SCHLAEPPI, K., VER LOREN VAN THEMAAT, E., AHMADINEJAD, N., ASSENZA, F., RAUF, P., HUETTEL, B., REINHARDT, R., SCHMELZER, E., PEPLIES, J., GLOECKNER, F. O., AMANN, R., EICKHORST, T. & SCHULZE-LEFERT, P. 2012. Revealing structure and assembly cues for *Arabidopsis* root-inhabiting bacterial microbiota. *Nature,* 488**,** 91-5.

CAIRD, M. A., RICHARDS, J. H. & DONOVAN, L. A. 2007. Nighttime stomatal conductance and transpiration in C3 and C4 plants. *Plant Physiology,* 143**,** 4-10.

CANARINI, A., KAISER, C., MERCHANT, A., RICHTER, A. & WANEK, W. 2019. Root exudation of primary metabolites: mechanisms and their roles in plant responses to environmental stimuli. *Frontiers in Plant Science,* 10**,** 157.

CAPORASO, J. G., KUCZYNSKI, J., STOMBAUGH, J., BITTINGER, K., BUSHMAN, F. D., COSTELLO, E. K., FIERER, N., PENA, A. G., GOODRICH, J. K. & GORDON, J. I. 2010. QIIME allows analysis of high-throughput community sequencing data. *Nature Methods,* 7**,** 335-336.

CAPORASO, J. G., LAUBER, C. L., WALTERS, W. A., BERG-LYONS, D., LOZUPONE, C. A., TURNBAUGH, P. J., FIERER, N. & KNIGHT, R. 2011. Global patterns of 16S rRNA diversity at a depth of millions of sequences per sample. *Proceedings of the National Academy of Sciences,* 108**,** 4516-4522.

CARDON, Z. G. & GAGE, D. J. 2006. Resource exchange in the rhizosphere: molecular tools and the microbial perspective. *Annual Review of Ecology, Evolution, and Systematics,* 37**,** 459-488.

CARRÉ, I. & VEFLINGSTAD, S. R. 2013. Emerging design principles in the *Arabidopsis* circadian clock. *Seminars in Cell & Developmental Biology*, 24, 393-398.

CARVALHAIS, L. C., DENNIS, P. G., BADRI, D. V., TYSON, G. W., VIVANCO, J. M. & SCHENK, P. M. 2013. Activation of the jasmonic acid plant defence pathway alters the composition of rhizosphere bacterial communities. *PLoS One,* 8**,** e56457.

CHA, J. Y., KIM, J., KIM, T. S., ZENG, Q., WANG, L., LEE, S. Y., KIM, W. Y. & SOMERS, D. E. 2017. GIGANTEA is a co-chaperone which facilitates maturation of ZEITLUPE in the *Arabidopsis* circadian clock. *Nature Communications,* 8**,** 1-12.

CHAPARRO, J. M., BADRI, D. V. & VIVANCO, J. M. 2014. Rhizosphere microbiome assemblage is affected by plant development. *The ISME Journal,* 8**,** 790-803.

CHEN, W. W., TAKAHASHI, N., HIRATA, Y., RONALD, J., PORCO, S., DAVIS, S. J., NUSINOW, D. A., KAY, S. A. & MAS, P. 2020. A mobile ELF4 delivers circadian temperature information from shoots to roots. *Nature Plants,* 6**,** 416-426.

CHUBERRE, C., PLANCOT, B., DRIOUICH, A., MOORE, J. P., BARDOR, M., GÜGI, B. & VICRÉ, M. 2018. Plant immunity is compartmentalized and specialized in roots. *Frontiers in Plant Science,* 9**,** 1692.

CLARKE, K. R. 1993. Non-parametric multivariate analyses of changes in community structure. *Australian Journal of Ecology,* 18**,** 117-143.

COHEN, S. E. & GOLDEN, S. S. 2015. Circadian rhythms in cyanobacteria. *Microbiology and Molecular Biology Reviews,* 79**,** 373-385.

CORREA, A., LEWIS, Z. A., GREENE, A. V., MARCH, I. J., GOMER, R. H. & BELL-PEDERSEN, D. 2003. Multiple oscillators regulate circadian gene expression in *Neurospora*. *Proceedings of the National Academy of Sciences,* 100**,** 13597-13602.

COUILLEROT, O., PRIGENT-COMBARET, C., CABALLERO-MELLADO, J. & MOËNNE-LOCCOZ, Y. 2009. *Pseudomonas fluorescens* and closely-related fluorescent pseudomonads as biocontrol agents of soil-borne phytopathogens. *Letters in Applied Microbiology,* 48**,** 505-512.

COVINGTON, M. F. & HARMER, S. L. 2007. The circadian clock regulates auxin signaling and responses in *Arabidopsis*. *PLoS Biology,* 5**,** e222.

CRANEY, A., HOHENAUER, T., XU, Y., NAVANI, N. K., LI, Y. & NODWELL, J. 2007. A synthetic *luxCDABE* gene cluster optimized for expression in high-GC bacteria. *Nucleic Acids Res,* 35**,** e46.

CROWTHER, T. W., BODDY, L. & JONES, T. H. 2012. Functional and ecological consequences of saprotrophic fungus–grazer interactions. *The ISME Journal,* 6**,** 1992-2001.

DARWENT, M. J., PATERSON, E., MCDONALD, A. J. & TOMOS, A. D. 2003. Biosensor reporting of root exudation from *Hordeum vulgare* in relation to shoot nitrate concentration. *Journal of Experimental Botany,* 54**,** 325-34.

DE BOER, W., HUNDSCHEID, M. P., KLEIN GUNNEWIEK, P. J., DE RIDDER-DUINE, A. S., THION, C., VAN VEEN, J. A. & VAN DER WAL, A. 2015. Antifungal rhizosphere bacteria can increase as response to the presence of saprotrophic fungi. *PLoS One,* 10**,** e0137988.

DE LEIJ, F. A. A. M., SUTTON, E. J., WHIPPS, J. M., FENLON, J. S. & LYNCH, J. M. 1995. Field release of a genetically modified *Pseudomonas fluorescens* on wheat: establishment, survival and dissemination. *Nature Biotechnology,* 13**,** 1488-1492.

DE PAULA, R. M., LEWIS, Z. A., GREENE, A. V., SEO, K. S., MORGAN, L. W., VITALINI, M. W., BENNETT, L., GOMER, R. H. & BELL-PEDERSEN, D. 2006. Two circadian timing circuits in *Neurospora crassa* cells share components and regulate distinct rhythmic processes. *Journal of Biological Rhythms,* 21**,** 159-168.

DE VRIEZE, J., PINTO, A. J., SLOAN, W. T. & IJAZ, U. Z. 2018. The active microbial community more accurately reflects the anaerobic digestion process: 16S rRNA (gene) sequencing as a predictive tool. *Microbiome,* 6**,** 63.

DE WEGER, L. A., KUIPER, I., VAN DER BIJ, A. J. & LUGTENBERG, B. J. 1997. Use of a *lux*-based procedure to rapidly visualize root colonisation by *Pseudomonas fluorescens* in the wheat rhizosphere. *Antonie Van Leeuwenhoek,* 72**,** 365-372.

DENG, L., CHEUNG, S. & LIU, H. 2020. Protistal grazers increase grazing on unicellular cyanobacteria diazotroph at night. *Frontiers in Marine Science*, 7, 135.

DENNIS, P., MILLER, A. & HIRSCH, P. 2006. 'Visualisation of rhizosphere bacterial colonisation patterns' in FINLAY, R. D., LUSTER, J. (ed.) *Handbook of Methods used in Rhizosphere Research*. Birmensdorf, Switzerland: Swiss Federal Research Institute, 386 – 387.

DESANTIS, T. Z., HUGENHOLTZ, P., LARSEN, N., ROJAS, M., BRODIE, E. L., KELLER, K., HUBER, T., DALEVI, D., HU, P. & ANDERSEN, G. L. 2006. Greengenes, a chimera-checked 16S rRNA gene database and workbench compatible with ARB. *Applied and Environmental Microbiology,* 72**,** 5069-5072.

DODD, A. N., PARKINSON, K. & WEBB, A. A. 2004. Independent circadian regulation of assimilation and stomatal conductance in the *ztl-1* mutant of *Arabidopsis*. *New Phytologist,* 162**,** 63-70.

DODD, A. N., SALATHIA, N., HALL, A., KÉVEI, E., TÓTH, R., NAGY, F., HIBBERD, J. M., MILLAR, A. J. & WEBB, A. A. 2005. Plant circadian clocks increase photosynthesis, growth, survival, and competitive advantage. *Science,* 309**,** 630-633.

DONG, Y., HUANG, C., PARK, J. & WANG, G. 2012. Growth inhibitory levels of salicylic acid decrease *Pseudomonas aeruginosa fliC* flagellin gene expression. *Journal of Experimental Microbiology and Immunology,* 16**,** 73-78.

DOORNBOS, R. F., VAN LOON, L. C. & BAKKER, P. A. 2012. Impact of root exudates and plant defense signaling on bacterial communities in the rhizosphere. A review. *Agronomy for Sustainable Development,* 32**,** 227-243.

DOWSON-DAY, M. J. & MILLAR, A. J. 1999. Circadian dysfunction causes aberrant hypocotyl elongation patterns in *Arabidopsis*. *The Plant Journal,* 17**,** 63-71.

DUINEVELD, B. M., KOWALCHUK, G. A., KEIJZER, A., VAN ELSAS, J. D. & VAN VEEN, J. A. 2001. Analysis of bacterial communities in the rhizosphere of chrysanthemum via denaturing gradient gel electrophoresis of PCR-amplified 16S rRNA as well as DNA fragments coding for 16S rRNA. *Applied and Environmental Microbiology,* 67**,** 172-178.

DUNLAP, P. V. & URBANCZYK, H. 2013. 'Luminous Bacteria' in ROSENBERG, E., DELONG, E., LORY, S., STACKEBRANDT, E., THOMPSON, F. (ed.) *The Prokaryotes.* Springer Reference, 495-528.

DVORNYK, V., VINOGRADOVA, O. & NEVO, E. 2003. Origin and evolution of circadian clock genes in prokaryotes. *Proceedings of the National Academy of Sciences,* 100**,** 2495-2500.

ECKARDT, 2005. Temperature entrainment of the *Arabidopsis* circadian clock. *Plant Cell*, 17, 645-647.

EDGAR, R. C. 2010. Search and clustering orders of magnitude faster than BLAST. *Bioinformatics,* 26**,** 2460-1.

EL ZAHAR HAICHAR, F., SANTAELLA, C., HEULIN, T. & ACHOUAK, W. 2014. Root exudates mediated interactions belowground. *Soil Biology and Biochemistry,* 77**,** 69-80.

EMERSON, J. B., ADAMS, R. I., ROMÁN, C. M. B., BROOKS, B., COIL, D. A., DAHLHAUSEN, K., GANZ, H. H., HARTMANN, E. M., HSU, T. & JUSTICE, N. B. 2017. Schrödinger's microbes: tools for distinguishing the living from the dead in microbial ecosystems. *Microbiome,* 5**,** 86.

ENGELMANN, W., SIMON, K. & PHEN, C. J. 1992. Leaf movement rhythm in *Arabidopsis thaliana*. *Zeitschrift für Naturforschung C,* 47**,** 925-928.

FIERER, N. 2017. Embracing the unknown: disentangling the complexities of the soil microbiome. *Nature Reviews Microbiology,* 15**,** 579-590.

FIERER, N., JACKSON, J. A., VILGALYS, R. & JACKSON, R. B. 2005. Assessment of soil microbial community structure by use of taxon-specific quantitative PCR assays. *Applied and Environmental Microbiology,* 71**,** 4117-20.

FISHER, R. A. 1925. 'Theory of statistical estimation' in *Mathematical Proceedings of the Cambridge Philosophical Society*. Cambridge University Press, 700-725.

FOWLER, S., LEE, K., ONOUCHI, H., SAMACH, A., RICHARDSON, K., MORRIS, B., COUPLAND, G. & PUTTERILL, J. 1999. *GIGANTEA*: a

circadian clock-controlled gene that regulates photoperiodic flowering in *Arabidopsis* and encodes a protein with several possible membrane-spanning domains. *The European Molecular Biology Organisation Journal,* 18**,** 4679-4688.

FUKUDA, H., UKAI, K. & OYAMA, T. 2012. Self-arrangement of cellular circadian rhythms through phase-resetting in plant roots. *American Physical Society Physical Review E,* 86**,** 041917.

GAIDOS, E., RUSCH, A. & ILARDO, M. 2011. Ribosomal tag pyrosequencing of DNA and RNA from benthic coral reef microbiota: community spatial structure, rare members and nitrogen-cycling guilds. *Environmental Microbiology,* 13**,** 1138-1152.

GANTNER, S., SCHMID, M., DURR, C., SCHUHEGGER, R., STEIDLE, A., HUTZLER, P., LANGEBARTELS, C., EBERL, L., HARTMANN, A. & DAZZO, F. B. 2006. *In situ* quantitation of the spatial scale of calling distances and population density-independent N-acylhomoserine lactone-mediated communication by rhizobacteria colonized on plant roots. *Federation of European Microbiology Societies Microbiology Ecology,* 56**,** 188-94.

GAO, Z., KARLSSON, I., GEISEN, S., KOWALCHUK, G. & JOUSSET, A. 2018. Protists: puppet masters of the rhizosphere microbiome. *Trends in Plant Science,* 24**,** 165-176.

GERLAND, P., RAFTERY, A. E., ŠEVČÍKOVÁ, H., LI, N., GU, D., SPOORENBERG, T., ALKEMA, L., FOSDICK, B. K., CHUNN, J. & LALIC, N. 2014. World population stabilization unlikely this century. *Science,* 346**,** 234-237.

GLYNN, E. F., CHEN, J. & MUSHEGIAN, A. R. 2006. Detecting periodic patterns in unevenly spaced gene expression time series using Lomb–Scargle periodograms. *Bioinformatics,* 22**,** 310-316.

GOODSPEED, D., CHEHAB, E. W., MIN-VENDITTI, A., BRAAM, J. & COVINGTON, M. F. 2012. *Arabidopsis* synchronizes jasmonate-mediated defense with insect circadian behavior. *Proceedings of the National Academy of Sciences,* 109**,** 4674-4677.

GOODWIN, S. B. 2014. 'Dothideomycetes: Plant Pathogens, Saprobes, and Extremophiles' in MARTIN, F. (ed.) *The Ecological Genomics of Fungi.* Ames, Iowa, United States: Wiley Blackwell, 119-147.

GOULD, P. D., LOCKE, J. C. W., LARUE, C., SOUTHERN, M. M., DAVIS, S. J., HANANO, S., MOYLE, R., MILICH, R., PUTTERILL, J., MILLAR, A. J. & HALL, A. 2006. The molecular basis of temperature compensation in the *Arabidopsis* circadian clock. *The Plant Cell*, 18, 1177-1187.

GOULD, P. D., UGARTE, N., DOMIJAN, M., COSTA, M., FOREMAN, J., MACGREGOR, D., ROSE, R., GRIFFITHS, J., MILLAR, A. J., FINKENSTÄDT, B., PENFIELD, S., RAND, D. A., HALLIDAY & K. J., HALL, A. J. W. 2013. Network balance via CRY signalling controls the *Arabidopsis* circadian clock over ambient temperatures. *Molecular Systems Biology*, 9:650.

GRAF, A., SCHLERETH, A., STITT, M. & SMITH, A. M. 2010. Circadian control of carbohydrate availability for growth in *Arabidopsis* plants at night. *Proceedings of the National Academy of Sciences,* 107**,** 9458-9463.

GREEN, R. & TOBIN, E. 1999. Loss of the circadian clock-associated protein 1 in *Arabidopsis* results in altered clock-regulated gene expression. *Proceedings of the National Academy of Sciences,* 96**,** 4176-4179.

GREEN, R. M., TINGAY, S., WANG, Z. Y. & TOBIN, E. M. 2002. Circadian rhythms confer a higher level of fitness to *Arabidopsis* plants. *Plant Physiology,* 129**,** 576-584.

GREENE, A. V., KELLER, N., HAAS, H. & BELL-PEDERSEN, D. 2003. A circadian oscillator in *Aspergillus* spp. regulates daily development and gene expression. *Eukaryotic Cell,* 2**,** 231-237.

GREENWOOD, M., DOMIJAN, M., GOULD, P. D., HALL, A. J. W. & LOCKE, J. C. W. 2019. Coordinated circadian timing through the integration of local inputs in *Arabidopsis thaliana*. *PLoS Biology,* 17**,** e3000407.

GRIFFITHS, R. I., WHITELEY, A. S., O'DONNELL, A. G. & BAILEY, M. J. 2000. Rapid method for coextraction of DNA and RNA from natural environments for analysis of ribosomal DNA-and rRNA-based microbial community composition. *Applied and Environmental Microbiology,* 66**,** 5488-5491.

GRUNDY, J., STOKER, C. & CARRÉ, I. A. 2015. Circadian regulation of abiotic stress tolerance in plants. *Frontiers in Plant Science,* 6**,** 648.

GUTIÉRREZ, R. A., STOKES, T. L., THUM, K., XU, X., OBERTELLO, M., KATARI, M. S., TANURDZIC, M., DEAN, A., NERO, D. C. & MCCLUNG, C. R. 2008. Systems approach identifies an organic nitrogen-responsive gene network that is regulated by the master clock control gene *CCA1*. *Proceedings of the National Academy of Sciences,* 105**,** 4939-4944.

HAAS, D. & DEFAGO, G. 2005. Biological control of soil-borne pathogens by fluorescent pseudomonads. *Nature Reviews Microbiology,* 3**,** 307-19.

HARMER, S. L., HOGENESCH, J. B., STRAUME, M., CHANG, H. S., HAN, B., ZHU, T., WANG, X., KREPS, J. A. & KAY, S. A. 2000. Orchestrated transcription of key pathways in *Arabidopsis* by the circadian clock. *Science,* 290**,** 2110-2113.

HARTMANN, A., ROTHBALLER, M. & SCHMID, M. 2008. Lorenz Hiltner, a pioneer in rhizosphere microbial ecology and soil bacteriology research. *Plant and Soil,* 312**,** 7-14.

HAYDON, M. J., MIELCZAREK, O., ROBERTSON, F. C., HUBBARD, K. E. & WEBB, A. A. 2013. Photosynthetic entrainment of the *Arabidopsis thaliana* circadian clock. *Nature,* 502**,** 689-92.

HERNANDEZ, R. R. & ALLEN, M. F. 2013. Diurnal patterns of productivity of arbuscular mycorrhizal fungi revealed with the Soil Ecosystem Observatory. *New Phytologist,* 200**,** 547-557.

HEVIA, M. A., CANESSA, P., MÜLLER-ESPARZA, H. & LARRONDO, L. F. 2015. A circadian oscillator in the fungus *Botrytis cinerea* regulates virulence when infecting *Arabidopsis thaliana*. *Proceedings of the National Academy of Sciences,* 112**,** 8744-8749.

HILTON, S., PICOT, E., SCHREITER, S., BASS, D., NORMAN, K., OLIVER, A. E., MOORE, J. D., MAUCHLINE, T. H., MILLS, P. R., TEAKLE, G. R., CLARK, I. M., HIRSCH, P. R., VAN DER GAST, C. J., BENDING, G. D. In press. Identification of microbial signatures linked to oilseed rape yield decline at the landscale scale. *Microbiome*.

HIRSCH, P. R. & MAUCHLINE, T. H. 2012. Who's who in the plant root microbiome? *Nature Biotechnology,* 30**,** 961.

HOLTZENDORFF, J., PARTENSKY, F., MELLA, D., LENNON, J. F., HESS, W. R. & GARCZAREK, L. 2008. Genome streamlining results in loss of robustness of the circadian clock in the marine cyanobacterium *Prochlorococcus marinus* PCC 9511. *Journal of Biological Rhythms,* 23**,** 187-199.

HÖRNLEIN, C., CONFURIUS-GUNS, V., STAL, L. J. & BOLHUIS, H. 2018. Daily rhythmicity in coastal microbial mats. *Nature Partner Journals Biofilms and Microbiomes,* 4**,** 1-11.

HUBBARD, C. J., BROCK, M. T., VAN DIEPEN, L. T., MAIGNIEN, L., EWERS, B. E. & WEINIG, C. 2017. The plant circadian clock influences rhizosphere community structure and function. *The ISME Journal,* 12**,** 400-410.

HUGHES, M., DONNELLY, C., CROZIER, A. & WHEELER, C. 1999. Effects of the exposure of roots of *Alnus glutinosa* to light on flavonoids and nodulation. *Canadian Journal of Botany,* 77**,** 1311-1315.

HUGHES, M. E., HOGENESCH, J. B. & KORNACKER, K. 2010. JTK_CYCLE: an efficient nonparametric algorithm for detecting rhythmic components in genome-scale data sets. *Journal of Biological Rhythms,* 25**,** 372-380.

IGIEHON, N. O. & BABALOLA, O. O. 2018. Rhizosphere microbiome modulators: contributions of nitrogen fixing bacteria towards sustainable

agriculture. *International Journal of Environmental Research and Public Health,* 15**,** 574.

IIJIMA, M., SAKO, Y. & RAO, T. 2003. 'A new approach for the quantification of root-cap mucilage exudation in the soil' in ABE, J. (ed.) *Roots: The Dynamic Interface between Plants and the Earth.* Springer: Science and Business Media, 399-407.

INGLE, R. A., STOKER, C., STONE, W., ADAMS, N., SMITH, R., GRANT, M., CARRE, I., RODEN, L. C. & DENBY, K. J. 2015. Jasmonate signalling drives time-of-day differences in susceptibility of *Arabidopsis* to the fungal pathogen *Botrytis cinerea*. *The Plant Journal,* 84**,** 937-948.

ISHIKAWA, C. M. & BLEDSOE, C. 2000. Seasonal and diurnal patterns of soil water potential in the rhizosphere of blue oaks: evidence for hydraulic lift. *Oecologia,* 125**,** 459-465.

JACKSON, R. W., PRESTON, G. M. & RAINEY, P. B. 2005. Genetic characterization of *Pseudomonas fluorescens* SBW25 rsp gene expression in the phytosphere and in vitro. *Journal of Bacteriology,* 187**,** 8477-88.

JAKOBSEN, H. H. & STROM, S. L. 2004. Circadian cycles in growth and feeding rates of heterotrophic protist plankton. *Limnology and Oceanography,* 49**,** 1915-1922.

JAMES, A. B., MONREAL, J. A., NIMMO, G. A., KELLY, C. L., HERZYK, P., JENKINS, G. I. & NIMMO, H. G. 2008. The circadian clock in *Arabidopsis* roots is a simplified slave version of the clock in shoots. *Science,* 322**,** 1832-1835.

JOHNSON, C. H., STEWART, P. L. & EGLI, M. 2011. The cyanobacterial circadian system: from biophysics to bioevolution. *Annual Review of Biophysics,* 40**,** 143-167.

JONES, D. L., HODGE, A. & KUZYAKOV, Y. 2004. Plant and mycorrhizal regulation of rhizodeposition. *New Phytologist,* 163**,** 459-480.

JONES, D. L., NGUYEN, C. & FINLAY, R. D. 2009. Carbon flow in the rhizosphere: carbon trading at the soil–root interface. *Plant and Soil,* 321**,** 5-33.

KANG, S., EVANS, P., MORRISON, M. & MCSWEENEY, C. 2013. Identification of metabolically active proteobacterial and archaeal communities in the rumen by DNA-and RNA-derived 16S rRNA gene. *Journal of Applied Microbiology,* 115**,** 644-653.

KAUR, G., PHILLIPS, C., WONG, K. & SAINI, B. 2013. Timing is important in medication administration: a timely review of chronotherapy research. *International Journal of Clinical Pharmacy,* 35**,** 344-358.

KAWAMOTO, N., ITO, H., TOKUDA, I. T. & IWASAKI, H. 2020. Damped circadian oscillation in the absence of KaiA in *Synechococcus*. *Nature Communications,* 11**,** 1-12.

KEBROM, T. H., MCKINLEY, B. A. & MULLET, J. E. 2020. Shade signals alter the expression of circadian clock genes in newly-formed bioenergy sorghum internodes. *Plant Direct,* 4**,** e00235.

KEVEI, E., GYULA, P., HALL, A., KOZMA-BOGNÁR, L., KIM, W. Y., ERIKSSON, M. E., TÓTH, R., HANANO, S., FEHÉR, B. & SOUTHERN, M. M. 2006. Forward genetic analysis of the circadian clock separates the multiple functions of ZEITLUPE. *Plant Physiology,* 140**,** 933-945.

KIM, J. A., SHIM, D., KUMARI, S., JUNG, H. E., JUNG, K. H., JEONG, H., KIM, W. Y., LEE, S. I. & JEONG, M. J. 2019. Transcriptome analysis of diurnal gene expression in chinese cabbage. *Genes,* 10, 130.

KIM, J. Y., SONG, H. R., TAYLOR, B. L. & CARRÉ, I. A. 2003. Light-regulated translation mediates gated induction of the *Arabidopsis* clock protein LHY. *The European Molecular Biology Organisation Journal,* 22**,** 935-944.

KÕLJALG, U., LARSSON, K. H., ABARENKOV, K., NILSSON, R. H., ALEXANDER, I. J., EBERHARDT, U., ERLAND, S., HØILAND, K., KJØLLER, R. & LARSSON, E. 2005. UNITE: a database providing web-based methods for the molecular identification of ectomycorrhizal fungi. *New Phytologist,* 166**,** 1063-1068.

KONDO, T., STRAYER, C. A., KULKARNI, R. D., TAYLOR, W., ISHIURA, M., GOLDEN, S. S. & JOHNSON, C. H. 1993. Circadian rhythms in prokaryotes: luciferase as a reporter of circadian gene expression in cyanobacteria. *Proceedings of the National Academy of Sciences,* 90**,** 5672-5676.

KOWALCHUK, G. A., BUMA, D. S., DE BOER, W., KLINKHAMER, P. G. & VAN VEEN, J. A. 2002. Effects of above-ground plant species composition and diversity on the diversity of soil-borne microorganisms. *Antonie Van Leeuwenhoek,* 81**,** 509.

LAI, A. G., DOHERTY, C. J., MUELLER-ROEBER, B., KAY, S. A., SCHIPPERS, J. H. & DIJKWEL, P. P. 2012. CIRCADIAN CLOCK-ASSOCIATED 1 regulates ROS homeostasis and oxidative stress responses. *Proceedings of the National Academy of Sciences,* 109**,** 17129-17134.

LAKSHMANAN, V., SELVARAJ, G. & BAIS, H. P. 2014. Functional soil microbiome: belowground solutions to an aboveground problem. *Plant Physiology,* 166**,** 689-700.

LEBEIS, S. L., PAREDES, S. H., LUNDBERG, D. S., BREAKFIELD, N., GEHRING, J., MCDONALD, M., MALFATTI, S., DEL RIO, T. G., JONES, C. D. & TRINGE, S. G. 2015. Salicylic acid modulates colonization of the root microbiome by specific bacterial taxa. *Science,* 349**,** 860-864.

LEE, H. J., HA, J. H., KIM, S. G., CHOI, H. K., KIM, Z. H., HAN, Y. J., KIM, J. I., OH, Y., FRAGOSO, V. & SHIN, K. 2016. Stem-piped light activates phytochrome B to trigger light responses in *Arabidopsis thaliana* roots. *Science Signaling,* 9**,** 106.

LEE, H. G. & SEO, P. J. 2018. Dependence and independence of the root clock on the shoot clock in *Arabidopsis*. *Genes & Genomics,* 40**,** 1063-1068.

LEE, S. J., KONG, M., MORSE, D. & HIJRI, M. 2018. Expression of putative circadian clock components in the arbuscular mycorrhizal fungus *Rhizoglomus irregulare*. *Mycorrhiza,* 28**,** 523-534.

LEE, S. J., MORSE, D. & HIJRI, M. 2019. Holobiont chronobiology: mycorrhiza may be a key to linking aboveground and underground rhythms. *Mycorrhiza***,** 1-10.

LEPP, P. W. & SCHMIDT, T. M. 1998. Nucleic acid content of *Synechococcus* spp. during growth in continuous light and light/dark cycles. *Archives of Microbiology,* 170**,** 201-207.

LEWIN, G. R., CARLOS, C., CHEVRETTE, M. G., HORN, H. A., MCDONALD, B. R., STANKEY, R. J., FOX, B. G. & CURRIE, C. R. 2016. Evolution and ecology of Actinobacteria and their bioenergy applications. *Annual Review of Microbiology,* 70**,** 235-254.

LI, H., SU, J. Q., YANG, X. R. & ZHU, Y. G. 2019. Distinct rhizosphere effect on active and total bacterial communities in paddy soils. *Science of The Total Environment,* 649**,** 422-430.

LI, R., LLORCA, L. C., SCHUMAN, M. C., WANG, Y., WANG, L., JOO, Y., WANG, M., VASSÃO, D. G. & BALDWIN, I. T. 2018. ZEITLUPE in the roots of wild tobacco regulates jasmonate-mediated nicotine biosynthesis and resistance to a generalist herbivore. *Plant Physiology,* 177**,** 833-846.

LILLEY, A., BAILEY, M., BARR, M., KILSHAW, K., TIMMS-WILSON, T., DAY, M., NORRIS, S., JONES, T. & GODFRAY, H. 2003. Population dynamics and gene transfer in genetically modified bacteria in a model microcosm. *Molecular Ecology,* 12**,** 3097-3107.

LITTHAUER, S., BATTLE, M. W. & JONES, M. A. 2016. Phototropins do not alter accumulation of evening-phased circadian transcripts under blue light. *Plant Signaling & Behavior,* 11**,** e1126029.

LIU, R., LIU, Y., CHEN, Y., ZHAN, Y. & ZENG, Q. 2019. Cyanobacterial viruses exhibit diurnal rhythms during infection. *Proceedings of the National Academy of Sciences,* 116**,** 14077-14082.

LIU, Y. & BELL-PEDERSEN, D. 2006. Circadian rhythms in *Neurospora crassa* and other filamentous fungi. *Eukaryotic Cell,* 5**,** 1184-1193.

LIVAK, K. J. & SCHMITTGEN, T. D. 2001. Analysis of relative gene expression data using real-time quantitative PCR and the 2(-Delta Delta C(T)) Method. *Methods,* 25**,** 402-8.

LOU, P., WU, J., CHENG, F., CRESSMAN, L. G., WANG, X. & MCCLUNG, C. R. 2012. Preferential retention of circadian clock genes during diploidization following whole genome triplication in *Brassica rapa*. *Plant Cell,* 24**,** 2415-26.

LOVE, M. I., HUBER, W. & ANDERS, S. 2014. Moderated estimation of fold change and dispersion for RNA-seq data with DESeq2. *Genome Biology,* 15**,** 550.

LOZA-CORREA, M., GOMEZ-VALERO, L. & BUCHRIESER, C. 2010. Circadian clock proteins in prokaryotes: hidden rhythms? *Frontiers in Microbiology,* 1**,** 130.

LU, H., MCCLUNG, C. R. & ZHANG, C. 2017. Tick tock: circadian regulation of plant innate immunity. *Annual Review of Phytopathology,* 55**,** 287-311.

LUGTENBERG, B. & KAMILOVA, F. 2009. Plant-growth-promoting rhizobacteria. *Annual Review of Microbiology,* 63**,** 541-556.

LUNDBERG, D. S., LEBEIS, S. L., PAREDES, S. H., YOURSTONE, S., GEHRING, J., MALFATTI, S., TREMBLAY, J., ENGELBREKTSON, A., KUNIN, V., DEL RIO, T. G., EDGAR, R. C., EICKHORST, T., LEY, R. E., HUGENHOLTZ, P., TRINGE, S. G. & DANGL, J. L. 2012. Defining the core *Arabidopsis thaliana* root microbiome. *Nature,* 488**,** 86-90.

MA, J. F. & NOMOTO, K. 1996. Effective regulation of iron acquisition in graminaceous plants. The role of mugineic acids as phytosiderophores. *Physiologia Plantarum,* 97**,** 609-617.

MA, P., MORI, T., ZHAO, C., THIEL, T. & JOHNSON, C. H. 2016. Evolution of KaiC-dependent timekeepers: a proto-circadian timing mechanism confers adaptive fitness in the purple bacterium *Rhodopseudomonas palustris*. *PLoS Genetics,* 12**,** e1005922.

MARASCO, R., ROLLI, E., ETTOUMI, B., VIGANI, G., MAPELLI, F., BORIN, S., ABOU-HADID, A. F., EL-BEHAIRY, U. A., SORLINI, C. & CHERIF, A. 2012. A drought resistance-promoting microbiome is selected by root system under desert farming. *PloS One,* 7**,** e48479.

MARCOLINO-GOMES, J., RODRIGUES, F. A., FUGANTI-PAGLIARINI, R., BENDIX, C., NAKAYAMA, T. J., CELAYA, B., MOLINARI, H. B. C., DE OLIVEIRA, M. C. N., HARMON, F. G. & NEPOMUCENO, A. 2014. Diurnal oscillations of soybean circadian clock and drought responsive genes. *PLoS One,* 9**,** e86402.

MASSALHA, H., KORENBLUM, E., MALITSKY, S., SHAPIRO, O. H. & AHARONI, A. 2017. Live imaging of root-bacteria interactions in a

microfluidics setup. *Proceedings of the National Academy of Sciences,* 114**,** 4549-4554.

MATIMATI, I., VERBOOM, G. A. & CRAMER, M. D. 2014. Do hydraulic redistribution and nocturnal transpiration facilitate nutrient acquisition in *Aspalathus linearis*? *Oecologia,* 175**,** 1129-1142.

MAVRODI, O. V., MAVRODI, D. V., THOMASHOW, L. S. & WELLER, D. M. 2007. Quantification of 2,4-diacetylphloroglucinol-producing *Pseudomonas fluorescens* strains in the plant rhizosphere by real-time PCR. *Applied and Environmental Microbiology,* 73**,** 5531-8.

MCCLUNG, C. R. 2006. Plant circadian rhythms. *The Plant Cell,* 18**,** 792-803.

MCCLUNG, C. R. 2019. The Plant Circadian Oscillator. *Biology,* 8, 14.

MELOUK, H. & HORNER, C. 1975. Cross protection in mints by *Verticillium nigrescens* against *V. dahliae*. *Phytopathology,* 65**,** 767-769.

MENDES, R., GARBEVA, P. & RAAIJMAKERS, J. M. 2013. The rhizosphere microbiome: significance of plant beneficial, plant pathogenic, and human pathogenic microorganisms. *Federation of European Microbiological Societies Microbiology Reviews,* 37**,** 634-663.

MICALLEF, S. A., SHIARIS, M. P. & COLÓN-CARMONA, A. 2009. Influence of *Arabidopsis thaliana* accessions on rhizobacterial communities and natural variation in root exudates. *Journal of Experimental Botany,* 60**,** 1729-1742.

MICHAEL, T. P., MOCKLER, T. C., BRETON, G., MCENTEE, C., BYER, A., TROUT, J. D., HAZEN, S. P., SHEN, R., PRIEST, H. D. & SULLIVAN, C. M. 2008. Network discovery pipeline elucidates conserved time-of-day–specific cis-regulatory modules. *PLoS Genetics,* 4**,** 14.

MILLAR, A. J., SHORT, S. R., CHUA, N.-H. & KAY, S. A. 1992. A novel circadian phenotype based on firefly luciferase expression in transgenic plants. *The Plant Cell,* 4**,** 1075-1087.

MINCHIN, P. R. 1987. 'An evaluation of the relative robustness of techniques for ecological ordination' In PRENTICE, I. C., VAN DER MAAREL, E. (ed.) *Theory and Models in Vegetation Science.* Dordrecht, Netherlands: Dr W. Junk Publishers, 89-107.

MIZOGUCHI, T., WHEATLEY, K., HANZAWA, Y., WRIGHT, L., MIZOGUCHI, M., SONG, H., CARRÉ, I. A. & COUPLAND, G. 2002. *LHY* and *CCA1* Are partially redundant genes required to maintain circadian rhythms in *Arabidopsis*. *Developmental Cell,* 2**,** 629-641.

MO, M., YOKAWA, K., WAN, Y. & BALUŠKA, F. 2015. How and why do root apices sense light under the soil surface? *Frontiers in Plant Science,* 6**,** 775.

MOORE, A., ZIELINSKI, T. & MILLAR, A. J. 2014. 'Online period estimation and determination of rhythmicity in circadian data, using the BioDare data infrastructure.' in STAIGER, D. (ed.) *Plant Circadian Networks.* Springer Science and Business Media, 13-44.

MOORE, J. C., MCCANN, K., SETÄLÄ, H. & DE RUITER, P. C. 2003. Top-down is bottom-up: does predation in the rhizosphere regulate aboveground dynamics? *Ecology,* 84**,** 846-857.

MULLINEAUX, C. W. & STANEWSKY, R. 2009. The rolex and the hourglass: a simplified circadian clock in *Prochlorococcus*? *Journal of Bacteriology,* 191**,** 5333-5335.

MURAKAMI, M., TAGO, Y., YAMASHINO, T. & MIZUNO, T. 2007. Comparative overviews of clock-associated genes of *Arabidopsis thaliana* and *Oryza sativa*. *Plant and Cell Physiology,* 48**,** 110-121.

NAKAMICHI, N., KUSANO, M., FUKUSHIMA, A., KITA, M., ITO, S., YAMASHINO, T., SAITO, K., SAKAKIBARA, H. & MIZUNO, T. 2009. Transcript profiling of an *Arabidopsis PSEUDO RESPONSE REGULATOR* arrhythmic triple mutant reveals a role for the circadian clock in cold stress response. *Plant and Cell Physiology,* 50**,** 447-462.

NAWAZ, A., PURAHONG, W., HERRMANN, M., KÜSEL, K., BUSCOT, F. & WUBET, T. 2019. DNA-and RNA-Derived fungal communities in subsurface aquifers only partly overlap but react similarly to environmental factors. *Microorganisms,* 7**,** 341.

NGUYEN, N. H., SONG, Z., BATES, S. T., BRANCO, S., TEDERSOO, L., MENKE, J., SCHILLING, J. S. & KENNEDY, P. G. 2016. FUNGuild: An open annotation tool for parsing fungal community datasets by ecological guild. *Fungal Ecology,* 20**,** 241-248.

NI, T. & ZENG, Q. 2016. Diel infection of cyanobacteria by cyanophages. *Frontiers in Marine Science,* 2**,** 123.

NIELSEN, K. M., JOHNSEN, P. J., BENSASSON, D. & DAFFONCHIO, D. 2007. Release and persistence of extracellular DNA in the environment. *Environmental Biosafety Research,* 6**,** 37-53.

NIMMO, H. G. 2018. Entrainment of *Arabidopsis* roots to the light: dark cycle by light piping. *Plant, cell & environment,* 41**,** 1742-1748.

NUNES-HALLDORSON, V. D. S. & DURAN, N. L. 2003. Bioluminescent bacteria: *lux* genes as environmental biosensors. *Brazilian Journal of Microbiology,* 34**,** 91-96.

O'KANE, D., LINGLE, W., WAMPLER, J., LEGOCKI, M., LEGOCKI, R. & SZALAY, A. 1988. Visualization of bioluminescence as a marker of gene

expression in rhizobium-infected soybean root nodules. *Plant Molecular Biology,* 10**,** 387-399.

OKSANEN, J., KINDT, R., LEGENDRE, P., O'HARA, B., STEVENS, M. H. H., OKSANEN, M. J. & SUGGESTS, M. 2007. The vegan package. *Community Ecology Package,* 10**,** 631-637.

OLIVEIRA, A. G., STEVANI, C. V., WALDENMAIER, H. E., VIVIANI, V., EMERSON, J. M., LOROS, J. J. & DUNLAP, J. C. 2015. Circadian control sheds light on fungal bioluminescence. *Current Biology,* 25**,** 964-968.

PARADA, A. E., NEEDHAM, D. M. & FUHRMAN, J. A. 2016. Every base matters: assessing small subunit rRNA primers for marine microbiomes with mock communities, time series and global field samples. *Environmental Microbiology,* 18**,** 1403-1414.

PARK, D. H., SOMERS, D. E., KIM, Y. S., CHOY, Y. H., LIM, H. K., SOH, M. S., KIM, H. J., KAY, S. A. & NAM, H. G. 1999. Control of circadian rhythms and photoperiodic flowering by the Arabidopsis *GIGANTEA* gene. *Science,* 285**,** 1579-1582.

PAULOSE, J. K., WRIGHT, J. M., PATEL, A. G. & CASSONE, V. M. 2016. Human gut bacteria are sensitive to melatonin and express endogenous circadian rhythmicity. *PLoS One,* 11**,** e0146643.

PHILIPPOT, L., RAAIJMAKERS, J. M., LEMANCEAU, P. & VAN DER PUTTEN, W. H. 2013. Going back to the roots: the microbial ecology of the rhizosphere. *Nature Reviews Microbiology,* 11**,** 789-799.

PINI, F., EAST, A. K., APPIA-AYME, C., TOMEK, J., KARUNAKARAN, R., MENDOZA-SUAREZ, M., EDWARDS, A., TERPOLILLI, J. J., ROWORTH, J., DOWNIE, J. A. & POOLE, P. S. 2017. Bacterial biosensors for in vivo spatiotemporal mapping of root secretion. *Plant Physiology,* 174**,** 1289-1306.

PRATAMA, A. A., TERPSTRA, J., DE OLIVERIA, A. L. M. & SALLES, J. F. 2020. The role of rhizosphere bacteriophages in plant health. *Trends in Microbiology*.

PREECE, C. & PEÑUELAS, J. 2020. A return to the wild: root exudates and food security. *Trends in Plant Science,* 25**,** 14-21.

PRITHIVIRAJ, B., BAIS, H., WEIR, T., SURESH, B., NAJARRO, E., DAYAKAR, B., SCHWEIZER, H. & VIVANCO, J. 2005. Down regulation of virulence factors of *Pseudomonas aeruginosa* by salicylic acid attenuates its virulence on *Arabidopsis thaliana* and *Caenorhabditis elegans*. *Infection and Immunity,* 73**,** 5319-5328.

QUAST, C., PRUESSE, E., YILMAZ, P., GERKEN, J., SCHWEER, T., YARZA, P., PEPLIES, J. & GLÖCKNER, F. O. 2012. The SILVA ribosomal RNA

gene database project: improved data processing and web-based tools. *Nucleic Acids Research,* 41**,** D590-D596.

RAAIJMAKERS, J. M., PAULITZ, T. C., STEINBERG, C., ALABOUVETTE, C. & MOËNNE-LOCCOZ, Y. 2009. The rhizosphere: a playground and battlefield for soilborne pathogens and beneficial microorganisms. *Plant and Soil,* 321**,** 341-361.

RAINEY, P. B. 1999. Adaptation of *Pseudomonas fluorescens* to the plant rhizosphere. *Environmental Microbiology,* 1**,** 243-257.

RATTRAY, E., PROSSER, J. I., GLOVER, L. A. & KILLHAM, K. 1995. Characterization of rhizosphere colonization by luminescent *Enterobacter cloacae* at the population and single-cell levels. *Applied and Environmental Microbiology,* 61**,** 2950-2957.

RAY, D. K., WEST, P. C., CLARK, M., GERBER, J. S., PRISHCHEPOV, A. V. & CHATTERJEE, S. 2019. Climate change has likely already affected global food production. *PloS One,* 14**,** e0217148.

RELLAN-ALVAREZ, R., LOBET, G., LINDNER, H., PRADIER, P. L., SEBASTIAN, J., YEE, M. C., GENG, Y., TRONTIN, C., LARUE, T., SCHRAGER-LAVELLE, A., HANEY, C. H., NIEU, R., MALOOF, J., VOGEL, J. P. & DINNENY, J. R. 2015. GLO-Roots: an imaging platform enabling multidimensional characterization of soil-grown root systems. *eLife,* 4.

RICHTER-HEITMANN, T., EICKHORST, T., KNAUTH, S., FRIEDRICH, M. W. & SCHMIDT, H. 2016. Evaluation of strategies to separate root-associated microbial communities: a crucial choice in rhizobiome research. *Frontiers in Microbiology,* 7**,** 773.

RIPPERGER, J. A., JUD, C. & ALBRECHT, U. 2011. The daily rhythm of mice. *Federation of European Biochemical Societies Letters,* 585**,** 1384-1392.

RODRIGUEZ, R., WHITE JR, J., ARNOLD, A. E. & REDMAN, A. R. A. 2009. Fungal endophytes: diversity and functional roles. *New Phytologist,* 182**,** 314-330.

RODRIGUEZ, R. J., HENSON, J., VAN VOLKENBURGH, E., HOY, M., WRIGHT, L., BECKWITH, F., KIM, Y. O. & REDMAN, R. S. 2008. Stress tolerance in plants via habitat-adapted symbiosis. *The ISME Journal,* 2**,** 404-416.

RODRIGUEZ-ROMERO, J., HEDTKE, M., KASTNER, C., MÜLLER, S. & FISCHER, R. 2010. Fungi, hidden in soil or up in the air: light makes a difference. *Annual Review of Microbiology,* 64.

ROESCH, L. F., FULTHORPE, R. R., RIVA, A., CASELLA, G., HADWIN, A. K., KENT, A. D., DAROUB, S. H., CAMARGO, F. A., FARMERIE, W. G. &

TRIPLETT, E. W. 2007. Pyrosequencing enumerates and contrasts soil microbial diversity. *The ISME Journal,* 1**,** 283-290.

ROHLAND, N. & REICH, D. 2012. Cost-effective, high-throughput DNA sequencing libraries for multiplexed target capture. *Genome Research,* 22**,** 939-946.

ROSBASH, M. & HALL, J. C. 1989. The molecular biology of circadian rhythms. *Neuron,* 3**,** 387-398.

RUDOLPH, N., VOSS, S., MORADI, A. B., NAGL, S. & OSWALD, S. E. 2013. Spatio-temporal mapping of local soil pH changes induced by roots of lupin and soft-rush. *Plant and Soil,* 369**,** 669-680.

SALICHOS, L. & ROKAS, A. 2010. The diversity and evolution of circadian clock proteins in fungi. *Mycologia,* 102**,** 269-278.

SALOMÉ, P. A. & MCCLUNG, C. R. 2005. *PSEUDO-RESPONSE REGULATOR 7* and *9* are partially redundant genes essential for the temperature responsiveness of the *Arabidopsis* circadian clock. *Plant Cell*, 17, 791-803.

SANCHEZ, S. E., RUGNONE, M. L. & KAY, S. A. 2020. Light perception: a matter of time. *Molecular Plant,* 13**,** 363-385.

SARTOR, F., EELDERINK-CHEN, Z., ARONSON, B., BOSMAN, J., HIBBERT, L. E., DODD, A. N., KOVÁCS, Á. T. & MERROW, M. 2019. Are there circadian clocks in non-photosynthetic bacteria? *Biology,* 8**,** 41.

SAYERS, E. W., BECK, J., BRISTER, J. R., BOLTON, E. E., CANESE, K., COMEAU, D. C., FUNK, K., KETTER, A., KIM, S. & KIMCHI, A. 2020. Database resources of the national center for biotechnology information. *Nucleic Acids Research,* 48**,** D9.

SCHAFFER, R., RAMSAY, N., SAMACH, A., CORDEN, S., PUTTERILL, J., CARRÉ, I. A. & COUPLAND, G. 1998. The late elongated hypocotyl mutation of *Arabidopsis* disrupts circadian rhythms and the photoperiodic control of flowering. *Cell,* 93**,** 1219-1229.

SCHMELLING, N. M., LEHMANN, R., CHAUDHURY, P., BECK, C., ALBERS, S. V., AXMANN, I. M. & WIEGARD, A. 2017. Minimal tool set for a prokaryotic circadian clock. *BioMed Central Evolutionary Biology,* 17**,** 1-20.

SCHMIDT, J. E., KENT, A. D., BRISSON, V. L. & GAUDIN, A. C. 2019. Agricultural management and plant selection interactively affect rhizosphere microbial community structure and nitrogen cycling. *Microbiome,* 7**,** 1-18.

SCHNEIDER, C. A., RASBAND, W. S. & ELICEIRI, K. W. 2012. NIH Image to ImageJ: 25 years of image analysis. *Nature Methods,* 9**,** 671-675.

SELENSKA, S. & KLINGMÜLLER, W. 1991. DNA recovery and direct detection of Tn*5* sequences from soil. *Letters in Applied Microbiology,* 13**,** 21-24.

SELOSSE, M.-A. & ROY, M. 2009. Green plants that feed on fungi: facts and questions about mixotrophy. *Trends in Plant Science,* 14**,** 64-70.

SHANNON, C. E. 1948. A mathematical theory of communication. *Bell System Technical Journal,* 27, 379-423.

SHARMA, M. & BHATT, D. 2015. The circadian clock and defence signalling in plants. *Molecular Plant Pathology,* 16**,** 210-218.

SHELDON, A. L. 1969. Equitability indices: dependence on the species count. *Ecology,* 50**,** 466-467.

SHI, S., NUCCIO, E., HERMAN, D. J., RIJKERS, R., ESTERA, K., LI, J., DA ROCHA, U. N., HE, Z., PETT-RIDGE, J. & BRODIE, E. L. 2015. Successional trajectories of rhizosphere bacterial communities over consecutive seasons. *mBio,* 6.

SHINDE, S., ZERBS, S., COLLART, F. R., CUMMING, J. R., NOIROT, P. & LARSEN, P. E. 2019. *Pseudomonas fluorescens* increases mycorrhization and modulates expression of antifungal defense response genes in roots of aspen seedlings. *BioMed Central Plant Biology,* 19**,** 4.

SILBY, M. W., CERDENO-TARRAGA, A. M., VERNIKOS, G. S., GIDDENS, S. R., JACKSON, R. W., PRESTON, G. M., ZHANG, X. X., MOON, C. D., GEHRIG, S. M., GODFREY, S. A., KNIGHT, C. G., MALONE, J. G., ROBINSON, Z., SPIERS, A. J., HARRIS, S., CHALLIS, G. L., YAXLEY, A. M., HARRIS, D., SEEGER, K., MURPHY, L., RUTTER, S., SQUARES, R., QUAIL, M. A., SAUNDERS, E., MAVROMATIS, K., BRETTIN, T. S., BENTLEY, S. D., HOTHERSALL, J., STEPHENS, E., THOMAS, C. M., PARKHILL, J., LEVY, S. B., RAINEY, P. B. & THOMSON, N. R. 2009. Genomic and genetic analyses of diversity and plant interactions of *Pseudomonas fluorescens*. *Genome Biology,* 10**,** R51.

SOMERS, D. E., WEBB, A., PEARSON, M. & KAY, S. A. 1998. The short-period mutant, *toc1-1*, alters circadian clock regulation of multiple outputs throughout development in *Arabidopsis thaliana*. *Development,* 125**,** 485-494.

SORIANO, M. I., ROIBÁS, B., GARCÍA, A. B. & ESPINOSA-URGEL, M. 2010. Evidence of circadian rhythms in non-photosynthetic bacteria? *Journal of Circadian Rhythms,* 8**,** 8.

SPAIN, A. M., KRUMHOLZ, L. R. & ELSHAHED, M. S. 2009. Abundance, composition, diversity and novelty of soil Proteobacteria. *The ISME Journal,* 3**,** 992-1000.

STALEY, C., FERRIERI, A. P., TFAILY, M. M., CUI, Y., CHU, R. K., WANG, P., SHAW, J. B., ANSONG, C. K., BREWER, H. & NORBECK, A. D. 2017. Diurnal cycling of rhizosphere bacterial communities is associated with shifts in carbon metabolism. *Microbiome,* 5**,** 1-13.

STEPHENSON, P., BAKER, D., GIRIN, T., PEREZ, A., AMOAH, S., KING, G. J. & ØSTERGAARD, L. 2010. A rich TILLING resource for studying gene function in *Brassica rapa*. *BioMed Central Plant Biology,* 10**,** 62.

SUKENIK, A., KAPLAN-LEVY, R. N., WELCH, J. M. & POST, A. F. 2012. Massive multiplication of genome and ribosomes in dormant cells (akinetes) of *Aphanizomenon ovalisporum* (Cyanobacteria). *The ISME Journal,* 6**,** 670-679.

SULPICE, R., FLIS, A., IVAKOV, A. A., APELT, F., KROHN, N., ENCKE, B., ABEL, C., FEIL, R., LUNN, J. E. & STITT, M. 2014. *Arabidopsis* coordinates the diurnal regulation of carbon allocation and growth across a wide range of photoperiods. *Molecular Plant,* 7**,** 137-155.

SUNDSTRÖM, J. F., ALBIHN, A., BOQVIST, S., LJUNGVALL, K., MARSTORP, H., MARTIIN, C., NYBERG, K., VÅGSHOLM, I., YUEN, J. & MAGNUSSON, U. 2014. Future threats to agricultural food production posed by environmental degradation, climate change, and animal and plant diseases–a risk analysis in three economic and climate settings. *Food Security,* 6**,** 201-215.

SWARUP, K., ALONSO-BLANCO, C., LYNN, J. R., MICHAELS, S. D., AMASINO, R. M., KOORNNEEF, M. & MILLAR, A. J. 1999. Natural allelic variation identifies new genes in the *Arabidopsis* circadian system. *The Plant Journal,* 20**,** 67-77.

TAKAHASHI, N., HIRATA, Y., AIHARA, K. & MAS, P. 2015. A hierarchical multi-oscillator network orchestrates the *Arabidopsis* circadian system. *Cell,* 163**,** 148-159.

TATAROGLU, O. & EMERY, P. 2015. The molecular ticks of the *Drosophila* circadian clock. *Current Opinion in Insect Science,* 7**,** 51-57.

TESTER, M. & MORRIS, C. 1987. The penetration of light through soil. *Plant, Cell & Environment,* 10**,** 281-286.

THARAYIL, N. & TRIEBWASSER, D. J. 2010. Elucidation of a diurnal pattern of catechin exudation by *Centaurea stoebe*. *Journal of Chemical Ecology,* 36**,** 200-204.

THOMPSON, I. P., LILLEY, A. K., ELLIS, R. J., BRAMWELL, P. A. & BAILEY, M. J. 1995. Survival, colonization and dispersal of genetically modified *Pseudomonas fluorescens* SBW25 in the phytosphere of field grown sugar beet. *Nature Biotechnology,* 13**,** 1493-1497.

TORSVIK, V., ØVREÅS, L. & THINGSTAD, T. F. 2002. Prokaryotic diversity--magnitude, dynamics, and controlling factors. *Science,* 296**,** 1064-1066.

URBINA, H., BREED, M. F., ZHAO, W., GURRALA, K. L., ANDERSSON, S. G., ÅGREN, J., BALDAUF, S. & ROSLING, A. 2018. Specificity in *Arabidopsis* thaliana recruitment of root fungal communities from soil and rhizosphere. *Fungal Biology,* 122**,** 231-240.

URICH, T., LANZÉN, A., QI, J., HUSON, D. H., SCHLEPER, C. & SCHUSTER, S. C. 2008. Simultaneous assessment of soil microbial community structure and function through analysis of the meta-transcriptome. *PloS One,* 3**,** e2527.

VACHERON, J., DESBROSSES, G., BOUFFAUD, M. L., TOURAINE, B., MOËNNE-LOCCOZ, Y., MULLER, D., LEGENDRE, L., WISNIEWSKI-DYÉ, F. & PRIGENT-COMBARET, C. 2013. Plant growth-promoting rhizobacteria and root system functioning. *Frontiers in Plant Science,* 4**,** 356.

VAGELAS, I. & LEONTOPOULOS, S. 2015. Cross-protection of cotton against *Verticillium wilt* by *Verticillium nigrescens*. *Emirates Journal of Food and Agriculture***,** 687-691.

VAN LOON, L., BAKKER, P. & PIETERSE, C. 1998. Systemic resistance induced by rhizosphere bacteria. *Annual Review of Phytopathology,* 36**,** 453-483.

VEIGA, R. S., FACCIO, A., GENRE, A., PIETERSE, C. M., BONFANTE, P. & VAN DER HEIJDEN, M. G. 2013. Arbuscular mycorrhizal fungi reduce growth and infect roots of the non-host plant *Arabidopsis thaliana*. *Plant, Cell, and Environment,* 36**,** 1926-37.

WAGG, C., JANSA, J., SCHMID, B. & VAN DER HEIJDEN, M. G. 2011. Belowground biodiversity effects of plant symbionts support aboveground productivity. *Ecology Letters,* 14**,** 1001-1009.

WANG, S. & KOOL, E. T. 1995. Origins of the large differences in stability of DNA and RNA helixes: C-5 methyl and 2'-hydroxyl effects. *Biochemistry*, 34, 4125-4132.

WANG, B. & QIU, Y. L. 2006. Phylogenetic distribution and evolution of mycorrhizas in land plants. *Mycorrhiza,* 16**,** 299-363.

WANG, W., BARNABY, J. Y., TADA, Y., LI, H., TÖR, M., CALDELARI, D., LEE, D. U., FU, X. D. & DONG, X. 2011. Timing of plant immune responses by a central circadian regulator. *Nature,* 470**,** 110-114.

WATT, M. & EVANS, J. R. 1999. Linking development and determinacy with organic acid efflux from proteoid roots of white lupin grown with low phosphorus and ambient or elevated atmospheric CO2 concentration. *Plant Physiology,* 120**,** 705-716.

WATT, M., SILK, W. K. & PASSIOURA, J. B. 2006. Rates of root and organism growth, soil conditions, and temporal and spatial development of the rhizosphere. *Annals of Botany,* 97**,** 839-55.

WEBB, A. A. 2003. The physiology of circadian rhythms in plants. *New Phytologist,* 160**,** 281-303.

WHITE III, R. A., RIVAS-UBACH, A., BORKUM, M. I., KÖBERL, M., BILBAO, A., COLBY, S. M., HOYT, D. W., BINGOL, K., KIM, Y. M. & WENDLER, J. P. 2017. The state of rhizospheric science in the era of multi-omics: a practical guide to omics technologies. *Rhizosphere,* 3**,** 212-221.

WHITE, T. J., BRUNS, T., LEE, S. & TAYLOR, J. 1990. 'Amplification and direct sequencing of fungal ribosomal RNA genes for phylogenetics' in SNINSKY, J. J., GELFAND, D. H., WHITE, T. J., INNIS, M. A. (ed.) *PCR protocols: a guide to methods and applications.* Academic Press, Inc., 18**,** 315-322.

WHITFIELD, W. A. D. 1974. 'The Soils of the National Vegetable Research Station, Wellesbourne' in *Report of the National Vegetable Research Station for 1973***,** 21-30.

WINSON, M. K., SWIFT, S., HILL, P. J., SIMS, C. M., GRIESMAYR, G., BYCROFT, B. W., WILLIAMS, P. & STEWART, G. S. 1998. Engineering the *luxCDABE* genes from *Photorhabdus luminescens* to provide a bioluminescent reporter for constitutive and promoter probe plasmids and mini-Tn*5* constructs. *Federation of European Microbiological Societies Microbiology Letters,* 163**,** 193-202.

WU, G., ANAFI, R. C., HUGHES, M. E., KORNACKER, K. & HOGENESCH, J. B. 2016. MetaCycle: an integrated R package to evaluate periodicity in large scale data. *Bioinformatics,* 32**,** 3351-3353.

XIAO, D., ZHANG, N.W., ZHAO, J.J., BONNEMA, G. & HOU, X.L. 2012. Validation of reference genes for real-time quantitative PCR normalisation in non-heading Chinese cabbage. *Functional Plant Biology,* 39.

XIE, Q., LOU, P., HERMAND, V., AMAN, R., PARK, H. J., YUN, D. J., KIM, W. Y., SALMELA, M. J., EWERS, B. E., WEINIG, C., KHAN, S. L., SCHAIBLE, D. L. & MCCLUNG, C. R. 2015. Allelic polymorphism of *GIGANTEA* is responsible for naturally occurring variation in circadian period in *Brassica rapa*. *Proceedings of the National Academy of Sciences*, 112**,** 3829-34.

YANOVSKY, M. J. & KAY, S. A. 2002. Molecular basis of seasonal time measurement in *Arabidopsis*. *Nature,* 419**,** 308-312.

YAZDANBAKHSH, N., SULPICE, R., GRAF, A., STITT, M. & FISAHN, J. 2011. Circadian control of root elongation and C partitioning in *Arabidopsis thaliana*. *Plant, Cell & Environment,* 34**,** 877-894.

YORK, L. M., CARMINATI, A., MOONEY, S. J., RITZ, K. & BENNETT, M. J. 2016. The holistic rhizosphere: integrating zones, processes, and semantics in the soil influenced by roots. *Journal of Experimental Botany,* 67**,** 3629-3643.

YOUNG, M. W. & KAY, S. A. 2001. Time zones: a comparative genetics of circadian clocks. *Nature Reviews Genetics,* 2**,** 702-715.

YU, K., PIETERSE, C. M., BAKKER, P. A. & BERENDSEN, R. L. 2019. Beneficial microbes going underground of root immunity. *Plant, Cell and Environment,* 42**,** 2860-2870.

ZARE, R., GAMS, W., STARINK-WILLEMSE, M. & SUMMERBELL, R. 2007. *Gibellulopsis*, a suitable genus for *Verticillium nigrescens*, and *Musicillium*, a new genus for *V. theobromae*. *Nova Hedwigia,* 85**,** 463-489.

ZHANG, C., XIE, Q., ANDERSON, R. G., NG, G., SEITZ, N. C., PETERSON, T., MCCLUNG, C. R., MCDOWELL, J. M., KONG, D. & KWAK, J. M. 2013. Crosstalk between the circadian clock and innate immunity in *Arabidopsis*. *PLoS Pathogens,* 9**,** e1003370.

ZHANG, N., CASTLEBURY, L. A., MILLER, A. N., HUHNDORF, S. M., SCHOCH, C. L., SEIFERT, K. A., ROSSMAN, A. Y., ROGERS, J. D., KOHLMEYER, J. & VOLKMANN-KOHLMEYER, B. 2006. An overview of the systematics of the Sordariomycetes based on a four-gene phylogeny. *Mycologia,* 98**,** 1076-1087.